ANTICANCER PROPERTY, MODE OF ACTION AND SELECTIVITY OF A SERIES OF COPPER COMPLEXES

By

KONG SIEW MING

A thesis submitted to Faculty of Engineering and Science,
Universiti Tunku Abdul Rahman,
in partial fulfillment of the requirements for the degree of
Master of Science
December 2012

ABSTRACT

ANTICANCER PROPERTY, MODE OF ACTION AND SELECTIVITY OF A SERIES OF COPPER COMPLEXES

Kong Siew Ming

Copper compounds can be an alternative to platinum-based anticancer drugs. Use of compounds involving endogenous metals, such as copper, may be less toxic than platinum-based anticancer drugs and may overcome the problems encountered by the latter. A previous study established that a series of ternary copper(II) complexes, $[Cu(phen)(aa)(H_2O)]NO_3$, exists as $[Cu(phen)(aa)(H_2O)]^+$ and NO^{3-}, and these species are stable up to at least 24 h. The effects of these compounds on MDA-MB-231 breast cancer cells and MCF10A non-cancerous cells, and some aspects of the mechanism involved were investigated in this study. Morphological analysis and MTT colorimetric assays showed that the compounds significantly inhibited cell proliferation in a dose-dependent manner, and there was significant difference in antiproliferative effect on these two cell lines for certain concentration range of ternary copper(II) complexes. Annexin V-FITC/PI double staining flow cytometry analysis of apoptosis assay demonstrated that the percentage of apoptotic cells induced by ternary copper(II) complexes was much higher in MDA-MB-231 tumor cells than MCF10A immortalized cells, suggesting selectivity of the compounds. Statistical analysis of the cell cycle data obtained using flow cytometry revealed that two of these compounds could

suppress growth of MDA-MB-231 cells through cell cycle arrest at G_0/G_1 phase. Accumulation of ubiquitinated proteins and IκB (NF-κB inhibitor) in MDA-MB-231 cells *via* Western blotting gave evidence for proteasome inhibition. With an assay using 2',7'-dichlorofluorescein diacetate (DCFH-DA), it was found that the compounds induced significant increase in reactive oxygen species (ROS) production in cancer cells at higher concentration (10 μM) and prolonged exposures (24 h) compared to untreated cells. However, similarly treated MCF10A cells showed minimal overall production of ROS under the same conditions. Detection of DNA damage-induced phosphorylation of H2AX at Ser^{139} in MDA-MB-231 cells suggested that the copper compounds induced double-strand breaks and activated signaling pathways leading to apoptosis. Overall, these findings suggested that ternary copper(II) complexes killed the cancer cells by inducing ROS production, DNA damage and arresting cell cycle at G_0/G_1 phase. In addition, these compounds inhibited proteasome function of the cancer cells. Thus, the anticancer property of these compounds involved multiple pathways and they were found to exhibit significant selectivity for cancer over non-cancerous cells.

ACKNOWLEDGEMENTS

I am grateful to a number of people around me who has contributed in various ways to the project and made this thesis possible. It is an honour for me to convey my gratitude to them in my humble acknowledgment.

Foremost, I owe my deepest gratitude to my supervisor, Dr Ng Chew Hee, who has shown extensive patience and supported me throughout my thesis with his excellent advice and unsurpassed knowledge. His understanding, encouragement and constructive comments have inspired my entire project.

Next, I would like to offer my sincerest gratitude and thanks to my co-supervisor, Dr Alan Khoo Soo Beng for his detailed supervision and guidance throughout this work. His scientific intuition and passion in science had been remarkably helpful for this study. He gave me an oasis of ideas and concepts which added great value to my project. I am indebted to him.

I would like to express my deep and sincere gratitude to Dr Munirah bt. Ahmad, for her motivation, patience, immense knowledge and enthusiasm. She provided me unflinching encouragement and support in various ways.

I am grateful to Institute for Medical Research (IMR) and Universiti Tunku Abdul Rahman for providing the necessary financial, academic and technical support for this research.

In my daily work I have been blessed with a friendly and cheerful group of fellow colleagues. I am indebted to Dr Tan Lu Ping, Susan Hoe, Chu Tai Lin, Maelinda Daker, Wayne Ng for their kindness, insightful comments and friendship. In many ways I have learnt much from them and I will cherish their generosity and encouragement towards me throughout the research. My sincere thanks also go to medical laboratory technologist Ms Tan, Sasela, Huraizah, Nurul, Syazwani, Amerul, Majid and Khuzairi for their help in diverse ways.

The project was a multidisciplinary one and it needed the assistance of others as I graduated with a degree in Biochemistry from University of Malaya. Here, I would like to extend my appreciation to Miss Wang Wai San who synthesized and characterized the series of ternary copper(II) complexes used in my research. To the crystallographers Associate Prof. Leong Weng Kee (Nanyang Technological University, Singapore) and Professor Fun H. K. (Universiti Sains Malaysia) who collected and solved the crystal structure of two of the ternary copper(II) complexes, I would also like to express my thanks.

Above all, I would like to thank my family for their unequivocal spiritual support and great patience at all times.

APPROVAL SHEET

This thesis entitled "**ANTICANCER PROPERTY, MODE OF ACTION AND SELECTIVITY OF A SERIES OF COPPER COMPLEXES**" was prepared by KONG SIEW MING and submitted as partial fulfillment of the requirements for the degree of Master of Science at Universiti Tunku Abdul Rahman.

Approved by:

_____

(Dr. NG CHEW HEE) Date:_____
Supervisor
Department of Chemical Science
Faculty of Science
Universiti Tunku Abdul Rahman

_____

(Dr. ALAN KHOO SOO BENG) Date:_____
Co-supervisor
Department of Molecular Pathology
Cancer Research Centre
Institute Medical of Research

FACULTY OF ENGINEERING AND SCIENCE
UNIVERSITI TUNKU ABDUL RAHMAN

Date: _____

SUBMISSION OF THESIS

It is hereby certified that **KONG SIEW MING** (ID No: **08UEM08134**) has completed this thesis entitled "**ANTICANCER PROPERTY, MODE OF ACTION AND SELECTIVITY OF A SERIES OF COPPER COMPLEXES**" under the supervision of Dr Ng Chew Hee (Supervisor) from the Department of Chemical Science, Faculty of Science, and Dr Alan Khoo Soo Beng (Co-Supervisor) from the Department of Molecular Pathology, Cancer Research Centre, Institute Medical of Research.

I understand that University will upload softcopy of my thesis in pdf format into UTAR Instituitional Repository, which may be made accessible to UTAR community and public.

Yours truly,

_____
(KONG SIEW MING)

DECLARATION

I KONG SIEW MING hereby declare that the thesis is based on my original work except for quotations and citations which have been duly acknowledged. I also declare that it has not been previously or concurrently submitted for any other degree at UTAR or other institutions.

Name: _____
(KONG SIEW MING)

Date :_____

TABLE OF CONTENTS

LIST OF TABLES

LIST OF FIGURES

LIST OF ABBREVIATIONS

%	Percentage
℃	Degree Celsius
μM	Micromolar
kDa	Kilodalton
g	Gram
N	Normality
L	Liter
mL	Millilitre
μL	Microlitre
mm	Millimeter
v/v	Volume/volume %
min	Minute
mg/mL	Milligrams/millilitre
ng/mL	Nanograms/millilitre
μg/mL	Micrograms/millilitre
U/mL	Units/millilitre
V	Volt
S. D.	Standard deviation
S. E. M.	Standard error of the mean
h	Hour
Fig	Figure
rpm	Revolutions per minute
APS	Ammonium persulfate

BSA	Bovine serum albumin
C-dMg	C-dimethylglycine
CO_2	Carbon dioxide
CP	Core particle
Cu	Copper
[Cu(8OHQ)$_2$]	Bis(8-hydroxyquionolinato)copper(II)
DCF	Fluorescent 2',7'-dichlorofluorescein
DCFH	Non-fluorescent 2',7'-dichlorofluorescein
DCFH-DA	2',7'-dichlorofluorescein diacetate
ddH_2O	Double distilled water
DMEM	Dulbecco's modified eagle medium
DMSO	Dimethyl sulfoxide
DNA	Deoxyribonucleic acid
DSB	Double-strand break
ECL	Enchanced chemiluminescence
EDTA	Ethylenediaminetetraacetic acid
F12	F-12 nutrient mixture
FCS	Fetal calf serum
FITC	Fluorescein isothiocyanate
Gly	Glycine
H_2O_2	Hydrogen peroxide
HCl	Hydrochloric acid
IC_{50}	Inhibitory concentration 50%
IκB-α	Inhibitory κB-α
DL-ala	DL-alanine

MTT	(3-[4,5-dimethylthiazol-2-yl]-2,5-diphenyltetrazolium bromide)
NaCl	Sodium chloride
$NaHCO_3$	Sodium bicarbonate
NaOH	Sodium hydroxide
NF-κB	Nuclear factor κB
PBS	Phosphate buffered salt
Phen	1,10-phenanthroline
PS	Phosphatidylserine
PVDF	Polyvinylidene fluoride
ROS	Reactive oxygen species
RP	Regulatory particle
RT	Room temperature
Sar	Sarcosine
SDS	Sodium dodecyl sulfate
TBST	Tris buffered saline tween-20
TEMED	Tetramethylethylenediamine
Tris-HCl	Tris(hydroxymethyl)aminomethane hydrochloride
Ub	Ubiquitin
UPP	Ubiquitin-proteasome pathway

CHAPTER 1.0

INTRODUCTION

Cancer is one of the most common causes of death worldwide. Lack of therapeutic selectivity (drug effects on cancer cells versus normal cells) and drug resistance limit the effectiveness of existing treatment options and remain the major challenge for current anticancer research (Bates, 1999; Gottesman *et al*., 2006). To date, a metal-based complex, *cis*-diamminedichloridoplatinum(II) (cisplatin) is one of the most effective chemotherapeutic drug in clinical application against several types of cancers (Abada and Howell, 2010; Boulikas and Vougiouka, 2003). In recent years, the clinical effectiveness of cisplatin has stimulated extensive investigation to find new, more effective metal-based anticancer drugs (Milacic *et al.,* 2008; Wang and Chiu, 2008). Nonetheless, side effects, acquired and intrinsic resistance of cancer cells to the drug and its high toxicity to some normal cells have been hampering its widespread use. As a result, there were efforts to develop various strategies to improve these limitations and challenges.

Daniel *et al.,* (2004) reported that the inability of many current chemotherapeutic drugs to discriminate between cancerous and normal cells lead to toxicity. Hence, it is important to discover the sensitivity and therapeutic efficacy of metal-based compounds that are capable of preserving normal tissue while still ensuring the effective killing of tumor cells. Thus, it is

useful to investigate the effect of new drugs on cancer cells and normal cells to find out any cellular biological differences. Optimizing the combination of factors such as dosage and treatment period of metal-based compounds is also necessary. This is not only to ensure their selectivity in preferentially killing cancer cells but also to reduce unintended damage to non-tumor cells and to minimize toxicity to normal or healthy tissue (Rajkumar *et al*., 2005).

Metal ion activities in biology offer a much more diverse chemistry and are important in therapeutic applications (Camakaris *et al*., 1999). Among all metals, copper (Cu) is an essential transition metal that takes part in the physiology and various biochemical functions of an organism (Harris and Gitlin, 1996) i.e. serves as a cofactor in the regulation of enzymatic reactions and is involved in redox biology (Harris, 1992). Copper, being an essential element, may be less toxic than non-essential metals such as platinum. (Wang and Guo, 2006; Gama *et al*., 2011). Copper(II) complexes of thiosemicarbazone are a family of the most promising non-platinum compounds with antitumor potential (Liberta and West, 1992; Ainscough *et al*., 1998; Jevtović *et al*., 2010). Casiopeinas® with abbreviated formulae: [Cu(N–N)(O–N)]NO_3 and [Cu(N–N)(O–O)]NO_3 were reported to exhibit high antitumor activity towards a variety of tumor cell lines (Serment-Guerrero *et al*., 2011; De Vizcaya-Ruiz *et al*., 2000). Furthermore, Guo *et al*., (2010) reported that copper(II) complex of ethyl 2-[bis(2-pyridylmethyl)amino] propionate ligand could kill tumor cells through multi-mechanisms. Copper(II) complexes described as [Cu(HL^I)(L^I)]OAc, where HL is the ligand 2,4-diiodo-6-((pyridine-2-ylmethylamino)methyl)phenol are able to induce proteasomal

inhibition and apoptosis *in vitro* (Hindo *et al*., 2009). Numerous studies on the antitumor activity of metal-based complexes suggest that copper(II) complexes are been developed as a promising candidates for anticancer therapy (Zhang *et al*., 2008a; Hernández *et al.*, 2005).

A series of ternary copper(II) complexes have been evaluated in this project. These ternary complexes can be represented as $[Cu(phen)(aa)(H_2O)]NO_3$. Phen is coordinated 1,10-phenanthroline, an N-aromatic π-acceptor ligand serving as the primary ligand. AA is a set of amino acids consisting of glycine and methylated glycine derivatives serving as secondary ligands. These secondary ligands are DL-alanine, sarcosine, glycine and C-dimethylglycine. Amino acids are building blocks of proteins and function as intermediates in metabolism and are able to form stable, planar, *bis*(aminoacidato)copper(II) complexes. Copper complexes containing certain amino acids were reported to have antitumor and artificial nuclease activities (Chaviara *et al*., 2005; Zhang and Zhou, 2008; Wang *et al*., 2010). The ligand 1,10-phenanthroline (phen) is known as a transition metal-chelator (Sun *et al*., 1997). Some ternary copper(II) complexes containing phen have been found to have anticancer property (Thati *et al*., 2007; Roy *et al*., 2010)

Bis(1,10-phenanthroline)copper(II), $[Cu(OP)_2]^{2+}$ was reported to induce cell death in human tumor cells although the exact molecular mechanism remains unclear (Tsang *et al*., 1996; Zhou *et al*., 2002). Other copper complexes were reported to have antitumor, anti-Candida, antimycobacterial and antiviral properties (Marzano *et al*., 2009; Wang and

Guo, 2006; Geraghty *et al*., 1999; Saha *et al*., 2004; Popescu *et al*., 1992). Various studies showed that some copper complexes could kill cancer cells *via* different mechanisms, as follows the induction of oxidative stress, DNA cleavage and proteasome inhibition (Valko *et al*., 2005; Cai *et al*., 2007; Zhou *et al*., 2003). Interest in the effectiveness of metal-based complexes has stimulated investigation of the *in vitro* anticancer property for the present series of ternary copper(II) complexes of 1,10-phenanthroline with amino acids and their mechanism of action. These complexes are abbreviated as $[Cu(phen)(aa)(H_2O)]NO_3$ and they have been fully characterized (Ng *et al*., 2012). The structure of the various $[Cu(phen)(aa)(H_2O)]^+$ cations have been determined by X-ray crystal structure crystallography to be square-pyramidal about the copper atom (Fig. 1.1) Electrospray Ionization Mass spectra (ESI-MS) of the methanolic solutions of these complexes show only peaks attributed to $[Cu(phen)(aa)]^+$, indicating only dissociation of coordinated water under ESI-MS conditions. Molar conductivity and UV-visible spectral data shows that the $[Cu(phen)(aa)(H_2O)]NO_3$ complexes exist as 1:1 electrolytes and are stable up to 24 h.

The primary goal of this study is aimed at finding new metal-based anticancer compounds based on copper(II). The anticancer property of this series of ternary copper complexes $[Cu(phen)(aa)(H_2O)]NO_3$ towards a breast cancer cell line MDA-MB-231 was investigated in conjunction with their harmfulness towards immortalized breast cell line MCF 10A. Moreover, targeting several molecular mechanisms could facilitate the development of new strategies for metal-based anticancer compounds. It can potentiate the

therapeutic benefits such as overcoming drug resistance and having therapeutic selectivity. To find out the anticancer property of the ternary copper(II) complexes, I tested this series of copper(II) compounds for (i) antiproliferative property by using MTT assay, (ii) apoptosis-inducing property by various methods, and (iii) ability to induce cell cycle by use of flow cytometry.

The goal of studying these ternary copper(II) complexes is to focus their selectivity properties and mode of action in human breast cell. In recent years, the development of copper(II) complexes as anticancer drugs is a very active field. It is clear that copper(II) can work by a variety of different routes although only a little understanding of the molecular basis of their mode of action has been documented. Ternary copper(II) complexes are likely to have mode of action, biodistribution and minimized side effects which are different from conventional platinum drugs and might be effective against human cancer. In principle, copper(II) complexes provide a broader spectrum of antitumor activity. The precise mode of action remains elusive and has resulted in great interest on how the ternary copper(II) complexes function which can add significantly to the current research. In the present study, proteasome inhibition, assay for reactive oxygen species and γ-H2AX assay were used to study their mode of action.

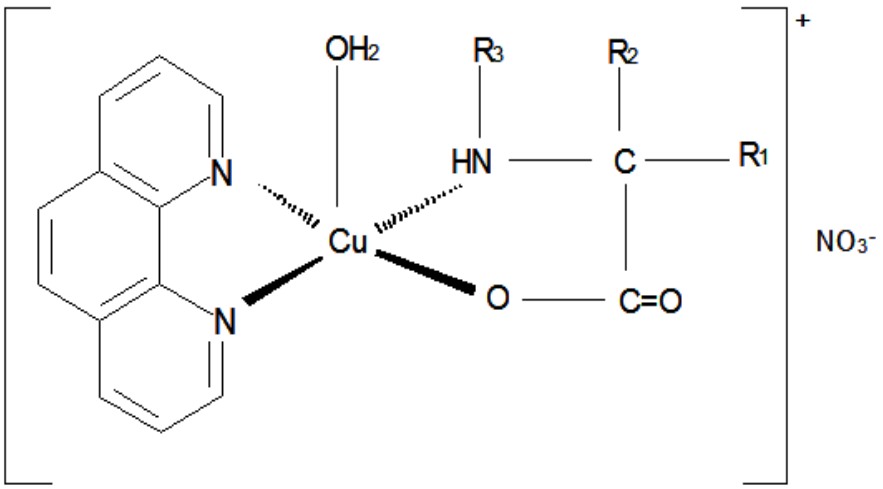

Fig. 1.1: Chemical structure of $[Cu(phen)(aa)(H_2O)]NO_3$ (gly: $R_1=R_2=R_3=H$; DL-ala: $R_1= CH_3$; $R_2=R_3=H$; C-dmg: $R_1= R_2= CH_3$, $R_3= H$; sar: $R_1=R_2=H$; $R_3= CH_3$).

Project objectives:

- To investigate antiproliferative and cellular morphological effects of ternary copper(II) complexes on MDA-MB-231 breast cancer cells and MCF 10A non-malignant breast epithelial cells.

- To investigate the mode of action for ternary copper(II) complexes: use of proteasome inhibition as well as reactive oxygen species and γ-H2AX assays.

- To determine the *in vitro* selectivity of ternary copper(II) complexes towards apoptosis.

CHAPTER 2.0

LITERATURE REVIEW

2.1 Breast cancer

Breast cancer continues to be the most common malignancy and remains the biggest threat for Malaysian women, as well as women in most parts of the world (Hisham and Yip, 2004). It is the number one leading cause of cancer deaths among women in Malaysia, according to the National Cancer Council (MAKNA). Breast cancer mortality is declining in certain countries such as United States, Canada and United Kingdom (Mettlin, 1999). Statistics from Breastcancer.org revealed that breast cancer incidence rate in the U.S decreased by about 2 % per year from 1999 to 2006. This decrease is possibly due to increased utilization of mammographic screening, reduced utilization of hormone replacement therapy (HRT) (Ries *et al.*, 2007), early detection of disease and availability of improved therapies.

In contrast to the West, according to Breast Health Info Centre in Radiology Malaysia, the incidence of breast cancer and death rate is on the rise in most Asian countries including Malaysia. According to Ferlay *et al.* (2002), this malignancy is diagnosed in 1,150,000 cases worldwide and caused 410,000 deaths in 2002. According to National Cancer Registry Report 2003-2005, a total of 67,792 new cases were diagnosed among 29,596 males and

38,196 females and the Age Standardised Rate (ASR) of female breast cancer is 47.4 per 100,000 population. In Malaysia, there is no complete and latest statistics report for breast cancer.

Malaysian women have approximately 1 in 20 (5%) chance of developing breast cancer over the course of their lifetime (Yip *et al.*, 2006; Leong *et al*., 2007). The risk factors of breast cancer include mode of presentation, environmental exposure, lifestyle, early menarche, nulliparity or late pregnancy, menopause status, prolonged oral contraceptive use and HRT (Silverman *et al*., 2011; Narod, 2010). In Malaysia, the main risk factors for developing breast cancer are positive family history, race with higher risk in Chinese, female gender and advancing age with the prevalent age group being 40-49 years (Hisham and Yip, 2004; Yip *et al*., 2008). Therefore, it is crucial to understand the etiology and pathogenesis of breast cancer among Asian women to discover its cures or treatment.

In the case of cancer, a chemotherapeutic agent is one that kills the rapidly dividing cells, thus slowing and stopping the cancer from spreading. According to MedicineWorld.Org, the commonly used chemotherapy drugs are doxorubicin, cyclophosphamide, methotrexate, paclitaxel, fluorouracil, epirubicin, docetaxel, vinorelbine, gemcitabine, capecitabine and carboplatin. The most frequent side effects were fatigue, nausea, vomiting and death of healthy cells (Williams and Schreier, 2004). Nasal septum perforation occurred at time of bevacizumab treated patient with metastatic breast cancer (Traina *et al*., 2006; Mailliez *et al*., 2010). In the case of cancer, a

chemotherapeutic agent is one that kills the rapidly dividing cells, thus slowing and stopping the cancer from spreading. According to MedicineWorld.Org, the commonly used chemotherapy drugs are doxorubicin, cyclophosphamide, methotrexate, paclitaxel, fluorouracil, epirubicin, docetaxel, vinorelbine, gemcitabine, capecitabine and carboplatin. The most frequent side effects of these drugs were fatigue, nausea, vomiting and death of healthy cells (Williams and Schreier, 2004). Nasal septum perforation was found to occur in using bevacizumab to treat patients with metastatic breast cancer (Traina *et al*., 2006; Mailliez *et al*., 2010). Other organic compounds, for example paclitaxel and docetaxel, were also found to have several major side effects, such as hypersensitivity reactions and neuropathies, and also impaired tumor penetration (Sparreboom *et al*., 1999; Vishnu and Roy, 2011). Besides numerous toxic side effects, many current organic anticancer compounds encounter cell resistance. These drawbacks have stimulated an extensive search for new organic and inorganic complexes with improved pharmacological properties. In addition, this has spurred scientists to employ different strategies in the development of metal-based anticancer agents with different metals and different targets.

The application of modern medicinal inorganic chemistry is a field of increasing prominence as metal-based compounds offer possibilities for the design of therapeutic agents not readily available to organic compounds. Although medicinal chemistry was almost exclusively based on organic compounds and natural products during the past three decades, investigation into metal complexes as chemotherapeutic drugs have gained growing interest

(Zhang and Lippard, 2003). Metal complexes, with a wide range of coordination numbers and geometries, accessible redox states, thermodynamic and kinetic characteristics, and the intrinsic properties of the cationic metal ion and ligand itself, offer the medicinal chemist a wide spectrum of reactivities that can be exploited (Bruijnincx and Sadler; 2008).

Metal ions and metal coordination compounds are known to affect cellular processes in a dramatic way. Although cisplatin is widely used in the successful treatment of various cancers, it has significant side effects and drug resistance which limited its clinical application. This has prompted investigation into other metal complexes for possible use as anticancer agents. Among these metal complexes, numerous complexes containing copper were found to be highly effective at killing cancer cells (Jevtović *et al.*, 2010). The functions of copper in biology have probably stimulated the development of new metallodrugs other than platinum drugs. Investigations into copper-based compounds, as alternatives to platinum-based anticancer compounds, to explore new mode of action and to obtain lower toxicity have been recently reviewed (Marzano *et al.*, 2009). Many copper complexes were found to be effective against several cancer cell lines (Tisato *et al.*, 2010).

2.2 Cell lines

Breast cell lines have been used extensively to test for cell proliferation, cell cycle progression and apoptosis (Gelbke *et al.*, 2004; Li *et al.*, 2008;

Raobaikady *et al*., 2005). The highly invasive human breast cancer cells MDA-MB-231 do not express steroid receptors (Horwitz *et al*., 1978) and estrogen receptor alpha (ERα) was not detectable (Aubé *et al*., 2011). MDA-MB-231 cells expressed higher mRNA and protein levels of protease-activated receptor (PAR)-1. This expression has been associated with tumor invasion and progression (Naldini *et al*., 2009). The etiology of breast cancer is associated with inflammatory processes. Naldini *et al*. (2010) have shown that interleukin (IL)-1β treatment resulted in accumulation of hypoxia-inducible factor (HIF)-1α, which is connected with the migratory capabilities of MDA-MB-231 breast cancer cells. Fibronectin adhesion led to Akt phosphorylation in highly metastatic MDA-MB-231 cells but not in non-metastatic cancer cells and suggests combination of conventional chemotherapeutic drugs with new drug enhancing sensitivity in breast cancer by targeting the PI-3K/Akt2 pathway (Xing *et al*., 2008).

MCF10A human mammary non-tumorigenic epithelial cells are frequently used as a normal control in breast cancer studies (Hsieh *et al*., 2005; Shun *et al*., 2004). These cells were derived from the mammary gland of a fibrocystic disease patient and have normal epithelial cell morphology (ATCC). They represent an important tool to characterize the biological properties of oncogenes due to their tight control and reversible expression of any transgene (Herr *et al*., 2011). MCF-10A cells are characterized as ERα-negative and null for the p16/p15 genes (Cowell *et al*., 2005). Genomic profiling shown that MCF10A cells correlate with the normal-like phenotype, but also to the basal-like and ERBB2+ subtypes (Miller *et al*., 2007; Jönsson

et al., 2007). All of these characteristics make MCF-10A cells widely use as a model of choice for breast tumor progression studies.

2.3 Copper

The transition metal copper (Cu) is an essential trace element found in stable oxidized [Cu(II)] and unstable reduced [Cu(I)] states and is involved in the biochemistry and physiology of all organism (Olivares and Uauy, 1996; De Romaña *et al*., 2011; Ding *et al*., 2011). Copper serves as a co-factor in redox reactions for metalloenzymes which is required for normal growth and development. Some enzymes which need copper are cytochrome c oxidase, Cu/Zn superoxide dismustase, ceruloplasmin, tyrosinease, peptidylglycine alpha-amidating mono-oxygenase and lysyl oxidase (Balamurugan and Schaffner, 2006; Ding *et al.*, 2011; Linder, 2001; Messerschmidt, 2010). Copper deficiency, overload or genetic predisposition cause certain diseases such as Alzheimer's disease, Menkes syndrome, Wilson disease, Indian childhood cirrhosis, aceruloplasminemia, Endemic Tyrolean infantile cirrhosis and idiopathic copper toxicosis (De Romaña *et al*., 2011; Tapiero *et al*., 2003; Balamurugan and Schaffner, 2006; Puig and Thiele, 2002; La Fontaine and Mercer, 2007**).**

Copper can be highly toxic to living systems due to its redox chemistry, which generates reactive oxygen species that can damage DNA, proteins and other cellular components *via* Fenton-like reactions (Bertini *et al*., 2010; Chen

and Dou, 2008). Therefore, copper homeostasis mechanisms in human are tightly regulated by different systems for its uptake, distribution, sequestration and elimination to ensure proper biological functions (Bertinato and L'Abbé, 2004).

Copper is necessary to stimulate proliferation and migration of human endothelial cells and enhance angiogenesis, which is the growth of new blood vessels (Gérard *et al*., 2010). It is required for the angiogenic process and it activates proangiogenic factors for tumor growth, invasion and metastasis (Nasulewicz *et al*., 2004). In normal tissues, angiogenesis is most commonly associated with wound healing, rheumatoid arthritis, psoriasis, retinitis or the menstrual cycles (Khanna *et al*., 2002; Moehler *et al*., 2003). However, significantly elevated serum and tumor copper concentration was found in cancerous tissues rather than normal tissues including breast, prostate, colon, lung and brain and leukemia (Zhai *et al*., 2010). Due to this cancer-associated copper elevation, in recent years, the interest in copper-targeting agents as more selective anticancer therapeutics have been developed by eliminating the copper in serum of human body (Daniel *et al*., 2005; Chen *et al*., 2009).

2.4 Copper(II) complexes

Copper(II) complexes of phen and its derivatives have previously been shown to exhibit numerous biological activities, such as antitumor, antimicrobial and antifungal (Katsarou *et al*., 2008; Rajendiran *et al*., 2007;

Marzano *et al*., 2009). The activity of copper(II) complexes as anticancer agents has been reviewed (Marzano *et al*., 2009; Collins *et al.*, 2000; Malon *et al*., 2001). Numerous studies showed that $[Cu(phen)_2]^{2+}$ induces apoptosis by attacking DNA (Tsang *et al*., 1996; Verhaegh *et al*., 1997; Zhou *et al*., 2003). Additionally, the copper(II) complex of 1,10-phenanthroline had been reported to exhibit nuclease activity in the presence of reducing agents and molecular oxygen (Lu *et al*., 2003).

Copper(II) complexes are regarded as the most promising alternatives to cisplatin as anticancer drugs (Reddy *et al*., 2011). An organic copper complexes dichlorido(1,10-phenanthroline)copper(II) effectively induced ubiquitinated protein accumulation and apoptosis in tumor cells (Daniel *et al*., 2004). Besides that, Zhang and co-worker (2008b) reported that a synthetic taurine Schiff base copper complex could suppress tumor cell growth and induce apoptosis via proteasome inhibition. However, the copper complex of tetrathiomolybdate (TM), an anti-copper drug and a potent copper chelator, was found to be unable to inhibit proteasomal activity (Daniel *et al.*, 2005). Therefore, it suggests that not all copper-binding compounds have proteasome-inhibitory and apoptosis inducing capability. However, the reason for cancer cells being more susceptible to attack by metal-binding compounds compared to non-malignant cells has not been fully elucidated (Zheng *et al*., 2010).

Copper(II) acts as a highly selective receptor in the 8-hydroxyquinoline containing tetraazacrown ethers, compared to Zn^{2+}, Cd^{2+},

Co^{2+}, Ni^{2+} and Pb^{2+} (Lee *et al*., 2001). Bis(8-hydroxyquionolinato)copper(II), [Cu(8OHQ)$_2$] inhibited proliferation in cultured human breast cancer cells, possessed apoptosis-inducing activities and proteasome-inhibitory activities (Zhai *et al*., 2010). Clioquinol (CQ), an analog of 8-hydroxyquinoline, is capable of forming a stable complex with copper, has been reported to possess antitumor effects and currently it is used in clinics for treatment of Alzheimer's disease (Chen *et al*., 2007). A series of organic-copper compounds and [Cu(8OHQ)$_2$] have been found to have antiproliferative activity and inhibit the chymotrypsin-like activity of the proteasome in human leukemia cancer cell line (Daniel *et al*., 2004). However, its precise mode of action is still unknown.

[Cu(phen)(Gly)(H_2O)]Cl·3H_2O had been prepared from the reactions of $CuCl_2$·2H_2O with amino acid and phen. Li *et al*. (2011) reported that the molar conductivity value in methanol indicates the ternary copper(II) complex is a 1:1 electrolytic. X-ray crystallography was used to determine the structure of this ternary copper(II) complexes. The geometry about the copper(II) ion is a distorted square pyramid (Liao *et al*., 2006). Chikira *et al*. (2002) showed the [Cu(phen)(aa)(H_2O)]$^+$ complexes dissociate partly into the amino acid and [Cu(phen)]$^{2+}$ on the DNA. Another ternary copper(II) complex, [Cu(L-ala)(phen)(H_2O)]NO_3, has been synthesized previously (Chetena *et al*., 2009). Ternary copper(II) complex, [Cu(phen)$_2$(mal)]·2H_2O (malH_2 = malonic acid) could induce a concentration-dependent cytotoxic effect and inhibited DNA synthesis (Deegan *et al*., 2007).

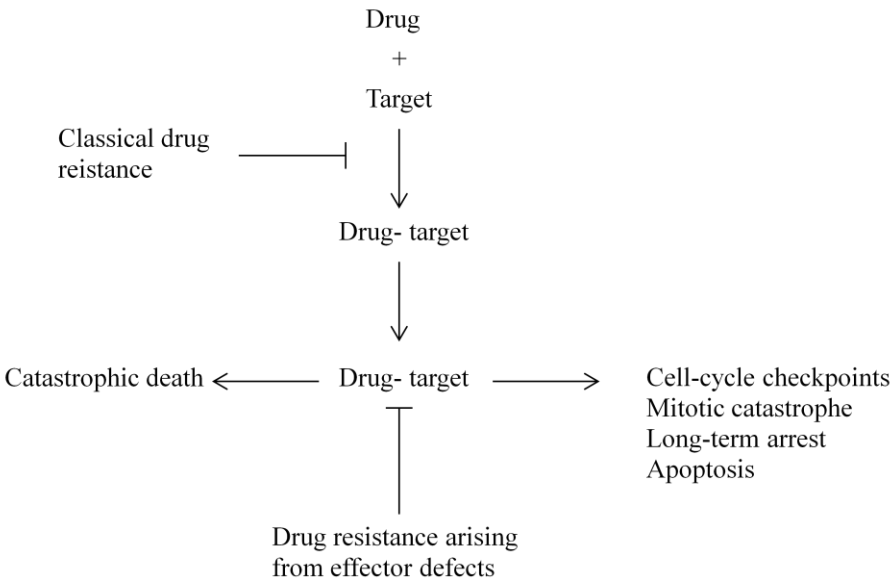

Fig. 2.1: Mechanisms of drug action. Redrawn from Johnstone *et al*., 2002.

2.5 Cisplatin

Cisplatin is one of the most potent antitumor agents known and widely used for the treatment of solid tumors. The dosage and efficacy of cisplatin are limited by its side effects which include nephrotoxicity, emetogenesis and neurotoxicity (Pabla and Dong, 2008). Cisplatin exerts cytotoxic effect by forming an intrastrand crosslink on DNA (Jamieson and Lippard, 1999). DNA damage-mediated apoptotic signals, however, can be attenuated and the resistance mechanisms include reduced drug uptake, increased drug inactivation and increased DNA adduct repair. This resistance is a major limitation of cisplatin-based chemotherapy (Siddik, 2003). In addition, the other limitation of cisplatin is poor oral bioavailability which may result in low cytotoxicity (Kelland, 2000). Human breast cancer cells such as MCF-7 are relatively resistant to cisplatin treatment compared to other breast cancer

cell lines (Yde *et al*., 2007; Yde and Issinger, 2006). Hence, the use of MCF-7 cell line seems appropriate. As a result of the problems encountered by cisplatin, improving the efficacy and reducing toxic side effects of metal-based drugs is a major challenge faced by current anticancer research.

2.6 Apoptosis and DNA cell cycle

Three processes, *viz.* apoptosis, autophagy and necrosis, serve to trigger cell death. Apoptosis (programmed cell death) is critical in pathological conditions to allow cell to commit suicide through the activation of specific signaling pathways (Fig. 2.2) and cellular self-destruction for the prevention of oncogenic transformation (Jacobson and Raff, 1997). Defects in apoptotic cell death regulation contribute to many diseases including tumor initiation, progression and metastases (Johnstone *et al*., 2002). Apoptosis is generally characterized by several distinct morphological characteristics and energy-dependent biochemical mechanisms including cell shrinkage, plasma membrane blebbing, DNA fragmentation, loss of the mitochondrial membrane potential and cellular condensation into apoptotic bodies that are removed by phagocytes (McConkey, 1998; Reed, 2000).

It is well documented that the key of killing mechanism for most anticancer therapies, *viz.* chemotherapy, γ-irradiation, immunotherapy and cytokines is induction of apoptosis in cancer cells (Lowe and Lin, 2000). There are two primary modes of apoptosis: the extrinsic (stimulation of cell

surface death receptors) and intrinsic (perturbation of mitochondria) pathways (Ashkenazi and Dixit, 1998; Green and Reed, 1998). The extrinsic pathway is mediated by death receptors of the Tumor Necrosis Factor Receptors (TNFR) superfamily. The intrinsic pathway is triggered by a variety of stimuli including disruption of cellular homeostasis and is initiated intracellularly.

In metal-induced apoptosis, the mitochondria play a crucial role in mediating apoptosis, putatively *via* metal-induced reactive oxygen species (Debatin *et al*., 2002; Chen *et al*., 2001). A series of cadmium(II) and nickel(II) complexes with 2-formylpyridine selenosemicarbazone possess ability to induce apoptosis *via* activation of mitochondrial pathway (Srdić-Rajić *et al*., 2011).

Cell move through four distinct phases of the cell cycle: G_1 phase, S phase (synthesis), G_2 phase and M phase (mitosis). The cell cycle stops at several checkpoints (G_1/S, G_2/M, and G_0/G_1) to maintain homeostasis. Dinnen and Ebisuzaki (1992) reported that anticancer drugs with various modes of action are known to block the cell cycle. Anticancer drugs exert their cytotoxicity effect by interfering with cell cycle or acting on apoptosis-related targets (Lévi, 2001).

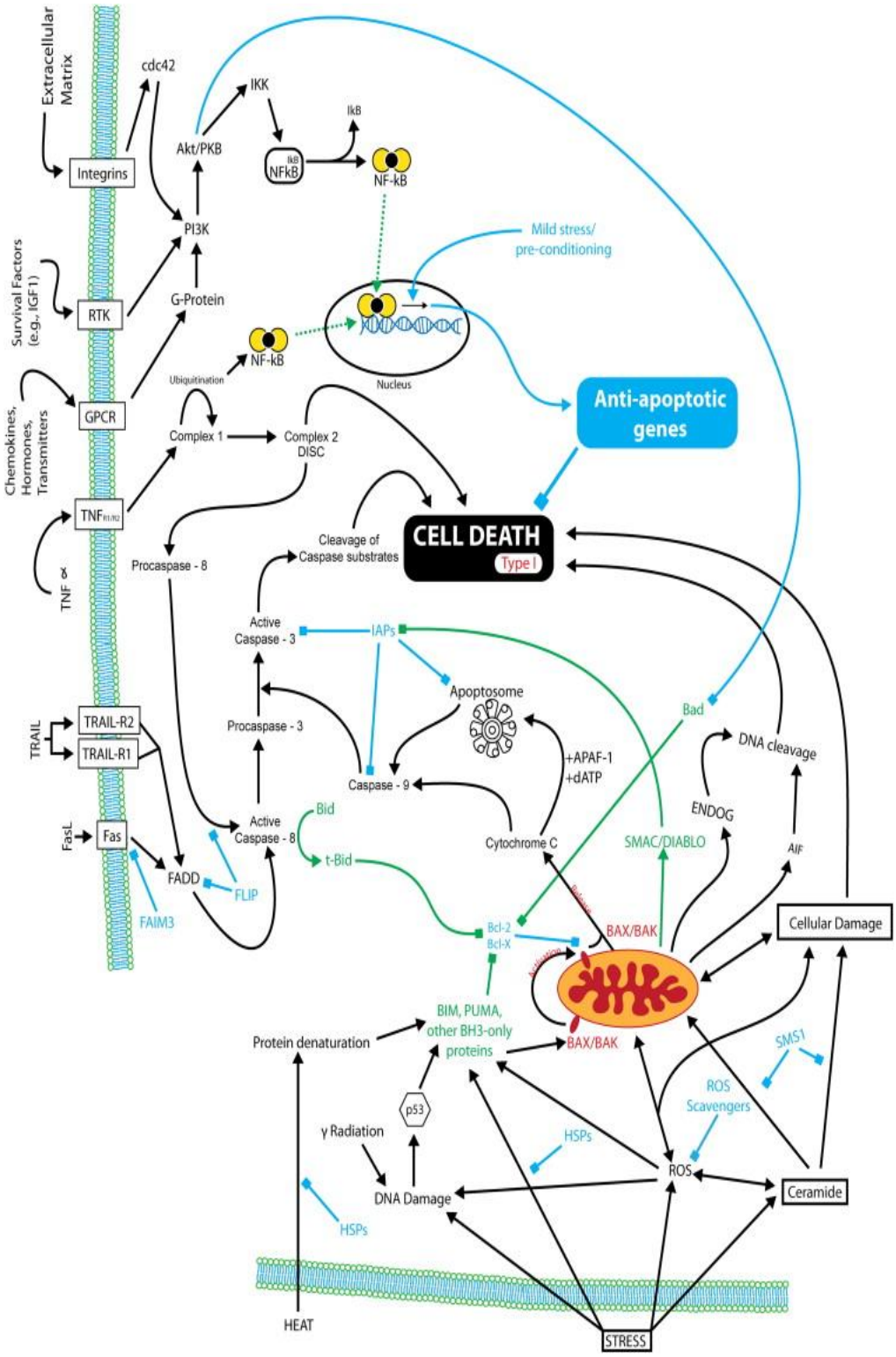

Fig. 2.2: Schematic representation of the cellular pathways of apoptosis. Taken from Portt *et al*., 2011.

2.7 Proteasome

The proteasome is one of the most fascinating and important topics currently addressed in either cellular or pharmacological sciences. Proteasome is a protein-destroying apparatus and is closely implicated in regulation of cell cycle, signal transduction pathway, protection of tumor cells against apoptosis, antigen processing for appropriate immune response, inflammatory responses, protection from oxidative stress relevant to neurodegenerative diseases, aging, HIV-transcription regulation, transcriptional activation and circadian rhythm control (Cvek and Dvorak, 2008; Naujokat, *et al*, 2006; Dou and Li, 1999; Kloetzel, 2004; Visekruna *et al*, 2006; Yamamoto *et al*., 2007; Dreiseitel *et al*., 2008). Inhibition of proteasome by interfering with degradation of some specific cellular proteins is involved in determining whether a cell proliferates or dies. Therefore proteasome has become a target for anticancer therapy.

The 26S proteasome is a 2.4 MDa large multisubunit, multifunctional ATP- and ubiquitin-dependent proteolytic complex which is localized in the cytosol, nucleus, endoplasmic reticulum and lysosomes of eukaryotic cells (Fenteany and Schreiber, 1996). The most common form of proteasome is composed of a proteolytic core particle (CP), referred to as the 20S proteasome (approximately 720 kDa) and 19S regulatory particle (RP) (approximately 890 kDa), also termed PA700 which bind on both ends of the 20S proteasome (Adams, 2003) (Fig. 2.3).

The RP contains two subcomplexes, the lid and the base which is capable of binding the polyubiquitin chain, cleaving and unfolding it from protein substrate prior to entry and controlling the access of substrates into the CP (Kisselev and Goldberg, 2001; Shibatani *et al*., 2006). The CP is a broad-spectrum, ATP-, Ub-independent protease, which contains multiple peptidase activities and functions as a catalytic machine. CP consists of 28 subunits, 14-α and 14-β, arranged in four heptameric, tightly stacked rings containing α7, β7, β7, α7 (Groll *et al*., 1999; Kurepa and Smalle, 2008; Lee and Glodberg, 1998; Grover *et al*., 2010). β-subunits conferring the unique and distinguishing proteasome feature have multiple peptidase activities with three primary distinct proteolytic activities, *viz.* chymotrypsin-like (cleavage after hydrophobic amino acids, mediated by the β5 subunits), trypsin-like (cleavage after basic residues, mediated by the β2 subunits), caspase-like or peptidylglutamyl peptide hydrolyzing-like, (PGPH)-like (cleavage after acidic residues, mediated by the β1 subunits) (Cvek and Dvorak , 2008). It has been reported that all three main types of activities contributed significantly to protein breakdown and their relative importance varied widely with the substrate (Naujokat *et al*., 2007).

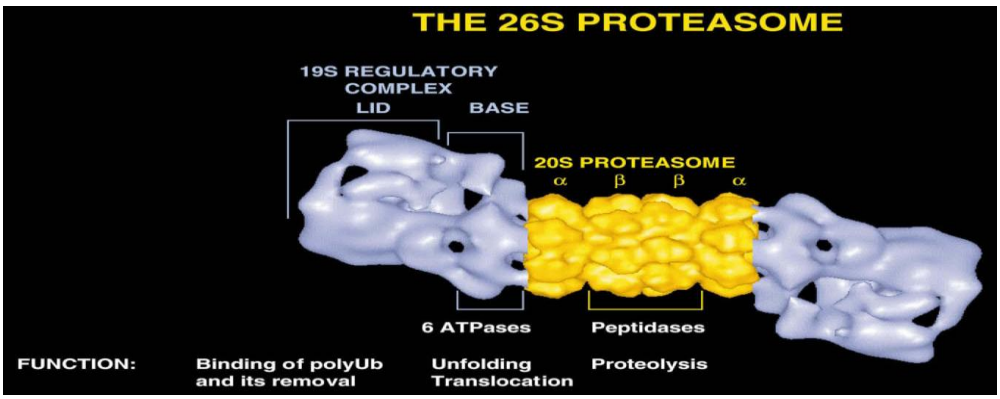

Fig. 2.3: Electron tomography image of the 26S proteasome and its components. Taken from Kisseleve and Goldberg, 2001.

2.7.1 Ubiquitin-proteasome pathway and proteasome inhibitors in cancer therapy

The Ubiquitin-proteasome pathway (UPP) is an ATP-dependent pathway and act as a major proteolytic system in the cytosol and nucleus of eukaryotic cells (Adams, 2002b). UPP plays a vital role in maintaining normal cellular homeostasis (Cvek and Dvorak, 2008), modulate many physiological processes and catalyzes the degradation of the majority of abnormal proteins that resulted from oxidative damage or mutation. It is involved in coordination and temporal degradation of short-lived and long-lived proteins as depicted in Table 2.1 (Chen and Dou, 2008; Zhai *et al*., 2010; Driscoll *et al*., 2011; Naujokat *et al*., 2007).

Currently targeting UPP in cancer therapy is a key to develop proteasome inhibitors as novel anticancer drugs. Inhibition of UPP can result in accumulation of tumor suppressor, pro-apoptotic proteins and lead to increase in sensitivity of cancer cells toward apoptosis (Ciechanover, 1998; Adams, 2004).

This proteolytic system involves two successive steps: ubiquitination of target protein and degradation of the tagged protein (Daniel *et al*., 2005). Ubiquitination is the first step in the UPP where the target protein is covalently ligated by C-terminal glycine residues of multiple 76-amino-acid-long peptide ubiquitin (Ub), a small 8 kDa protein (Rajkumar *et al*., 2005). This ubiquitination is carried out by a multi-enzymatic system consisting of

Ub-activating (E1), Ub-conjugating (E2) and Ub-ligating (E3) enzymes in sequential manner which ultimately results in the specific proteins being selectively recognized by the proteasome complex from other proteins for degradation (Dou and Li, 1999).

The second step is degradation of identified proteins by the 26S proteasome. Ubiquitin-tagged proteins (at least four ubiquitins on sequential lys48 residues) are recognized by the 19S RP for degradation and the ubiquitin is released and recycled (Jensen *et al.*; 1995; Almond and Cohen, 2002). Multiple proteolytic sites on the β-subunits hydrolyze proteins without releasing polypeptide intermediates but cleave the polypeptides into smaller peptides which range from 3 to 22 amino acids in length with a median size of six residues (Kisselev *et al*., 1999; Rajkumar *et al*., 2005) that are further hydrolyzed to amino acids by other peptidases.

This UPP has been validated as a novel target for anticancer therapy with the success of bortezomib as a proteasome inhibitor to treat patient with relapsed and refractory multiple myeloma (Mateos and San Miguel, 2007). It is of particular interest to develop other UPS-directed drugs that have greater efficacy to overcome drug resistance and lesser side effects. Almond and Cohen (2002) concluded the mechanism of proteasome inhibitor-induced apoptosis are through increased p53 activity, accumulation of the growth inhibitory molecules (p27, p21), accumulation of pro-apoptotic Bcl-2 family proteins, activation of the stress-activated protein kinases (SPAK) and overcoming the anti-apoptotic effects of NF-κB (nuclear factor κB) (Table

2.1). Preclinical studies have shown that proteasome inhibitors are able to induce cell death rapidly and selectively in malignant, proliferating and transformed cells, including those resistant to conventional chemotherapeutic agents, compared to normal or untransformed cells.

Table 2.1: Physiological functions and selected substrates of ubiquitin-proteasome pathway. Source: (Kisselev and Goldberg, 2001); (Adams, 2002a); (Adam, 2003); (Lee and Goldberg, 1998).

Function	**Substrate**
Apoptosis	Bcl-2, cIAP, XIAP, bax
Cell cycle progression	$p27^{Kip1}$, p21, cyclins A,B,D,E
CDK1/cyclin B phosphatase	cdc25 phosphatase
Inflammation	IκB, p105 precursor of NF-κB
Long-term memory	Protein kinase A (regulatory subunit)
Regulation of metabolic pathways	Ornithine decarboxylase, HMG-CoA reductase
Relieves DNA supercoiling	Topoisomerase I, Topoisomerase IIα
Regulation of cyclin activity	Cyclin-dependent kinase (CDK) inhibitors, p21 CIP/WAF1
Immune surveillance	Most cytosolic and nuclear proteins
Protein quality control	CFTRΔF508, α_1-antitrypsin (Z-variant), aged calmodulin
Photomorphogenesis in plants	Hy5
Oncogenesis	p53, $p27^{Kip1}$, bax, IκB
Regulation of gene expression	c-Jun, E2F1, IκB, β-catenin

Kazi *et al*. (2003) reported genistein-mediated proteasome inhibition and selective apoptosis in SV40-transformed derivative (VA-13) but not in human fibroblast cell line WI-38. Anthocyanins and anthocyanidins also possess proteasome inhibition activity (Dreiseitel *et al*., 2008; Bazzaro *et al*., 2006) and the tested ovarian carcinoma cell lines exhibited greater sensitivity to apoptosis in response to proteasome inhibitors than in immortalized ovarian surface epithelial cells. L-glutamine schiff base copper complexes and pyrrolidine dithiocarbamate-metal complexes could inhibit proteasome activity and induce cell death selectively in MDA-MB-231 breast cancer cells

but not normal, immortalized breast cells (Xiao *et al*., 2008; Milacic *et al*., 2008).

2.8 Reactive oxygen species

Reactive oxygen species (ROS) are continuously produced in eukaryotic cells by a variety of pathways in aerobic metabolism and are in balance with antioxidants (Xia *et al*., 2007; Curtin *et al*., 2002). ROS are derived from metabolism involving molecular oxygen. They exist in radical and non-radical structures, *viz.* superoxide anion (O_2^-), hydrogen peroxide (H_2O_2), hydroxyl radical (OH), hypochlorous acid (HOCl), nitric oxide (NO), peroxyl radical (ROO ·), singlet oxygen ($^1O_2$), with their half-lives generally ranging in seconds or minutes (Curtin *et al*., 2002; Simon *et al*., 2000; Han *et al*., 2008).

ROS are regulated by redox reactions and they act as second messengers in metabolic and other signal-transduction pathways, such as mitogen-activated protein kinases (MAPK), protein phosphatases and transcription factors (Renschler, 2004; Gupte and Mumper, 2007). Excess ROS generation or down regulation of ROS scavengers and antioxidant enzymes, or both are well known to be cytotoxic and these can lead to human diseases, including cancer, degenerative diseases, and other pathological conditions (Waris and Ahsan, 2006; Kamat and Devasagayam, 2000).

Endogenous systems that generate ROS include the NADPH oxidase complex, cytochrome P450, lipoxygenase, mitochondria, cycloxygenase, xanthine oxidase and peroxisomes (Galanis *et al*., 2008). ROS generation through nonenzymatic glycosylation reaction, membrane-bound NADPH oxidase and mitochondrial electron transport chain where the electrons escaping from their transport complexes, react with oxygen to form O_2^- (Lu *et al*., 2007; Kaneto *et al*., 2010). As most ROS have short half-life and have limited diffusion distance, they cause damage near the sites of production. Cellular redox balance is regulated through antioxidant defense systems that consist of primary defense (superoxide dismutase, catalase, glutathione peroxidase, heme peroxidase) and secondary defense termed as free-radical scavengers (α-tocopherol, ascorbate, reduced glutathione (GSH), thioredoxin, cytochrome c, coenzyme Q) (Hervouet *et al*., 2007; Bandyopadhyay *et al*., 1999).

ROS at low or medium level are important components of normal cell signaling to mediate cell growth, migration, differentiation and gene expression (Ushio-Fukai and Nakamura, 2008; Ruiz-Ramos *et al*., 2009). However, high amounts of ROS, antioxidants depletion, or both are known to cause tissue damage, apoptosis or necrosis by reacting with sulphydrl groups in proteins, nucleotides in DNA and lipids peroxidation in membranes leading to damage of cell structure and function (Xu *et al*., 2010). Oxidative damage induce DNA sequence changes in the form of mutations, deletions, gene amplification and rearrangements which results in the initiation of apoptosis signalling leading to cell death, or to the initiation and progression of

multistage carcinogenesis (Matés and Sánchez-Jiménez, 2000; Waris and Ahsan, 2006). Excessive ROS leading to oxidative damage disrupt mitochondrial membrane potential and impair the membrane integrity, result in release of apoptogenic molecules such as cytochrome c and activate downstream caspases leading to apoptosis (Chen *et al*., 2008b; Van Remmen and Richardson, 2001; Dhanasekaran *et al*., 2005; Han *et al*., 2008).

Experiments conducted by Cai *et al*. (2007) reported that liver carcinoma Bel-7402 treated with $[Cu(phen)_2]^{2+}$ caused over production of ROS and decreased GSH/GSSG ratio, which led to oxidative DNA damage and subsequent apoptosis. Studies of Gupte and Mumper (2007) demonstrated that D-penicillamine (a copper-chelating agent) had effectively generated ROS in the tumor tissue due to significantly elevated copper level. Furthermore, Chen *et al*. (2009) reported HeLa cells treated with clioquinol dramatically stimulated production of ROS in the presence of copper ion and eventually executed programmed cell death. Numerous studies found that exposure of cancer cells to different compounds resulted in significant increase of ROS which led to apoptosis (Lu *et al*., 2006; Yang *et al*., 2006; Renschler, 2004). Significantly increased copper level in breast cancer was also found to lead to increase oxidative stress in patient (Huang *et al*., 1999).

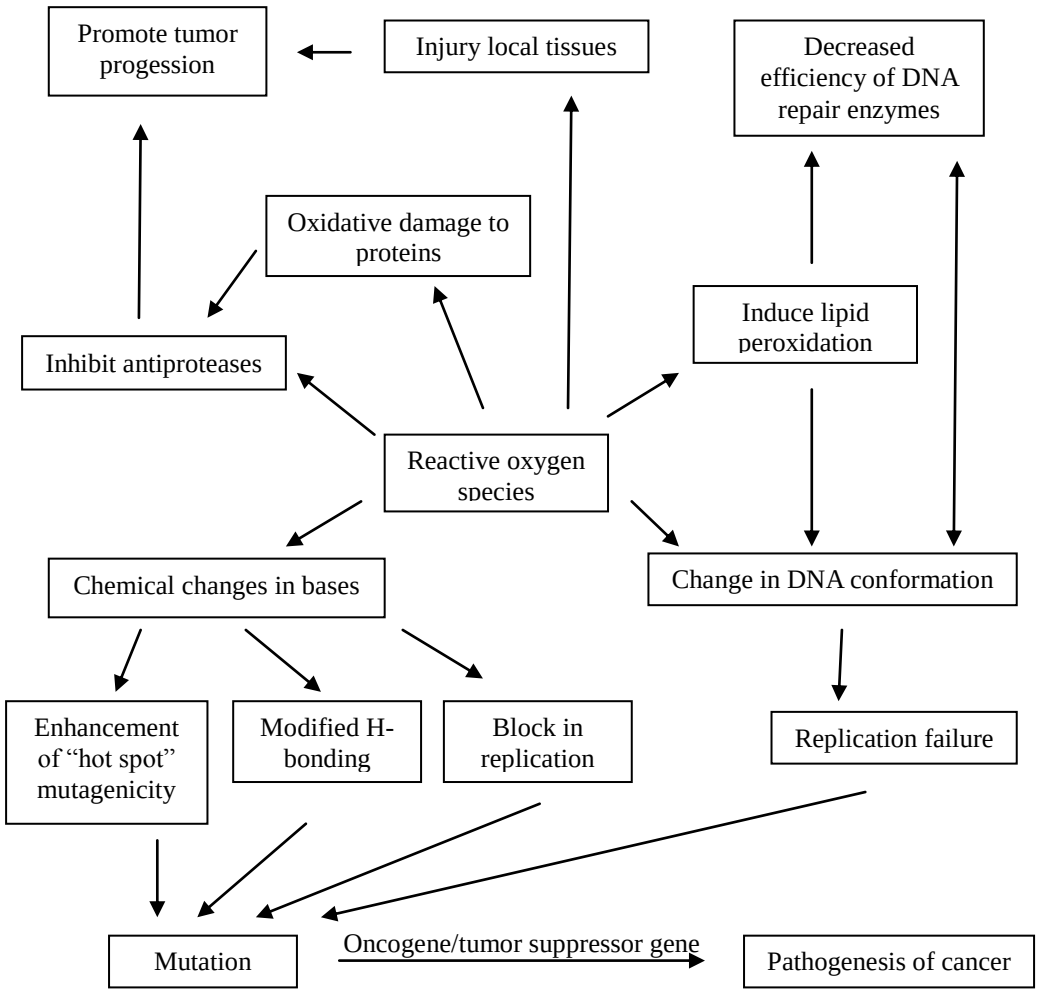

Fig. 2.4: Response of overproduction of ROS. Redrawn from Matés and Sánchez-Jiménez, 2000.

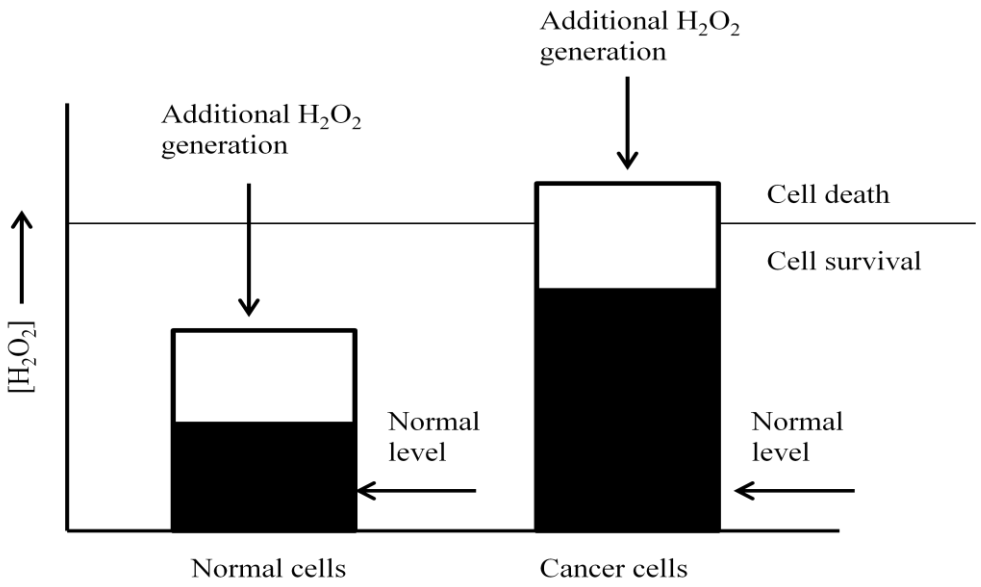

Fig. 2.5: Mechanism of ROS-based anticancer therapies. Redrawn from López-Lázaro, 2007.

2.9 Histone H2AX phosphorylation and DNA damage

The nucleosome forms the basic building block of chromatin which is a histone-DNA complex. Histones are a family of small, positively charged proteins. The nucleosome core particle is composed of 145 base pairs of DNA wrapped around a histone core, assembled in two H2A/H2B dimmers and one H3/H4 heterotetramer). The H2A histone family contained three members, *viz.* H2A1-H2A2, H2AZ, and H2AX (Rogakou *et al.*, 1998). The isoform H2AX levels in the cell line or tissue represent 2-25% of the mammalian histone pool (Fernandez-Capetillo *et al*., 2004; Sluss and Davis, 2006).

Histones play a central role in transcription regulation, DNA repair, DNA replication and chromosomal stability. H2AX is a core histone H2A variant that becomes rapidly phosphorylated at C-terminal serine^{139} (known as γ-H2AX) within 1-3 minutes in the chromatin. The phosphorylated form of H2AX, also called γ-H2AX, is necessary to facilitate the recruitment of other factors surrounding the sites of each nascent DNA double-strand break (DSB) and further forms discrete foci at break sites (Celeste *et al*., 2003, Paull *et al*., 2000). Interestingly, this modification (γ-H2AX) has been employed as a sensitive and reliable molecular marker for monitoring of genome damage and repair in terminally differentiated cells (Gavrilov *et al*., 2006). One of the hall marks of the terminal stages of apoptosis is concurrent chromosomal DNA cleavage into oligonucleosomal pieces (Mukherjee *et al*., 2006)**.** Phosphorylated H2AX is in response to arrest of cell cycle progression, relocalization of DNA repair factors and triggers cells to undergo apoptosis.

Therefore, these are linked to counteract mutagenesis or oncogenic transformation (Hanasoge and Ljungman, 2007; Paull *et al*., 2000).

Several factors, either exogenous or endogenous, are known to be involved in DSB induction that result in molecular lesion responsible for genomic instability, chromosome aberrations, cell killing, mutation and lead to the induction of DNA damage-signaling cascade (Hanasoge and Ljungman, 2007; Kato *et al*., 2007). Rebbaa *et al*., (2006) demonstrated that drug-induced DSBs often correlated with apoptosis and not cell proliferation arrest. Moreover, formation of γ-H2AX appears during apoptosis concurrently with endonuclease-mediated DNA fragmentation downstream from caspase activation (Rogakou *et al.*, 2000).

An approach to treat cancer is to induce DSBs because DSBs are the most deleterious DNA lesions, more difficult to repair compared to base damage or single-strand DNA breaks (SSBs) and more toxic in tumor cells (Ismail *et al*., 2007). DSBs can arise by exposure to ionizing radiation, ultraviolet light (UV) irradiation or by many chemotherapeutic agents. DSBs are repaired by two major pathways, homologous recombination (HR) and non-homologous end joining (NHEJ) (Mah *et al*., 2011). It is critical for the correction of DSBs to restore genomic integrity and to prevent cell death, chromosomal aberrations and mutations (Srivastava *et al*., 2009).

Protein kinases of the phosphatidylinositol 3-OH-kinase-related kinase (PI3KK) family including ataxia telangiectasia mutated (ATM), ataxia

telangiectasia related (ATR) or DNA-dependent protein kinase (DNA-PK) are produced in respond to DSBs, resulting in initial H2AX phosphorylation (Fig. 2.6). ATM is a primarily kinase that phosphorylates H2AX in response to DNA damage at low doses of ionizing radiation and H2AX is phosphorylated by ATR in response to DNA replication stress (Fernandez-Capetillo, 2004).

γ-H2AX induction was found to occur only in apoptotic nuclei with characteristic chromatin condensation (Mukherjee *et al.*, 2006). Several studies had shown that DNA damage induced phosphorylation of H2AX was associated with DNA repair, cell cycle checkpoints, induction of apoptosis and tumor suppression. For example, Liu *et al*., (2008) showed that transient overexpression of H2AX was associated with increase apoptosis in gastrointestinal stromal tumor (GIST) cells treated with protein kinase inhibitor imatinib mesylate. Oxaliplatin induced DNA strand breaks were found to result in apoptosis in colorectal cancer cells (Chiu *et al.*, 2009). Additionally, Jane and Pollack (2010) reported that enzastaurin induced γ-H2AX to regulate apoptosis in malignant glioma cells *via* MAPK signaling pathway.

Podhorecka *et al.*, (2010) also found DNA damage was induced by many anticancer drugs. My present study was designed to evaluate γ-H2AX levels which can be used to detect or evaluate the efficiency of genotoxic effect for different ternary copper(II) complexes in breast cancer cell and immortalized breast cell lines. Analysis of expression γ-H2AX with anticancer treatment would allow monitoring of DSB formation in tumor cell as well as

normal cells.

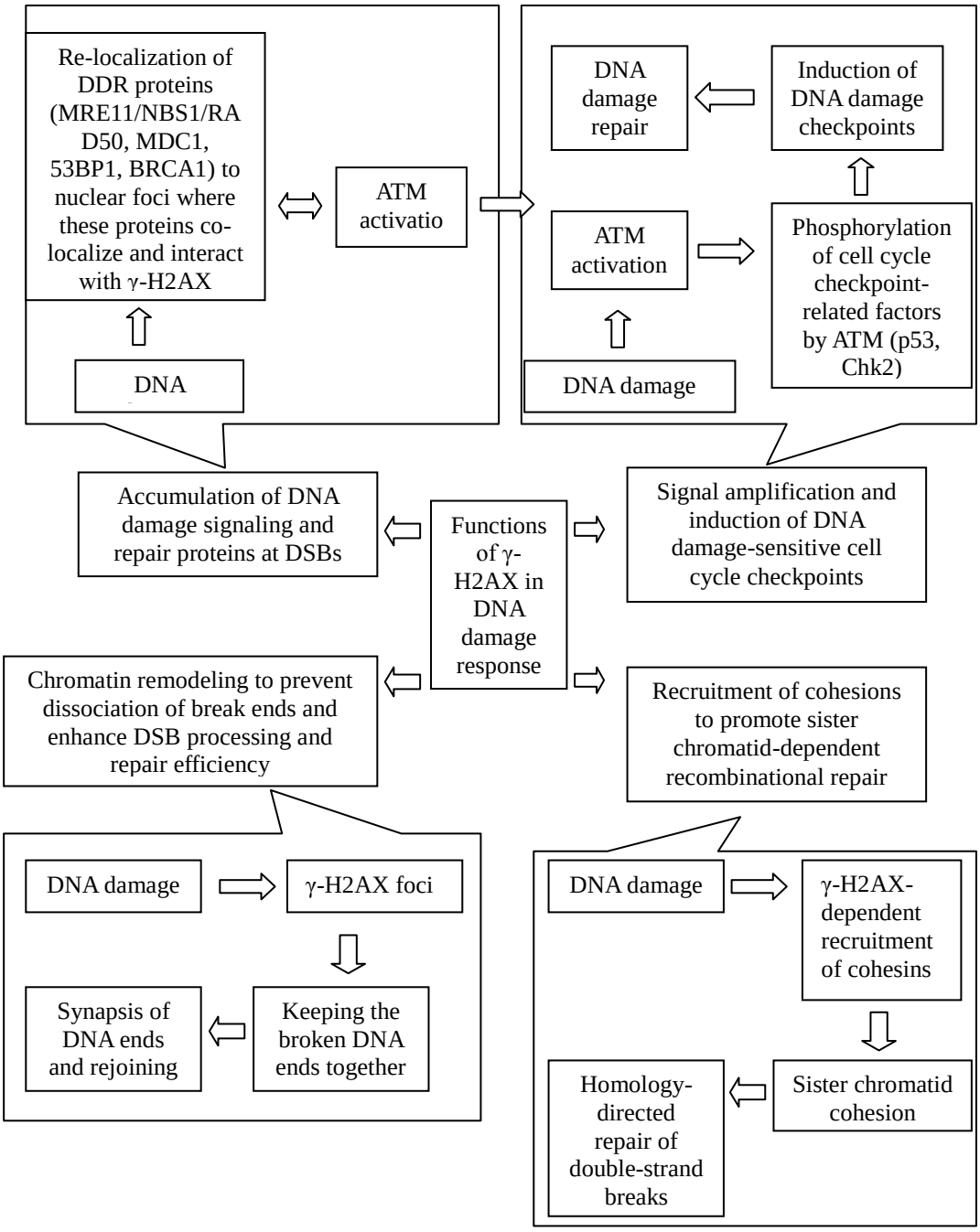

Fig. 2.6: H2AX phosphorylation and its role in DNA damage response. Redrawn from Podhorecka *et al*., 2010.

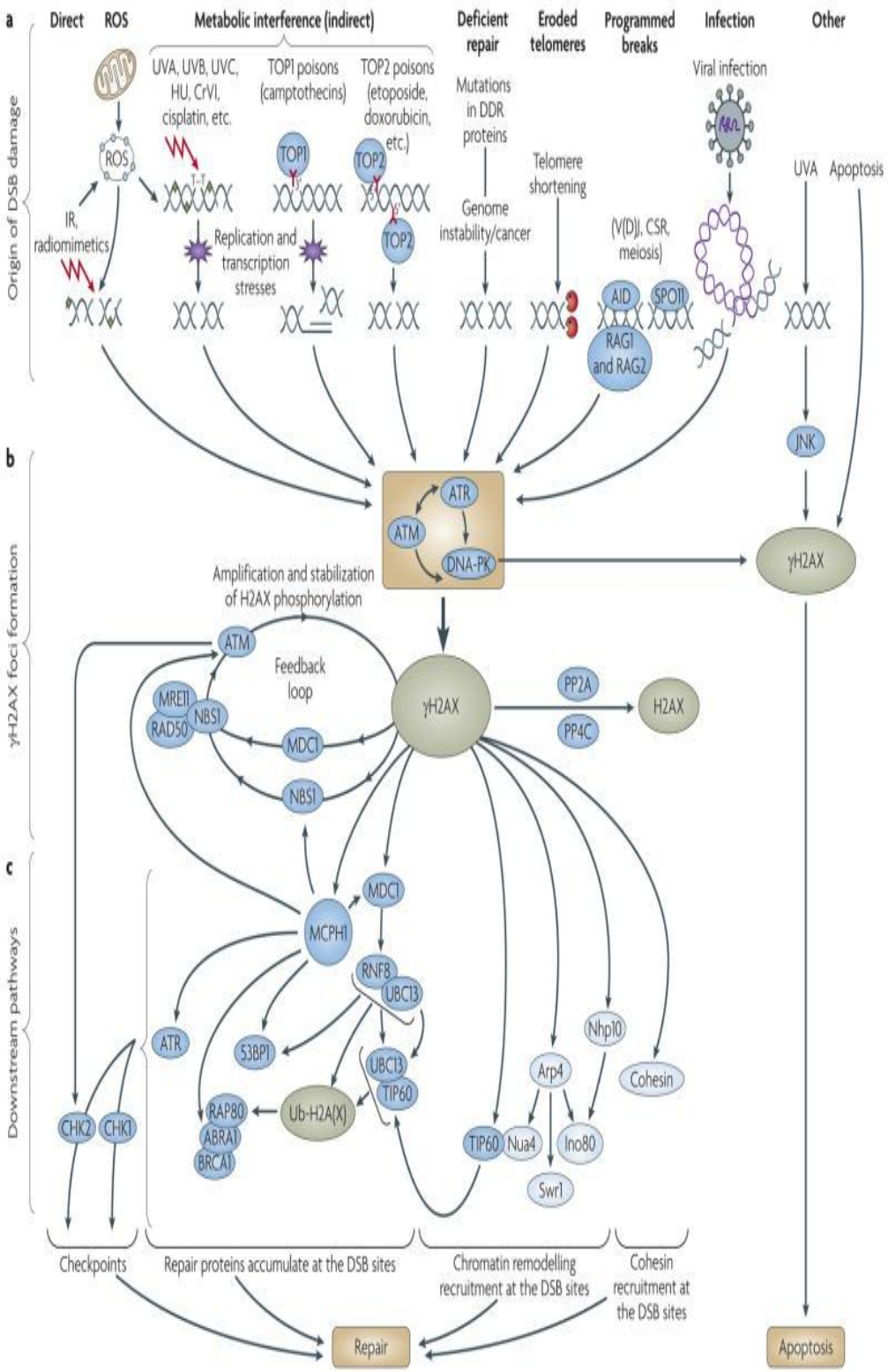

Fig. 2.7: H2AX is a central component of numerous signaling pathways in response to DSBs. Taken from Bonner *et al.*, 2008.

CHAPTER 3.0

MATERIALS AND METHODS

To investigate the anticancer property of ternary copper(II) complexes on transformed (MDA-MB-231) and non-transformed (MCF 10A) breast cell lines, four assays were used. Initially, morphology study was carried out by observing morphological changes of the cells before and after treatment with ternary copper(II) complexes microscopic examination. Quantification of cell viability and proliferation of the cells was determined by colorimetric MTT (3-[4,5-dimethylthiazol-2-yl]-2,5-diphenyltetrazolium bromide) assay that involved reduction of yellow tetrazolium salt (MTT) to purple formazan by viable cells.

The third assay (apoptosis assay) involved flow cytometry and the use of annexin V-FITC staining to detect apoptotic cells. Annexin V-FITC is a conjugate consisting of annexin V (a phospholipid protein) and the fluorescent dye fluorescein isothiocyanate (FITC). After the induction of apoptosis, phosphatidylserine (PS) is translocated from the inner (cytoplasmic) leaflet to the outer (cell surface) leaflet of the plasma membrane. Annexin V is a calcium-dependent phospholipid-binding protein that has a high affinity for binding exposed PS on the surface of apoptotic cell. The fourth assay involved flow cytometric technique which enabled quantification of cells in different phases of cell cycle. Propidium iodide (PI) was used to stain the

nucleus. The fluorescent PI was intercalated into cellular DNA and the enhanced fluorescence intensity of bonded PI was directly proportional to cellular DNA content.

Understanding the mechanism of action is vital to discover the potential of ternary copper(II) complexes as new therapeutic agents. Three assays were carried out to determine their mode of action, namely proteasome inhibition, ROS detection and γ-H2AX assay. Western blot analysis with specific antibodies to ubiquitin and IκB-α protein were use to detect proteasome inhibition. Proteasome inhibition was measured as accumulation of ubiquitinated proteins. Absence of ubiquitinated proteins implies no proteasome inhibition.

A cell permeable substrate, 2',7'-dichlorofluorescein diacetate (DCFH-DA), a reliable fluorogenic marker for ROS detection was used to determine the amount of intracellular hydrogen peroxide (H_2O_2). The nonpolar and non-ionic DCFH-DA can passively diffuse into cells and be deacetylated by intracellular esterases to form non-fluorescent 2',7'-dichlorofluorescein (DCFH). This DCFH compound is then trapped inside the cells. In the presence of ROS, DCFH is oxidized to fluorescent 2',7'-dicholofluorescein (DCF).

Histone H2AX is a variant histone and H2AX is emerging as an intriguing gene in tumor biology. The presence of phosphorylated H2AX on serine^{139} (γ-H2AX) in cells serve to amplify the DNA double-strand breaks

(DSBs) or aid repair of persistent lesion. It was studied by immunofluorescence analysis. γ-H2AX facilitates the recruitment of proteins required for DNA damage signaling and repair surrounding DNA damage site. It was revealed by using an antibody against phosphorylated H2AX which provided a measure of the signal of DSBs within a cell. Cells were imaged by fluorescence microscope.

3.1 Materials

Ternary copper(II) complexes were supplied by Dr Ng Chew Hee and their synthesis was similar to the method used for preparing (1,10-phenanthroline)(*N*,*N'*-ethylenediaminediacetato)metal(II) (Ng *et al*., 2008). Copper(II) 8-hydroxyquinoline complex [$Cu(8OHQ)_2$] was obtained from Sigma-Aldrich (St. Louis, MO) and was used without further purification. All cell culture products were purchased from Invitrogen (Grand Island, NY). Annexin V-FITC Apoptosis Detection Kit II, Alexa Fluor® 488 Mouse anti-H2AX (pS139), PI and Alexa Fluor® 488 Mouse IgG1 κ Isotype control were purchased from BD Biosciences (MA, USA). Ubiquitin (P4D1) and IκB-α (C-15) antibodies were purchased from Santa Cruz Biotechnology (Santa Cruz, CA). β-actin antibody was purchased from Cell Signaling (MA, USA). Insulin, hydrocortisone, DMSO (dimethyl sulfoxide), DCFH-DA, BSA (bovine serum albumin) and MTT were purchased from Sigma-Aldrich (St. Louis, MO). SuperSignal West Pico Chemiluminescent Substrate was purchased from Thermo Scientific (Rockford, USA). Western Lighting™ Chemiluminescence

Reagent Plus was purchased from PerkinElmer (MA, USA).

3.2 Synthesis and characterization of ternary copper(II) complexes

The series of $[Cu(phen)(aa)(H_2O)]NO_3$ complexes (aa: gly, DL-ala, C-dmg, sar; lattice water molecules, if present, are omitted for simplicity in subsequent chapters) have been synthesized and characterized by FTIR, elemental analysis, ESI-MS, UV-visible spectroscopy, molar conductivity measurement and X-ray diffraction by others (Ng *et al*, 2012). These complexes were synthesized by similar method. An example is given for the preparation of $[Cu(phen)(DL\text{-}ala)(H_2O)]NO_3$. L-alanine (0.09 g, 0.001 mol) was added to a water-ethanol mixture of $Cu(NO_3)_2.3H_2O$ (0.25 g, 0.001 mol) and 1,10-phenanthroline (0.20 g, 0.001 mol) to give a dark blue solution. The pH was adjusted to pH 8.1 by adding NaOH solution. The resultant solution was heating overnight in a water bath at 45^{o}C to obtain the blue needle crystals. Yield: 0.18 g, 40%. Repeated attempts yielded suitable crystals of $[Cu(phen)(DL\text{-}ala)(H_2O)]NO_3] \cdot 2½H_2O$ and $[Cu(phen)(C\text{-}dmg)(H_2O)]NO_3$ for X-ray crystal structure analysis. The crystallographic data for these two complexes have been deposited at Cambridge Crystallographic Data Centre as CCDC 809125 and 809126 respectively. The crystal structure of $[Cu(phen)(gly)(H_2O)]NO_3 \cdot 1½H_2O$ had been determined previously (Zhang and Zhou, 2008).

The elemental analysis and FTIR spectral data are reproduced herein.

[Cu(phen)(gly)(H_2O)]NO_3 ·1.5H_2O**.** Calc. for $C_{14}H_{17}N_4O_{7.5}Cu$: C, 39.58; H, 3.32; N, 13.19%. Found: C, 39.75; H, 3.88; N, 13.08%. FTIR (cm^{-1}): 3400, 3273, 3188, 3116, 3056, 2929, 1653, 1625, 1588, 1521, 1493, 1474, 1458, 1430, 1384, 1224, 1160, 1108, 1042, 921, 874, 856, 833, 781, 739, 723, 563, 431. ν_{OH}(water) 3400s; ν_{NH}(amino) 3273s; $\nu_{COO\text{-}}$(asym,sym) 1625vs, 1384vs; ρ_{CH}(phen) 856s, 723s.

[Cu(phen)(DL-ala)(H_2O)]NO_3 2½H_2O**.** Calc. for $C_{15}H_{19}N_4O_{7.5}Cu$: C, 41.05; H, 4.36; N, 12.77%. Found: C, 41.13; H, 4.25; N, 12.76%. FTIR (cm^{-1}): 3468, 3230, 3121, 3042, 2969, 2930, 1654, 1636, 1521, 1497, 1458, 1430, 1384, 1284, 1225, 1183, 1157, 1122, 1108, 929, 874, 858, 825, 780, 738, 723, 562, 474, 431. ν_{OH}(water) 3468s; ν_{NH}(amino) 3230s; $\nu_{COO\text{-}}$(asym,sym) 1636vs, 1384vs; ρ_{CH}(phen) 858s, 723s.

[Cu(phen)(C-dmg)(H_2O)]NO_3. Calc. for $C_{16}H_{18}N_4O_6Cu$: C, 45.12; H, 4.26; N, 13.16%. Found: C, 45.43; H, 4.09; N, 13.24%. FTIR (cm^{-1}): 3437, 3235, 3163, 3118, 3063, 2972, 2931, 2907, 2869, 1663, 1609, 1586, 1560, 1521, 1494, 1474, 1428, 1384, 1346, 1257, 1220, 1206, 1142, 1126, 1107, 967, 897, 874, 848, 820, 775, 738, 722, 569, 497, 431. ν_{OH}(water) 3437s; ν_{NH}(amino) 3235s; $\nu_{COO\text{-}}$(asym,sym) 1663vs, 1384vs; ρ_{CH}(phen) 848s, 722s.

[Cu(phen)(sar)(H_2O)]NO_3. Calc. for $C_{15}H_{16}N_4O_6Cu$: C, 43.74; H, 3.92; N, 13.60%. Found: C, 43.69; H, 3.95; N, 13.49%. FTIR (cm^{-1}): 3331, 3197, 3131, 3070, 3002, 2981, 2934, 1655, 1629, 1587, 1523, 1492, 1431, 1405,

1384, 1360, 1315, 1265, 1257, 1197, 1141, 1107, 1076, 1038, 990, 927, 905, 874, 859, 826, 782, 736, 724, 556, 431. ν_{OH}(water) 3331s; ν_{NH}(amino) 3197s; ν_{COO-}(asym,sym) 1655vs, 1384vs; ρ_{CH}(phen) 859s, 724s.

3.3 Media preparation

3.3.1 Dulbecco's modified eagle medium (DMEM) preparation

A pack of DMEM powder (high glucose) (Product #12800-017, GIBCO®) was dissolved in roughly 95% double distilled water (ddH_2O). 3.7 g of sodium bicarbonate ($NaHCO_3$) was then added. The pH of resultant solution was adjusted to 0.2 to 0.3 units below pH 7.0-7.4 by adding 1 M sodium hydroxide (NaOH) or 1 M hydrochloric acid (HCl) with stirring and then topped up with ddH_2O to the 1 L mark of the volumetric flask. This medium was filtered by using Millipore vacuum 0.22 μm filter top and kept at 4 ℃. Some medium was pipetted into 35 mm culture dish and was incubated at NuAire CO_2 incubator overnight to check for any contamination. MDA-MB-231 breast cancer cell line were maintained in DMEM containing 10% fetal calf serum (FCS), 50 U/mL penicillin and 50 μg/mL streptomycin at 37 ℃ in 5% CO_2 incubator.

3.3.2 F-12 Nutrient mixture preparation

A pack of F12 nutrient mixture (Ham) powder (Product #21700-075,

GIBCO®) was dissolved in ddH_2O to approximately 95% of the final required volume (1 L). 1.176 g/L of $NaHCO_3$ was added. The pH was adjusted between 0.2 and 0.3 below the pH 7.0-7.4 by adding either 1 M NaOH or 1 M HCl. The medium was topped up to the desired volume with ddH_2O and stirred until dissolved. The medium was immediately filtered by using Millipore vacuum 0.22 µm filter top and kept at 4 ℃. Some medium was pipetted into 35 mm petri dish and was incubated in a NuAire CO_2 incubator overnight to check for any contamination prior to use.

3.3.3 Preparation of DMEM/F12 growth medium

1:1 DMEM/F12 mixture was supplemented with 5% (v/v) horse serum, 1× MEM non essential amino acid, 1× L-glutamine, 10 ug/mL insulin, 20 ng/mL epidermal growth factor (recombinant human), 0.5 µg/mL hydrocortisone, 50 U/mL penicillin and 50 µg/mL streptomycin. This growth medium was used to culture MCF 10A cells and stored in a 4 ℃ refrigerator.

3.4 Phosphate buffered salt preparation

One tablet of phosphate buffered salt (PBS) (Takara Bio INC) was dissolved in 100 mL ddH_2O. The solution was autoclaved at 121 ℃ for 15 min. Then, it was tightly sealed and stored at 4 ℃.

3.5 Cell culture

3.5.1 Maintenance of cultured cells

Immortalized human mammary epithelial cells (MCF 10A) were cultured in growth medium (1:1 DMEM/F12) prepared in Section 3.3.3. MDA-MB-231 breast cancer cells were cultured in DMEM medium. Both media were supplemented with 10% heat-inactivated fetal calf serum, 50 U/mL penicillin and 50 µg/mL streptomycin. Both cell lines were purchased from American Type Culture Collection (ATCC), (Manassas, VA, USA). Passage numbers of all the cell lines used in this research are not known and new record of passage number could not be continued.

Both types of breast cells are adherent cells and need to be subcultured to avoid overcrowding and to prevent the culture from dying. Subculturing was done in the following manner. The old media were aspirated and each culture was rinsed with 3 mL PBS. The PBS was aspirated and 1 mL of trypsin-EDTA (TrypLE^{TM} Express) was added to ensure that the monolayer was completely covered with it. The cells were incubated at 37 ℃ in a CO_2 incubator for 5 min (NuAire). The cells were checked and gently tapped to ensure the cells were well trypsinized. 5 mL of appropriate growth medium was added to resuspend the cells. The suspension was transferred to a 15 mL polystyrene conical centrifuge tube (BD Falcon^{TM}) for centrifugation at 1000 rpm for 5 min (Kubota) at room temperature (RT). The medium was aspirated and the pellet was resuspended in 1 mL appropriate growth medium. The appropriate volume of cell suspension was transferred to a new petri dish

(Corning®) containing pre-warmed medium. Cultured cells were maintained at 37 ℃ in a humidified incubator with an atmosphere of 5% CO_2 (NuAire). The cells from each cell line were subcultured every four days.

3.5.2 Cryopreservation of cell lines

MDA-MB-231 and MCF 10A cell lines were cryopreserved cultures in log phase of growth to yield the highest number of viable cells. The degree of cell density and general appearance of the culture were assessed by using an inverted microscope. The cells were trypsinized to detach them by following the procedure used during the subculture (Section 3.5.1). The total number of cells and percent viability was determined using the Countess® Automated Cell Counter (Section 3.6). Each collected pellet was resuspended in 500 µL ice-cold medium with 10% FCS and the cell suspension was aliquoted into pre-chilled cryogenic vial (Nalgene®). The 500 µL ice-cold medium was supplemented with 10% FCS and 10% DMSO which acted as cryoprotectant. Immediately, the cryovial was placed at -20 ℃ for 4 h and then transferred to a -80 ℃ freezer overnight. The frozen cells were kept in liquid nitrogen for permanent storage.

3.5.3 Reviving of cell lines

A vial of frozen cells was thawed quickly in 37 ℃ water bath

(Memmert). The vial was observed and removed from the water bath when there was just a small piece of ice remaining. The cells were immediately transferred to a sterile 15 mL conical tube containing 10 mL appropriate cold medium and resuspended gently, followed by spinning at 1000 rpm for 10 min. The supernatant was poured off and the cells were resuspended in 10 mL appropriate pre-warmed growth medium with 10% FCS. The cells were then transferred to a culture plate and were incubated in a 5% CO_2 incubator at 37 ℃.

3.6 Cell quantification

Cell counting and viability counts were determined by Countess® Automated Cell Counter (Invitrogen). 10 µL of sample was mixed with 10 µL of trypan blue and pipetted into Countess® chamber slide. The slide was inserted into the instrument and the cell count was recorded.

3.7 Cell morphology Assay

MDA-MB-231 and MCF 10A cells (1×10^4 cells per well) were cultured in separate 96 flat test plates (Orange Scientific) overnight. The culture medium in each well was replaced with new medium with or without the indicated test drug concentration and reincubated for 24 h at 37 ℃ in a 5% CO_2 incubator. Serial dilution was carried out to give a range of drug

concentration (25, 12.5, 6.25, 3.12 and 1.56 μM) of ternary copper(II) complexes and [Cu(8OHQ)$_2$]. An inverted microscope (Leica DM IRB) was used for all microscopic imaging with bright field for cellular morphology. Morphological changes were observed and photographed.

3.8 MTT viability assay

Cells were harvested from exponential growth phase maintenance cultures. Cells were seeded at density 1 × 10^5 cells/mL in 100 μL medium per well in a 96-well flat bottom tissue culture plate (Orange Scientific), followed by incubation at 37 ℃ in a 5% CO_2 incubator overnight to allow the cells to attach to the wells. The media from the plates were removed and then replaced with 100 μL of culture media with or without the test compounds. The cells were incubated for 24 h, in a 37 ℃ humidified incubator with 5% CO_2 to allow the compounds to take effect. Cells were treated with six different test drug concentrations (25, 12.5, 6.25, 3.12 and 1.56 μM) of ternary copper(II) complexes and [Cu(8OHQ)$_2$].

After the drug exposure period, 5 mg/mL MTT was dissolved in PBS just prior to culture application. 20 μL MTT solution per well was added and the plate was incubated (37 ℃, 5% CO_2) for a further 4 h to allow the MTT to be metabolized. The plate was centrifuged at 1000 rpm for 5 min. The viable cells producing formazan were inspected microscopically and the media were slowly aspirated. Then, 100 μL DMSO per well was added to dissolve the

formazan using a multichannel pipette. The optical density was measured using enzyme-linked immunosorbent assay (ELISA) plate reader (Dynatech MRX) at a wavelength of 570 nm with background subtraction at 630 nm. Every experiment included a set of negative controls (untreated cultures), blank wells without cells and a set of control [$Cu(8OHQ)_2$]. Percentage of cell viability was calculated using Microsoft Excel and IC_{50} values (the concentration of the complex causing 50% growth inhibition) were estimated from dose response curves. For all viability experiments, each set of drug concentrations was in triplicate and each experiment was repeated three times.

Calculation:

$$Cell\ viability\ (\%) = \frac{\text{Mean Optical Density of sample}}{\text{Mean Optical Density of Control}} \text{ x } 100$$

3.9 Annexin V-FITC/PI double staining in flow cytometric analysis of apoptosis

Cells were treated with 5 μM ternary copper(II) complexes and [$Cu(8OHQ)_2$] in separate 60 mm petri dish for 24 h when cell confluency reached 70-80%. Cells were also cultured without treatment as control. Apoptosis assay was performed using Annexin V-FITC Apoptosis Detection Kit II (BD Pharmingen^{TM}). Unstained cells, cells stained with Annexin V-FITC alone and cells stained with PI alone were used as control to set up compensation and quadrants.

Each sample was treated as described herein. Culture medium with suspension cells was collected and cells were washed with PBS. PBS was then collected. Cells were trypsinised with 1 mL accutase (Millipore) at 37 ℃ for 5 min to completely detach the cells. Accutase with suspension cells were collected and centrifuged at 1000 rpm for 5 min. The pellet was resuspended in 1× binding buffer. Cell count was performed and 1×10^6 cells/mL was prepared. 100 µL of the solution (1×10^5 cells) was transferred into a 12 × 75-mm, 5 mL polystyrene round bottom test tube (Becton, Dickson and company). 5 µL of FITC Annexin V and 5 µL PI was added. Cells were mixed gently and incubated for 15 min at room temperature (RT) in the dark. 400 µL of 1× binding buffer was added. The samples were filtered into labeled 12 × 75-mm, 5 mL polystyrene round bottom test tubes with cell strainer caps and analyzed immediately by fluorescent activated cell sorter (FACSCalibur, Becton-Dickinson). BD CellQuest Pro software was used to analyze the data.

3.10 DNA staining of isolated nuclei for cell cycle analysis

Different sets of cells were exposed to 5 µM ternary copper(II) complexes for 24 h when cells have grown to 70% confluence in a 60 mm tissue culture dishes. Cells were cultured without treatment as control. Culture media with floating cells were collected and the cells were washed with PBS. Cells were trypsinised with 1 mL accutase and then incubated at 37 ℃ in a 5% CO_2 incubator for 5 min until cells detached completely. Cells were collected, centrifuged for 5 min at 1000 rpm at RT and finally the pellets were

resuspended in PBS. Cell count was performed by Countess® Automated Cell Counter. The concentration of cells was adjusted to 0.5-1.0 $\times 10^6$ cells/mL and spun at 1000 rpm for 5 min. Supernatant was discarded and pellets was mixed well with 300 uL of hypotonic DNA staining buffer (0.25 g sodium citrate, 0.75 mL Triton™ X-100, 0.025 g propidium iodide, 0.005 g ribonuclease A and 250 mL distilled water). Each sample was filtered into a labeled 12 × 75-mm tube with cell strainer cap and kept at 4 ℃ protected from light for at least 10 min before analysis. The samples were mixed well and 20,000 cells were analyzed per sample by passage through a FACSCalibur employing the BD CellQuest Pro software. The percentage of cells in each phase of the cell cycle was analyzed using ModFit LT™ software (Verity Software House, Inc. ME).

3.11 Western blot analysis for proteasome inhibition

3.11.1 Preparation of whole cell extraction

MDA-MB-231 cells were grown until 80-90% confluence in a series of 10 cm petri dishes and were treated with 1 μM and 10 μM of ternary copper(II) complexes and [Cu(8OHQ)$_2$] for 24 h. After that, cells were harvested and lysated as described herein. Some of the petri dishes contained floating cells and attached monolayer cells after 24 h treatment.

All the petri dishes were placed in ice. Method for process of floating cells in petri dish was collected as described. Culture media with suspended cells were collected carefully and centrifuged at 1000 rpm for 5 min at 4 ℃.

Pellets were washed with cold PBS and followed by centrifugation at 1000 rpm for 5 min at 4 ℃ (Eppendorf, Centrifuges 5810 R). Washing and centrifugation were repeated again. Supernatant was removed and lysis buffer (50 mM Tris–HCl, pH 8.0, 5 mM EDTA, 150 mM NaCl, 0.5% Nonidet P-40, 0.5 mM phenylmethylsulfonyl fluoride, and 0.5 mM dithiothreitol) was added into each pellet to produce cell lysate. Cell monolayer left on each petri dish after removal of floating cells was washed twice with cold PBS. Lysis buffer was added into the plate and cells were collected by cell scraper from petri dish into microcentrifuge tube as cell lysate.

Both of the cell lysates were combined and further disrupted and homogenized by sonication. This combined cell lysate was then rocked at 4 ℃ for 30 min. Afterwards, cell lysate was centrifuged at 11400 rpm for 30 min at 4 ℃. Pellet was discarded. The supernatants containing proteins were known as whole cell extracts. The supernatants were kept in ice until used for further analysis.

3.11.2 Protein assay

Protein concentration was determined using Braford method (Bio-Rad protein assay). 2 µL of supernatant was added into 798 µL ddH_2O into an eppendorf tube. 800 µL of ddH_2O was prepared as a blank. 200 µL of dye reagent concentrate was pipetted into each tube and vortexed. Samples were incubated for 5 min at RT. Absorbance was measured at 595 nm by using

NanoDrop™ 8000.

3.11.3 Sodium dodecyl sulfate - polyacrylamide gel electrophoresis (SDS-PAGE)

Table 3.1: Tris-glycine SDS-Polyacrilamide Gel Electrophoresis

Reagent	8% Resolving Gel Volume (mL)	10% Resolving Gel Volume (mL)	5% Stacking Gel Volume (mL)
ddH_2O	4.6	4.0	2.1
30% acrilamide	2.7	3.3	0.5
Tris 0.5M, pH 8.8	2.5	2.5	-
Tris 0.5M, pH 6.8	-	-	0.38
10% SDS	0.1	0.1	0.03
10% APS	0.1	0.1	0.03
TEMED	0.006	0.004	0.003
Total	10	10	3

Stacking gel and resolving gel were prepared according to Table 3.1. The ingredients needed to prepare the resolving gel of the chosen percentage were mixed well and it was poured quickly into the assemble plates without trapping any bubbles. A layer of 70% ethanol was placed on top of the resolving gel. The resolving gel needs 30 min to polymerize completely. Then, ethanol was poured off, replaced with ddH_2O and dried with filter paper. 5% stacking gel solution was prepared and poured onto the resolving gel. A comb was inserted and left for 30 min to allow solidification. The gel was placed into the tank.

Both the bottom and the top of the gel were immersed with running buffer (Tris [tris(hydroxymethyl)aminomethane], glycine, 10% SDS). 1 part of

4× SDS and 2% mercaptoethanol were added to 3 parts of each whole cell extract and immediately heated at 95 ℃ for 5 min. The comb was removed and 20 μg whole cell extracts per well were loaded. Gel was run at 80 V until blue dye passed the stacking gel. Then, the voltage was increased to 110 V until the blue dye front reaches the bottom.

3.11.4 Wet transfer

The size-separated protein from the gel was transferred to polyvinylidene fluoride (PVDF) membrane by wet transfer. PVDF was soaked in methanol for a few seconds and then rinsed with distilled water. PVDF, sponges, SDS-PAGE gel and filter papers were soaked in transfer buffer prior to use. Sandwich blot was assembled in the following order: black panel (negative electrode), sponges, two pieces of filter papers, SDS-PAGE gel, PVDF membrane, two pieces of filter paper and red panel (positive electrode). The sandwich blot was put into a transfer tank which contains transfer buffer and run at 15 V overnight at RT. The gel pack was disassembled and PVDF membrane was gently dislodged from the sandwich and transferred to a small container containing ddH_2O.

3.11.5 Antibodies and detection

The PVDF membrane was rinsed with ddH_2O and incubated with

blocking solution (5% milk in Tris buffered saline Tween-20 (TBST) pH 7.3, 0.05% Tween-20) at RT for 45 min. This was followed by 1 h incubation with a primary antibody against target protein (ubiquitinated protein, IκB-α, β-actin) in blocking solution at RT. The volume of primary antibody with blocking solution was enough to cover the membrane and it was allowed to float freely when agitated. The membrane was washed 3 times with TBST [1 × Tris buffered saline (TBS), 0.05% Tween-20] for 10 min each time. Afterwards, the wash solution was decanted and incubated with peroxidase-conjugated anti-IgG as secondary antibody, diluted in blocking buffer for 45 min at RT. The membrane was washed three times with TBST in the order of 10 – 15 – 20 min. All of these steps were performed on a shaker with extensive agitation. Then, the following steps were performed in a dark room. Enchanced chemiluminescence (ECL) working solution of the SuperSignal West Pico Chemiluminescent Substrate or Western lighting^{TM} Chemiluminescence Reagent Plus by mixing reagent 1 and reagent 2 at 1:1 ratio was used for detection of proteins from Western blots. Membrane was incubated in ECL working solution for 5 min. The blot was ready to be detected by putting inside the film cassette. The film was exposed for a few minutes/seconds depending on the protein to be detected. Finally, the film is developed in an X-ray processor. The level of β-actin was used as a total protein loading control. Prestained protein standards (10-250 kDa, Bio-Rad) were used as protein markers to determine the size of target proteins. The western blot of protein bands are quantified using ImageJ program.

3.12 Intracellular reactive oxygen species (ROS) detection

MDA-MB-231 cells and MCF 10A cells at 70-80% confluence were treated with indicated concentration of ternary copper(II) complexes and time points. The incubation time for one set treatment involving 5 μM and 10 μM ternary copper(II) complexes was 6 h whereas another set involving 5 μM of same complexes was 24 h. Cells were also cultured without treatment as control. Cells were rinsed with PBS. Then, trypsinization was performed by using accutase to detach cells and spun down at 1000 rpm for 5 min. Each pellet was suspended with 500 μL of 10 μM DCFH-DA (Sigma) solubilized in PBS and then incubated for 30 min at 37 ℃ in the dark. The cells were again spun down, the excess DCFH-DA was aspirated and the pellets were washed three times with PBS. Finally, the cells were suspended in PBS. The DCF fluorescence was measured immediately at 488 nm excitation and 525 nm emission (fluorescein isothiocyanate filter) using FACSCalibur with 20,000 events recorded. Data were analyzed by using BD CellQuest Pro software. The amount of ROS was quantified as the mean fluorescence intensity.

3.13 γ-H2AX assay

MDA-MB-231 cells and MCF 10A cells were seeded in 2-well Lab-Tek II Chambered with cover glass slide (Nalge Nunc International) at a density of 1.2×10^5 cells/well and incubated overnight. Media were removed from the wells and the cells were treated for 6 h with fresh media with 5 μM

ternary copper(II) complexes. Extra wells were prepared for untreated cells and 1 μM adriamycin-treated cells as control for this assay. An isotype control was used to confirm that the antibody H2AX binding is specific and not a result of non-specific binding of the fluorescent antibody.

After treatment, the media were removed and cells washed with PBS. Cells were fixed with 3.7% formaldehyde in PBS and incubated for 10 min at RT. The fixative was removed and the cells were washed twice with PBS. The cells were permeabilized by using 0.1% Triton™ X-100 in PBS and incubated for 5 min at RT. The permeabilization buffer was removed and cells were washed twice with PBS. After Alexa Fluor® 488 Mouse anti-H2AX (pS139) was diluted at 1:10 ratio in 3% BSA/PBS and added to each well. The isotype control (concentration as primary antibody) was added to untreated well and Adriamycin treated well. The cells were incubated for 60 min at RT in the dark. The antibody was removed and washed three times with 0.05% Tween-20 in PBS. The nuclei were counter-stain with 1 μg/mL solution of DAPI for 5 min. Slide was mounted using Vectasheild® mounting medium before imaging. Fluorescence images were captured using a Nikon microscope equipped with a CCD camera and NIS software. All the images were obtained using same parameters (exposure time and brightness) for direct comparisons and cell scoring analyzed by MetaMorph® microscopy automation and image analysis software.

3.14 Statistical analysis

Statistical analysis was conducted using statistical software of GraphPad Prism 5 (GraphPad software, Inc. San Diego, CA). Differences between untreated and compound-treated samples were compared by one-way analysis of variance (ANOVA) with post hoc Dunnett's tests. Data were expressed as mean ± S.E.M and for significant differences were set up at *= $p<0.05$, **=$p<0.01$, ***$p<0.005$.

CHAPTER 4.0

RESULT

4.1 Effect of compounds on cancer and non-cancer cell morphology using microscopic techniques

The morphological effects of ternary copper(II) complexes on MDA-MB-231 and MCF10A cells were examined and imaged. The aim was to find out whether the ternary copper(II) complexes could change their morphology and induce apoptosis. In the observation of morphological changes in human breast carcinoma MDA-MB-231 cells by ternary copper(II) complexes, untreated cells maintained their morphology, appeared robust, elongated, adherent and showed cellular crowding, suggestive of proliferation. The morphology of cells was altered after treatment with ternary copper(II) complexes. The cells seemed to grow slower, losing their characteristic morphology, retracting and forming islets of more rounded cells with elevated concentrations of ternary copper(II) complexes after 24 h of treatment [Figs. 4.1(a) - 4.1(j)]. The characteristic morphological features of apoptotic cells are cell rounded and shrunken by cleavage of lamins and actin filaments in the cytoskeleton, nuclear condensation, membrane blebs and formation of apoptotic bodies (Van Cruchten and Van Den Broeack, 2002; Rello *et al*., 2005).

As shown in Figs. 4.1(a) - (j), it was observed that MDA-MB-231 and MCF 10A apoptotic cells became altered in shape and lost their normal cellular morphology including cell size (diameter or area, shape and granularity) after treatment with ternary copper(II) complexes in a dose-dependent manner. Ternary copper(II) complexes at 3.1- 6.3 μM induced apparent MDA-MB-231 cell shrinkage and made the cells rounded-up. These cells underwent further induced cell retraction and become less confluent when incubated with 12.5 - 25 μM ternary copper(II) complexes. Similarly, the known anticancer [$Cu(8OHQ)_2$] also induced concentration-dependent apoptotic morphological changes in the same concentration range [Fig. 4.1(i) - (j)]. These data suggest that ternary copper(II) complexes have the similar apoptosis-inducing effect as [$Cu(8OHQ)_2$] in MDA-MB-231 cells.

Morphologically, all the ternary copper(II) complexes-treated cells at 3.1 μM showed obvious change after 24 h in MDA-MB-231 cells [Figs. 4.1 (a), (c), (e), (g)], while at the same concentration, MCF 10A cells maintained a normal morphology [Figs. 4.1(b), (d), (f), (h)]. Nevertheless, morphological changes were only observed at higher doses of ternary copper(II) complexes in MCF 10A. Apoptotic morphological changes such as shrunken cells and characteristic apoptotic blebbing were detected for MCF 10A cells at 6.3 - 25 μM of ternary copper(II) complexes after 24 h of treatment. However, [$Cu(8OHQ)_2$] induced morphology change (a reduction in cell size) in both MDA-MB-231 and MCF 10A cells was observed at low concentration (3.1 μM) [Fig. 4.1(i) - (j)], suggesting its equal toxicity to both cell lines.

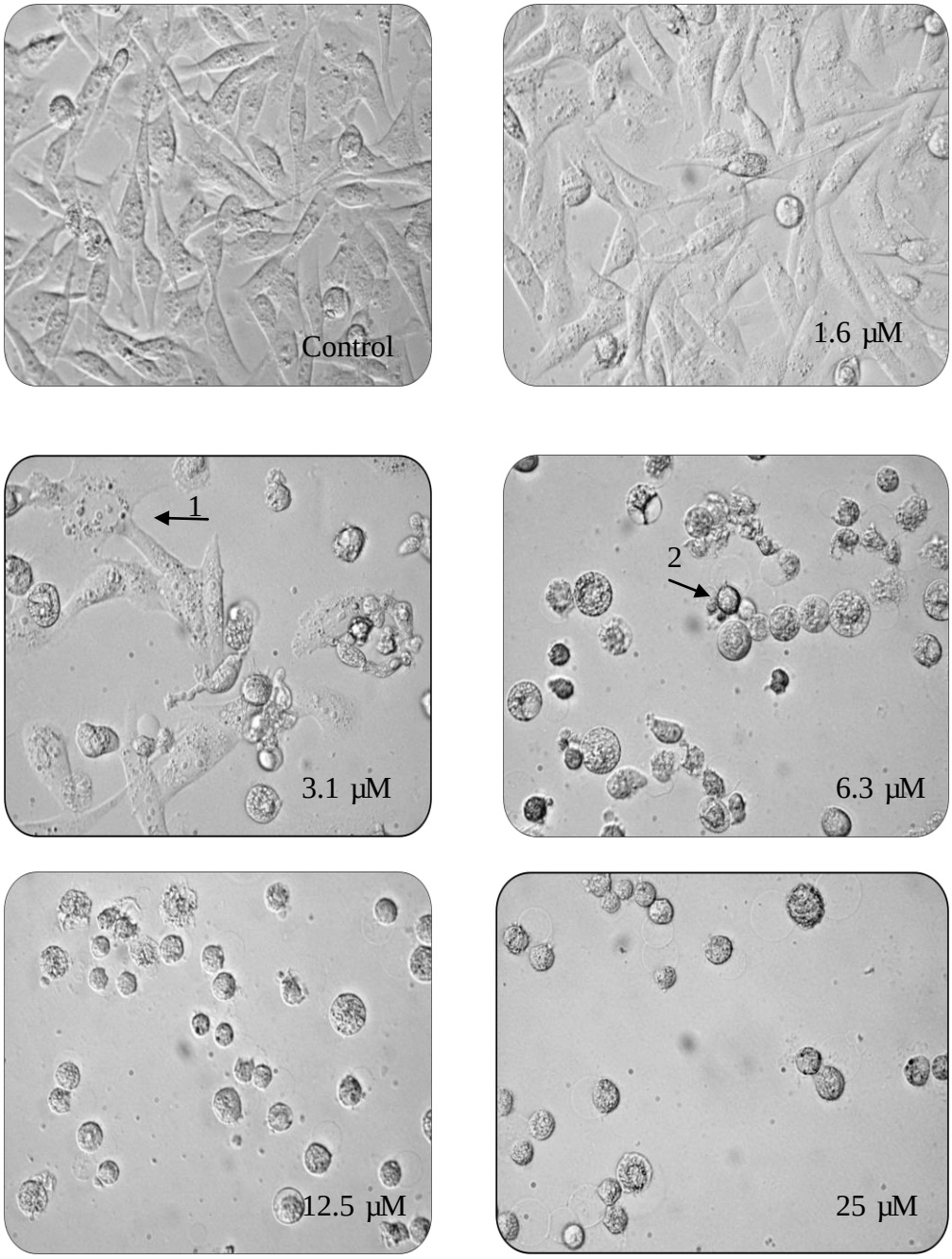

Fig. 4.1(a): Morphological changes in MDA-MB-231 cells treated for 24 h with $[Cu(phen)(DL\text{-}ala)(H_2O)]NO_3\ 2½H_2O$ at different concentrations as compared to untreated cells. (Microscope magnification 400×). All pictures are typical of three independent experiments each performed under identical conditions. Arrow (1) condensation of chromatin, (2) membrane bleb.

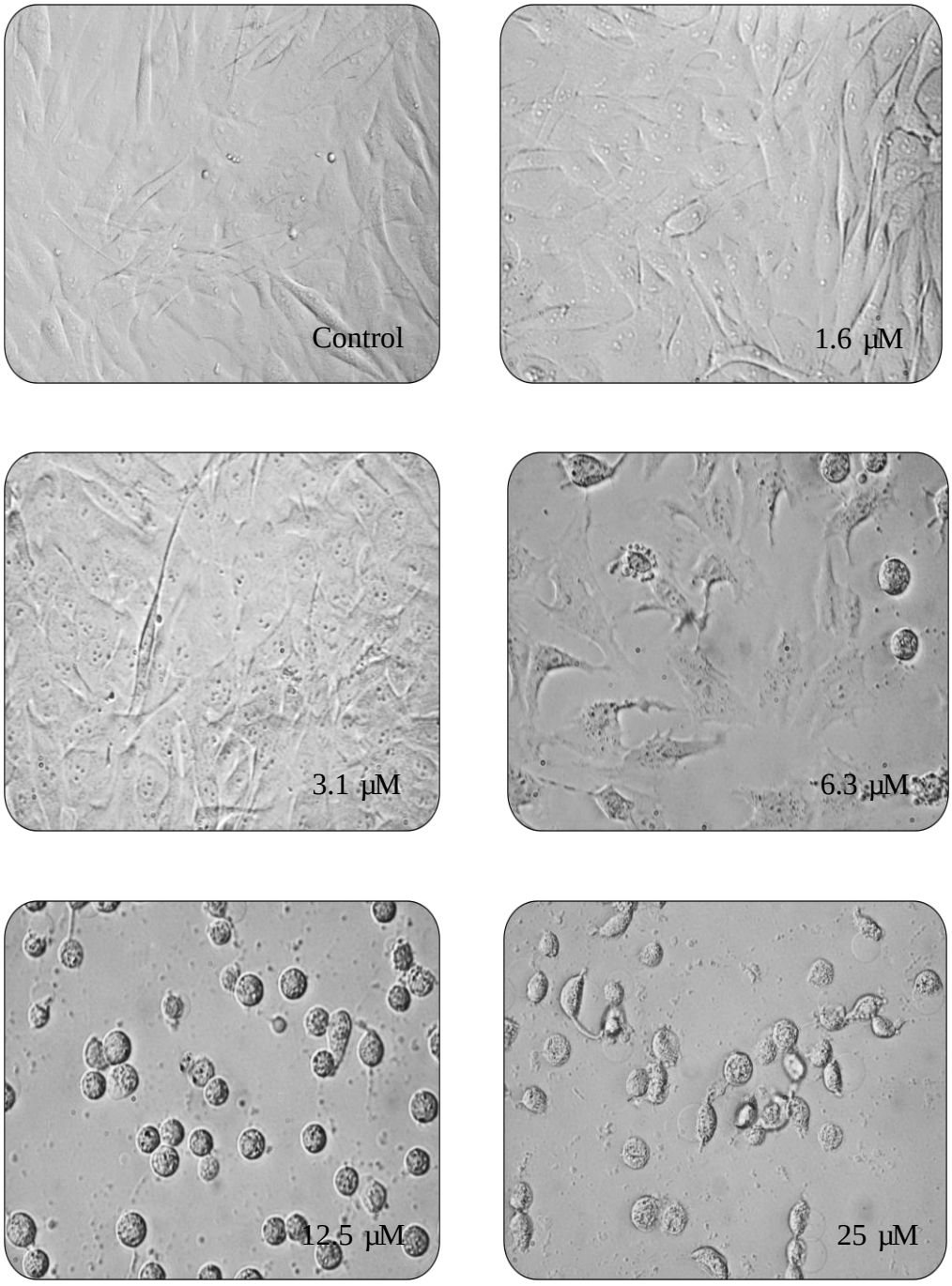

Fig. 4.1(b): Morphological changes in MCF 10A cells treated for 24 h with [Cu(phen)(DL-ala)(H_2O)]NO_3 2½H_2O at different concentrations as compared to untreated cells. (Microscope magnification 400×). All pictures are typical of three independent experiments each performed under identical conditions.

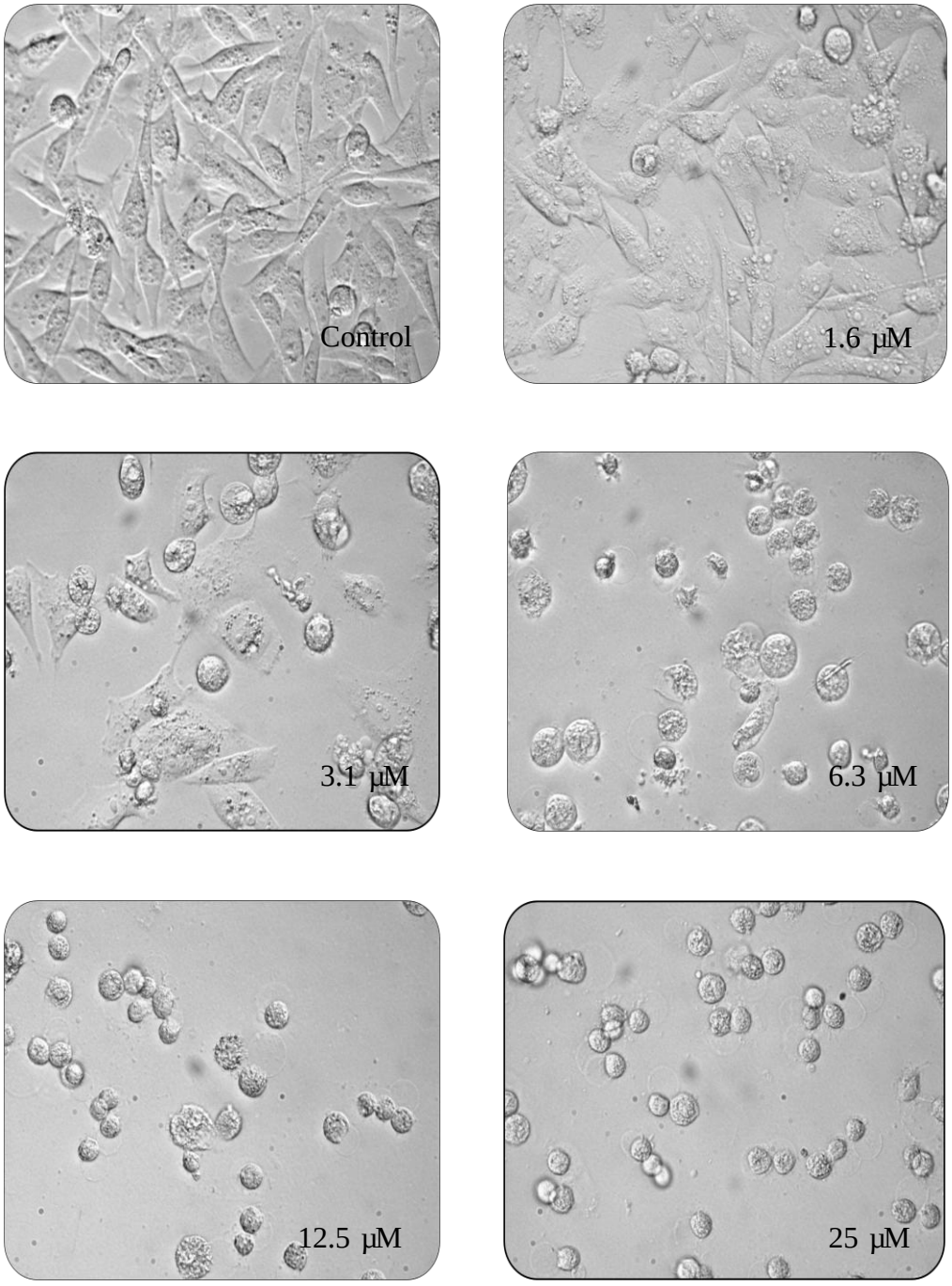

Fig. 4.1(c): Morphological changes in MDA-MB-231 cells treated for 24 h with $[Cu(phen)(sar)(H_2O)]NO_3$ at different concentrations as compared to untreated cells. (Microscope magnification 400×). All pictures are typical of three independent experiments each performed under identical conditions.

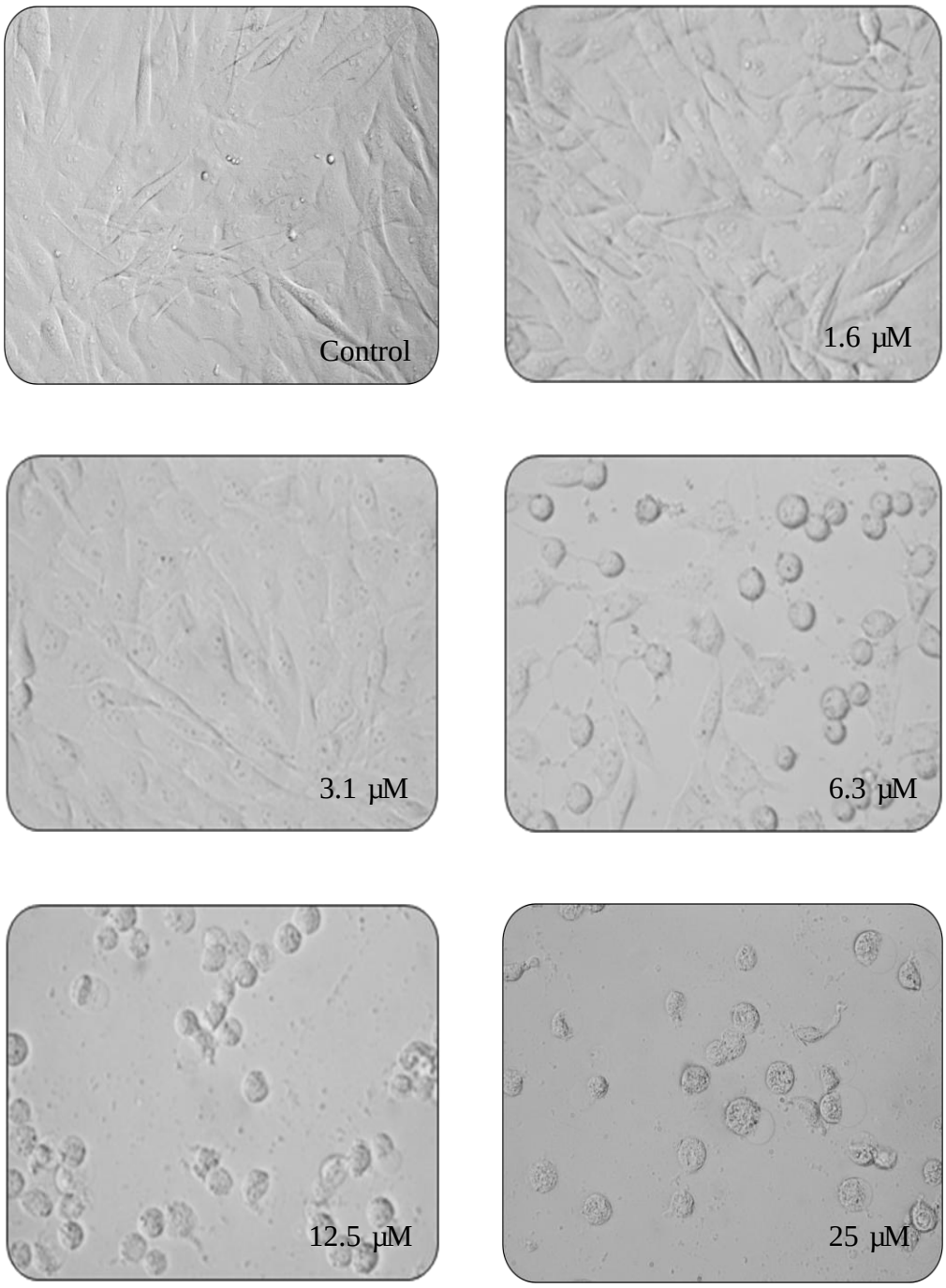

Fig. 4.1(d): Morphological changes in MCF 10A cells treated for 24 h with [Cu(phen)(sar)(H_2O)]NO_3 at different concentrations as compared to untreated cells. (Microscope magnification 400×). All pictures are typical of three independent experiments each performed under identical conditions.

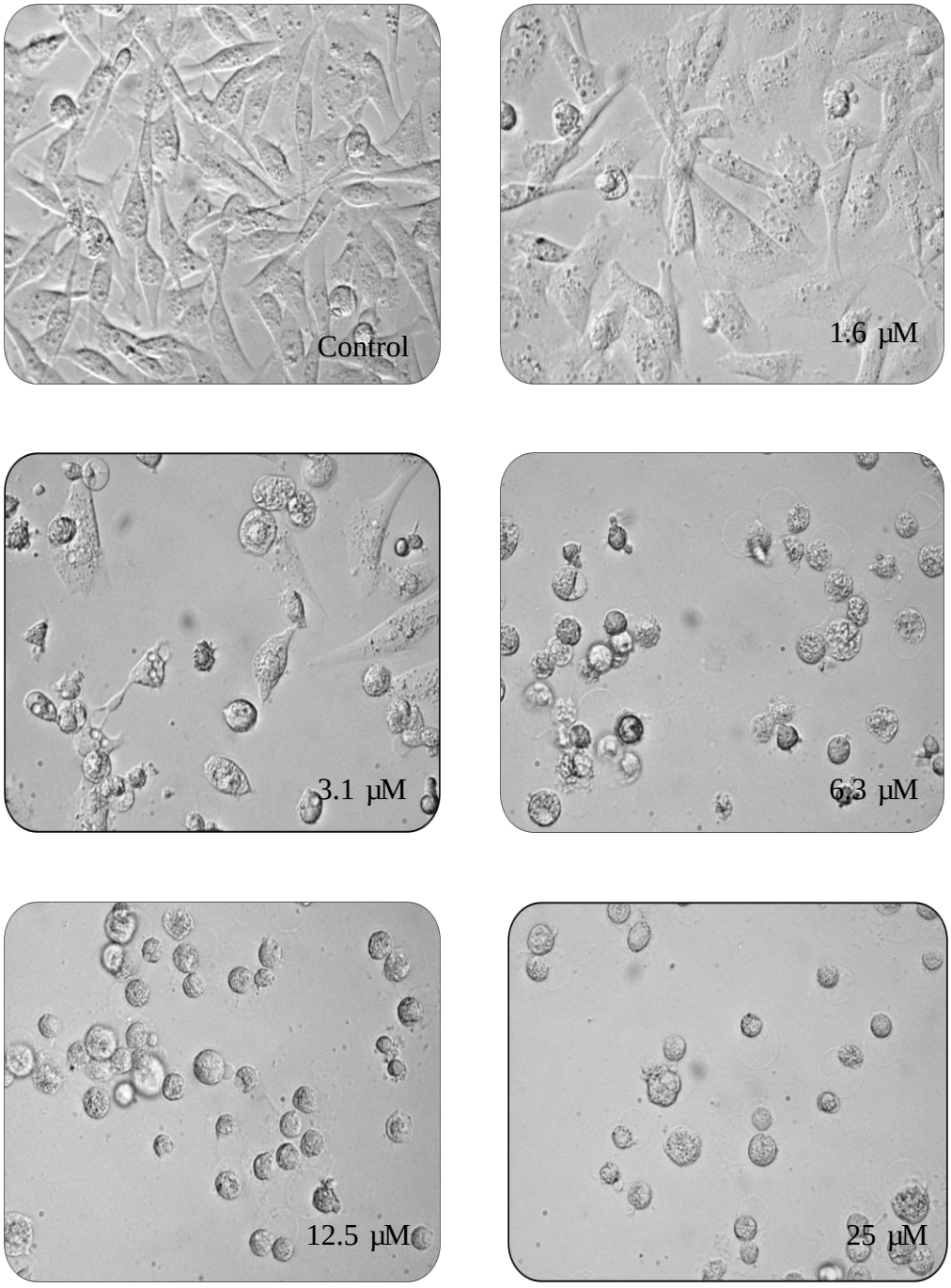

Fig. 4.1(e): Morphological changes in MDA-MB-231 cells treated for 24 h with $[Cu(phen)(gly)(H_2O)]NO_3 \cdot 1.5H_2O$ at different concentrations as compared to untreated cells. (Microscope magnification 400×). All pictures are typical of three independent experiments each performed under identical conditions.

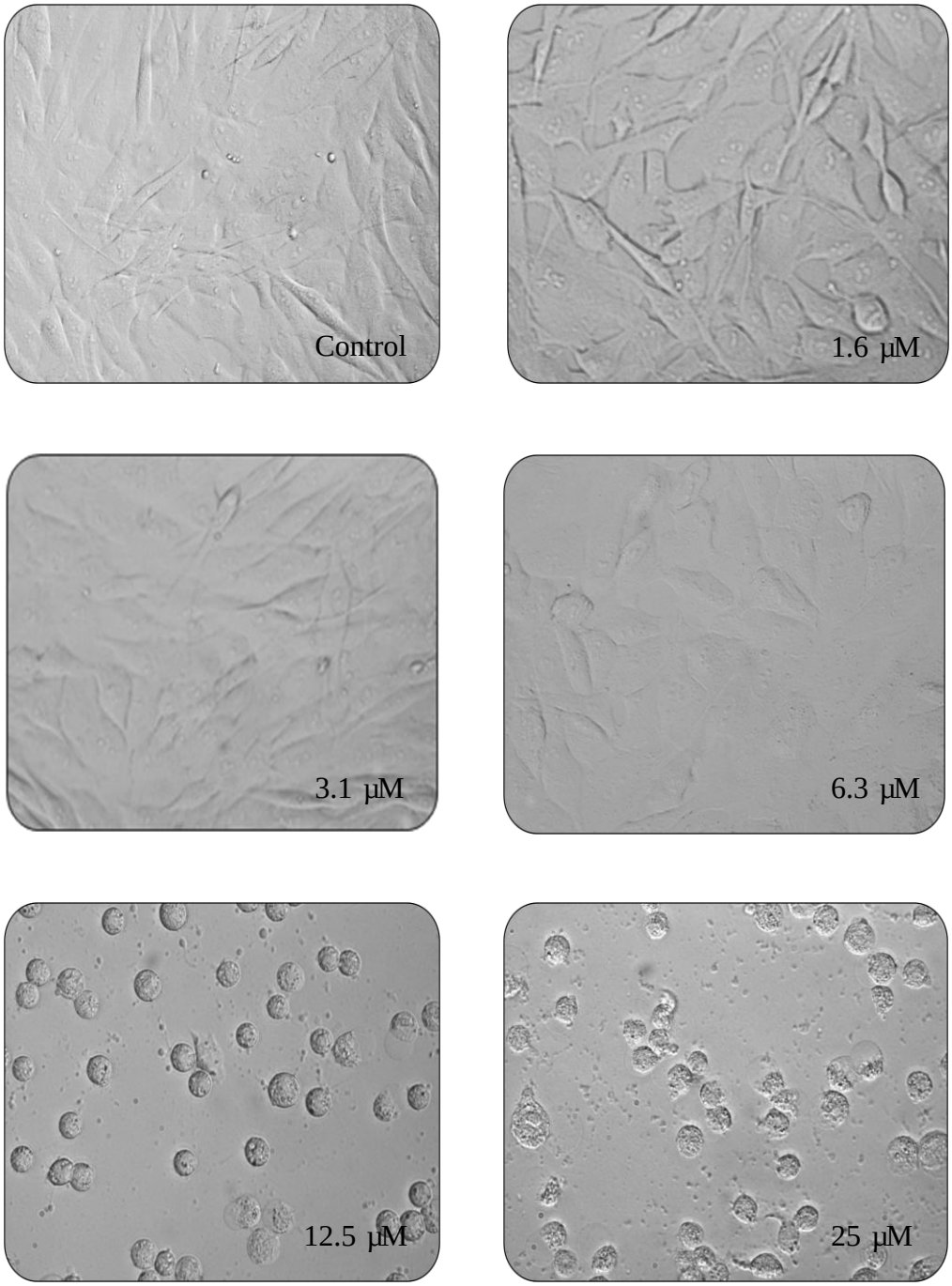

Fig. 4.1(f): Morphological changes in MCF 10A cells treated for 24 h with $[Cu(phen)(gly)(H_2O)]NO_3 \cdot 1.5H_2O$ at different concentrations as compared to untreated cells. (Microscope magnification 400×). All pictures are typical of three independent experiments each performed under identical conditions.

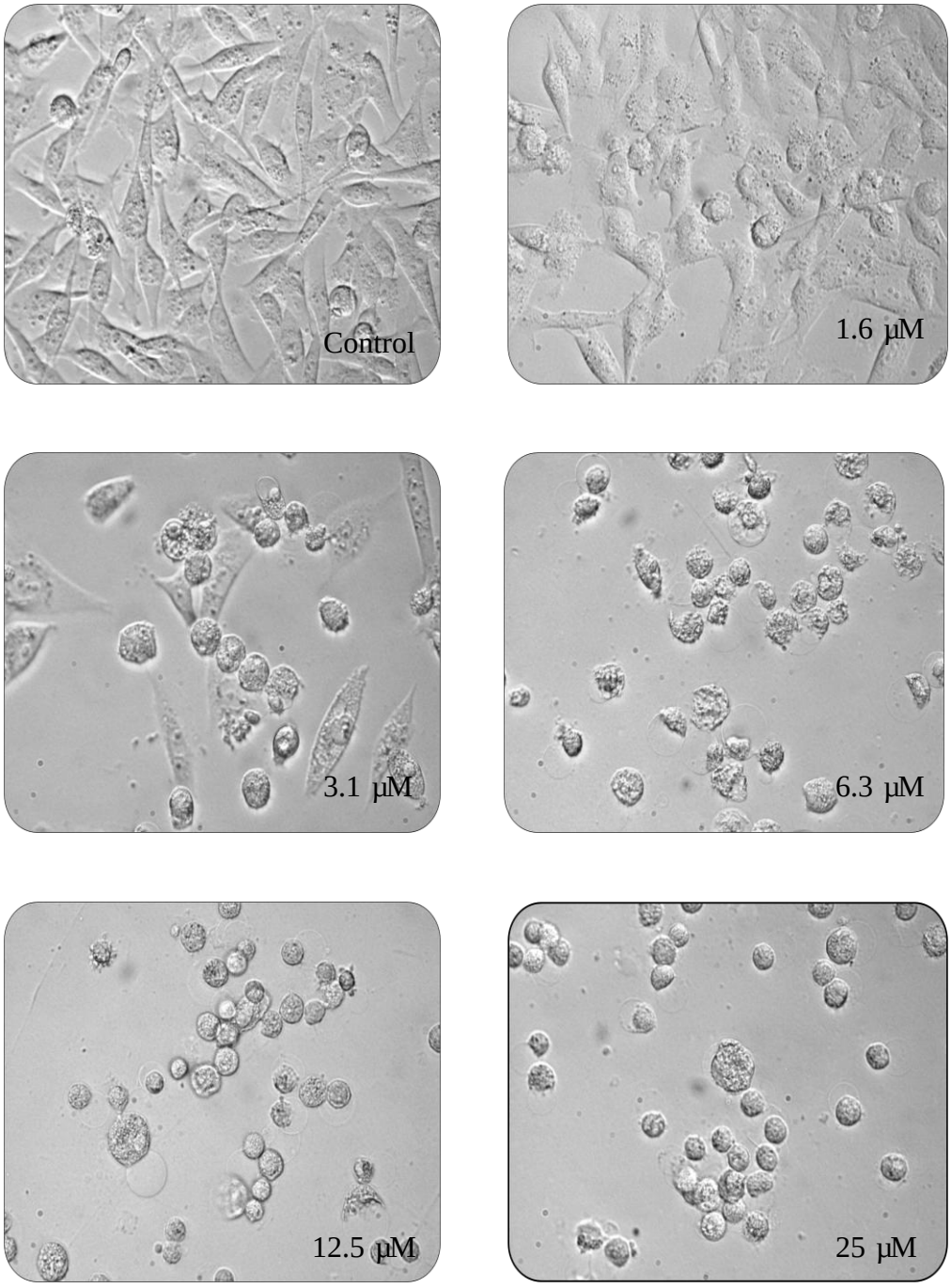

Fig. 4.1(g): Morphological changes in MDA-MB-231 cells treated for 24 h with [Cu(phen)(C-dmg)(H_2O)]NO_3 at different concentrations as compared to untreated cells. (Microscope magnification 400×). All pictures are typical of three independent experiments each performed under identical conditions.

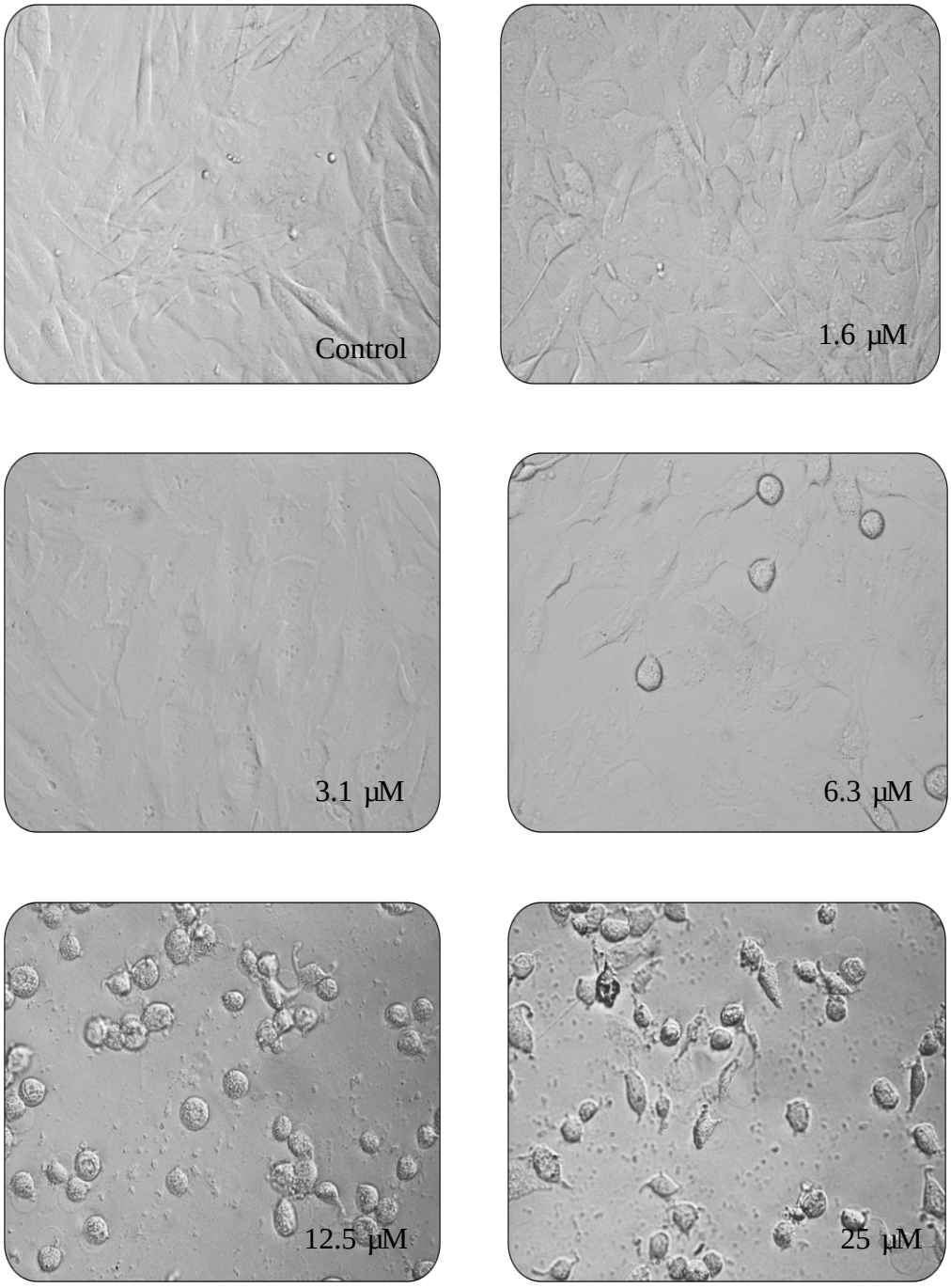

Fig. 4.1(h): Morphological changes in MCF 10A cells treated for 24 h with [Cu(phen)(C-dmg)(H_2O)]NO_3 at different concentrations as compared to untreated cells. (Microscope magnification 400×). All pictures are typical of three independent experiments each performed under identical conditions.

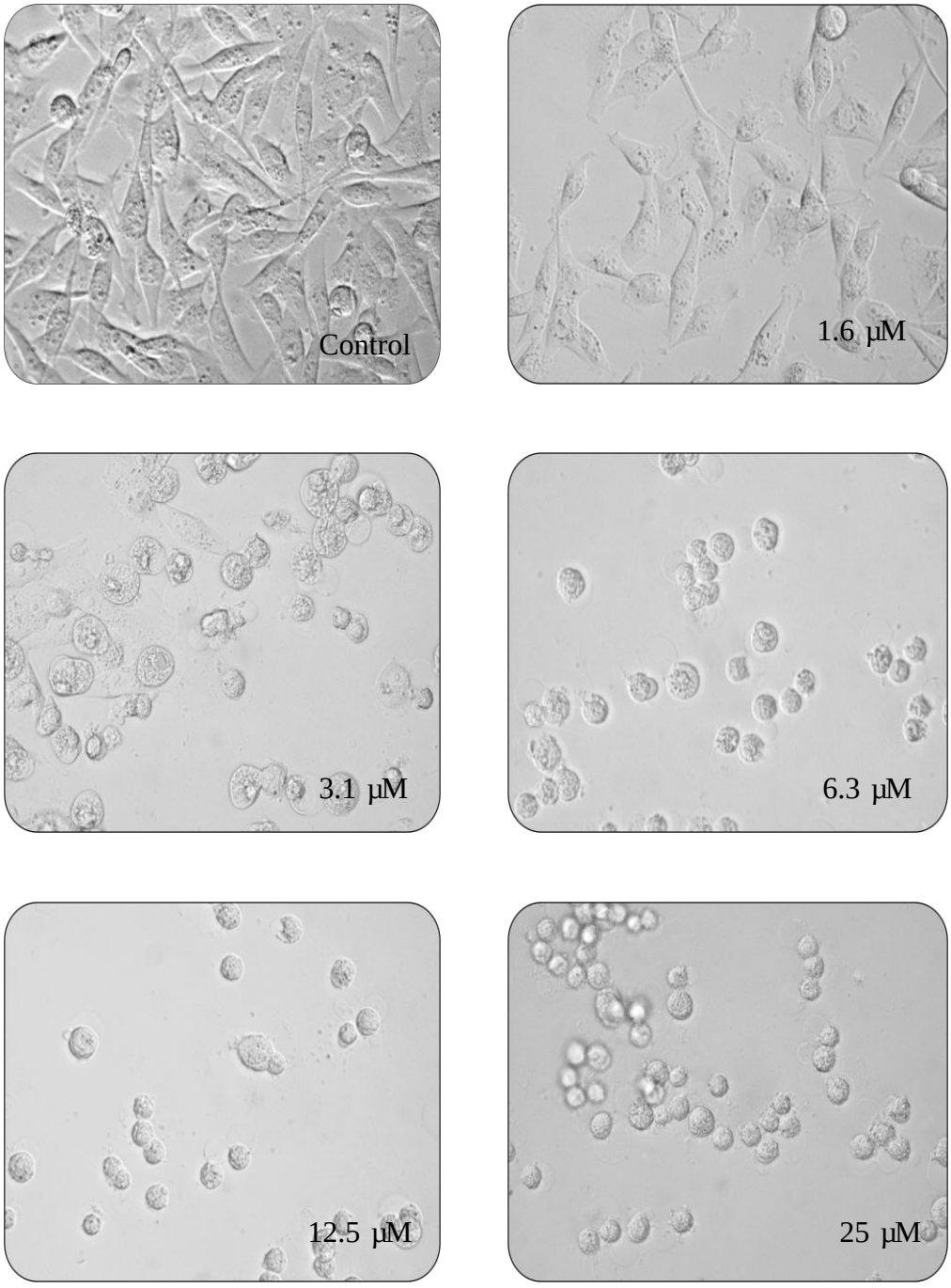

Fig. 4.1(i): Morphological changes in MDA-MB-231 cells treated for 24 h with [$Cu(8OHQ)_2$] at different concentrations as compared to untreated cells. (Microscope magnification 400×). All pictures are typical of three independent experiments each performed under identical conditions.

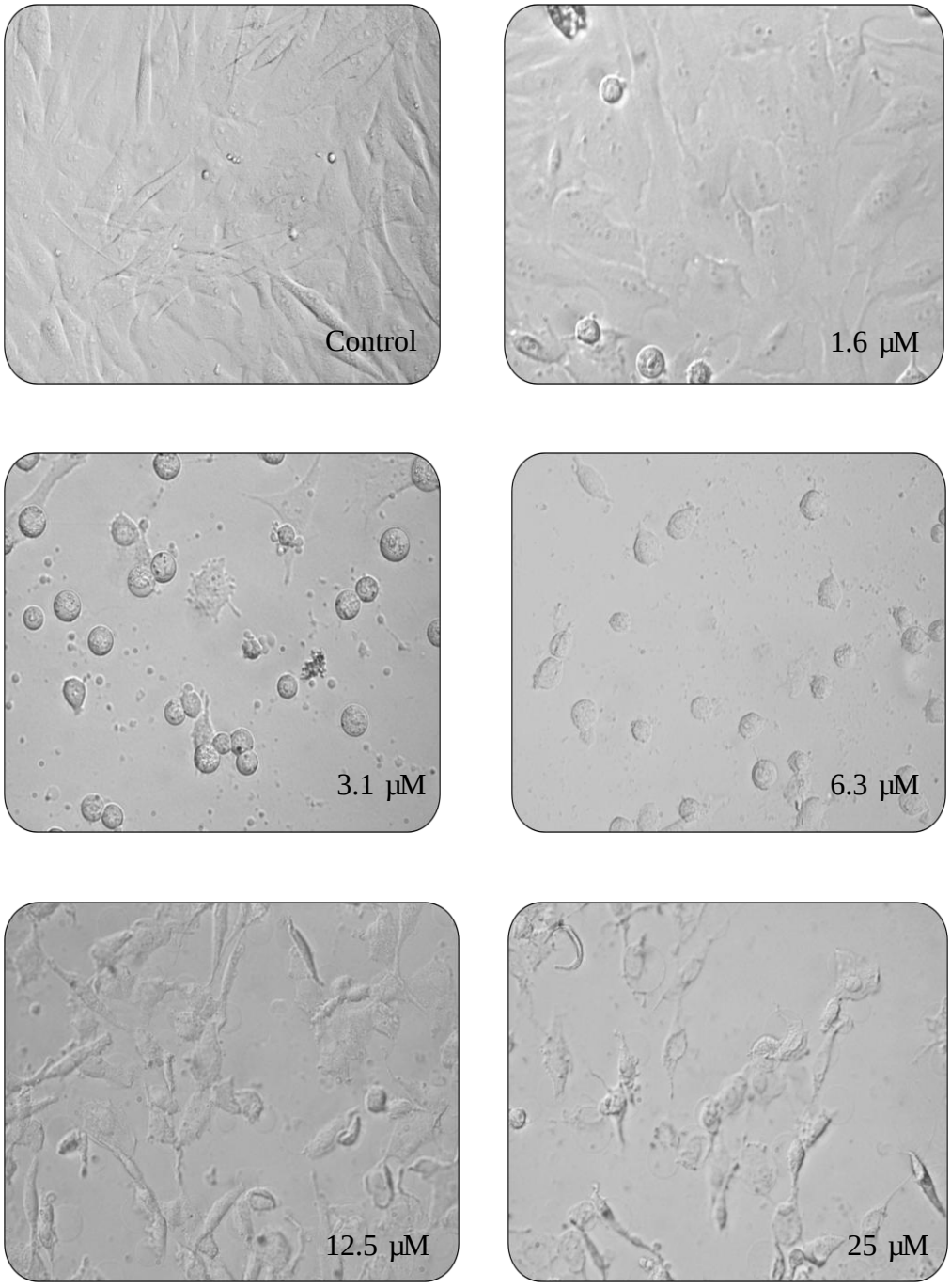

Fig. 4.1(j): Morphological changes in MCF 10A cells treated for 24 h with [Cu(8OHQ)$_2$] at different concentrations as compared to untreated cells. (Microscope magnification 400×). All pictures are typical of three independent experiments each performed under identical conditions.

4.2 The effect of compounds on cell viability measured by MTT assay

For analyzing the antiproliferative effect of ternary copper(II) complexes on cell viability, MTT assay on both cell lines was performed to show their sensitivity and selectivity. MTT assay is associated with cellular proliferation inhibition and the decrease in the percentage of formazan product which is directly related to the increase concentration of the antiproliferative compound. In this study, the tumorigenic human breast cancer cells (MDA-MB-231) and non-tumorigenic human breast epithelial cell line (MCF 10A) were treated with increasing concentration of tested compounds (1 - 25 μM) for 24 h. Figs. 4.2 (a) - (e) illustrated the dose response curves of the series of ternary copper(II) complexes and $[Cu(8OHQ)_2]$ for both cell lines. MTT assay results showed ternary copper(II) complexes mediated dose-dependent decline in the viability of MDA-MB-231 and MCF 10A cell lines.

There was only a slight reduction in cell viability at 1.6 μM compound-treated MDA-MB-231 cells. After that, the cell viability decreased more sharply with every compound from 3.1 to 12.5 μM. Inhibition of the cell growth was greater than 90% when cells were treated with 25 μM of every compound [Figs. 4.2(a) - (e)]. All the ternary copper(II) complexes exhibited similar results for both cell lines. Besides that, the gaps between the dose response curves of both cell lines as shown in the Figs. 4.2(a) – (d) are wider in the concentration range 6.25 to 12.5 μM of the ternary copper(II) complexes. Analysis of the results for $[Cu(phen)(sar)(H_2O)]NO_3$ is described in detail here as an example. For MDA-MB-231 cells treated with

[Cu(phen)(sar)(H_2O)]NO_3, the cell viability is 87% when treated with 3.1 μM and decreased to approximately 10% cell viability at 12.5 μM [Fig. 4.2(b)]. However, the immortalized cells (MCF 10A) were more resistant to the ternary copper(II) complexes. It was observed that 98% and 63% cell viabilities resulted from MCF 10A cells treated with 3.1 and 12.5 μM respectively.

The results of 24 h MTT assay revealed that [Cu(8OHQ)$_2$] (known with anticancer properties compound) employed as control, inhibited equally the cell viability and decreased proliferation of both cell lines in a dose-dependent manner. Cell viabilities for MDA-MB-231 cells treated with 3.1 and 6.3 μM of [Cu(8OHQ)$_2$] were 24% and 4% respectively while corresponding values for MCF 10A treated cells were 17% and 3% respectively [Fig. 4.2(e)]. Antiproliferative results were in agreement with morphological changes observed in Section 4.1 as compound treated cells reacted in a dose-dependent manner.

The antiproliferative property of each compound was determined in the form of IC_{50} concentration (50% growth inhibitory concentration) from Figs. 4.2 (a) - (e). The data of all the compounds are tabulated in Table 4.1. Interestingly, IC_{50} of [Cu(phen)(gly)(H_2O)]NO_3·1.5H_2O in MDA-MB-231 cell is 8.5 μM ± 0.3 and those for all the ternary copper(II) compounds with methylated glycine derivatives (DL-ala, Sar, C-dmg) are 5.5 μM ± 1.1, 5.2 μM ± 0.2 and 6.2 μM ± 1.1, respectively. They have slightly lower IC_{50} values compared to glycinate compound. In contrast, the IC_{50} values of ternary

copper(II) complexes in MCF 10A ranged from 14 -17 μM and are higher than in MDA-MB-231 (5 - 9 μM). Therefore, ternary copper(II) compounds with methylated glycine derivatives are considered more antiproliferative than $[Cu(phen)(gly)(H_2O)]NO_3 \cdot 1.5H_2O$. On the other hand, $[Cu(8OHQ)_2]$ served as a positive control in this assay. The IC_{50} value for the MCF 10A treated with $[Cu(8OHQ)_2]$ is 1.7 μM ± 0.4 lower than that for MDA-MB-231 (2.7 μM ± 0.2) and this difference is statistically significant. P value for the percentage of MDA-MB-231 and MCF 10A cell viability is less than 0.05. Table 4.1 shown that the IC_{50} values from the dose response curve which were obtained from the three independent experiments. IC_{50} values was calculated based on the data of each of independent experiment (also see Appendix A). The IC_{50} trend of values for $[Cu(8OHQ)_2]$ is the reverse.

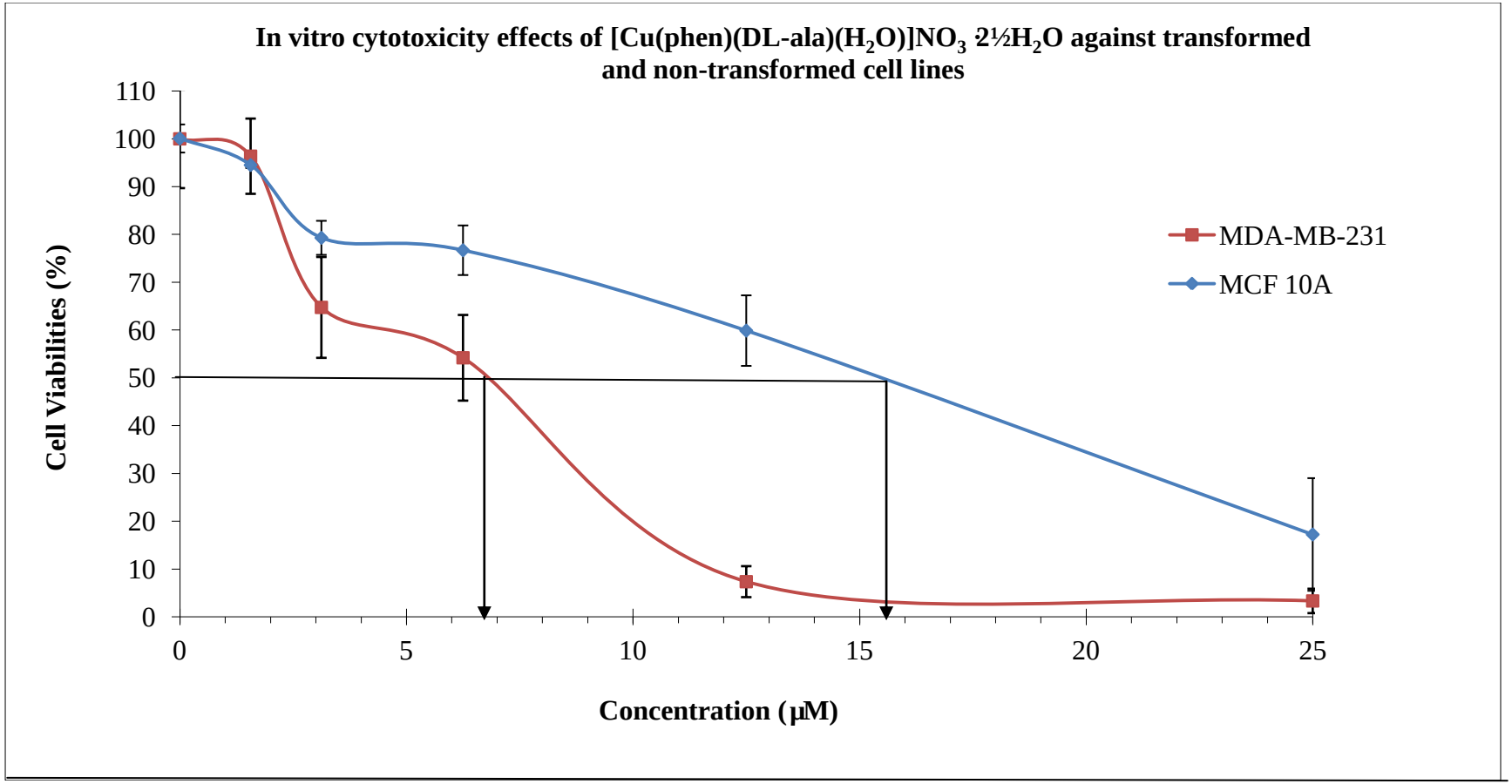

Fig. 4.2(a): Dose response curves of the antiproliferative activity (% cell viability) of [Cu(phen)(DL-ala)(H_2O)]NO_3 2½H_2O, in MDA-MB-231 and MCF 10A cells at 24 h. Cell viability is expressed as relative activity of control cells (100%). Results are shown represent one experiment and error bars show the S.D.

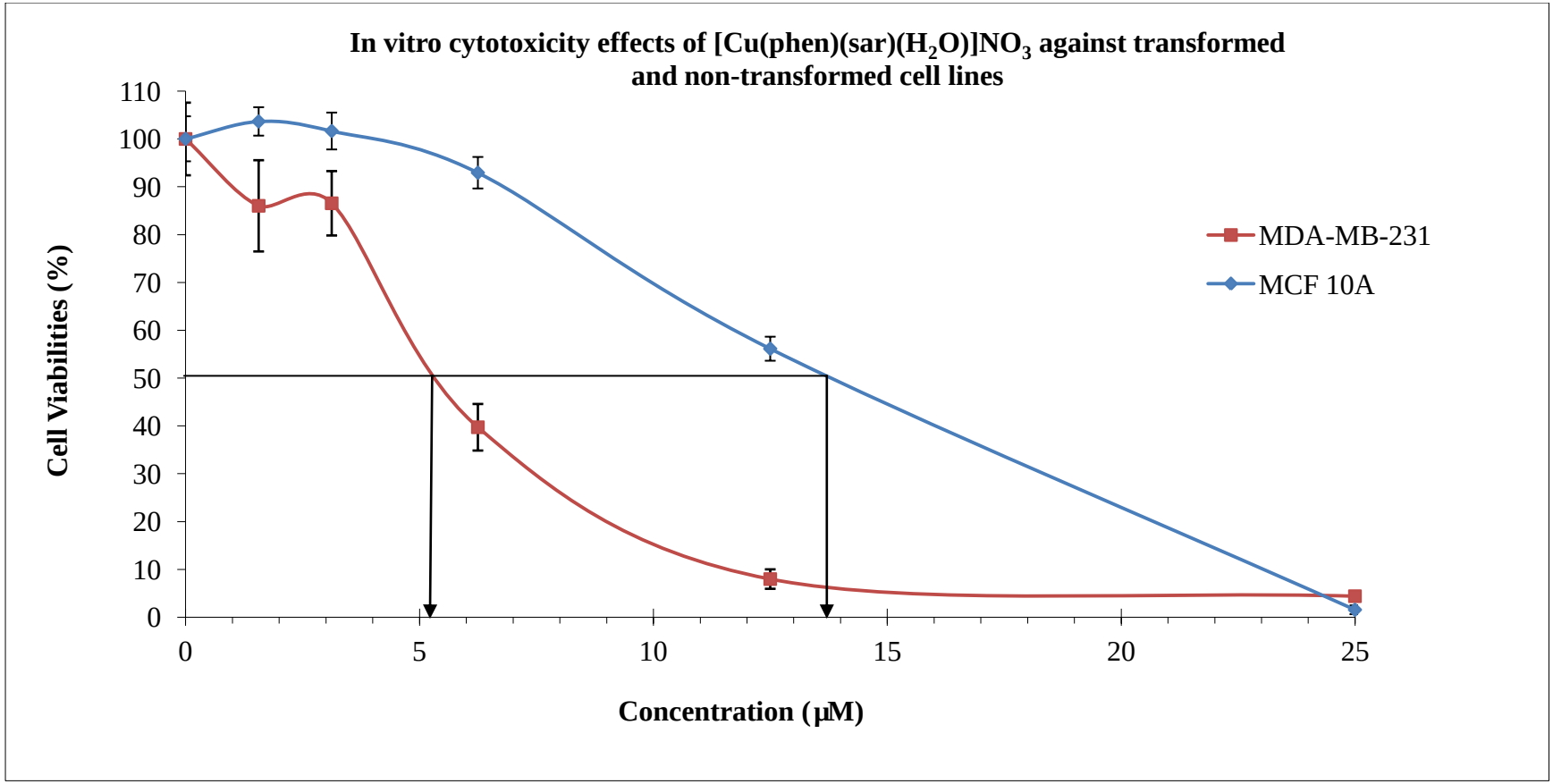

Fig. 4.2(b): Dose response curves of the antiproliferative activity (% cell viability) of $[Cu(phen)(sar)(H_2O)]NO_3$ in MDA-MB-231 and MCF 10A cells at 24 h. Cell viability is expressed as relative activity of control cells (100%). Results are shown represent one experiment and error bars show the S.D.

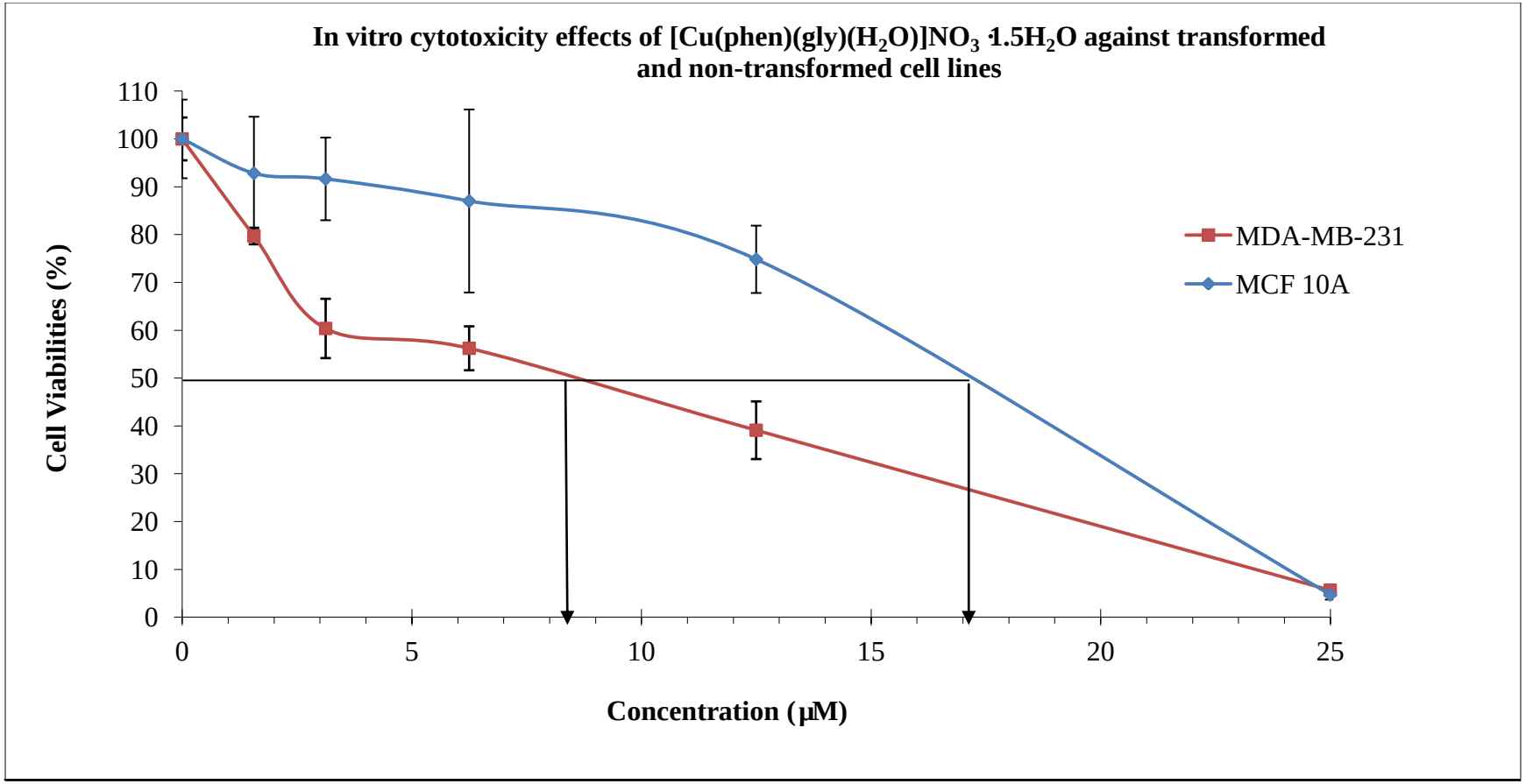

Fig. 4.2(c): Dose response curves of the antiproliferative activity (% cell viability) of $[Cu(phen)(gly)(H_2O)]NO_3 \cdot 1.5H_2O$ in MDA-MB-231 and MCF 10A cells at 24 h. Cell viability is expressed as relative activity of control cells (100%). Results are shown represent one experiment and error bars show the S.D.

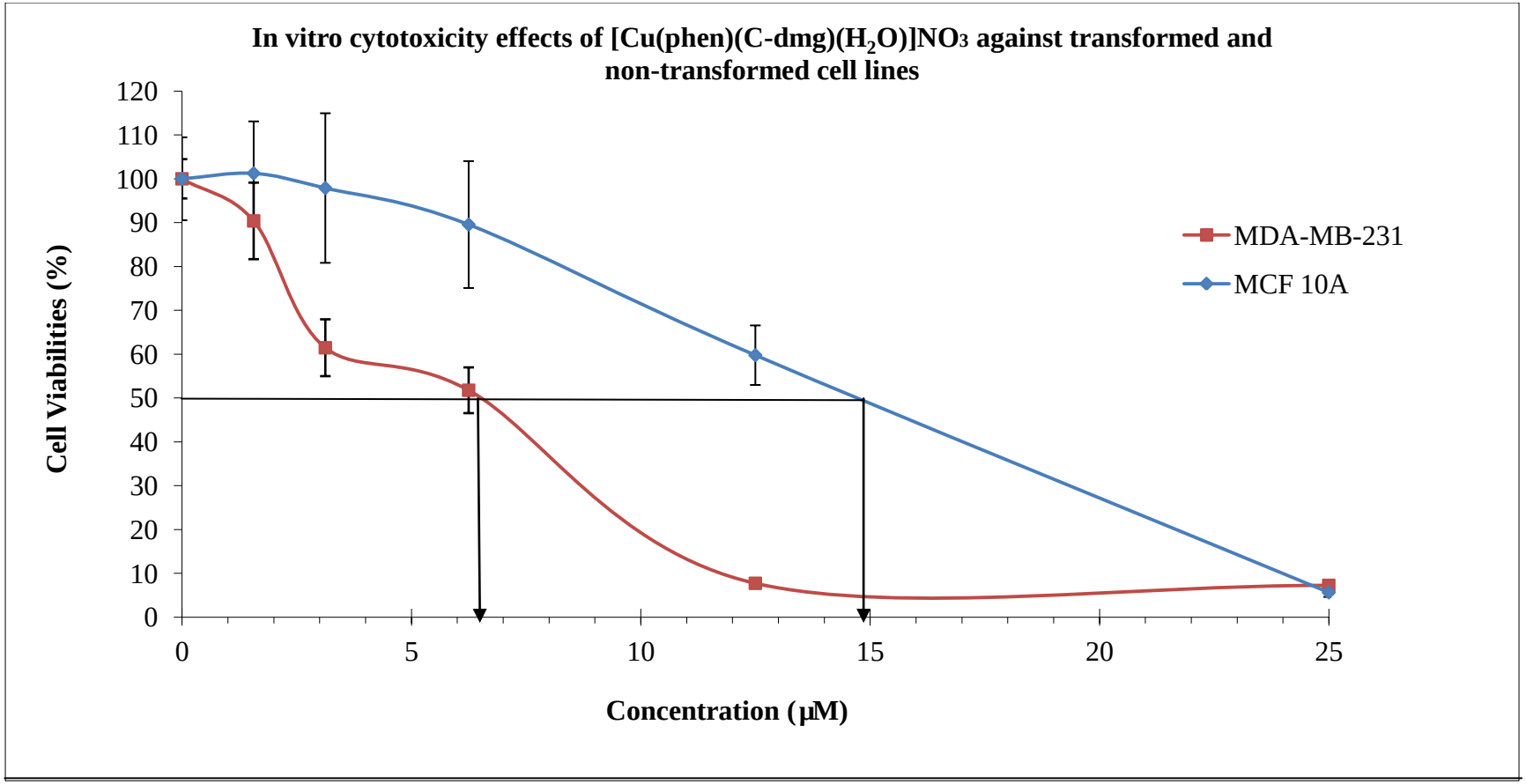

Fig. 4.2(d): Dose response curves of the antiproliferative activity (% cell viability) of $[Cu(phen)(C\text{-}dmg)(H_2O)]NO_3$ in MDA-MB-231 and MCF 10A cells at 24 h. Cell viability is expressed as relative activity of control cells (100%). Results are the mean of at least three independent experiments and error bars show the S.D.

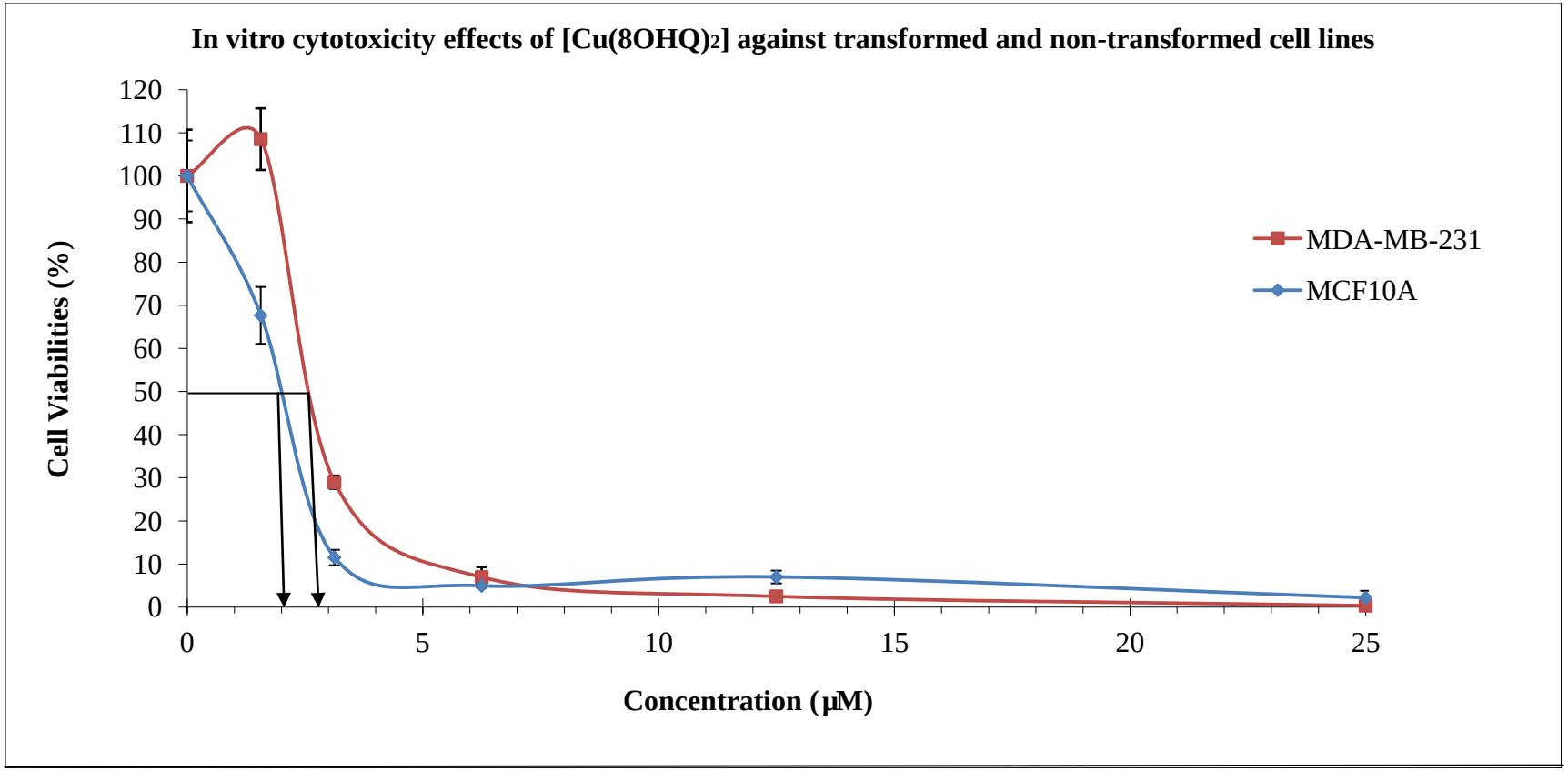

Fig. 4.2(e): Dose response curves of the antiproliferative activity (% cell viability) of [Cu(8OHQ)$_2$] in MDA-MB-231 and MCF 10A cells at 24 h. Cell viability is expressed as relative activity of control cells (100%). Results are shown represent one experiment and error bars show the S.D.

Table 4.1: IC_{50} values (μM) for proliferation inhibition by ternary copper(II) complexes for 24 h treatment. IC_{50} values were calculated from dose-response curves. Data are mean ± S. D.

Compounds	IC_{50} (μM)	
	MDA-MB-231	MCF10A
$[Cu(phen)(DL\text{-}ala)(H_2O)]NO_3 \cdot 2½H_2O$	5.5 ± 1.1	13.9 ± 2.1
$[Cu(phen)(sar)(H_2O)]NO_3$	5.2 ± 0.2	16.5 ± 2.3
$[Cu(phen)(gly)(H_2O)]NO_3 \cdot 1.5H_2O$	8.5 ± 0.3	15.8 ± 0.6
$[Cu(phen)(C\text{-}dmg)(H_2O)]NO_3$	6.2 ± 1.1	15.1 ± 1.6
$[Cu(8OHQ)_2]$	2.7 ± 0.2	1.7 ± 0.4

4.3 Analysis of apoptosis by flow cytometry

The potential of ternary copper(II) complexes-induced cell death in adherent MDA-MB-231 and MCF 10A cells was quantitatively examined by apoptosis assay using annexin V-FITC/PI double staining. Cells were treated for 24 h with 5 μM of compounds and 10000 cells were analysed by the flow cytometer. The number of apoptotic cells was calculated by adding the percentage of cells with early apoptotic cells (lower right) to late apoptotic cells (upper right). The mean of three independent experiments results are shown as bar charts Fig. 4.4. However, data in Figs. 4.3(a) - (b) are representative of three independent experiments.

Very low percentage of apoptotic cells were detected in the untreated MDA-MB-231 cells as well as in untreated MCF 10A demonstrating normal cell viability (Fig. 4.4). Treatment of MDA-MB-231 cells with 5 μM [Cu(phen)(DL-ala)(H_2O)]NO_3·2½H_2O, [Cu(phen)(sar)(H_2O)]NO_3, [Cu(phen)(gly)(H_2O)]NO_3·1.5H_2O, [Cu(phen)(C-dmg)(H_2O)]NO_3 resulted in 46.33, 56.84, 41.14, 55.64% apoptotic cells (Fig. 4.4). Further analysis of flow cytometric data clearly showed treatment with ternary copper(II) complexes increased cell death more than fourfold relative to untreated for MDA-MB-231 cells. On the contrary, the percentage of apoptotic cells for compound-treated MCF 10A ranged from 7 to 10%, which are comparable to that found for untreated cells (Fig. 4.4). Therefore, no increase in apoptotic cells was observed in MCF 10A cells treated with ternary copper(II) complexes.

[$Cu(8OHQ)_2$] treatment of both cell lines resulted in approximately 90% apoptotic cells [Fig.4.2(e)]. As depicted in Figs. 4.3(a) - (b), cells treated with 5 μM [$Cu(8OHQ)_2$] became 90.21% apoptotic in MDA-MB-231 and 94.64% apoptotic in MCF 10A. [$Cu(8OHQ)_2$] exhibited similar high cytotoxicity towards both cell lines. For 24 h exposure, there was significant induced apoptosis in ternary copper(II) complexes treated MDA-MB-231 cells compared to untreated cells. In contrast, there was insignificant induced apoptosis in the immortalized MCF 10A cells treated with 5 μM of these compounds (Fig. 4.4).

(a)Untreated

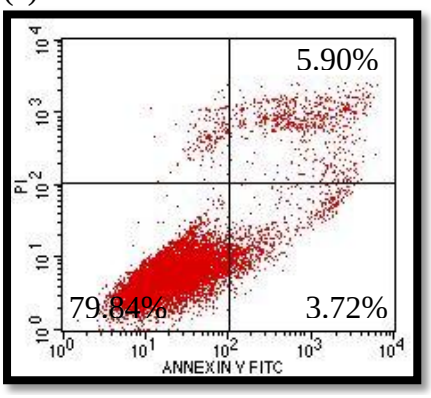

(b)[Cu(phen)(DL-ala)(H_2O)]NO_3 ·2½H_2O

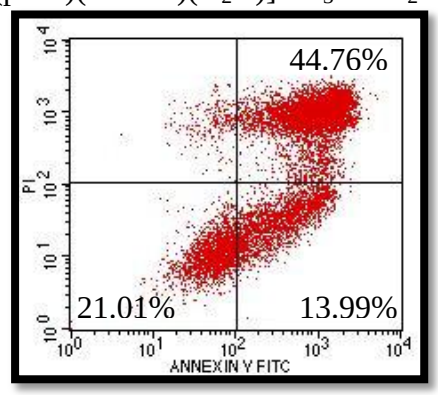

(c)[Cu(phen)(sar)(H_2O)]NO_3

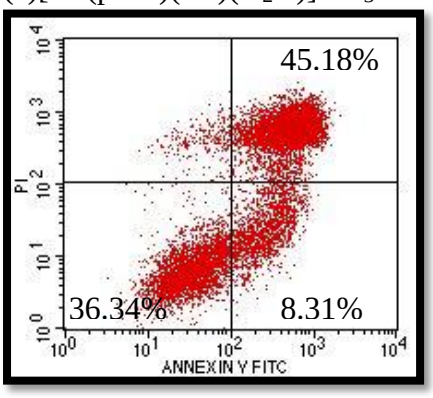

(d)[Cu(phen)(gly)(H_2O)]NO_3 ·1.5H_2O

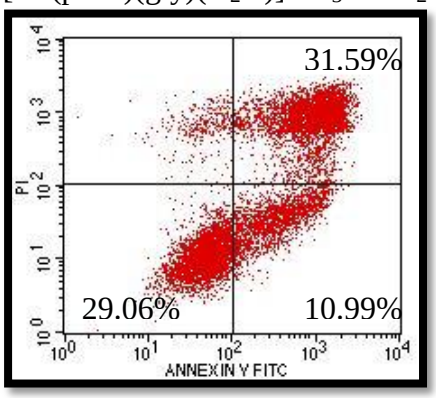

(e)[Cu(phen)(C-dmg)(H_2O)]NO_3

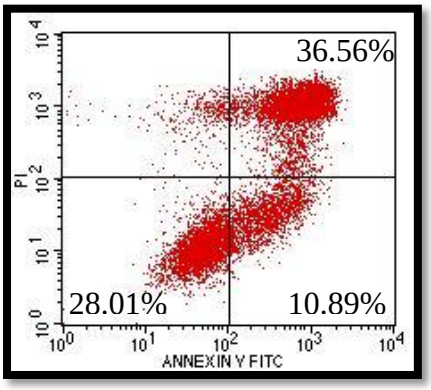

(f)[Cu(8OHQ)$_2$]

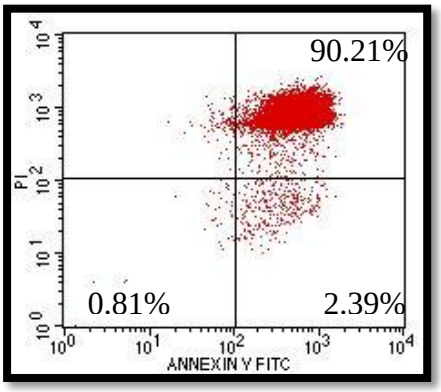

Fig. 4.3(a): A comparison between untreated and treated MDA-MB-231 cells in expression of apoptosis after incubation with 5 μM ternary copper(II) complexes for 24 h by flow cytometry analysis. Percentage of total cells is shown for each quadrant. Results are representative of three independent experiments.

(a)Untreated

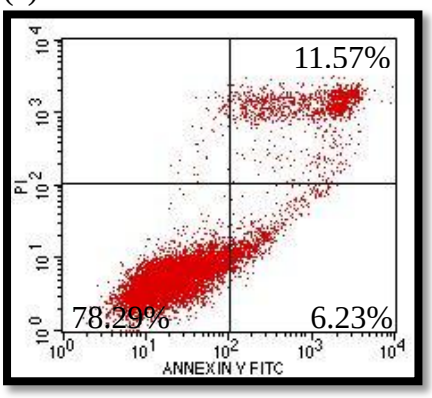

(b)[Cu(phen)(DL-ala)(H_2O)]NO_3 ·2½H_2O

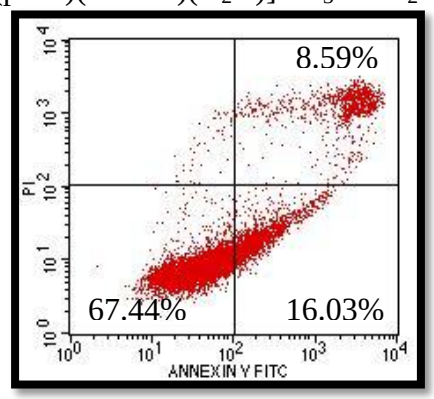

(c)[Cu(phen)(sar)(H_2O)]NO_3

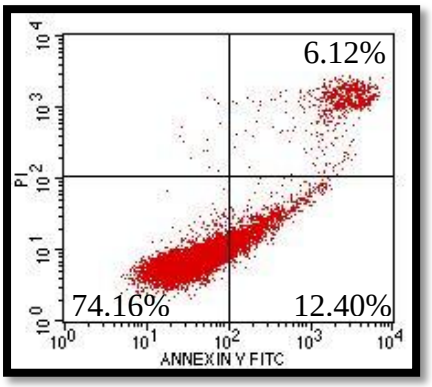

(d)[Cu(phen)(gly)(H_2O)]NO_3 ·1.5H_2O

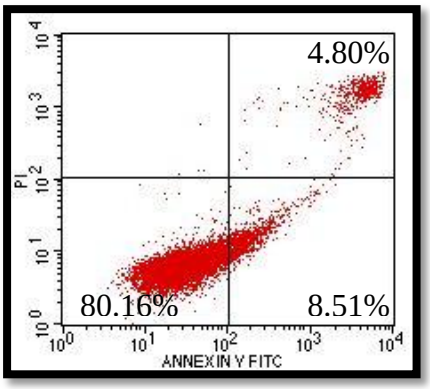

(e)[Cu(phen)(C-dmg)(H_2O)]NO_3

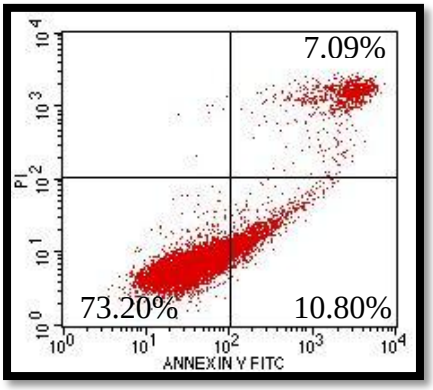

(f)[Cu(8OHQ)$_2$]

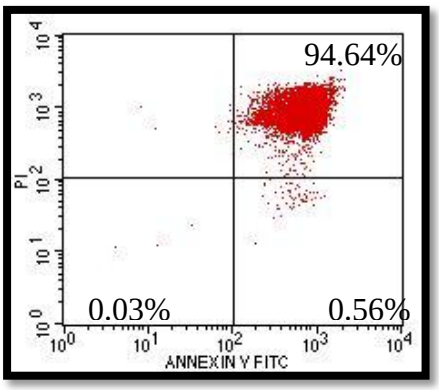

Fig. 4.3(b): A comparison between untreated and treated MCF 10A cells in expression of apoptosis after incubation with 5 μM ternary copper(II) complexes for 24 h by flow cytometry analysis. Percentage of total cells is shown for each quadrant. Results are representative of three independent experiments.

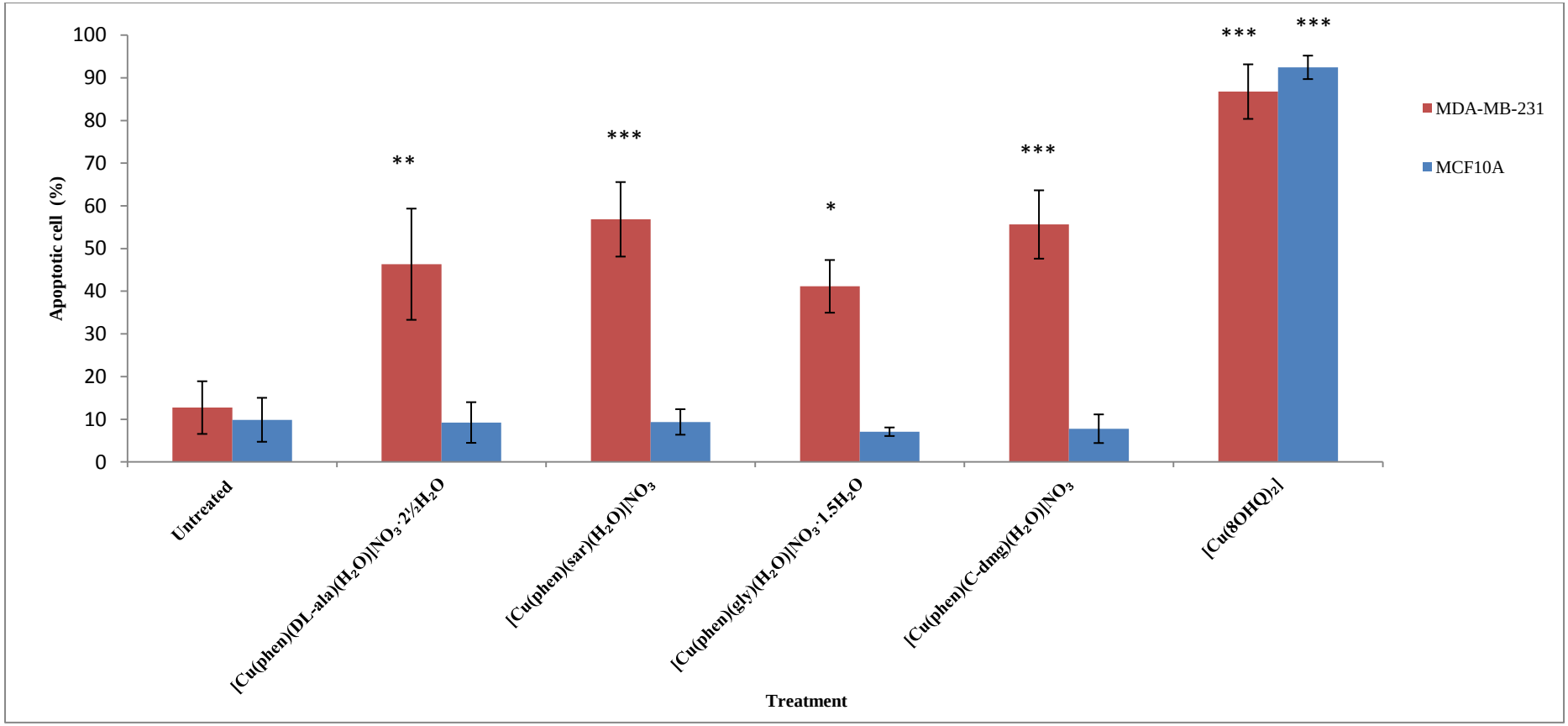

Fig 4.4: Percentage of apoptotic cells after treatment with 5 µM ternary copper(II) complexes and $[Cu(8OHQ)_2]$ for 24 h in MDA-MB-231 and MCF 10A cell lines. Results are the mean of three independent experiments and error bars show the S. D. * = ($p < 0.05$), ** = ($p < 0.01$), *** = ($p < 0.005$) indicates significantly different from untreated.

4.4 Effect of ternary copper(II) complexes on cell cycle

The effects on cell cycle distribution of ternary copper(II) complexes were examined by flow cytometry after staining of cells with propidium iodide. MDA-MB-231 and MCF 10A cells were treated with 5 μM ternary copper(II) complexes for 24 h. The percentage of cells in each phase of the cell cycle G_0/G_1, S and G_2/M was determined by using Modfit LT software (Verity Software House, Topsham, ME).

Figures. 4.5(a) - (b) showed distribution of cells in three major phases of the cycle (G_0/G_1, S, G_2/M) in DNA historgram of MDA-MB-231 cells and MCF 10A cells after treatment 24 h with 5 μM ternary copper(II) complexes. Fig. 4.6(a) compares the average percentage of cells in different phases for MDA-MB-231 cells treated with ternary copper(II) complexes with those of untreated cells. As depicted in Fig. 4.6(a), G_0/G_1, S phase and G_2/M of untreated MDA-MB-231 cells were 56.28% ± 2.5 (mean ± S. D.), 33.98% ± 2.5 and 9.73% ± 0.2 respectively. For MDA-MB-231 cells treated with [Cu(phen)(DL-ala)(H_2O)]NO_3 2½H_2O, the percentage of cell population at G_0/G_1 phase increased to 69.34% ± 2.7 but those at S phase and G_2/M decreased to 26.06% ± 3.1 and 4.6% ± 0.4 respectively. This indicated that [Cu(phen)(DL-ala)(H_2O)]NO_3 2½H_2O induced cell cycle arrest at G_0/G_1. Treatment with all ternary copper(II) complexes resulted in a rise in the percentage of cells in G_0/G_1 with a concomitant decrease in the percentage S phase and G_2/M phase in MDA-MB-231 [Fig. 4.6(a)]. Similar results were obtained with other ternary copper(II) complexes.

The results for the immortalized breast cell line, MCF 10A, are different. The percentage of cells in G_0/G_1, S and G_2/M phases for cells treated with 5 μM ternary copper(II) complexes are comparable to those for untreated cells [Fig. 4.6(b)]. Thus, the copper(II) complexes did not affect the cell cycle of MCF10A cells, i.e. there is no cell cycle arrest, for 24 h incubation.

(a)Untreated

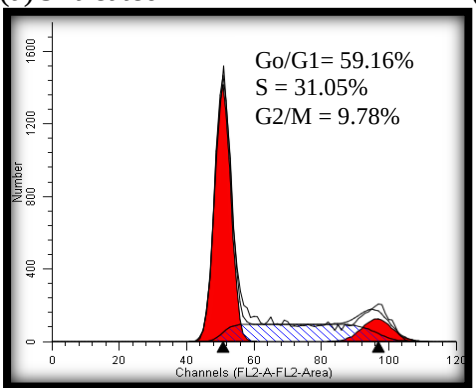

(b)[Cu(phen)(DL-ala)(H_2O)]NO_3 ·2½H_2O

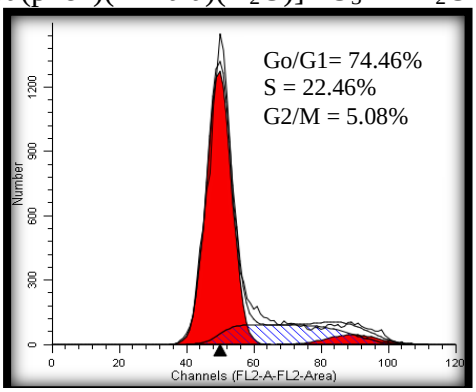

(c)[Cu(phen)(sar)(H_2O)]NO_3

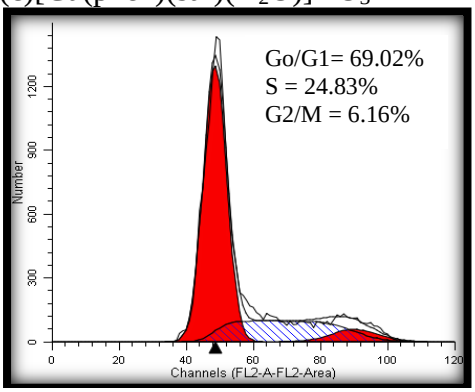

(d)[Cu(phen)(gly)(H_2O)]NO_3 ·1.5H_2O

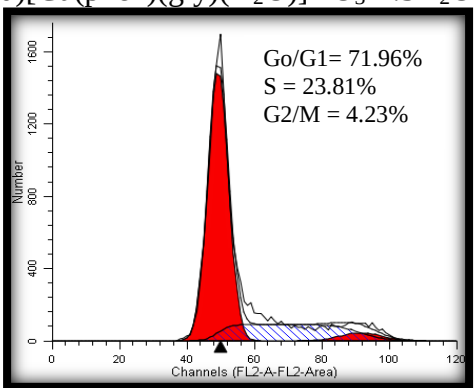

(e)[Cu(phen)(C-dmg)(H_2O)]NO_3

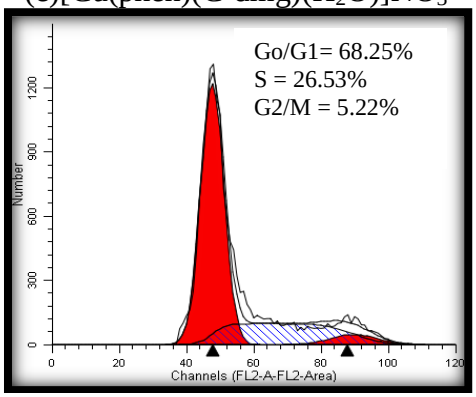

Fig. 4.5(a): DNA histograms from MDA-MB-231cells treated with 5 µM ternary copper(II) complexes, harvested at 24 h. Untreated and treated cells were stained with propidium iodide, measured by FACSCalibur and cell phase distributions were determined using the ModFit software. Results are representative of three independent experiments.

(a)Untreated

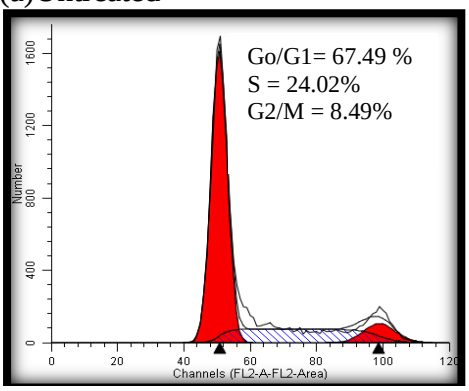

(b)[Cu(phen)(DL-ala)(H_2O)]NO_3 ·2½H_2O

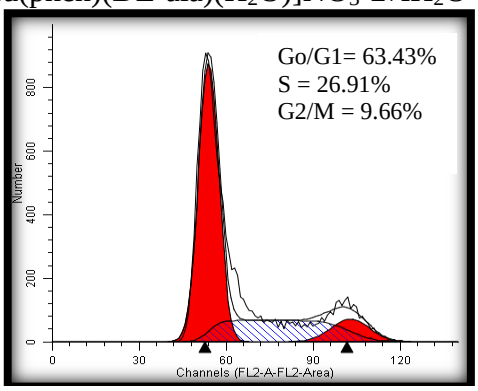

(c)[Cu(phen)(sar)(H_2O)]NO_3

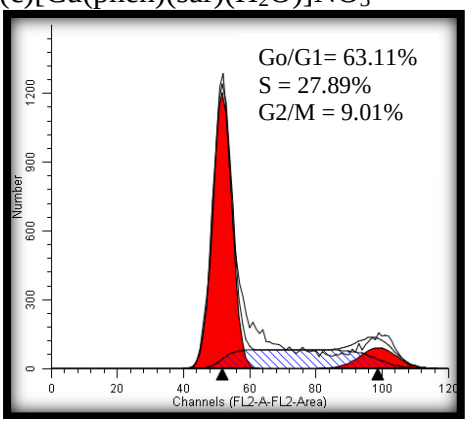

(d)[Cu(phen)(gly)(H_2O)]NO_3 ·1.5H_2O

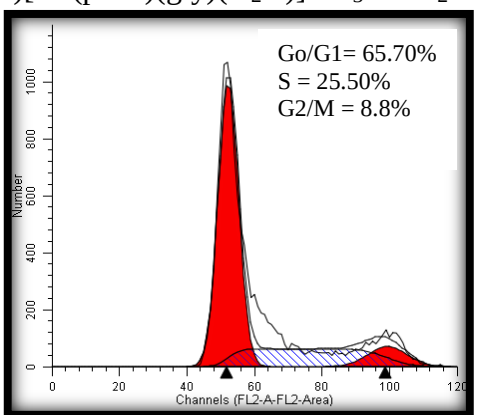

(e)[Cu(phen)(C-dmg)(H_2O)]NO_3

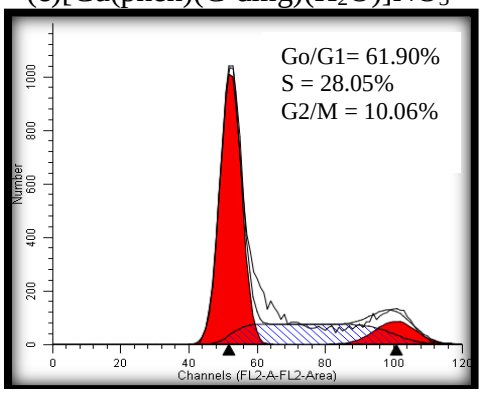

Fig. 4.5(b): DNA histograms from MCF 10A treated with 5 µM ternary copper(II) complexes, harvested at 24 h. Untreated and treated cells were stained with propidium iodide, measured by FACSCalibur and cell phase distributions were determined using the ModFit software. Results are representative of three independent experiments.

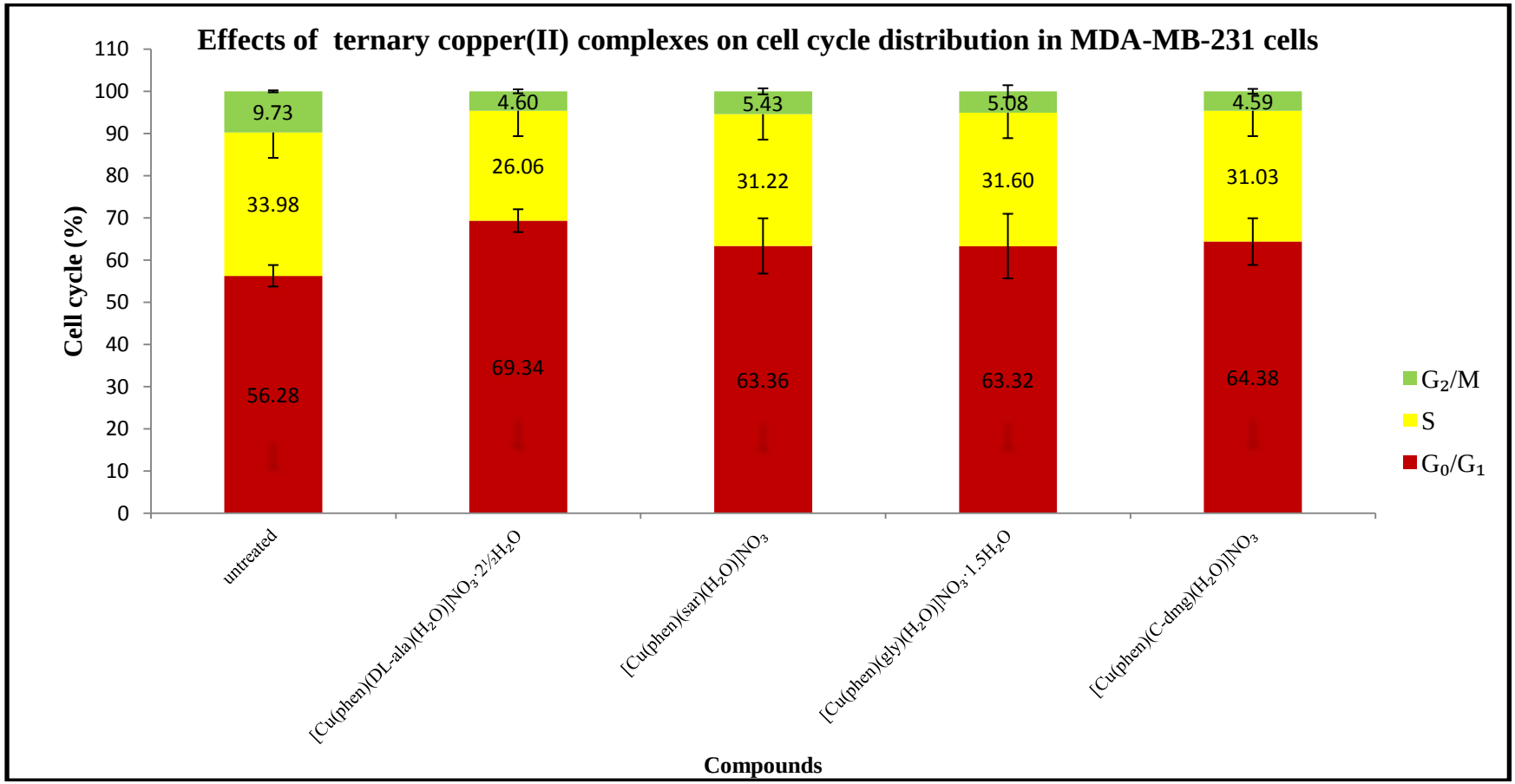

Fig. 4.6(a): Cell cycle distribution of MDA-MB-231 cells in the absence or presence of 5 μM ternary copper(II) complexes at 24 h. Data are presented as means of the percentage of cells in G_0/G_1, S or G_2/M phase from three independent experiments with S.D.

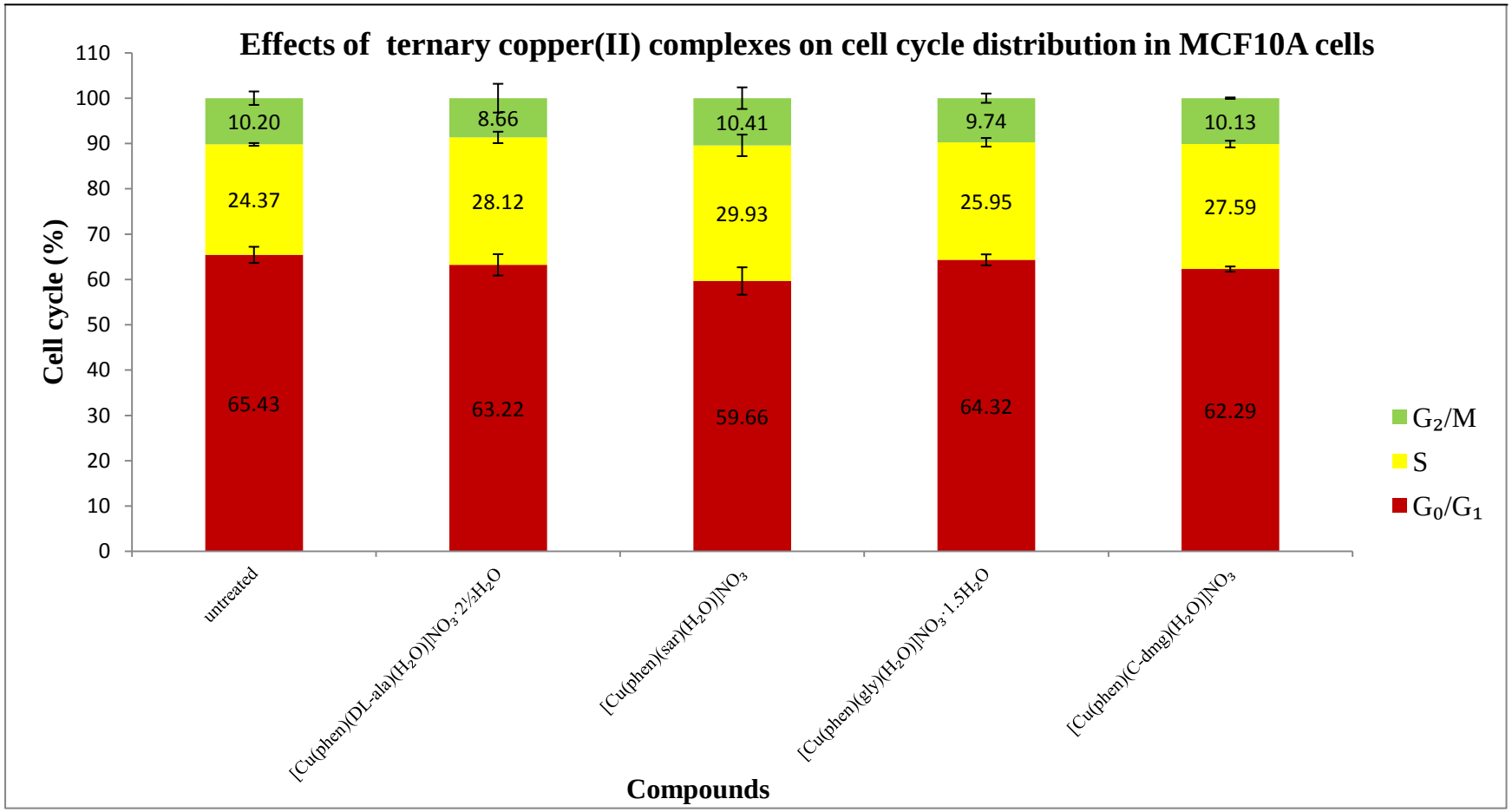

Fig. 4.6(b): Cell cycle distribution of MCF 10A cells in the absence or presence of 5 µM ternary copper(II) complexes at 24 h. Data are presented as means of the percentage of cells in G_0/G_1, S or G_2/M phase from three independent experiments with S.D.

Table 4.2: Statistical analysis of the cell cycle analysis after cells treated with ternary copper(II) complexes at 24 h. * = ($p < 0.05$), ** = ($p < 0.01$), *** = ($p < 0.005$) indicates significantly different from untreated. NS = non-significant.

	MDA-MB-231 cells			MCF10A cells		
	G_0/G_1 phase	S phase	G_2/M phase	G_0/G_1 phase	S phase	G_2/M phase
Untreated vs [Cu(phen)(DL-ala)(H2O)]NO_3 ·2½H_2O	**	*	***	NS	**	NS
Untreated vs [Cu(phen)(sar)(H_2O)]NO_3	NS	NS	***	*	***	NS
Untreated vs [Cu(phen)(gly)(H_2O)]NO_3 ·1.5H_2O	NS	NS	***	NS	NS	NS
Untreated vs [Cu(phen)(C-dmg)(H_2O)]NO_3	*	NS	***	NS	*	NS

4.5 Proteasome inhibition

To elucidate whether ternary copper(II) complexes could induce inhibition of proteasome activity *in vitro*, western blot analysis was performed. MDA-MB-231 cells were treated with 1 μM and 10 μM of each compound for 24 h, followed by Western blotting using specific antibodies to ubiquitin, IκB-α and β-actin. β-actin was used as a loading control. All the ternary copper(II) complexes inhibited the proteasome activity in a concentration-dependent manner as shown in Fig. 4.7(a).

Fig. 4.7(a) shows higher intensity and accumulation of ubiquitinated proteins from cells treated with higher concentration (10 μM) for all four ternary copper(II) complexes. According to lane 1, a very low intensity of ubiquitinated proteins was observed in the absence of treatment. The greater intensity band in lane 11 indicates [$Cu(8OHQ)_2$] is good proteasomal inhibitor in MDA-MB-231 cells, in agreement with similar reported results (Daniel *et al.*, 2004; Milacic *et al*., 2009).

Cells treated with lower concentration (1 μM) of ternary copper(II) complexes showed results similar to that of the untreated cells. The levels of ubiquitinated proteins after 10 μM ternary copper(II) complexes treatment in MDA-MB-231 cells are similar with [$Cu(8OHQ)_2$], a well-known proteasome inhibitor which serves as control. This data suggest that treatment with sufficient ternary copper(II) complexes can lead to accumulation of ubquitinated proteins and contribute to proteasome inhibition.

The abundance of putative ubiquitinated IκB-α, a proteasome target protein (56 kDa) and decreased degraded IκB-α (37 kDa) protein band were observed with 10 μM [Cu(8OHQ)$_2$] treatment. In contrast, treatment with 1 μM [Cu(8OHQ)$_2$] result in decreased intensity of the putative ubiquitinated IκB-α band and increased intensity of the degraded IκB-α protein band. A single protein band of putative ubiquitinated IκB-α was also detected in cells treated with 10 μM ternary copper(II) complexes. Overall, it was observed that putative ubiquitinated IκB-α (56 kDa) protein bands for cells treated with ternary copper(II) complexes had much less intensity under identical conditions compared to [Cu(8OHQ)$_2$] (Fig 4.7(a): e.g. lane 9 versus lane 11). Results from these experiments revealed that [Cu(8OHQ)$_2$] treatment was more effective in increasing ubiquitinated IκB-α than treatment with ternary copper(II) complexes. Therefore, ternary copper(II) complexes are weaker inhibitors for IκB-α.

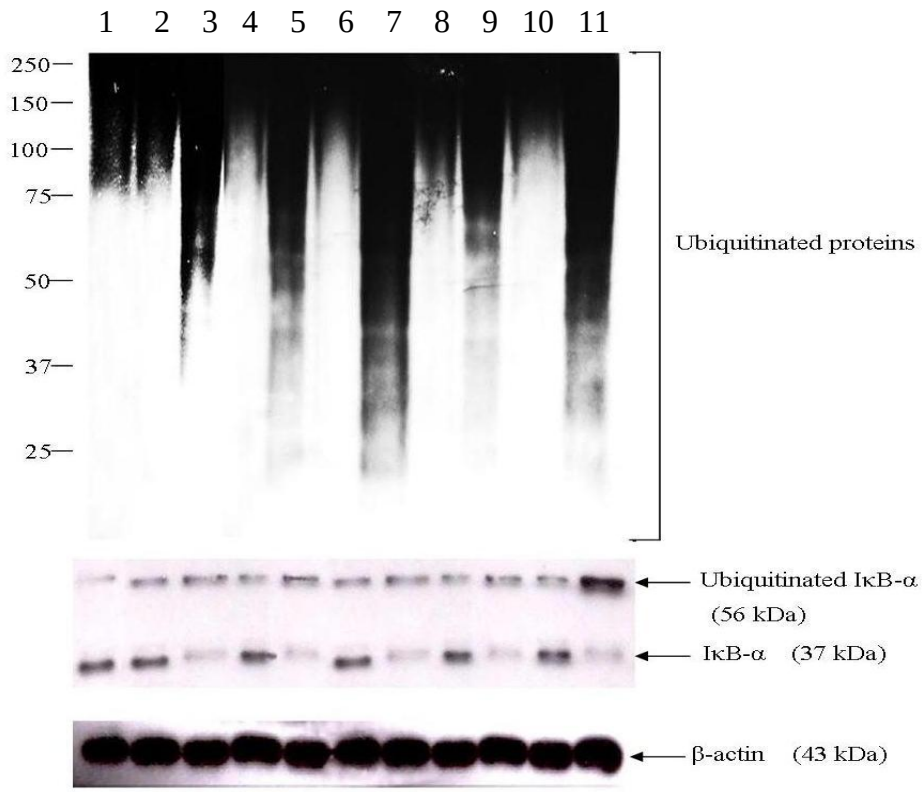

Fig. 4.7(a) Western blot analysis for ubiquitinated protein and IκB-α expression (20 µg of total protein lysate/lane) obtained from human breast cancer MDA-MB-231 cells, treated with ternary copper(II) complexes and $[Cu(8OHQ)_2]$ for 24 h. β-actin was used as the loading control. The experiment was repeated three times with similar results. Lane 1, untreated; Lane 2, 1 µM $[Cu(phen)(DL\text{-}ala)(H_2O)]NO_3 \cdot 2½H_2O$; Lane 3, 10 µM $[Cu(phen)(DL\text{-}ala)(H_2O)]NO_3 \cdot 2½H_2O$; Lane 4, 1 µM $[Cu(phen)(sar)(H_2O)]NO_3$; Lane 5, 10 µM $[Cu(phen)(sar)(H_2O)]NO_3$; Lane 6: 1 µM $[Cu(phen)(gly)(H_2O)]NO_3 \cdot 1.5H_2O$; Lane 7, 10 µM $[Cu(phen)(gly)(H_2O)]NO_3 \cdot 1.5H_2O$; Lane 8, 1 µM $[Cu(phen)(C\text{-}dmg)(H_2O)]NO_3$; Lane 9, 10 µM $[Cu(phen)(C\text{-}dmg)(H_2O)]NO_3$; Lane 10, 1 µM $[Cu(8OHQ)_2]$; Lane 11, 10 µM $[Cu(8OHQ)_2]$.

.

Lane 1

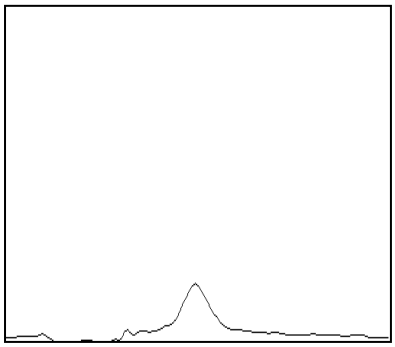

Lane 2

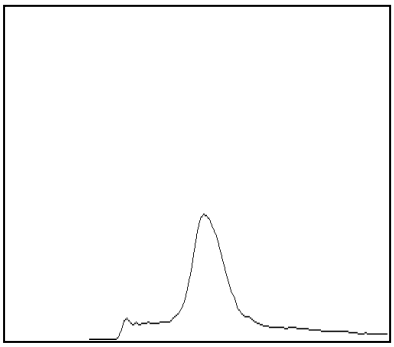

Lane 3

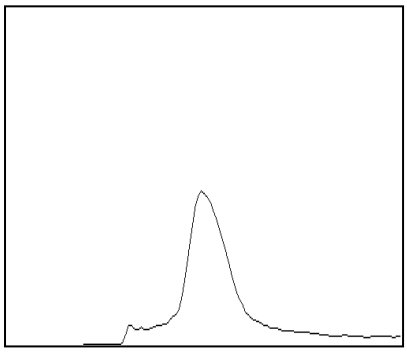

Lane 4

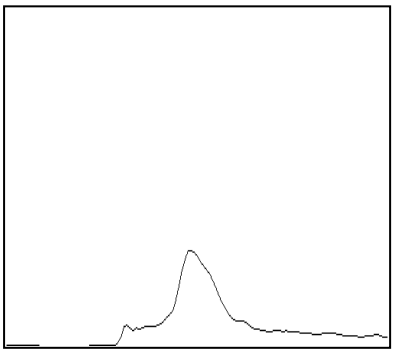

Lane 5

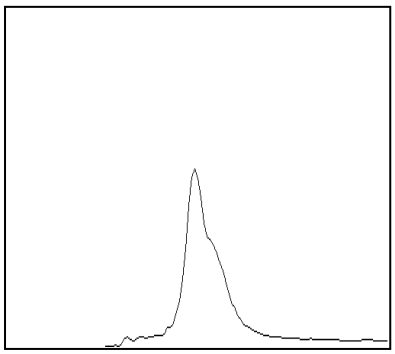

Lane 6

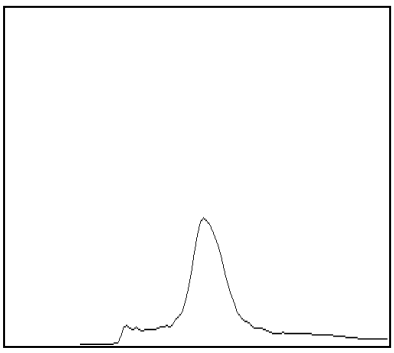

Lane 7

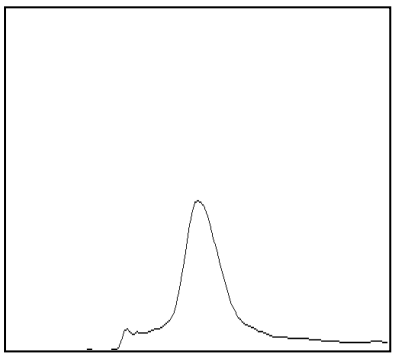

Lane 8

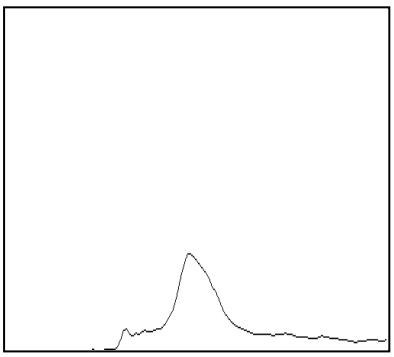

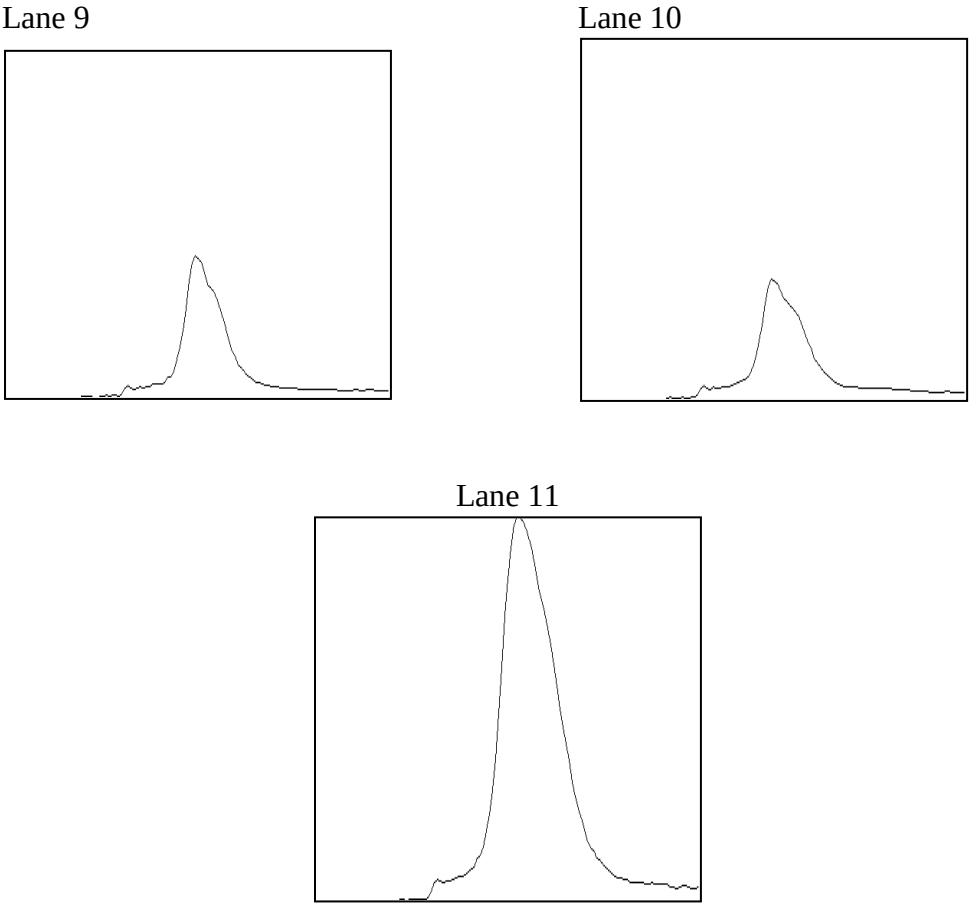

Fig. 4.7(b) Histogram of ubiquitinated IκB-α (56 kDa) obtained from human breast cancer MDA-MB-231 cells treated with ternary copper(II) complexes and [Cu(8OHQ)$_2$] for 24 h. Lane 1, untreated; Lane 2, 1 μM [Cu(phen)(DL-ala)(H$_2$O)]NO$_3$·2½H$_2$O; Lane 3, 10 μM [Cu(phen)(DL-ala)(H$_2$O)]NO$_3$·2½H$_2$O; Lane 4, 1 μM [Cu(phen)(sar)(H$_2$O)]NO$_3$; Lane 5, 10 μM [Cu(phen)(sar)(H$_2$O)]NO$_3$; Lane 6: 1 μM [Cu(phen)(gly)(H$_2$O)]NO$_3$·1.5H$_2$O; Lane 7, 10 μM [Cu(phen)(gly)(H$_2$O)]NO$_3$·1.5H$_2$O; Lane 8, 1 μM [Cu(phen)(C-dmg)(H$_2$O)]NO$_3$; Lane 9, 10 μM [Cu(phen)(C-dmg)(H$_2$O)]NO$_3$; Lane 10, 1 μM [Cu(8OHQ)$_2$]; Lane 11, 10 μM [Cu(8OHQ)$_2$].

Lane 1

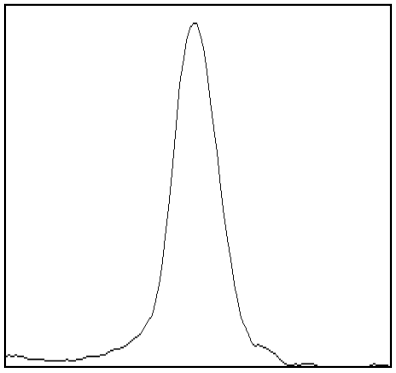

Lane 2

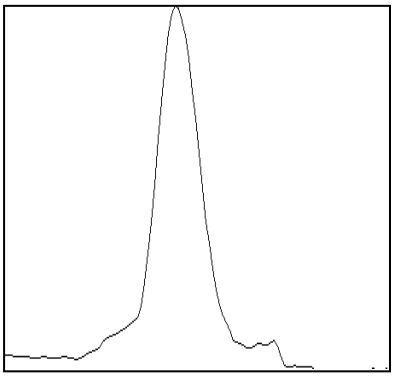

Lane 3

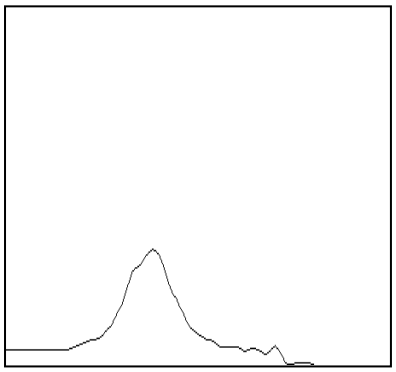

Lane 4

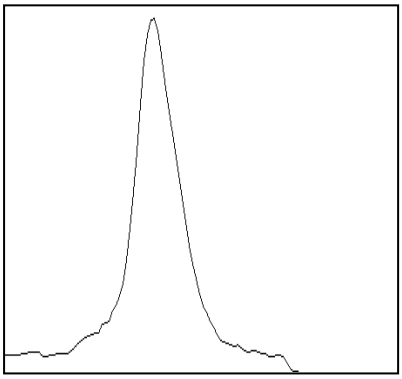

Lane 5

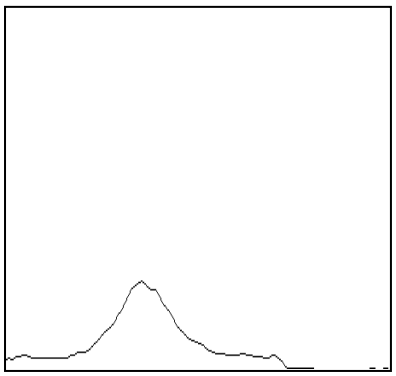

Lane 6

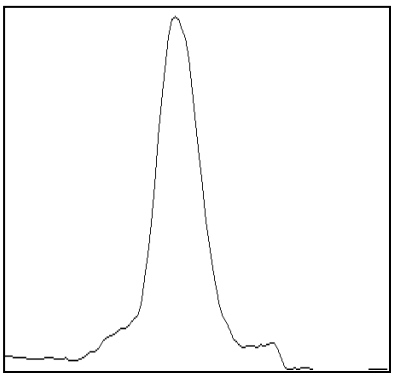

Lane 7

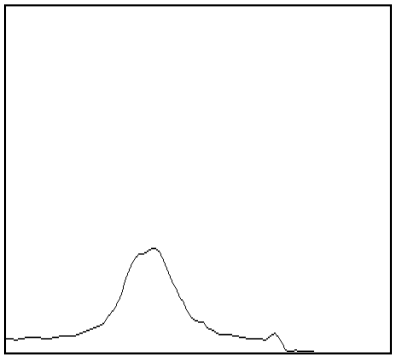

Lane 8

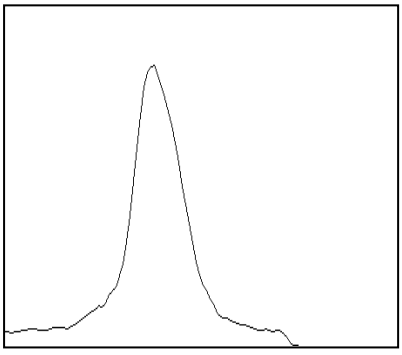

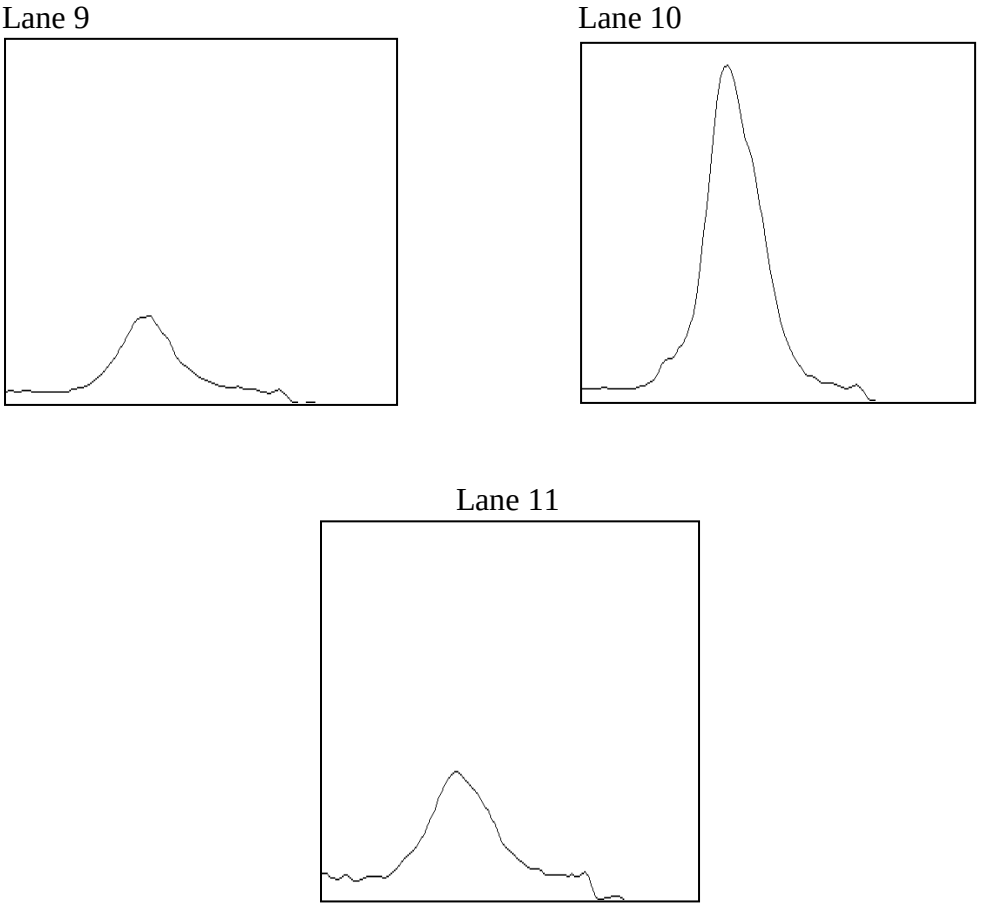

Fig. 4.7(c) Histogram of IκB-α (37 kDa) obtained from human breast cancer MDA-MB-231 cells treated with ternary copper(II) complexes and [Cu(8OHQ)$_2$] for 24 h. Lane 1, untreated; Lane 2, 1 μM [Cu(phen)(DL-ala)(H$_2$O)]NO$_3$·2½H$_2$O; Lane 3, 10 μM [Cu(phen)(DL-ala)(H$_2$O)]NO$_3$·2½H$_2$O; Lane 4, 1 μM [Cu(phen)(sar)(H$_2$O)]NO$_3$; Lane 5, 10 μM [Cu(phen)(sar)(H$_2$O)]NO$_3$; Lane 6: 1 μM [Cu(phen)(gly)(H$_2$O)]NO$_3$·1.5H$_2$O; Lane 7, 10 μM [Cu(phen)(gly)(H$_2$O)]NO$_3$·1.5H$_2$O; Lane 8, 1 μM [Cu(phen)(C-dmg)(H$_2$O)]NO$_3$; Lane 9, 10 μM [Cu(phen)(C-dmg)(H$_2$O)]NO$_3$; Lane 10, 1 μM [Cu(8OHQ)$_2$]; Lane 11, 10 μM [Cu(8OHQ)$_2$].

4.6 ROS study

To investigate the possible generation of ROS in breast cells (MDA-MB-231 and MCF 10A) by ternary copper(II) complexes, both cell lines were treated with indicated concentration (5, 10 μM) and time point (6 , 24 h) as described in Section 3.12. The intracellular ROS levels were detected by flow cytometric analysis using the fluorophore, DCFH-DA. Increase in DCF fluorescence will reflect increase in ROS level.

Exposure of MDA-MB-231 cells to 10 μM of ternary copper(II) complexes for 6 h led to significant increase in ROS production as shown in Fig. 4.10. The results for [Cu(phen)(DL-ala)(H_2O)]NO_3·2½H_2O is described to illustrate this. On incubation of MDA-MB-231 cells with 10 μM [Cu(phen)(DL-ala)(H_2O)]NO_3·2½H_2O, the ROS generation increased 2-fold compared to the untreated cells (6 h) (Fig. 4.10). The exposure of the MDA-MB-231 and MCF 10A to any compound at 5 μM for 6 h resulted in insignificant increase in relative fluorescence compared to untreated cells. The intensities of DCF fluorescence in 5 μM compound-treated in both cell lines were similar (109-132) to that of untreated cells (100) (Fig. 4.10). The subsequent data are only presented for 24 h incubation period for 5 μM compound-treated cells (Fig. 4.11).

Notably strong fluorescence up to 3-fold was observed in compound-treated MDA-MB-231 cells after 24 h treatment. However, the production of ROS in 10 μM compound-treated MCF 10A remained relative low even after

24 h incubation. Collectively, these data imply that ROS production in ternary copper(II) complexes-treated cells was concentration- and time-dependent in MDA-MB-231 cell line.

(a) [Cu(phen)(DL-ala)(H_2O)]NO_3 ·2½H_2O (b) [Cu(phen)(sar)(H_2O)]NO_3

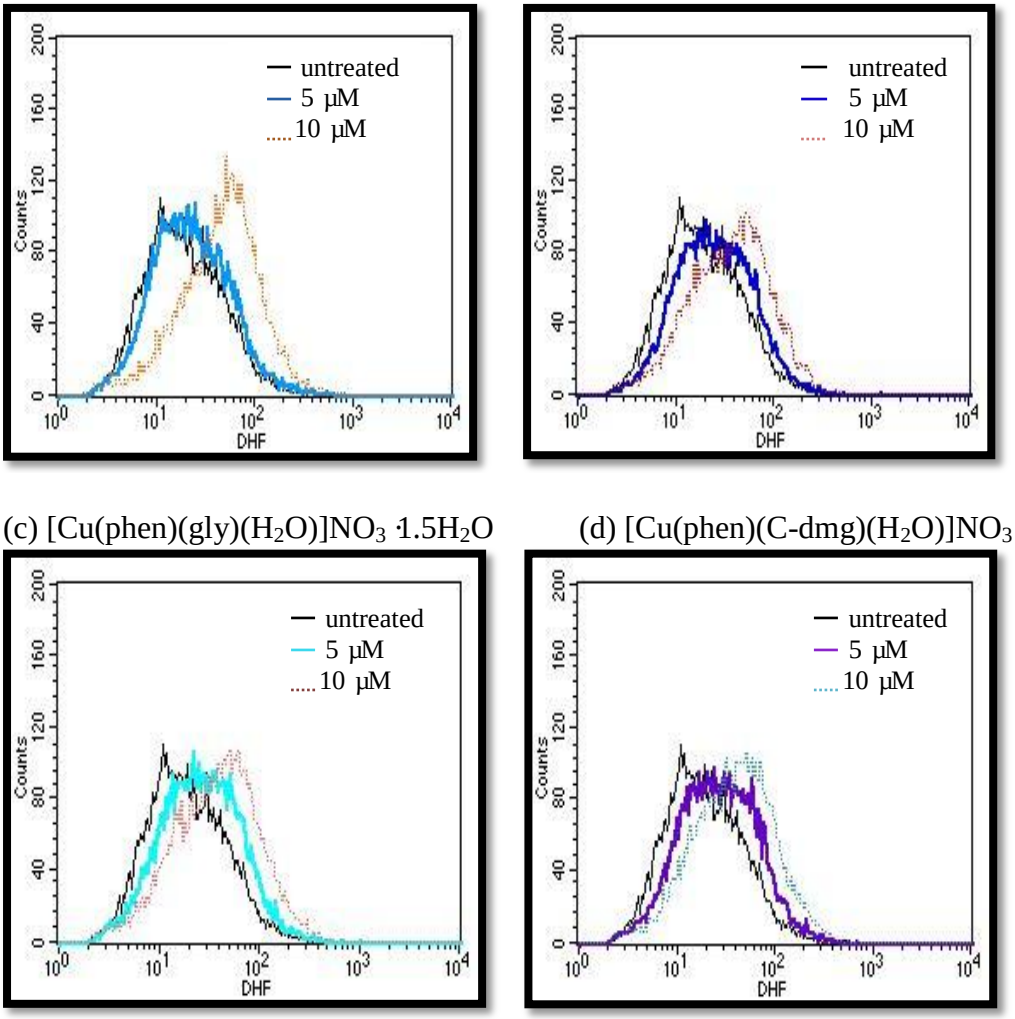

(c) [Cu(phen)(gly)(H_2O)]NO_3 ·1.5H_2O (d) [Cu(phen)(C-dmg)(H_2O)]NO_3

Fig. 4.8(a): MDA-MB-231 cells were untreated or treated with (a) [Cu(phen)(DL-ala)(H_2O)]NO_3 ·2½H_2O, (b) [Cu(phen)(sar)(H_2O)]NO_3, (c) [Cu(phen)(gly)(H_2O)]NO_3 ·1.5H_2O, (d) [Cu(phen)(C-dmg)(H_2O)]NO_3 for 6 h, then stained with DCFH-DA and the fluorescence intensity was measured by flow cytometry. An experiment representative of three is shown.

(a) $[Cu(phen)(DL\text{-}ala)(H_2O)]NO_3 \cdot 2½H_2O$ (b) $[Cu(phen)(sar)(H_2O)]NO_3$

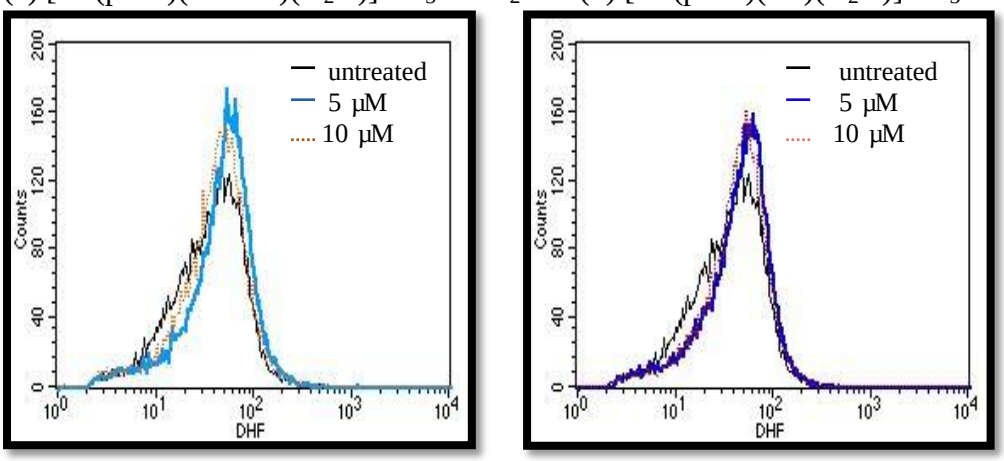

(c) $[Cu(phen)(gly)(H_2O)]NO_3 \cdot 1.5H_2O$ (d) $[Cu(phen)(C\text{-}dmg)(H_2O)]NO_3$

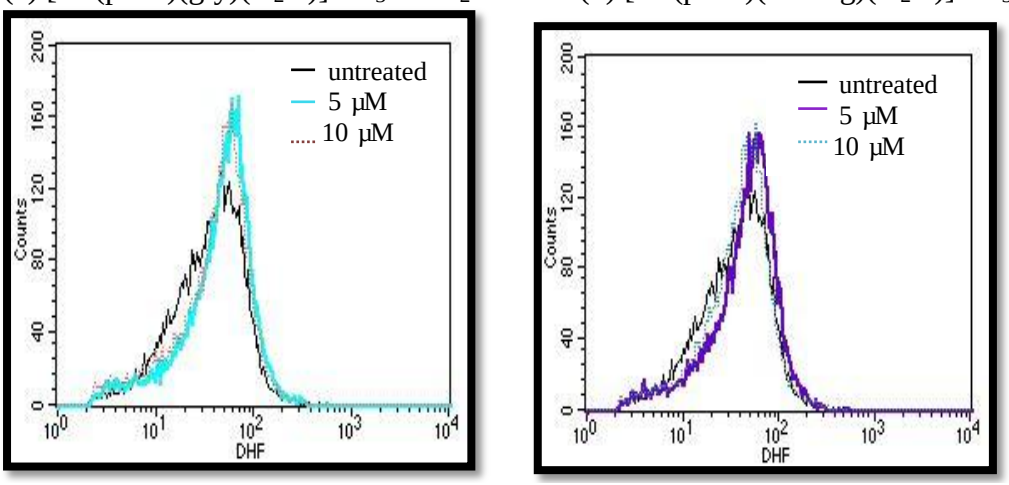

Fig. 4.8(b): MCF 10A cells were untreated or treated with (a) $[Cu(phen)(DL\text{-}ala)(H_2O)]NO_3 \cdot 2½H_2O$, (b) $[Cu(phen)(sar)(H_2O)]NO_3$, (c) $[Cu(phen)(gly)(H_2O)]NO_3 \cdot 1.5H_2O$, (d) $[Cu(phen)(C\text{-}dmg)(H_2O)]NO_3$ for 6 h, then stained with DCFH-DA and the fluorescence intensity was measured by flow cytometry. An experiment representative of three is shown.

(a) [Cu(phen)(DL-ala)(H_2O)]NO_3 2½H_2O (b) [Cu(phen)(sar)(H_2O)]NO_3

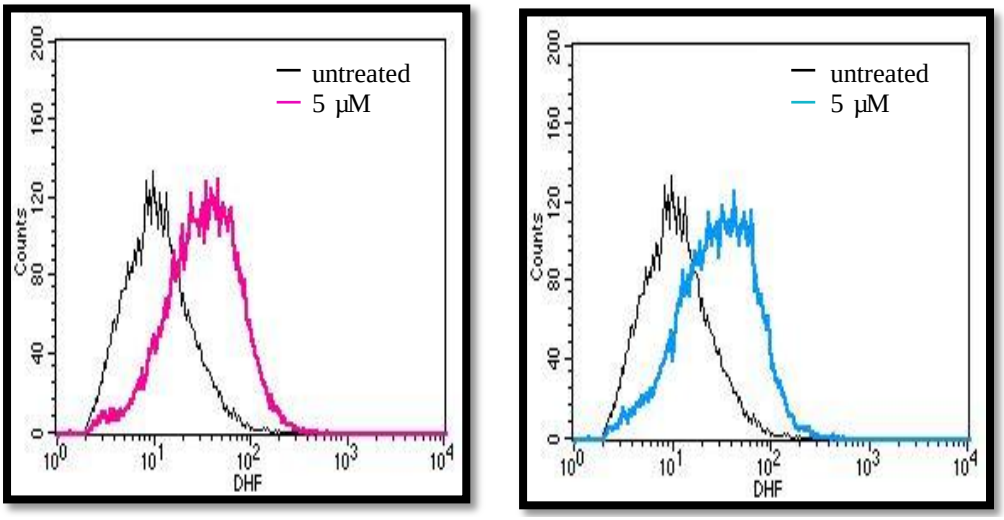

(c) [Cu(phen)(gly)(H_2O)]NO_3 ·1.5H_2O (d) [Cu(phen)(C-dmg)(H_2O)]NO_3

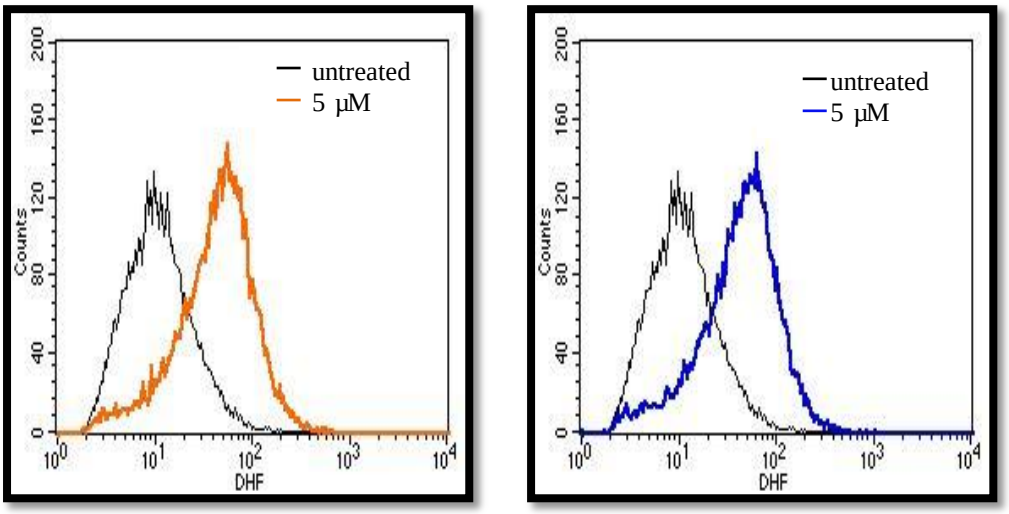

Fig. 4.9(a): MDA-MB-231 cells were untreated or treated for 24 h with (a) [Cu(phen)(DL-ala)(H_2O)]NO_3 2½H_2O, (b) [Cu(phen)(sar)(H_2O)]NO_3, (c) [Cu(phen)(gly)(H_2O)]NO_3 ·1.5H_2O, (d) [Cu(phen)(C-dmg)(H_2O)]NO_3 then stained with DCFH-DA and the fluorescence intensity was measured by flow cytometry. An experiment representative of three is shown.

(a) [Cu(phen)(DL-ala)(H_2O)]NO_3 ·2½H_2O (b) [Cu(phen)(sar)(H_2O)]NO_3

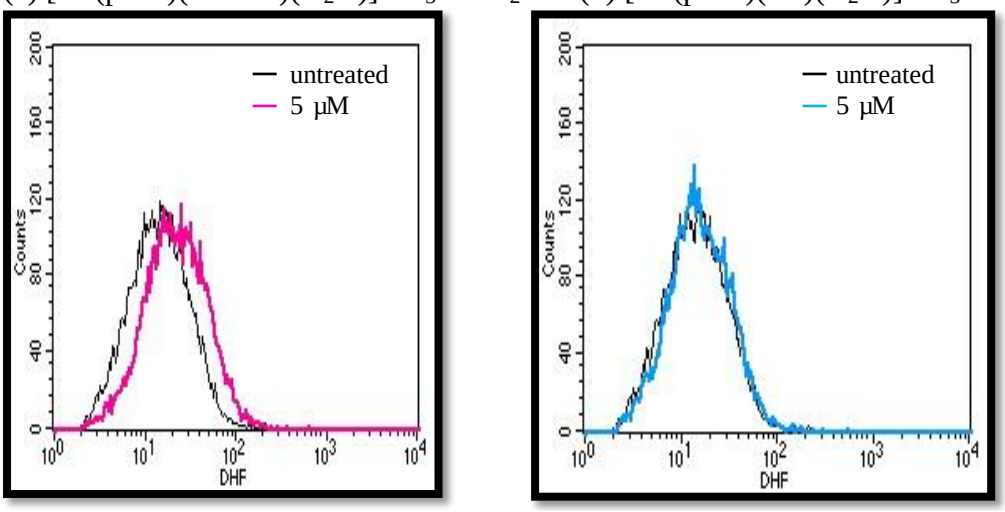

(c) [Cu(phen)(gly)(H_2O)]NO_3 ·1.5H_2O (d) [Cu(phen)(C-dmg)(H_2O)]NO_3

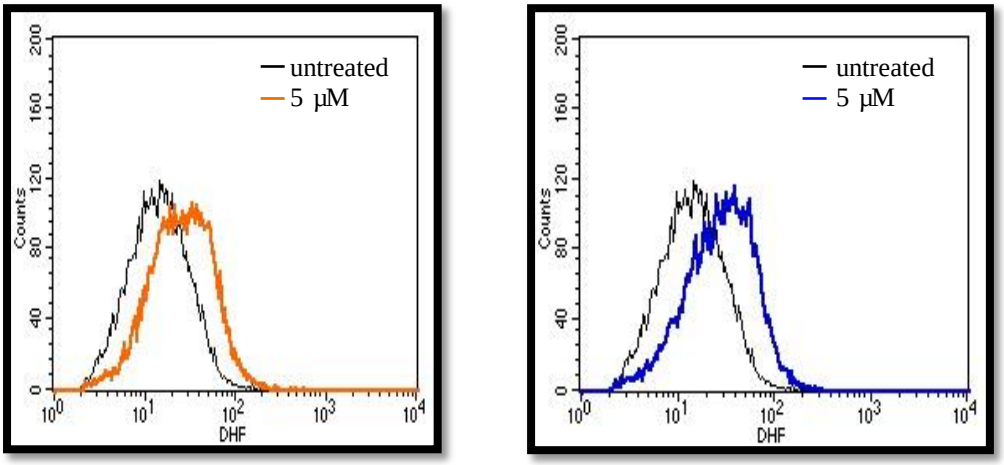

Fig. 4.9(b): MCF 10A cells were untreated or treated for 24 h with (a) [Cu(phen)(DL-ala)(H_2O)]NO_3 2½H_2O, (b) [Cu(phen)(sar)(H_2O)]NO_3, (c) [Cu(phen)(gly)(H_2O)]NO_3 ·1.5H_2O, (d) [Cu(phen)(C-dmg)(H_2O)]NO_3 then stained with DCFH-DA and the fluorescence intensity was measured by flow cytometry. An experiment representative of three is shown.

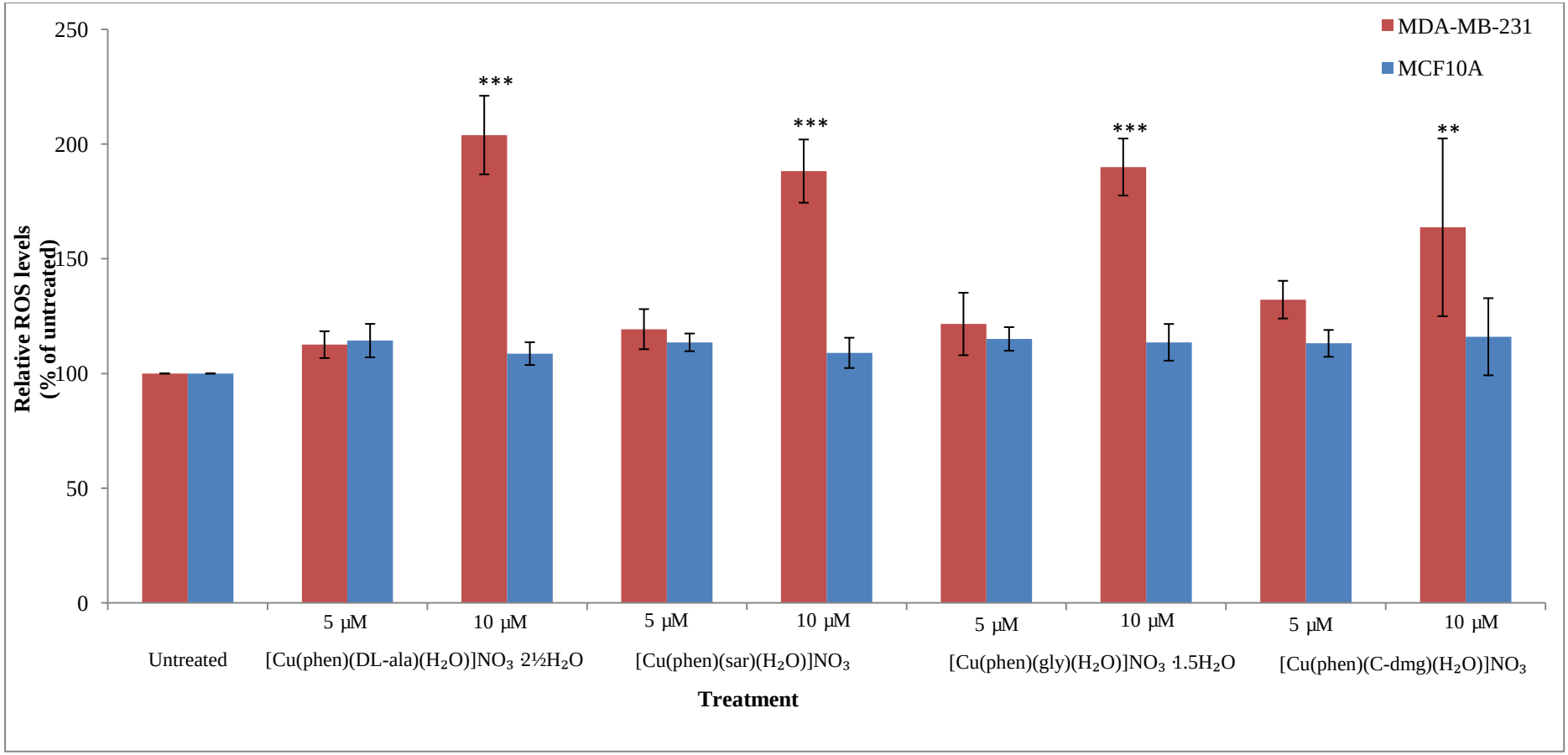

Fig. 4.10: ROS production induced by ternary copper(II) complexes treatment with different concentration for 6 h. The average of data obtained in three independent experiments. Results are mean ± S.D. (n=3).

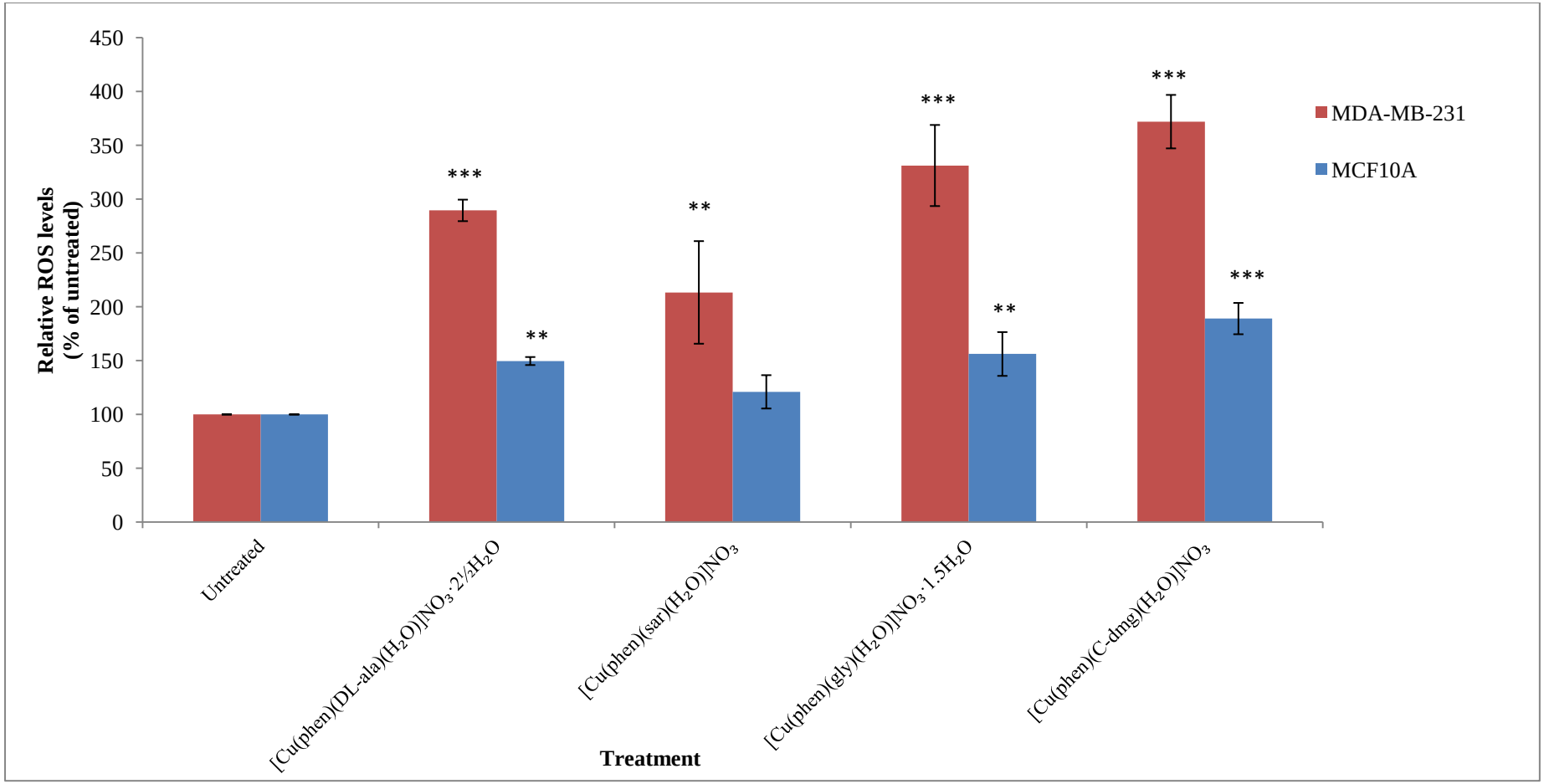

Fig. 4.11: ROS production induced by 5 μM ternary copper(II) complexes treatment for 24 h. The average of data obtained in three independent experiments. Results are mean ± S.D. (n=3).

4.7 Effect of ternary copper(II) complexes on the phosphorylation of H2AX

Histone H2AX phosphorlyation on Ser^{139} assay was used to investigate DNA double-strand breaks induced by ternary copper(II) complexes in MDA-MB-231 and MCF 10A. Adriamycin, as control, could induce γ-H2AX which can be detected in both MDA-MB-231 and MCF 10A cells incubated with Alexa Fluor® 488-tagged specific antibodies against γ-H2AX by immunofluorescence staining and fluorescence microscopy. For image analysis, three images were taken as follows DAPI (4', 6-diamidino-2-phenylindole) channel, FITC channel and phase contrast. DAPI was used for DNA staining. DAPI specifically stains nuclei.

As shown in Fig. 4.12, MDA-MB-231 cells treated with 5 μM ternary copper(II) complexes induced a massive increase in γ-H2AX levels (green fluorescence) at 6h incubation. Image (right panel) obtained from the FITC channel of the color camera represents phosphorylated H2AX (γ-H2AX). γ-H2AX was easily identified with clearly increased fluorescence intensity detectable in MDA-MB-231 cells treated with 5 μM [Cu(phen)(DL-ala)(H_2O)]NO_3·2½H_2O. Similar results were obtained in experiments for MDA-MB-231 cells treated with 5 μM [Cu(phen)(sar)(H_2O)]NO_3, [Cu(phen)(gly)(H_2O)]NO_3·1.5H_2O, [Cu(phen)(C-dmg)(H_2O)]NO_3 (Fig. 4.12).

To quantify the amount of γ-H2AX, cell scoring was performed by using MetaMorph® software. These data showed that the number of cells

stained positive for γ-H2AX induced by ternary copper(II) complexes in MDA-MB-231 cells is higher compared to MCF 10A cells (Fig. 4.13). The effect of compounds induced H2AX phosphorylation towards immortalized MCF 10A cells was also studied. Results revealed obvious nuclei staining with DAPI (blue) but at the same position no phosphorylation or no green fluorescence was detected in compounds-treated cells (Fig. 4.14). In conclusion, there was induction of γ-H2AX in MDA-MB-231 cells treated with ternary copper(II) complexes but none for the correspondingly treated MCF 10A cells.

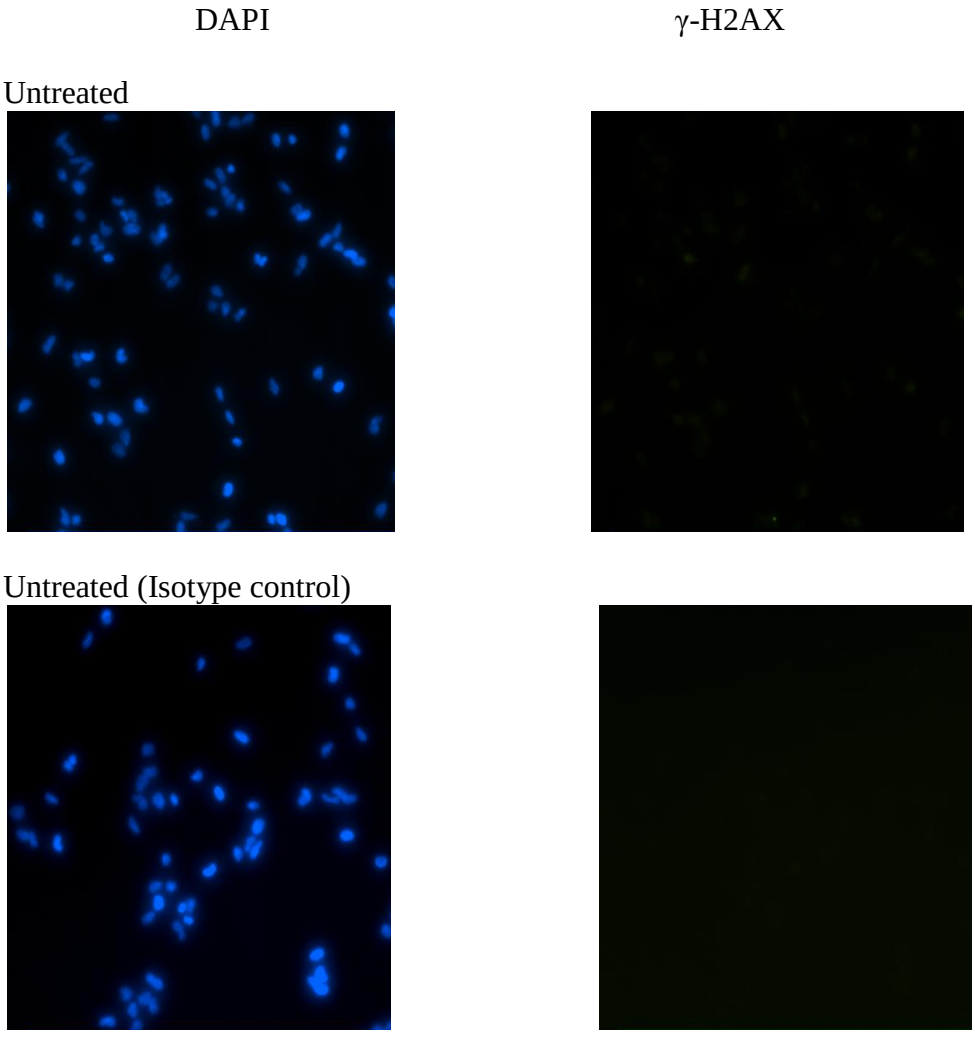

DAPI γ-H2AX

Adriamycin

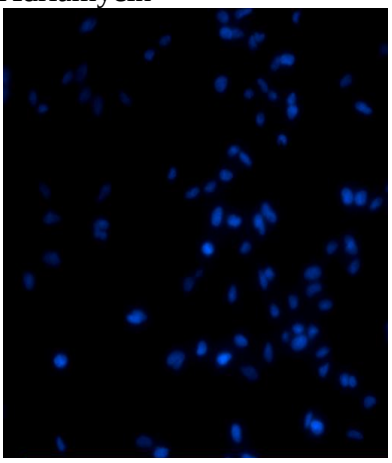

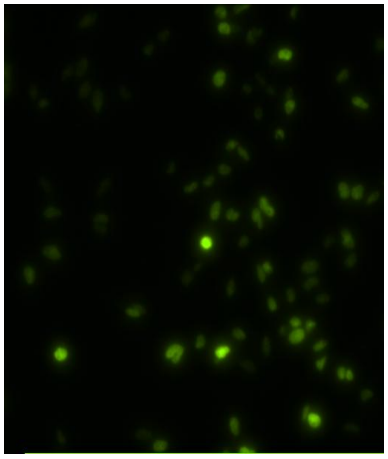

Adriamycin (Isotype control)

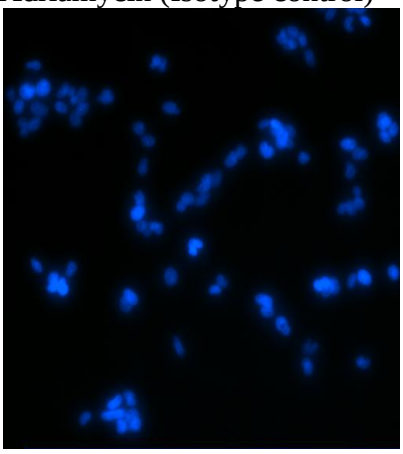

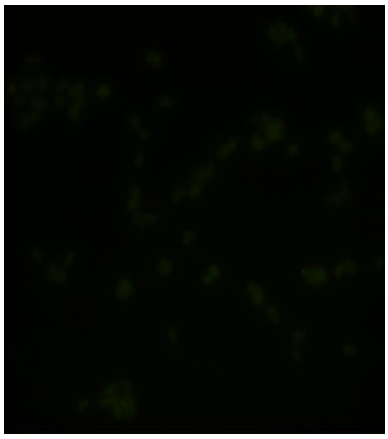

[Cu(phen)(DL-ala)(H_2O)]NO_3 2½H_2O

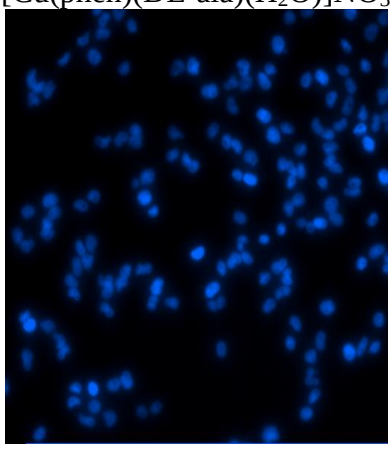

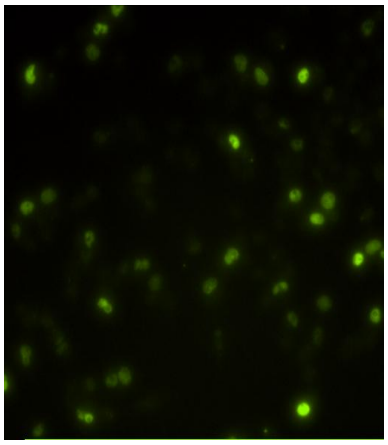

DAPI γ-H2AX

[Cu(phen)(sar)(H_2O)]NO_3

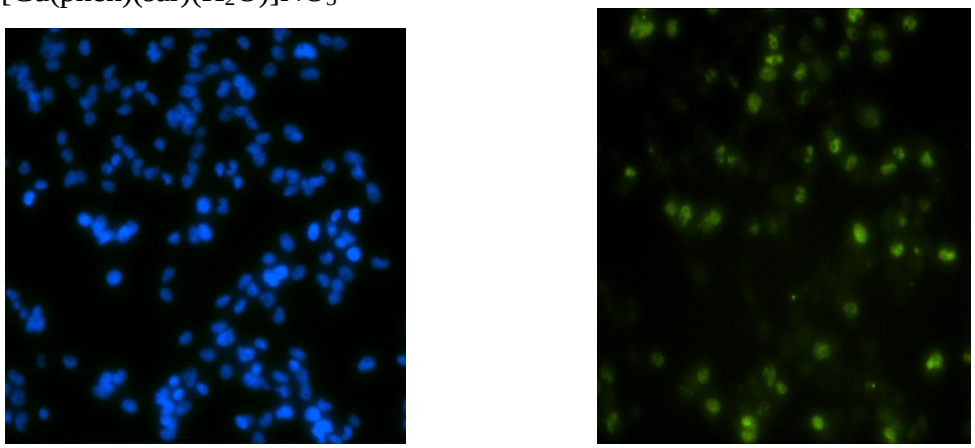

[Cu(phen)(gly)(H_2O)]$NO_3 \cdot 1.5H_2O$

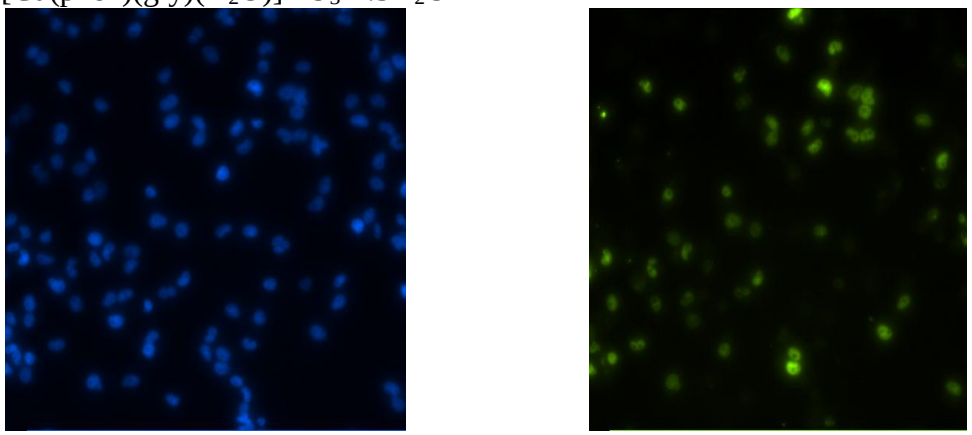

[Cu(phen)(C-dmg)(H_2O)]NO_3

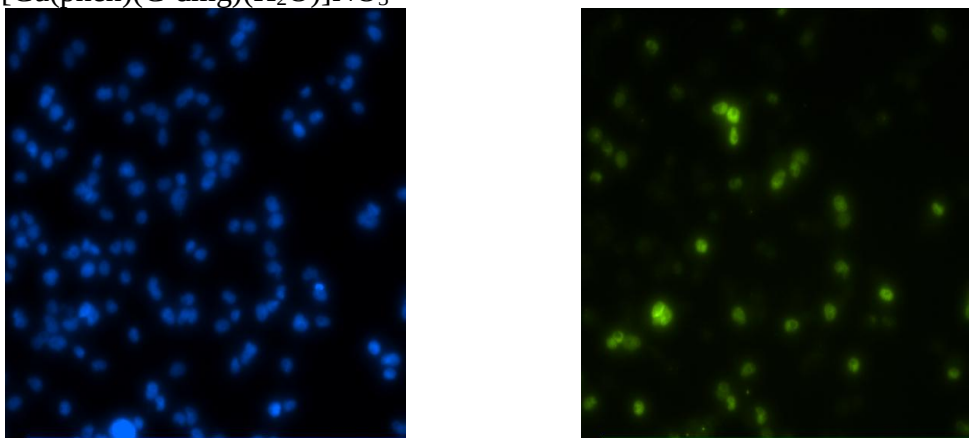

Fig. 4.12: Immunofluorescence staining for γ-H2AX (green) in MDA-MB-231 cells after 6 h treatment with 5 µM ternary copper(II) complexes compared to control cells. DNA counterstaining is with DAPI (blue). Results are representative of three independent experiments.

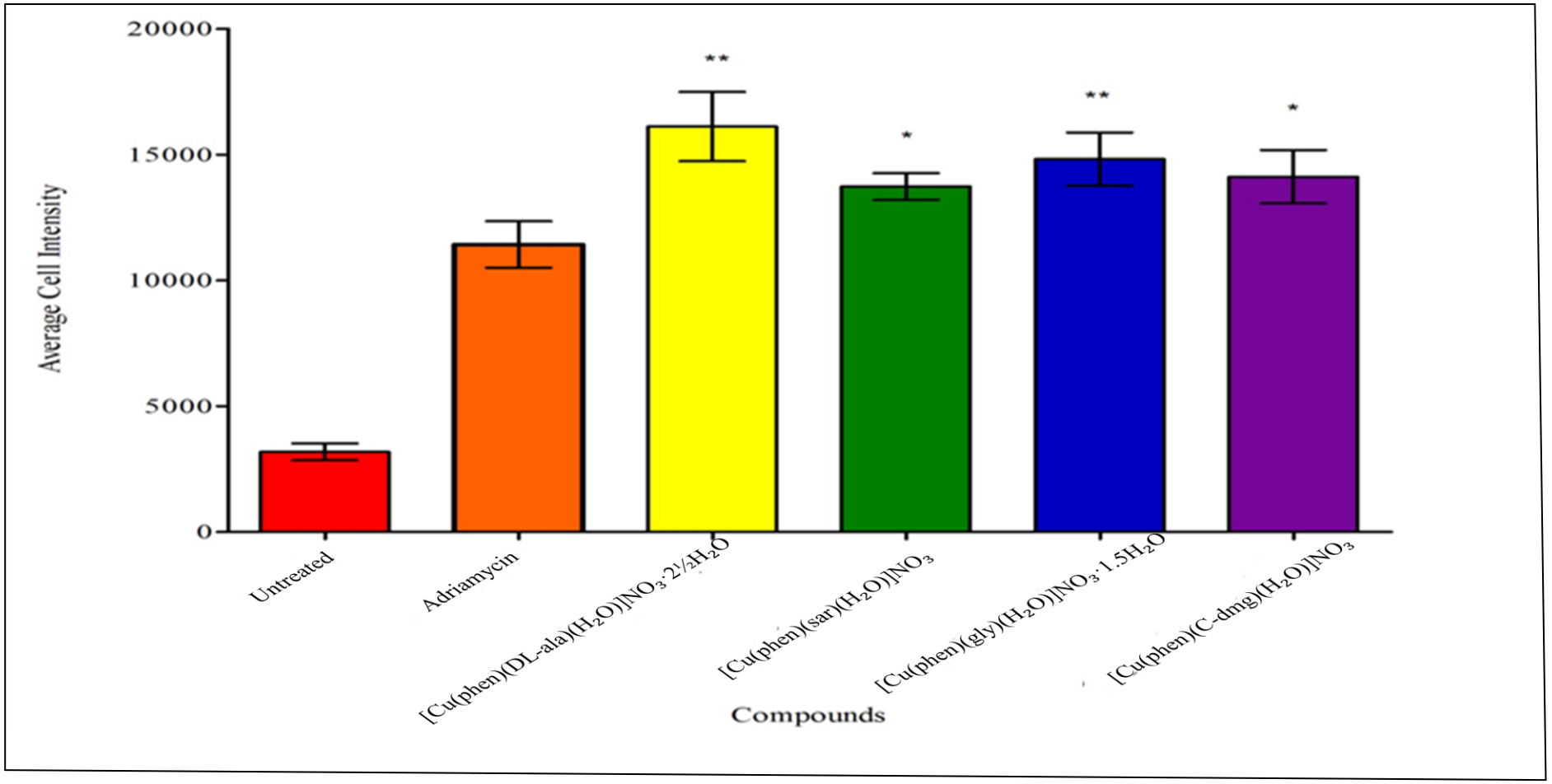

Fig. 4.13: Cell intensity of γH2AX production induced by ternary copper(II) complexes in MDA-MB-231 cells. Results are mean ± S.E.M.

DAPI γ-H2AX

Untreated

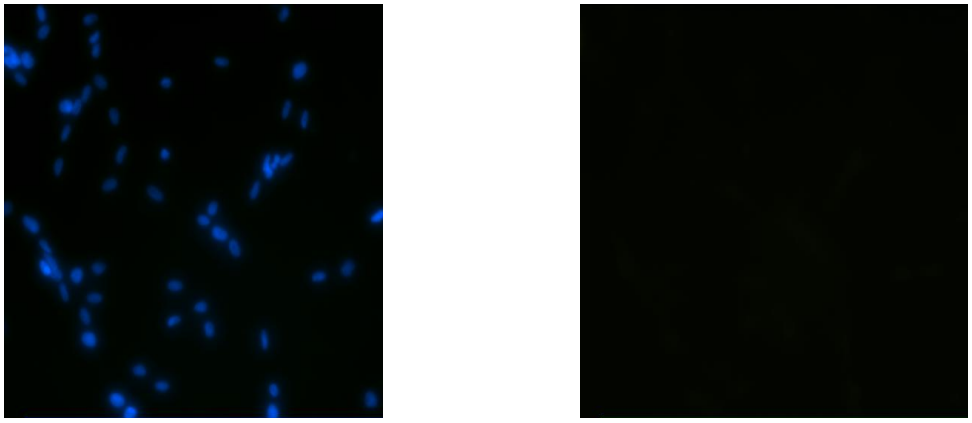

Untreated (Isotype control)

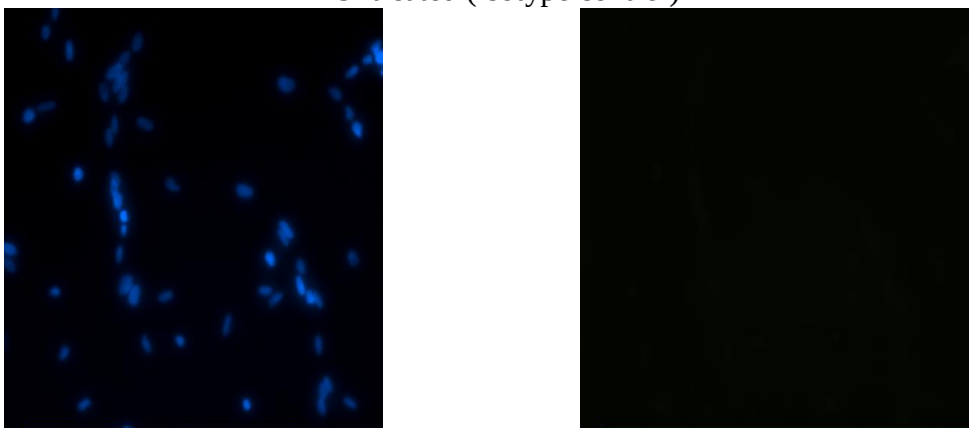

Adriamycin

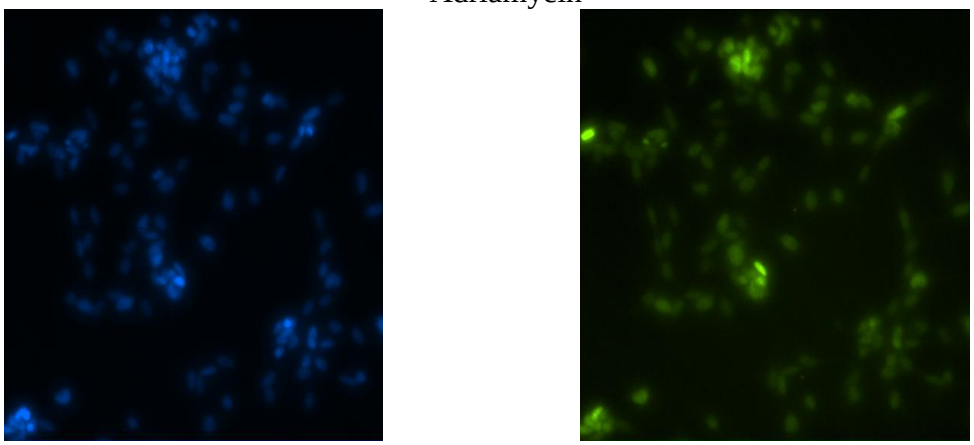

DAPI γ-H2AX

Adriamycin (Isotype control)

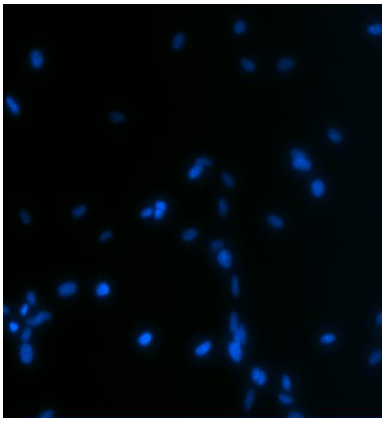
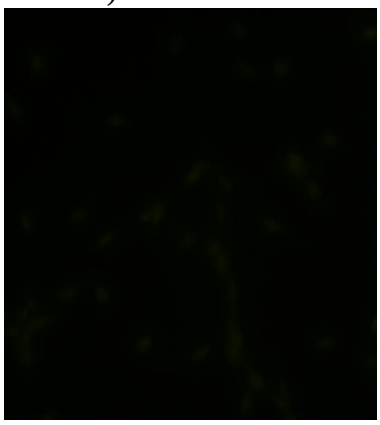

[Cu(phen)(DL-ala)(H_2O)]NO_3 ·2½H_2O

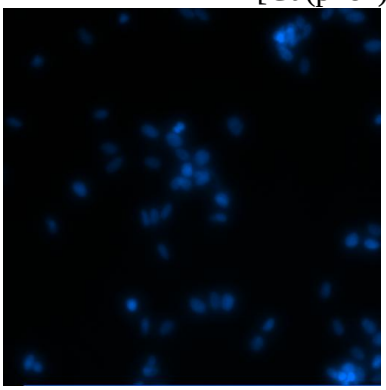
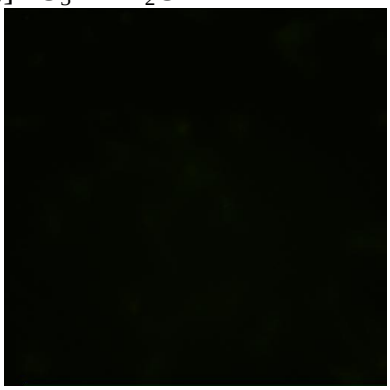

[Cu(phen)(sar)(H_2O)]NO_3

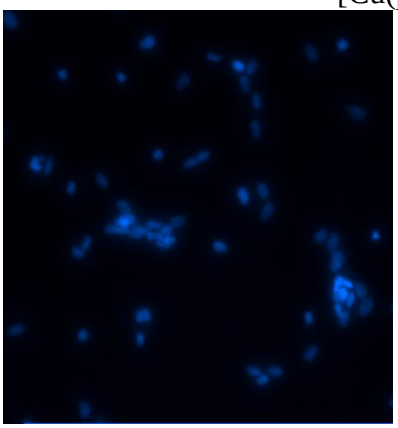


DAPI γ-H2AX

[Cu(phen)(gly)(H_2O)]NO_3 ·1.5H_2O

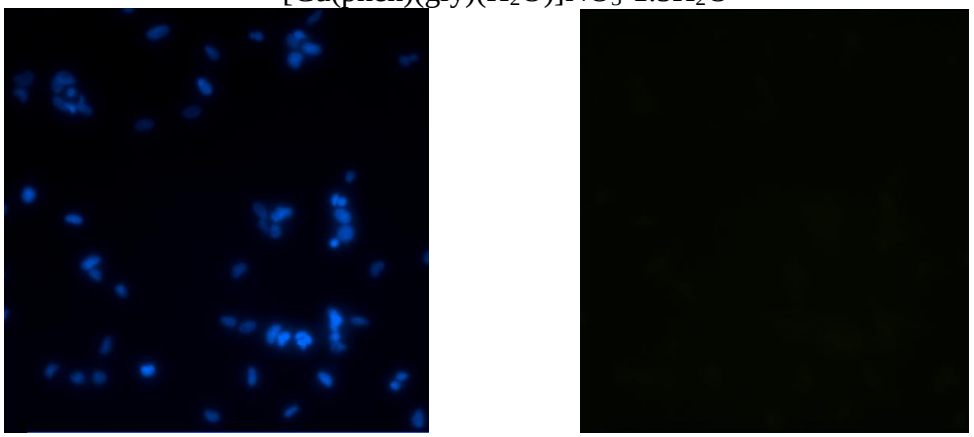

[Cu(phen)(C-dmg)(H_2O)]NO_3

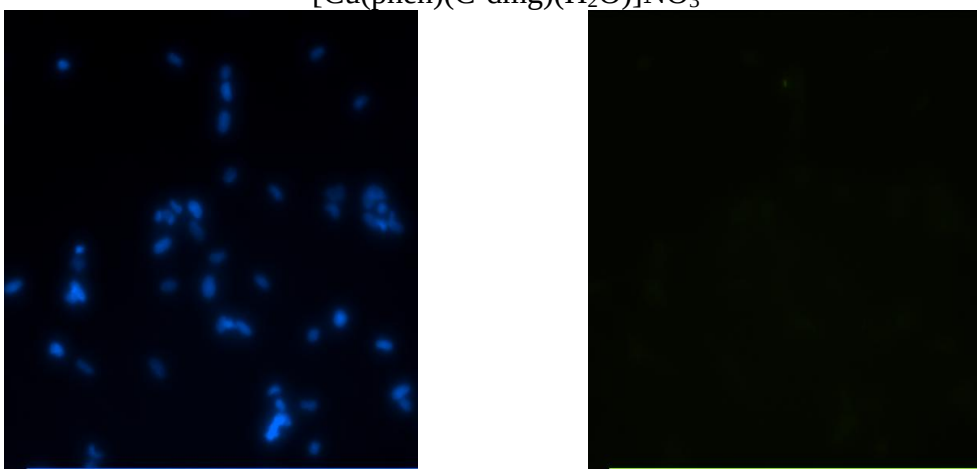

Fig. 4.14: Immunofluorescence staining for γ-H2AX (green) in MCF 10A cells after 6 h treatment with 5 μM ternary copper(II) complexes compared to control cells. DNA counterstaining is with DAPI (blue). Results are representative of three independent experiments.

CHAPTER 5.0

DISCUSSION

5.1 Anticancer properties of ternary copper(II) complexes

Strikingly, long-term treatment with chemotherapeutic agents can cause problems of unexpected toxicity to normal cells or drug resistance. Therefore, it is necessary to discover novel drugs which can potentially target cell differentially. The primary objective of this study is to identify the potential of ternary copper(II) complexes as anticancer compounds and to investigate their mode of action. Nevertheless, this study does not represent a thorough investigation of their mode of action but only involve a few aspects of their mechanism of action.

Human breast cancer cell line MDA-MB-231 and immortalized breast cell line MCF 10A were chosen and used throughout this study to evaluate the cyto-selective nature of the above ternary copper(II) complexes toward them and to provide comparison between these cell lines. MDA-MB-231 cells are highly malignant, metastatic and invasive, whereas, MCF 10A cells are not cancer cells, highly uninvasive and lack of functional estrogen receptor and progesterone receptor. Both cell lines belong to the Basal B category (Neve *et al*., 2006; Shekhar *et al*., 1998). MCF 10A cells retain many of the characteristics of normal human cells (Miller *et al*., 1993). Morphology assay

was an important step carried out to determine the extent and nature of cytological effects of treatment with the ternary copper(II) complexes.

5.1.1 Morphological changes and cell proliferation analysis

Biological responses of anticancer drugs are mediated by proliferation arrest and cell death (Herr and Debatin, 2001). Untreated cells maintained their morphology, appeared robust, elongated, adherent and showed normal proliferation. Microscopical examination displays distinct dose-dependent decline in the population of viable estrogen receptor α-negative MDA-MB-231 breast cancer cells and MCF 10A non-malignant breast epithelial cells upon exposure to compounds compared to control [Figs. 4.1(a) – (j)]. In addition, the results showed that the reduced cell viability and significant morphological changes (irregular in shape, cell shrinkage and floating cells) after treatment with individual ternary copper(II) complexes in both cell lines. Colonies of clumped up and floating dead cells in the medium were observed during visual inspection of cells treated with higher concentration of compounds. However, initiation of morphological change was dependent on dose and it was observed that morphological change in MCF 10A cells required higher dosage of ternary copper(II) complexes compared to that in MDA-MB-231 cells. These observations (results) indicated that ternary copper(II) complexes could inhibit cell proliferation and induce apoptosis. In order to highlight the potential advantage of ternary copper(II) compounds, a metal-based complex, $[Cu(8OHQ)_2]$ was used for comparative studies in

antiproliferative study. [$Cu(8OHQ)_2$] exhibited higher cytotoxicity in both cell lines than that shown by ternary copper(II) complexes [Figs 4.1(a) - (j)]. The results of morphology assay [Figs 4.1(a) - (h)] indicated that ternary copper(II) complexes were antiproliferative in a dose-dependent manner and displayed selective degree of growth inhibition towards both cell lines at low concentration (3 μM).

Previous studies have indicated the importance of metal compounds in cancer treatment (Huang *et al*., 2005). Morphological analysis showed that ternary copper(II) complexes possess antitumor activity by inhibiting the proliferation of cancer cells. In this assay, sufficiently low concentration (<3 μM) of the compounds could induce different degree of morphological changes such as cell surface, volume, and shape in MDA-MB-231 cells, while maintaining the phenotype of MCF 10A cells.

MTT assay was also used to study cell viability or proliferation in cell population. It is based on reduced mitochondria activity which indicates reduced cell viability (Usta *et al*., 2009). It is widely used in determining drug sensitivity profiles *in vitro* and in primary screening of potential chemotherapeutic drugs. Screening with this assay on both cell lines can provide a means of showing differential/selective antiproliferative property of the ternary copper(II) complexes. The study showed that ternary copper(II) complexes produced a stronger decrease in MDA-MB-231 cell proliferation than in the MCF10A in the concentration range (3.1 – 12.5 μM) used. It may be considered as a promissory compound for further studies.

All ternary copper(II) complexes exhibited relatively high antiproliferative activity in MDA-MB-231 cells. In this study, the results of the MTT assay showed that ternary copper(II) complexes exerted a concentration-dependant antiproliferative effect on both treated cell lines at 24 h treatment. However, the rate of decrease of viability for MDA-MB-231 was higher than that for MCF 10A [Fig. 4.2(a) – (d)]. These results may indicate that inhibition of growth was due to cytotoxicity of the drugs. The gaps between the dose response curves of both cell lines as shown in the Figs. 4.2(a) – (d) are wider in the concentration range 6.25 to 12.5 μM of the ternary copper(II) complexes, showing the more pronounced rate of reduced proliferation for the cancer cells over the normal cells. Treatment with ternary copper(II) complexes at 24 h showed the maximum reduction in cell viability (>90%) in both cell lines was reached at the complex concentration of 25 μM. In contrast, $[Cu(8OHQ)_2]$ is not antiproliferatively selective. MTT assay showed that cell viabilities for MDA-MB-231 cells treated with 3.1 μM and 6.3 μM of $[Cu(8OHQ)_2]$ were 29% and 7% respectively while corresponding values for MCF10A treated cells were 12% and 5% respectively [Fig 4.2(e)]. Overall, the quantitative analysis of MTT assay supports the qualitative morphology study. Barceló-Oliver *et al*., 2009 reported that copper-hippurate derivative-phenanthroline ternary complexes which were found to be anticancer. Similar antiproliferative behaviour of other metal complexes of phen towards human derived cancer cell lines had been reported. In fact, some of the phen complexes are more active than cisplatin (Deegan *et al*., 2007; Thati *et al*., 2009).

Data presented in Table 4.1 reveal small differences in IC_{50} value among individual ternary copper(II) complexes for MDA-MB-231 and MCF 10A cells. It indicates that type of ligand (different amino acid) itself does play a small role in mediating cytotoxicity by inducing variable reduction of cell viability. The three ternary copper(II) complexes with methylated glycine are slightly more cytotoxic than the $[Cu(phen)(gly)(H_2O)]NO_3 \cdot 1.5H_2O$. Methylation of the precursor glycine resulted in enhancement of the IC_{50} of the resultant ternary copper(II) complexes. The anticancer property of these ternary copper(II) complexes towards MDA-MB-231 is better than that of cisplatin as the latter has IC_{50} value of 66 μM at 24 h incubation (Rubino *et al*., 2009). Again analysis of IC_{50} values shows that these ternary copper(II) complexes are more antiproliferative towards MDA-MB-231 than MCF10A.

Based on the IC_{50} values, this finding clearly showed that ternary copper(II) complexes were more efficient in reducing 50% population growth of progesterone receptor-rich MDA-MB-231 cells in the concentration range of 5 to 9 μM, whereas higher concentration of compound (14 - 17 μM) is needed to inhibit 50% proliferation of MCF 10A cells. Similar result was obtained by Afrasiabi *et al*., (2003) who reported that [Cu(PQTSC)Cl] (PQTSC=phenanthrenequinone thiosemicarbazone) exhibited antipoliferative activity against progesterone receptor-rich human breast cancer cell line. Consequently, the ternary copper(II) complexes deserve more attention.

Interestingly, MTT assay showed that IC_{50} values for MDA-MB-231 cells treated with ternary copper(II) complexes were lower compared to MCF

10A cells, suggesting that ternary copper(II) complexes were more antiproliferative towards MDA-MB-231 cells at lower μM concentrations. MCF 10A cells only show similar cytotoxicity profile (50% growth inhibition) when treated with higher concentration of ternary copper(II) complexes. In contrast, $[Cu(8OHQ)_2]$ has slightly higher IC_{50} values for MDA-MB-231 cells (2.7 ± 0.2 μM) compared to MCF 10A cells (1.6 ± 0.4 μM). $[Cu(8OHQ)_2]$ is slightly more antiproliferative towards normal MCF10A cells rather than cancerous MDA-MB-231 cells. These results indicated that $[Cu(8OHQ)_2]$ was much more antiproliferative but not selective towards both cell lines.

Consistent with the findings in breast cancer cells, ternary copper(II) complexes were found to be more effective against tumorigenic nasopharyngeal cell line (HK1) than corresponding non-tumorigenic cell line (NP69). HK1 and NP69 cells treated with the same ternary copper(II) complexes had a dose-dependent growth inhibition as breast cell lines (data not shown).

5.1.2 Assessment of apoptosis and cell cycle

For the subsequent assays (apoptosis assay and cell cycle analysis), the concentration of ternary copper(II) complexes (IC_{50} values) and the incubation time (24 h) were selected based on results from the MTT assay. In order to explore the hypothesis that ternary copper(II) complexes exhibit selectivity in apoptosis induction towards transformed (MDA-MB-231) and non-

transformed (MCF 10A) cell lines, flow cytometric analysis was used to examine the effect of ternary copper(II) complexes on both cell cycle and cell death (Figs. 4.3 - 4.6).

To find out the cause of antiproliferation, apoptosis assay was performed to quantitate the percentage of early and late apoptotic cells. In apoptotic cells, the exposure of phosphatidylserine to the outer layer of the membrane was detected by using Annexin V-FITC/PI double staining (Vermes *et al*., 1995). Very low percentage of apoptotic cells were detected in both untreated MDA-MB-231 and MCF10A cells, demonstrating normal cell viability [Figs. 4.3(a) – (b)]. Analysis of results presented in Fig. 4.4 shows that apoptotic death produced in MDA-MB-231 cells by treatment with 5 μM of ternary copper(II) complexes was up to 4-fold more than that in MCF 10A cells. However, the number of MCF 10A apoptotic cells treated with ternary copper(II) complexes remained low (~10%) and did not increase with respect to the untreated cells. Previously, Zhou *et al*., (2002) reported that a copper-1,10-phenanthroline, $[Cu(OP)_2]^{2+}$ could induce G_1 phase specific apoptotic cell death in liver carcinoma cell line (Bel-7402). De Vizxaya-Ruiz *et al*., (2000) demonstrated the ability of a novel copper-based anticancer compound, Casiopeina II, to induce apoptotic death in two cancer cell lines. In contrast, $[Cu(8OHQ)_2]$ exhibited similar high cytotoxicity towards both cell lines. It's induction of apoptosis is therefore indiscriminate or non-cytoselective.

Based on the data presented, ternary copper(II) complexes were found to be an apoptosis-inducer in MDA-MB-231 cells at 5 μM but not in MCF

10A. This is in agreement with the results of the morphological study and MTT assay. There is enhancement of this apoptosis-inducing property of the ternary copper(II) complexes towards cancerous cell line compared to non-tumorigenic cell line. A major finding in this study with these compounds is that they showed obvious higher growth inhibition and induction of apoptosis in cancer cell lines, with less toxicity exhibited towards non-transformed cells. This property is good reason for further testing and evaluation of these compounds as anticancer drugs.

Cell cycle assay was performed on MDA-MB-231 and MCF 10A. Untreated cells and cells exposed to 5 μM ternary copper(II) complexes for 24 h and the percentage of cells entering each stage of the cell cycle was determined by software. Analysis of the graphical result presented in Fig. 4.5(a) and the histograms in Fig. 4.6(a) for all the ternary copper(II) complexes shows that there was increase in percentage of cells entering the G_0/G_1 while there was decrease in the percentage of cells in G_2/M phase. The percentage of MDA-MB-231 cells in S phase remains static. This indicates that all the ternary copper(II) complexes were capable of arresting the cells at G_0/G_1 and preventing cell cycle progress to G_2/M phase. However, statistical analysis ($p<0.05$) shows that only the increases in G_0/G_1 phase for Cu(phen)(DL-ala)NO_3 and Cu(phen)(C-dmg)NO_3 are significant. This means that these two complexes induced cell cycle arrest at G_0/G_1 and the methyl substituent at the α-carbon of the amino acid may be important. Kaznica *et al.*, (2009) had similarly reported that platinum(IV) complex, $[PtCl_2(6mp)_2]$

induced cell cycle arrest in G_0/G_1 phase in B16 mouse melanoma tumors after 12, 24 and 48 h of incubation.

However, under the same conditions, there was no statistically significant cell cycle arrest in MCF 10A cells treated with the ternary copper(II) complexes [Figs. 4.5(b) and Fig. 4.6(b)]. It was reported that proliferation of cells were slowed down at certain checkpoints in respond to growth signals, repair of damaged DNA and alterations in cell size (Rebbaa *et al*., 2006; Garret *et al*., 2001; Giacinti and Gioradano, 2006). The data demonstrate that these ternary copper(II) complexes may act on G_0/G_1 checkpoints for MDA-MB-231 cells but not MCF 10A cells and prevent further cell division. Based on the finding, ternary copper(II) complexes do not just inhibit cell viability, but also act on the machinery associated with blockage in cell cycle event and ultimately induce cell death in cancer cells. Collectively, these data support that treatment of ternary copper(II) complexes at 5 μM are less harmful to MCF 10A non-transformed cells but are toxic to MDA-MB-231 cancer cells.

Based on the studies stated above (Figs. 4.1 - 4.6), ternary copper(II) complexes were involved in regulating cell viability, cell cycle and apoptosis. Similar results were obtained by Zhou *et al*. (2003) who reported that copper-1,10-phenanthroline, $[Cu(OP)_2]^{2+}$ is a chemical nuclease that nicks DNA and upregulates the DNA-binding activity of p53 which was critical for cell survival, cell progression and apoptosis. The present study reveals that ternary copper(II) compounds showed higher growth inhibition and apoptosis in

cancer cell lines, with less toxicity exhibited toward non-transformed cells in a concentration-dependent manner. It suggested that treatment with ternary copper(II) could result in highly effective and selective cancer cell killing that avoids toxicity. The value of ternary copper(II) complexes in having selectivity for cancer cells over non-cancerous cells led me to investigate the mechanism of ternary copper(II) complexes on both cell lines.

5.2 Mode of action for ternary copper(II) complexes

Up to now, despite the enormous effort by worldwide researchers in finding copper complexes with multi-targeting function, very diverse mechanisms underlying their antitumor activity have been proposed. Other researchers have reported that certain copper complexes exerted multiple mode of action, such as inducing oxidative stress in mitochondria (Johnson and Thomas, 1999) and causing damage to nuclear DNA (Liu *et al.*, 1999). In an attempt to elucidate the mode of action of ternary copper(II) complexes in response to cytotoxicity, ROS assay, proteasome inhibition assay and H2AX assay were conducted *in vitro*.

$[Cu(8OHQ)_2]$ was used in cytotoxicity assay except cell cycle analysis. It was not possible to perform analysis for the chosen concentrations of $[Cu(8OHQ)_2]$ after 24 h for ROS generation study and cell cycle analysis, due to the resultant small number of living cells after the chosen incubation period. $[Cu(8OHQ)_2]$ is a known apoptosis inducer in human cancer cell and

proteasome inhibitor. In the cytotoxicity study, [$Cu(8OHQ)_2$] serves as a more suitable comparison compound than cisplatin for the investigated ternary copper(II) complexes because the former has the same copper(II) ion and is redoxs-active. For γ-H2AX study, adriamycin serves as a positive control instead of [$Cu(8OHQ)_2$]. Adriamycin is suitable as it had been widely used as DNA damaging agents which caused DSBs whereas [$Cu(8OHQ)_2$] has not been reported to induce DSBs.

5.2.1 Proteasome inhibition in whole-cell extract

The proteasome inhibitor, bortezomib is an effective drug for the treatment of multiple myeloma. However, adverse effects due to its toxicity were reported (Corso *et al*., 2010; Cusack, 2003). A large amount of research related to proteasome inhibitors has been carried out. Daniel *et al*., (2004) reported that dichlorido(1,10-phenanthroline)copper(II) (DCPTC) inhibited proteasome activity and caused apoptosis in Jurkat T cells. Hindo *et al*., (2009) reported that 1:1 (2,4-diiodo-6-((pyridine-2-ylmethylamino)methyl)phenol): copper chloride mixture could inhibit the cellular proteasome in prostate cancer cell extract but the ligand alone had a negligible effect. Dou and coworkers described that organic copper compounds with the mixture bidentate ligand able to inhibit the proteasomal chymotrypsin-like activity and followed by induction of apoptosis whereas [$CuCl_2$] alone inhibited proteasome activity at a lower extent and 8-hydroxyquinolines alone showed

no inhibition. Therefore, with the choice of appropriate bidentate ligands could enhance the copper-mediated proteasome inhibitory activity.

Milacic *et al*. (2008) reported that the bis(1-pyrrolidinecarbodithioato-κS, κS')copper(II), [$(PyDT)_2Cu$], had greater proteasomal inhibition in MDA-MB-231 breast cancer compared to copper(II) chloride, suggesting that chelation of the PyDT ligand to copper have contributed to higher proteasome inhibitory effect. Fig. 4.7(a) shows the increased levels of ubiquitinated proteins at 24 h, associated with the inhibition of proteasome activity in the cancer cells treated with 10 μM ternary copper(II) complexes. In sharp contrast, ternary copper(II) complexes had no or slight effect on MDA-MB-231 cells treated at 1 μM concentration compared to untreated cells [Fig. 4.7(a)]. [$Cu(8OHQ)_2$] was very effective at inhibiting proteasome activity in concentration-dependent manner, and treated cells showed accumulation of ubiquitinated protein as shown at Fig. 4.7(a). Previously, it had been reported that [$Cu(8OHQ)_2$] could inhibit the proteasomal activity, suppress growth and induce apoptosis in cancer cells (Daniel *et al*., 2004; Zhai *et al*., 2010). In the present study, levels of ubiquitinated proteins were increased in a dose-dependent manner for the [$Cu(phen)(aa)(H_2O)]NO_3$-treated MDA-MB-231 cells, consistent with the results for the known proteasome inhibitor, [$Cu(8OHQ)_2$]. The species responsible for proteasome inhibition are likely to be $[Cu(phen)(aa)(H_2O)]^+$ as they are detected by ESI-MS (as $[Cu(phen)(aa)]^+$) and their stability up to 24h is supported by spectroscopic and conductivity data.

Screening for proteasome inhibition and finding out structure-activity relationship in new metal complexes is thus a good approach to discover more efficient anticancer drugs. However, early *in vitro* screening for selectivity is needed. Ubiquitin-proteasome pathway (UPP) dysregulation in tumorigenesis and its inhibition have formed the basis for a rational strategy to prevent tumor progression and overcome drug resistance (Dees and Orlowski, 2006). Evidence from studies in the literature showed that proteasome inhibitors are potent apoptosis inducers for cancer treatment. It was found that cancer cells were more sensitive to proteasome inhibitors than normal or untransformed cells. This approach contributes to the potential of metal complexes as anticancer drugs (Nam *et al*., 2001). Although [$Cu(8OHQ)_2$] is a good proteasome inhibitor, we found that it is not selective. It was equally cytotoxic to MDA-MB-231 cancer cell and MCF 10A non-cancerous cells. In fact, the ternary copper(II) complexes were more selective and modestly efficient anticancer drugs.

Inactive NF-κB (nuclear factor κB) are bound to inhibitor IκB in the cytoplasm and prevent its translocation to nucleus. NF-κB activation is regulated by phosphorylation of IκB which results in its ubiquitination and its subsequent degradation by proteasome. Proteasome inhibitor functions to block the nuclear translocation and transcriptional activity of NF-κB and this can result in accumulation of ubiquitinated IκB-α. Functional proteasome will cause degradation of the ubiquitinated IκB-α to smaller fragmented IκB-α (37 kDa) (Fig. 4.7(a) untreated control, lane 1). Extract from cancer cells treated with 1 μM of all tested compounds showed pattern of IκB-α bands similar to

that from untreated cells, suggesting no inhibition of proteasome. However, extraction from MDA-MB-231 cells treated with 10 μM of [$Cu(8OHQ)_2$] showed an intense band of ubiquitinated IκB-α (56 kDa) and a faint band of degraded IκB-α (37 kDa), suggesting degradation of the IκB-α (56 kDa) due to the proteasomal inhibition induced by [$Cu(8OHQ)_2$] (Fig. 4.7(a), lane 11). In the experiment, the intensities of protein level of ubiquitinated IκB-α (56 kDa) and degraded IκB-α (37 kDa) for ternary copper(II) complexes-treated cancer cells (1 and 10 μM respectively) were similar to those of [$Cu(8OHQ)_2$] treated cells. This indicated that 10 μM of ternary copper(II) complexes could also inhibit proteasome. These data suggest that the proteasome is a target of ternary copper(II) complexes in human tumor cells and this inhibition contribute to their anticancer property. However, most of the other ubiquinated proteins (smearing) that were not degraded by the proteasome have not yet been identified and investigated (Fig. 4.7(a) Upper section).

5.2.2 Ternary copper(II) complexes induced intracellular ROS

Proteasome inhibition may not be the only mechanism for antitumor activity by ternary copper(II) complexes. Copper ions and complexes may undergo redox reactions and can damage biomolecules by formation of ROS (Linder, 1991). For example, copper participates in catalyzing the formation of ROS through superoxide and hydrogen peroxide *via* a Haber-Weiss reaction (Garrow *et al*., 2000). Tardito *et al*., (2007) stated that the production of ROS through copper(II) complexes-mediated cytotoxicity results in cell death. The

potential of copper-mediated oxidative stress by production of ROS in mediating killing cancer cells can be exploited therapeutically for cancer treatment (Gupte and Mumper, 2009). Live cell imaging study using microscopy technique showed that these complexes were able to induce morphology changes (diameter, shape and granularity) at 6 h in MDA-MB-231 cells (data not shown). Based on this finding, 6 h had been selected for ROS study and H2AX assay in this study.

In order to determine the level of ROS generation, two doses (5 μM and 10 μM) and two incubation time (6 h or 24 h) were chosen for treatment of MDA-MB-231 and MCF 10A. For the 24 h treatment, 10 μM concentration was not chosen in this assay because more than 70% of cells underwent cell death in the MTT assay when cells were treated with 10 μM ternary copper(II) complexes. The ROS production measurements in relation to incubation time and drug concentration are shown in Figs. 4.8 – 4.11. The exposure of the MDA-MB-231 and MCF10A to any compound at 5 μM for 6 h resulted in insignificant increase in relative fluorescence compared to untreated cells (Fig. 4.10). Results for higher dose (10 μM) of $[Cu(phen)(X_{aa})(H_2O)]NO_3$ or longer incubation time (24 h, 5 μM) revealed that the generation of ROS was significantly increased. It showed that the increased production of ROS in MDA-MB-231 cells versus time (Figs 4.10 - 4.11). As shown in Fig 4.10, the generation of ROS by ternary copper(II) complexes is dose-dependent in MDA-MB-231 cells. Byrnes *et al*., (1992) stated that metal chelating agent (1,10-phenanthroline) enhanced DNA damage for metal-catalyzed generation of oxygen-derived radicals. The cytotoxic action of ternary copper(II)

complexes may involve similar increase in ROS generation. On the other hand, 10 μM ternary copper(II) complexes still has no effect on the ROS levels in MCF10A treated cells for 6 h as there is no statistically significant increase in ROS compared to untreated cells (Fig. 4.10). This reveals that there is a safe minimum dosage of ternary copper(II) complexes to induce significant ROS increase in cancer cells without altering the ROS levels in normal cells.

Previous studies of Zhou *et al*., (2002) reported that copper(II)-1,10-phenanthroline, $[Cu(OP)_2]^{2+}$, was known to promote hydroxyl radical formation from molecular oxygen by redox-cycling and the hydroxyl radicals were responsible for DNA damage. In our studies, the ROS assay showed that cellular ROS induced by each ternary copper(II) complex was 2 - 4 fold higher in MDA-MB-231 cells treated for longer period (24 h) compared to basal levels of ROS in untreated cells. However, remarkably lower ROS production was observed in treated MCF 10A cells under the same condition. The result showed a uptrend in the level of ROS in MDA-MB-231 cells with respect to increasing concentration of the ternary copper(II) complexes at 6 h incubation. It is feasible to manipulate concentration of ternary copper(II) complexes and incubation time to generate significantly higher ROS in cancer cells compared to untreated cancer cells without affecting ROS levels in normal cells or merely raising to ROS levels to non-dangerous levels. Many types of cancer cells have higher basal ROS and decreased antioxidants. The greater generation of ROS in MDA-MB-231 than in MCF10A could easily push the ROS level to reach the ROS threshold without adequate antioxidants, and thus preferentially initiate apoptosis in the former.

Ternary copper(II) complexes have minimal effect on generation of ROS in non-tumorigenic MCF 10A, in sharp contrast to their effect on breast tumor MDA-MB-231. The increased ROS can directly affect cell survival pathways (PI3-kinase/Akt pathway) (Clerkin *et al*., 2008). On the other hand, Pelicano *et al*., (2004) reported a characteristic of many cancer cells in exhibiting increased ROS stress due to oncogenic stimulation, increased metabolic activity and mitochondrial malfunction. It was said that it was possible to use anticancer agents to induce ROS generation to selectively kill cancer cells (Pelicano *et al*., 2003). Therefore, the strategy of preferential cell death by increasing ROS in cancer cells can provide a prospect of selective cancer treatment (Gupte and Mumper, 2009). Many studies suggest significant decrease of the antioxidant enzymes such as catalase and glutathione perioxidase in breast tumors compared to nonmalignant cells and accumulation of oxidatively induced DNA damage in human breast cancer cell lines (Francisco *et al*., 2008; Nyaga *et al*., 2006). These data revealed that the resistance against chemotherapy was dependent on the ability of different cell types to defend themselves against ROS. Collectively, these results imply that ternary copper(II) complexes are capable of enhancing cytotoxicity *via* increased generation of ROS in malignant cells and thereby inducing cell death.

5.2.3 Relation of γH2AX to ternary copper(II) complexes

Published data demonstrated that copper(II) complexes can be used as metallodrugs to cause DNA damage and lead to decrease cell viability, cell cycle arrest and apoptotic cell death (Annaraj *et al*., 2005; Liu *et al.*, 1999; Chikira *et al*., 2002; Wang *et al*., 2010). It is, therefore important to identify DNA as one of the targets for ternary copper(II) complexes. DNA damage that lead to formation of DNA double strand breaks (DSBs) will induce phosphorylated H2AX on Ser^{139} (denoted as γH2AX) (Srivastava *et al*., 2009; Mukherjee *et al*., 2006). γH2AX can serve as an indicator for induction of apoptosis. The detection of γH2AX in nuclei is based on immunofluorescence using antibody tagged with Alexa Fluor® 488. Counter staining with DAPI was used to locate nuclear DNA in the cells.

DSBs are among the most cytotoxic DNA lesions. γH2AX provides a marker of DSBs (Huang and Darzynkiewicz, 2006). If DNA repair is successful, cells exposed to antineoplastic drugs will keep entering the cycle and develop resistance to the drugs. Isotype control used in the study was to distinguish the DSBs induced by test agents (adriamycin) versus the intrinsically formed DSBs in untreated cell (Figs. 4.12 - 4.14). Zhou *et al.* (2011) have investigated the percentage of cells expressing γH2AX which was found to increase in a dose-dependent manner after exposure to adriamycin. In this study, the intensity of FITC indicates γH2AX was significantly elevated in each individual ternary copper(II) complexes-treated MDA-MB-231 cells (Fig 4.12). This result suggests 5 μM ternary copper(II) complexes induced DSBs

at short incubation period (6 h) in cancer cells. One of the substrate phosphorylated by ataxia telangiectasia mutated (ATM) is histone H2AX, and the expression of γH2AX is mediated by ATM. Once ATM is activated, it lead to the downstream events such as recruitment of DNA repair machinery, engagement of cell cycle checkpoints, and activation of apoptotic pathway (Tanaka *et al*., 2007). Accordingly, the results suggest that the transient treatment (6 h) with ternary copper(II) complexes induced formation of γH2AX and induced oxidative DNA damage and lead to downstream apoptosis pathway (Figs. 4.12 – 4.13).

Intriguingly, in contrast to MDA-MB-231, a negative response for the γH2AX was observed after treatment of MCF 10A with 5 μM ternary copper(II) complexes under the same conditions (Fig. 4.14). This difference may be because MCF 10A cells could still conserve their viability at that particular ternary copper(II) concentration and time point. Therefore, sufficiently low concentration of ternary copper(II) complexes did not cause DSBs in MCF 10A cells. This indicates their relative non-toxicity towards immortalized cells. Further testing and investigation are needed to prove their efficacy as anticancer drugs. Taken together, these findings imply that this method could be useful to screen for the mechanism of this series of ternary copper(II) complexes.

The metal chelator phen and copper salts form stable copper bis-phen complexes. Ligand is responsible for directing the metal to different molecular targets (Tardito and Marchio, 2009). Tardito *et al.* (2011) reported that

lipophilicity is one determinant in the cytotoxicity of a copper complex. In this study, the different amino aicds with methyl substituent(s) serve as subsidiary ligand in this series of ternary copper(II) complexes does not seem to greatly affect and regulate their biological activities. Although the four members of this series of ternary copper(II) complexes showed similar effectiveness, only two of them, with one or two methyl substituent(s) at the α–carbon of the amino acid, could induced cell cycle arrest at G_o/G_1. Attempt has been made to improve hydrophilicity by choosing amino acid with hydrophobic methyl subsituent(s) as ligand. By including amino acid as a component, all these ternary copper(II) complexes are found to easily dissolve in water and to be less cytotoxic compared to $[Cu(8OHQ)_2]$. However, the exact role of the amino acid has not been elucidated and the evidence of a synergic effect between the copper and the ligands is till lacking.

CHAPTER 6.0

CONCLUSION

Platinum is not the only transition metal used in the treatment of cancer. Copper is an essential cofactor in number of enzymes and it participates in a broad spectrum of intracellular processes under normal and pathological conditions. For example, copper is essential for tumor angiogenesis and it is found to be elevated in various human cancer tissues. Up to now, a great variety of copper complexes have been tested as cytotoxic agents and found to have anticancer activity *in vitro* and *in vivo*. Due to copper redox behavior and variable coordination modes, there still exist enormous prospect in the design of more potent and less toxic copper complexes-based antiproliferative drugs with enhanced bioavailability and anticancer efficacy. The usage of ligand-bound essential metal ions, such as copper, may participate in a variety of biological redox chemistry and interact with different biological substrates to widen the spectrum of anticancer activity. In this connection, copper complexes may serve as effective cytotoxic agents.

Ternary copper(II) complexes described in this study show diverse *in vitro* biological activities, ranging from anticancer properties and different modes of action (proteasome inhibition, ROS generation study and phosphorylation of H2AX) leading to apoptosis pathway. At molecular level, it has become clear that ternary copper(II) complexes can act by different

mechanisms which involve interaction with DNA leading to an oxidative cell damage, production of ROS by redox-cycling, and inhibition of proteasome activity. Generally, these intracellular molecular events trigger cancer cell death through an apoptotic mechanism.

These findings suggest that ternary copper(II) complexes are capable of decreasing cell proliferation in a dose-dependent manner. Microscopic image demonstrated that MDA-MB-231 and MCF10A cells treated with ternary copper(II) complexes are able to induce morphological changes and decreases the number of cells in a concentration-dependent manner. The growth inhibition and apoptosis induction were observed with the treatment of ternary copper(II) complexes at micromolar concentrations and selectivity against cancer cells was established through the MTT assay and apoptosis study. $[Cu(phen)(DL\text{-}ala)(H_2O)]NO_3$, $[Cu(phen)(sar)(H_2O)]NO_3$, $[Cu(phen)(C\text{-}dMg)(H_2O)]NO_3$, $[Cu(phen)(gly)(H_2O)]NO_3$ are antiproliferative against MDA-MB-231 cells in a concentration dependent manner with IC_{50} values of 5.5 ± 1.1 μM, 5.2 ± 0.2 μM, 6.2 ± 1.1 μM and 8.5 ± 0.3 μM respectively for 24 h incubation. At relatively low range of concentrations, these compounds had exhibited anticancer activity by selectively killing cancer cells rather non-cancerous cells. This needs to be extended to different cell lines as well as to *in vivo* studies. Staining with annexin V-FITC and propidium iodide showed that 5 μM of these compounds could induce cell cycle arrest at G_0/G_1 phase at 24 h incubation for MDA-MB-231 breast cancer cells, while MCF10A immortalized cells were not affected by this series of ternary copper(II) complexes at this concentration. There is a link among

proteasome inhibition, copper and cancer. Indeed, copper has a strong implication in proteasome activity. Data suggested that these ternary copper(II) complexes act as proteasome inhibitors and apoptosis inducers to tumor cells. Apoptosis-inducing effect may be mediated by ternary copper(II) complexes through the generation of ROS and DSBs in cancer cells. Collectively, these results indicate that ternary copper(II) complexes is a potent anticancer compounds that induces cell death at relatively low range of concentration.

Experimental evidences suggest that generation of ROS by redox cycling showed obvious cellular effects in cancer cells treated with ternary copper(II) complexes and avoids toxicity in immortalized cells. Hence, there is a safe minimum dosage of ternary copper(II) complexes to induce the redox unbalance which is responsible for triggering cell death. However, more evidence and the exact molecular mechanism underlying the selective cytotoxicity of these compounds remain to be collected and elucidated. Understanding pathways of metabolism of these newly metal-based compounds and identification of metabolites and their roles require extensive studies. In addition, it is not totally clear why drug-treated oncogene-transformed cells are more sensitive and selective to the ternary copper(II) complexes than untransformed cells. Therefore, further research is needed to address further downstream mechanism, specifically the selectivity and specificity of killing cancer cells. Thus, these experiments will form a significant portion of the intended future studies, along with elucidation of the detailed mechanism which led to cell death.

In conclusion, this project has established the potential of ternary copper(II) complexes for further development into new anticancer drugs. Results suggest that ternary copper(II) complexes showed promising antitumor activity in breast cancer cell line. These complexes might offer a unique approach to treating human cancers, including drug resistant tumors.

List of References

Abada, P. and Howell, S. B. (2010). Regulation of Cisplatin Cytotoxicity by Cu Influx Transporters Metal-Based Drugs, 2010: 317581, 9 pages.

Adams J. (2003). The proteasome: structure, function, and role in the cell**.** *Cancer Treat Rev.*, 29 Suppl 1:3-9.

Adams, J. (2002a). Development of the proteosome inhibitor PS-341. *The Oncologist*, 7, 9-16.

Adams, J. (2002b). Proteasome inhibition: a novel approach to cancer therapy. *Trends in Molecular Medicine*, 8, S49-S54.

Adams, J. (2004). The development of proteasome inhibitors as anticancer drugs. *Cancer* Cell, 5, 417-421.

Afrasiabi, Z., Sinn, E., Padhye, S., Dutta, S., Padhye, S., Newton, C., Anson, C. E, Powell, A. K. (2003). Transition metal complexes of phenanthrenequinone thiosemicarbazone as potential anticancer agents: synthesis, structure, spectroscopy, electrochemistry and in vitro anticancer activity against human breast cancer cell-line. T47D. *J Inorg Biochem.*, 95,306-314.

Ainscough, E. W., Brodie, A. M., Denny, W. A., Finlay, G. J. and Ranford, J. D (1998). Nitrogen, sulfur and oxygen donor adducts with copper(II) complexes of antitumor 2-formylpyridinethiosemicarbazone analogs: physicochemical and cytotoxic studies. *J Inorg Biochem.*, 70, 175-185.

Almond, J. B. and Cohen, G. M. (2002) The proteasome: a novel target for cancer chemotherapy. *Leukemia*, 16, 433-443.

Annaraj, J., Srinivasan, S., Ponvel, K. M. and Athappan, P. R. (2005). Mixed ligand copper(II) complexes of phenanthroline/bipyridyl and curcumin diketimines as DNA intercalators and their electrochemical behavior under Nafion® and clay modified electrodes. *Journal of Inorganic Biochemistry*, 99, 669-676.

Ashkenazi, A. and Dixit, V. M. (1998). Death receptors: signaling and modulation. *Science*, 281, 1305-1308.

Aubé, M., Larochelle. C. and Ayotte, P. (2011). Differential effects of a complex organochlorine mixture on the proliferation of breast cancer cell lines. *Environ Res.*, 111, 337-347.

Balamurugan, K. and Schaffner, W. (2006). Copper homeostasis in eukaryotes: Teetering on a tightrope. *Biochim Biophys Acta.*, 1763, 737-746.

Bandyopadhyay, U., Das, Dipak. and Banerjee, R. K. (1999). Reactive oxygen species: Oxidative damage and pathogenesis. *Current Science*, 77, 658-666.

Barceló-Oliver, M.; García-Raso, A.; Terrón, A.; Molins, E.; Prieto, M. J.; Moreno, V.; Martínez-Serra, J.; Lladó, V.; López, I.; Gutiérrez, A. and Escribá, P. V., (2009). Ternary copper(II) complexes with hippurate derivatives and 1,10-phenanthroline: synthesis and biological activity. *Inorganica Chimica Acta*, 362, 4744-4753.

Bates, S. E. (1999). Drug resistance: still on the learning curve. *Clin Cancer Res.*, 5, 3346-3348.

Bazzaro, M., Lee, M. K., Zoso, A., Stirling, W. L. H., Santillan, A., Ie-Ming S. and Richard B. S. R. (2006). Ubiquitin-Proteasome System Stress Sensitizes Ovarian Cancer to Proteasome Inhibitor–Induced Apoptosis. *Cancer Res.*, 66, 3754-3763.

Bertinato, J. and L'Abbé, M. R. (2004). Maintaining copper homeostasis: Regulation of Copper-trafficking proteins in response to copper deficiency or overload. *J. Nutr. Biochem.*, 15, 316-322.

Bertini, I., Cavallaro, G. and McGreevy, K.S. (2010). Cellular copper management-a draft user's guide. *Coordination Chemistry Reviews*, 254, 506-524.

Bonner. W. M. Redon, C. E., Dickey, J. S., Nakamura, A. J., Sedelnikova, O. A., Solier, S. and Pommier, Y. (2008). γH2AX and cancer. *Nat Rev Cancer.*, 8, 957-967.

Boulikas, T. and Vougiouka, M. (2003). Cisplatin and platinum drugs at the molecular level. (Review). *Oncol Rep.*, 10, 1663-1682.

Bruijnincx, P. C and Sadler, P. J (2008). New trends for metal complexes with anticancer activity. *Curr Opin Chem Biol*,12, 197-206.

Byrnes, R. W., Antholine, W. E and Petering, D. H. (1992). Interactions of 1,10-phenanthroline and its copper complex with Ehrlich cells. *Free Radic Biol Med.*, 12,457-469.

Cai, X., Pan, N. and Zou, G. (2007). Copper-1,10-phenanthroline-induced apoptosis in liver carcinoma Bel-7402 cells associates with copper overload, reactive oxygen species production, glutathione depletion and oxidative DNA damage. *Biometals*, 20, 1-11.

Camakaris, J., Voskoboinik, I. and Mercer, J. F. (1999). Molecular mechanisms of copper homeostasis. *Biochem Biophys Res Commun.*, 261, 225-232.

Celeste, A., Fernandez-Capetillo, O., Kruhlak, M. J., Pilch, D. R., Staudt, D. W., Lee, A., Bonner, R. F., Bonner, W. M. and Nussenzweig, A. (2003). Histone H2AX phosphorylation is dispensable for the initial recognition of DNA breaks. *Nat Cell Biol.*, 5,675-679.

Chaviara, A. T., Christidis, P. C., Papageorgiou, A., Chrysogelou, E., Hadjipavlou-Litina, D. J. and Bolos, C. A. (2005). In vivo anticancer, anti-inflammatory, and toxicity studies of mixed-ligand Cu(II) complexes of dien and its Schiff dibases with heterocyclic aldehydes and 2-amino-2-thiazoline. Crystal structure of [Cu(dien)(Br)(2a-2tzn)](Br)(H(2)O). *J Inorg Biochem.*, 99, 2102-2109.

Chen, D. and Dou, Q. P. (2008). New uses for old copper-binding drugs: converting the proangiogenic copper to a specific cancer cell death inducer. *Expert Opin. Ther. Targets*, 12, 739-748.

Chen, D., Cui, Q. C., Yang, H., Barrea, R. A., Sarkar, F. H., Sheng, S., Yan, B., Reddy, G. P. and Dou, Q. P. (2007). Clioquinol, a therapeutic agent for Alzheimer's disease, has proteasome-inhibitory, androgen receptor-suppressing, apoptosis-inducing, and antitumor activities in human prostate cancer cells and xenografts. *Cancer Res.*, 67, 1636-1644.

Chen, F., Vallyathan, V., Castranova, V. and Shi, X. (2001). Cell apoptosis induced by carcinogenic metals. *Mol. Cell. Biochem.*, 222, 183-188.

Chen, H. L., Chang, C. Y., Lee, H. T., Lin, H. H., Lu, P. J., Yang, C. N., Shiau, C. W. and Shaw, A. Y. (2009). Synthesis and pharmacological exploitation of clioquinol-derived copper-binding apoptosis inducers triggering reactive oxygen species generation and MAPK pathway activation. *Bioorg Med Chem.*, 17, 7239-7247.

Chen, W., Zhao, Z., Li, L., Wu, B., Chen, S. F., Zhou, H., Wang, Y. and Li, Y. Q. (2008b). Hispolon induces apoptosis in human gastric cancer cells through a ROS-mediated mitochondrial pathway. *Free Radic Biol Med.*, 45, 60-72.

Chetana, P. R., Rao, R., Roy, M. and Patra, A. K. (2009). New ternary copper(II) complexes of l-alanine and heterocyclic bases: DNA binding and oxidative DNA cleavage activity. *Inorganica Chimica Acta*, 362, 4692-4698.

Chikira, M., Tomizawa, Y., Fukita, D., Sugizaki, T., Sugawara, N., Yamazaki, T., Sasano, A., Shindo, H., Palaniandavar, M. and Antholine, W. E. (2002). DNA-fiber EPR study of the orientation of Cu(II) complexes of 1,10-phenanthroline and its derivatives bound to DNA: mono(phenanthroline)-copper(II) and its ternary complexes with amino acids. *J Inorg Biochem.*, 89, 163-173.

Chiu, S. J., Lee, Y. J., Hsu, T. S. and Chen, W. S. (2009). Oxaliplatin-induced gamma-H2AX activation via both p53-dependent and -independent pathways but is not associated with cell cycle arrest in human colorectal cancer cells. *Chem Biol Interact.*, 182, 173-182.

Ciechanover, A. (1998). The ubiquitin–proteasome pathway: on protein death and cell life. *EMBO J.*, 17, 7151-7160.

Clerkin, J. S., Naughton, R., Quiney, C. and Cotter, T. G. (2008). Mechanisms of ROS modulated cell survival during carcinogenesis. *Cancer Lett.*, 266, 30-36.

Collins, M., Ewing, E., Mackenzie, G., Sinn, E., Sandbhor, U., Padhye and S., Padhye, G. S. (2000). Metal Complexes as Anticancer Agents. 2. Synthesis, Spectroscopy, Magnetism, Electrochemistry, X-ray Crystal Structure and Antimelanomal Activity of the Copper(II) Complex of 5-amino-1-tolylimidazole-4-carboxylate in B16F10 Mouse Melanoma Cells. *Inorg. Chem. Comm.*, 3, 453-457.

Corso, A., Mangiacavalli, S., Varettoni, M., Pascutto, C., Zappasodi, P., and Lazzarino, M. (2010). Bortezomib-induced peripheral neuropathy in multiple myeloma: A comparison between previously treated and untreated patients. *Leuk Res.*, 34, 471-474.

Cowell, J. K., LaDuca, J., Rossi, M. R., Burkhardt, T., Nowak, N. J. and Matsui, S. (2005). Molecular characterization of the t(3;9) associated with immortalization in the MCF10A cell line. *Cancer Genet Cytogenet.*,163, 23-29.

Curtin, J. F, Donovan, M. and Cotter, T. G. (2002). Regulation and measurement of oxidative stress in apoptosis. *J Immunol Methods.*, 265, 49-72.
Cusack, J. C. (2003). Rationale for the treatment of solid tumors with the proteasome inhibitor bortezomib. *Cancer Treat Rev.*, 29, 21-31.

Cvek, B. and Dvorak, Z. (2008). The value of proteasome inhibition in cancer. Can the old drug, disulfiram, have a bright new future as a novel proteasome inhibitor? *Drug Discovery Today*, 13, 716-722.

McConkey, D. J. (1998). Biochemical determinants of apoptosis and necrosis. *Toxicol. Lett.*, 99, 157-168.

Daniel, K. G, Chen, D., Orlu, S., Cui, Q. C., Miller, F. R. and Dou, Q. P. (2005). Clioquinol and pyrrolidine dithiocarbamate complex with copper to form proteasome inhibitors and apoptosis inducers in human breast cancer cells. *Breast Cancer Res.*, 7, R897-908.

Daniel, K. G., Gupta, P., Harbach, R. H., Guida, W. C., Dou, Q. P. (2004). Organic copper complexes as a new class of proteasome inhibitors and apoptosis inducers in human cancer cells. *Biochem Pharmacol*, 67, 1139-1151.

De Romaña, D. L., Olivares, M., Uauy, R. and Araya, M. (2011). Risks and benefits of copper in light of new insights of copper homeostasis. *Journal of Trace Elements in Medicine and Biology*, 25, 3-13.

De Vizcaya-Ruiz, A., Rivero-Muller, A., Ruiz-Ramirez, L., Kass, G. E., Kelland, L. R., Orr, R. M., Dobrota, M. (2000). Induction of apoptosis by a novel copper-based anticancer compound, casiopeina II, in L1210 murine leukaemia and CH1 human ovarian carcinoma cells. *Toxicol In Vitro*, 14, 1-5.

Debatin, K. M., Poncet, D. and Kroemer, G. (2002). Chemotherapy: targeting the mitochondrial cell death pathway. *Oncogene*, 21, 8786-8803.

Deegan, C., McCann, M., Devereux, M., Coyle, B. and Egan, D.A. (2007). In vitro cancer chemotherapeutic potential and mechanism of action of 1,10-Phenanthroline (phen), $[Ag_2(phen)_3(mal)]\ 2H_2O$, $[Cu(phen)_2(mal)]\ 2H_2O$ and $[Mn(phen)_2(mal)]\ 2H_2O$ ($malH_2$=malonic acid), using human cancer cells, *Cancer Lett.*, 247, 224-233.

Dees, E. C., and Orlowski, R. Z. (2006). Targeting the ubiquitin-proteasome pathway in breast cancer therapy. *Future Oncol.*, 2(1):121-135.

Dhanasekaran, A., Kotamraju, S., Karunakaran, C., Kalivendi, S. V., Thomas, S., Joseph, J. and Kalyanaraman, B. (2005). Mitochondria superoxide dismutase mimetic inhibits peroxide-induced oxidative damage and apoptosis: Role of mitochondrial superoxide. *Free Radical Biology & Medicine*, 39, 567-583.

Ding, X., Xie, H. and Kang, Y. J. (2011). The significance of copper chelators in clinical and experimental application. *The Journal of Nutritional Biochemistry*, 22, 301-310.

Dinnen, R. D. and Ebisuzaki, K. (1992). The linking of anticancer drugs, cell cycle blocks, and differentiation: implications in the search for antineoplastic drugs. *Leuk Res.*, 16, 491-495.

Dou, Q. P. and Li, B., (1999). Proteasome inhibitors as potential novel anticancer agents. *Drug Resist. Updates*, 2, 215-223.

Dreiseitel, A., Schreier, P., Oehme, A., Locher, S., Rogler, G., Piberger, H., Hajak, G. and Sand, P. G. (2008). Inhibition of proteasome activity by anthocyanins and anthocyanidins. *Biochem Biophys Res Commun.*, 372, 57-61.
Driscoll, J. J., Minter, A., Driscoll, D. A. and Burris, J. K. (2011). The Ubiquitin+Proteasome Protein Degradation Pathway as a Therapeutic Strategy in the Treatment of Solid Tumor Malignancies. *Anticancer Agents Med Chem.*, 11, 242-246.

Fenteany. G. and Schreiber, S. L. (1996). Specific inhibition of the chymotrypsin-like activity of the proteasome induces a bipolar morphology in neuroblastoma cells. *Chem Biol*., 3, 905-912.

Ferlay, J., Bray, F., Pisani, P., et al (2002). Globocan 2002: Cancer Incidence, Mortality and Prevalence Worldwide. Lyon: International Agency for Research on Cancer Press.

Fernandez-Capetillo, O., Lee, A., Nussenzweig, M. and Nussenzweig, A. (2004). H2AX: the histone guardian of the genome. *DNA Repair (Amst).*, 3, 959-967.

Francisco, D. C., Peddi, P., Hair, J. M., Flood, B.A., Cecil, A.M., Kalogerinis, P. T., Sigounas, G. and Georgakilas, A. G. (2008). Induction and processing of complex DNA damage in human breast cancer cells MCF-7 and nonmalignant MCF-10A cells. *Radical Biology and Medicine*, 44. 558-569.

Galanis, A., Pappa, A., Giannakakis, A., Lanitis, E., Dangaj, D. and Sandaltzopoulos, R. (2008). Reactive oxygen species and HIF-1 signalling in cancer. *Cancer Lett.*, 266, 12-20.

Gama, S., Mendes, F., Marques, F., Santos, I. C., Carvalho, M. F., Correia, I., Pessoa, J. C., Santos, I. and Paulo, A. (2011). Copper(II) complexes with tridentate pyrazole-based ligands: synthesis, characterization, DNA cleavage activity and cytotoxicity. *J Inorg Biochem.*, 105, 637-644.

Garrett, S., Barton, W. A., Knights, R., Jin, P., Morgan, D. O. and Fisher, R. P. (2001). Reciprocal activation by cyclin-dependent kinases 2 and 7 is directed by substrate specificity determinants outside the T loop. *Mol Cell Biol.*, 21, 88-99.

Garrow, J. S., Ralph, A., James, W. P. T. and Ralph, A. (2000). Human nutrition and dietetics (pg 252). Churchill Livingstone.

Gavrilov, B., Vezhenkova, I., Firsanov, D., Solovjeva, L., Svetlova, M., Mikhailov, V. and Tomilin, N. (2006). Slow elimination of phosphorylated histone c-H2AX from DNA of terminally differentiated mouse heart cells in situ. *Biochemical and Biophysical Research Communications*, 347, 1048-1052.

Gelbke, H. P., Kayser, M. and Poole, A. (2004). OECD test strategies and methods for endocrine disruptors. *Toxicology*. 205, 17-25.

Geraghty, M., Sheridana, V., McCanna, M., Devereuxb, M. and McKeec, V. (1999). Synthesis and anti-Candida activity of copper(II) and manganese(II) carboxylate complexes: X-ray crystal structures of [Cu(sal)(bipy)] C2H5OH H2O and [Cu(norb)(phen)2] 6.5H2O (salH2=salicylic acid; norbH2=cis-5-norbornene-endo-2,3-dicarboxylic acid; bipy=2,2′-bipyridine; phen=1,10-phenanthroline). *Polyhedron*, 18, 2931-2939.

Gérard, C., Bordeleau, L. J., Barralet, J. and Doillon, C. J. (2010). The stimulation of angiogenesis and collagen deposition by copper. *Biomaterials*, 31, 824-831.

Giacinti, C. and Gioradano, A. (2006). RB and cell cycle progression. *Oncogene*, 25, 5220-5227.

Gottesman, M.M., Ludwig, J., Xia, D. and Szakács, G. (2006). Defeating drug resistance in cancer. *Discov Med.*, 6, 18-23.

Green, D. R. and Reed, J. C. (1998). Mitochondria and apoptosis, *Science*, 281, 1309-1312.

Groll, M., Heinemeyer, W., Jager, S., Ullrich, T., Bochtler, M., Wolf, D.H., Huber, R., (1999). The catalytic sites of 20S proteasomes and their role in subunit maturation: a mutational and crystallographic study. *Proc. Natl. Acad. Sci. (USA)* 96, 10976-10983.

Grover, A., Shandilya, A., Bisaria, V. S. and Sundar, D. (2010). Probing the anticancer mechanism of prospective herbal drug Withaferin A on mammals: a case study on human and bovine proteasomes. *BMC Genomics.*, 11, Suppl 4:S15.

Guo, W. J., Ye, S. S., Cao, N., Huang, J., Gao, J. and Chen, Q. Y. (2010). ROS-mediated autophagy was involved in cancer cell death induced by novel copper(II) complex. *Exp Toxicol Pathol.*, 62, 577-582.

Gupte, A. and Mumper, R. J. (2007). Copper chelation by D-penicillamine generates reactive oxygen species that are cytotoxic to human leukemia and breast cancer cells. F*ree Radic Biol Med.*, 43, 1271-1278.

Gupte, A. and Mumper, R. J. (2009). Elevated copper and oxidative stress in cancer cells as a target for cancer treatment. *Cancer Treat. Rev.*, 35, 32-46.

Han, Y. H., Kim, S. H., Kim, S. Z. and Park, W. H. (2008). Antimycin A as a mitochondria damage agent induces an S phase arrest of the cell cycle in HeLa cells. *Life Sci.*, 83, 346-355.

Hanasoge, S. and Ljungman, M. (2007). H2AX phosphorylation after UV irradiation is triggered by DNA repair intermediates and is mediated by the ATR kinase. *Carcinogenesis.*, 28, 2298-2304.

Harris, E. D. (1992). Copper as a cofactor and regulator of copper, zinc superoxide dismutase. *J Nutr.*, 122 (3 Suppl):636-640.

Harris, Z. H. and Gitlin, J. D. (1996). Genetic and molecular basis of copper toxicity. *Am J Clin Nutr.*, 63, 836S-841S.

Hernández, W., Spodine, E., Beyer, L., Schröder, U., Richter, R., Ferreira, J. and Pavani, M. (2005). Synthesis, characterization and antitumor activity of copper(II) complexes, [CuL2] [HL1-3=N,N-Diethyl-N'-(R-Benzoyl)Thiourea (R=H, o-Cl and p-NO2)]. Bioinorg Chem Appl., 3, 299-316.

Herr, I. and Debatin, K. M. (2001). Cellular stress response and apoptosis in cancer therapy. Blood., 98, 2603-2614.

Herr, R., Wöhrle, F. U., Danke, C., Berens, C. and Brummer, T. (2011). A novel MCF-10A line allowing conditional oncogene expression in 3D culture. *Cell Commun Signal.*, 9, 17-30.

Hershko, A. (1991). The ubiquitin pathway for protein degradation. *Trends Biochem Sci.*, 16, 265-268.

Hervouet, E., Simonnet, H. and Godinot, C. (2007). Mitochondria and reactive oxygen species in renal cancer. *Biochimie.*, 89, 1080-1088.

Hindo. S. S., Frezza, M., Tomco, D., Heeg, M. J., Hryhorczuk, L., McGarvey, B. R., Dou, Q. P. and Verani, C. N. (2009). Metals in anticancer therapy: copper(II) complexes as inhibitors of the 20S proteasome. *Eur J Med Chem.*, 44, 4353-4361.

Hisham, A. N. and Yip, C. H. (2004). Overview of breast cancer in Malaysian women: a problem with late diagnosis. *Asian J Surg.*, 27,130-133.

Horwitz, K. B., Zava, D. T., Thilager, A. K., Jenson, E. M. and McGuire, W. L. (1978). Steroid receptor analyses of nine breast cancer cell lines. *Cancer Res.*, 38, 2434–2437.

http://www.breastcancer.org/symptoms/understand_bc/statistics.jsp Accessed on 16th March 2011.

http://www.imaginis.com/breast-health/breast-cancer-statistics-on-incidence-survival-and-screening-2 Accessed on 20th March 2011.

http://www.makna.org.my/breastcancer.asp Accessed on 19th March 2011.

http://www.radiologymalaysia.org/breasthealth/About/FactsNStats.htm Accessed on 19th March 2011.

http://www.utusan.com.my/utusan/info.asp?y=2010&dt=0706&pub=Utusan_Malaysia&sec=Kesihatan&pg=kn_01.htm Accessed on 18th March 2011.

Hsieh, T. C, Wijeratne, E. K., Liang, J. Y., Gunatilaka, A. L and Wu, J. M. (2005). Differential control of growth, cell cycle progression, and expression of NF-kappaB in human breast cancer cells MCF-7, MCF-10A, and MDA-MB-231 by ponicidin and oridonin, diterpenoids from the chinese herb Rabdosia rubescens. Biochem Biophys Res Commun**,** 337, 224-231.

Huang, R., Wallqvist, A. and Covell, D. G. (2005). Anticancer metal compounds in NCI's tumor-screening database: putative mode of action. *Biochem Pharmacol.*, 69, 1009-1039

Huang, X. and Darzynkiewicz, Z. (2006). Cytometric Assessment of Histone H2AX Phosphorylation: A Reporter of DNA Damage. *Methods Mol Biol.*, 314, 73-80.

Huang, Y. L., Sheu, J. Y. and Lin, T. H. (1999). Association between oxidative stress and changes of trace elements in patients with breast cancer. *Clin Biochem.*, 32, 131-136.

Ismail, I. H, Wadhra, T. I. and Hammarsten, O. (2007). An optimized method for detecting gamma-H2AX in blood cells reveals a significant interindividual

variation in the gamma-H2AX response among humans. *Nucleic Acids Res.*, 35, e36.

Jacobson, M. D., Weil, M. and Raff, M. C. (1997). Programmed cell death in animal development. *Cell*, 88,347-354.

Jamieson, E. R. and Lippard, S. J. (1999). Structure, recognition, and processing of cisplatin-DNA adducts. *Chem. Rev.*, 99, 2467-2498.

Jane, E. P. and Pollack, I. F. (2010). Enzastaurin induces H2AX phosphorylation to regulate apoptosis via MAPK signalling in malignant glioma cells. *Eur J Cancer.*, 46, 412-419.

Jensen, T. J., Loo, M. A., Pind, S., Williams, D. B., Goldberg, A. L, Riordan and J. R. (1995). Multiple proteolytic systems, including the proteasome, contribute to CFTR processing. *Cell*, 83, 129-135.

Jevtović, V., Ivković, S., Kaisarević, S., Kovačevi, R. (2010). Anticancer activity of new copper(II) complexes incorporating apyridoxal-semicarbazone ligand. *Contemporary material I*, 2, 133-137.

Johnson, W. T and Thomas, A. C. (1999). Copper deprivation potentiates oxidative stress in HL-60 cell mitochondria. *Proc Soc Exp Biol Med.*, 221, 147-152.

Johnstone, R. W., Ruefli, A. A. and Lowe, S. W. (2002). Apoptosis: a link between cancer genetics and chemotherapy. *Cell*, 108, 153-164.

Jönsson, G., Staaf, J., Olsson, E., Heidenblad, M., Vallon-Christersson, J., Osoegawa, K., de Jong, P., Oredsson, S., Ringnér, M., Höglund, M. and Borg, A. (2007). High-resolution genomic profiles of breast cancer cell lines assessed by tiling BAC array comparative genomic hybridization. *Genes Chromosomes Cancer*, 46, 543-558.

Kamat, J. P. and Devasagayam, T. P. (2000). Oxidative damage to mitochondria in normal and cancer tissues, and its modulation. *Toxicology.*, 155, 73-82.

Kaneto, H., Katakami, N., Matsuhisa, M. and Matsuoka, T. A. (2010). Role of reactive oxygen species in the progression of type 2 diabetes and atherosclerosis. *Mediators Inflamm.*, 2010:453892. Pg11.

Kato, T. A., Okayasu, R. and Bedford, J. S. (2007). Comparison of the induction and disappearance of DNA double strand breaks and gamma-H2AX foci after irradiation of chromosomes in G1-phase or in condensed metaphase cells. *Mutat Res.*, 639, 108-112.

Katsarou, M. E., Efthimiadou, E. K., Psomas, G., Karaliota, A. and Vourloumis, D. (2008). Novel copper(II) complex of N-propyl-norfloxacin and

1,10-phenanthroline with enhanced antileukemic and DNA nuclease activities. *J Med Chem*., 51, 470-478.

Kazi, A., Daniel, K.G., Smith, D.M., Kumar, N.B. and Dou, Q.P. (2003). Inhibition of the proteasome activity, a novel mechanism associated with the tumor cell apoptosis-inducing ability of genistein. *Biochem. Pharmacol.*, 66, 965-976.

Kaznica, A., Drewa, T., Lakomska, I., Ryta-Stamirowska, P., Debski, R., Styczynski, J., Drewa, G. and Szlyk, E. (2009). Influence of two Pt(IV) complexes on viability, apoptosis and cell cycle of B16 mouse melanoma tumors. *Exp Oncol.*, 31, 33-36.

Kelland, L.R. (2000). Preclinical perspectives on platinum resistance. *Drugs*, 59, 1-8.

Khanna, S., Venojarvi, M., Roy, S., Sharma, N., Trikha, P., Bagchi, D., Bagchi, M. and Sen, C. K. (2002). Dermal wound healing properties of redox-active grape seed proanthocyanidins. *Free Radical Biology and Medicine*, 33, 1089-1096.

Kisselev, A. F and Goldberg, A. L. (2001). Proteasome inhibitors: from research tools to drug candidates. *Chem Biol.*, 8,739-758.

Kisselev, A. F., Akopian, T. N., Woo, K. M. and Goldberg, A.L. (1999). The sizes of peptides generated from protein by mammalian 26S and 20S proteasomes: implications for understanding the degradative mechanism and antigen presentation. *J. Biol. Chem.*, 274, 3363-3371.

Kloetzel, P. M. (2004). The proteasome and MHC class I antigen processing, *Biochim. Biophys. Acta.*, 1695, 217-225.

Kurepa, J. and Smalle, J. A. (2008). Structure, function and regulation of plant proteasome. *Biochimie.*, 90, 324-335.

La Fontaine, S. and Mercer, J. F. B. (2007). Trafficking of the copper-ATPases, ATP7A and ATP7B: Role in copper homeostasis. *Archives of Biochemistry and Biophysics*, 463, 149-167.

Lee, D. H. and Goldberg, A. L. (1998). Proteasome inhibitors: valuable new tools for cell biologists. *Trends Cell Biol.*, 8, 397-403.

Lee, S. C., Izatt, R. M., Zhang, X. X., Nelson, E. G., Lamb, J. D., Savage, P. B. and Bradshaw, J. S. (2001). Highly selective copper(II) ion receptors: tetraazacrown ethers bearing two 8-hydroxyquinoline side arms. *Inorganica Chimica Acta*, 317, 174-180.

Leong, B. D., Chuah, J. A., Kumar, V. M., Yip, C. H. (2007). Breast cancer in Sabah, Malaysia: a two year prospective study. *Asian Pac J Cancer Prev.*, 8, 525-529.

Lévi, F. (2001). Circadian chronotherapy for human cancers. *Lancet Oncol.*, 2, 307-315.

Li, X., Zhang, Z., Wang, C., Zhang, T., He, K. and Deng, F. (2011). Synthesis, crystal structure and action on Escherichia coli by microcalorimetry of copper complexes with 1,10-phenanthroline and amino acid. *J Inorg Biochem*. 105, 23-30.

Li, Z., Li, J., Mo, B., Hu, C., Liu, H., Qi, H., Wang, X and Xu, J. (2008). Genistein induces cell apoptosis in MDA-MB-231 breast cancer cells via the mitogen-activated protein kinase pathway. *Toxicol In Vitro*, 22, 1749-1753.

Liao, S. R., Le, X. Y., Lin, Q. B., Lu, Q. M., Liu, X. P., Xiong, Y. H. and Feng, X. L. (2006). Synthesis, characterization and SOD-like activity of phen-Cu(II)-amino acid complexes . *Chin. J. Inorg. Chem.*, 22, 201-206.

Liberta, A. E. and West, D. X. (1992). Antifungal and antitumor activity of heterocyclic thiosemicarbazones and their metal complexes: current status. *Biometals*, 5, 121-126.

Linder, M. C. (2001). Copper and genomic stability in mammals. *Mutat Res.*, 475, 141-152.

Linder, M. C. Biochemistry of copper. New York: Plenum Press; 1991.

Liu, C., Zhou, J., Li, Q., Wang, L., Liao, Z. and Xu, H. (1999). DNA damage by copper(II) complexes: coordination-structural dependence of reactivities. *J Inorg Biochem.*, 75, 233-240.

Liu, Y., Parry, J. A., Chin, A., Duensing, S. and Duensing, A. (2008). Soluble histone H2AX is induced by DNA replication stress and sensitizes cells to undergo apoptosis. *Molecular Cancer.*, 7, 61.

López-Lázaro, M. (2007). Dual role of hydrogen peroxide in cancer: possible relevance to cancer chemoprevention and therapy. Cancer Lett.; 252, 1-8.

Lowe, S. W. and Lin, A. W. (2000). Apoptosis in cancer. *Carcinogenesis*, 21, 485-495.

Lowndes, S. A. and Harris, A. L. (2006). The Role of Copper in Tumour Angiogenesis. *Journal of Mammary Gland Biology and Neoplasia*, 10, 299-310.

Lu, L. P., Zhu, M. L. and Yang, P. (2003). Crystal structure and nuclease activity of mono(1,10-phenanthroline) copper complex. *J Inorg Biochem.*, 95, 31-36.

Lu, W., Ogasawara, M. A. and Huang, P. (2007). Models of reactive oxygen species in cancer. *Drug Discov Today Dis Model*, 4, 67-73.

Lu, Z., Tao, Y., Zhou, Z., Zhang, J., Li, C., Ou, L and Zhao, B. (2006). Mitochondrial reactive oxygen species and nitric oxide-mediated cancer cell apoptosis in 2-butylamino-2-demethoxyhypocrellin B photodynamic treatment. *Free Radic Biol Med.*, 41, 1590-1605.

Mah, L. J., Orlowski, C., Ververis, K., Vasireddy, R. S., El-Osta, A. and Karagiannis, T. C. (2011). Evaluation of the efficacy of radiation-modifying compounds using γH2AX as a molecular marker of DNA double-strand breaks. *Genome Integr.*, 2, 3-11.

Mailliez, A., Baldini, C., Van, J. T., Servent, V., Malle. Y. and Bonneterre, J. (2010). Nasal septum perforation: a side effect of bevacizumab chemotherapy inbreast cancer patients. *Br J Cancer*, 103, 772-775.

Maloň, M., Trávníček, Z., Maryško, M., Zbořil, R., Mašláň, M., Jaromír Marek, Doležal, K., Rolčík, J., Kryštof, V., Strnad, M. (2001). Metal complexes as anticancer agents 2. Iron(III) and copper(II) bio -active complexes with N-6-benzylaminopurine derivatives. *Inorganica Chimica Acta*, 119-129.

Marzano, C., Pellei, M., Tisato, F. and Santini, C. (2009). Copper complexes as anticancer agents. *Anticancer Agents Med Chem.*, 9, 185-211.

Mateos, M. V. and San Miguel, J. F.(2007). Bortezomib in multiple myeloma. *Best Pract Res Clin Haematol.*, 20, 701-715.

Matés, J. M. and Sánchez-Jiménez, F. M. (2000). Role of reactive oxygen species in apoptosis: implications for cancer therapy. *Int J Biochem Cell Biol.*, 32, 157-170.

Messerschmidt, A. (2010). Copper Metalloenzymes. Comprehensive Natural Products II, Chapter 8.14, Pages 489-545.

Mettlin, C. (1999). Global Breast Cancer Mortality Statistics. *CA CancerJ Clin.*, 49, 138 - 144.

Milacic, V., Chen, D., Giovagnini, L., Diez, A., Fregona, D., Dou, Q. P. (2008). Pyrrolidine dithiocarbamate-zinc(II) and -copper(II) complexes induce apoptosis in tumor cells by inhibiting the proteasomal activity. *Toxicol Appl Pharmacol.*, 231, 24-33.

Milacic, V., Jiao, P., Zhang, B., Yan, B. and Dou, Q. P. (2009). Novel 8-hydroxylquinoline analogs induce copper-dependent proteasome inhibition and cell death in human breast cancer cells. *Int J Oncol*., 35, 1481-1491.

Miller, L. D. and Liu, E. T. (2007). Expression genomics in breast cancer research: microarrays at the crossroads of biology and medicine. *Breast Cancer Res*., 9, 206.

Miller, F. R., Soule, H. D., Tait, L., Pauley, R. J., Wolman, S. R., Dawson, P. J. and Heppner, G. H. (1993). Xenograft model of progressive human proliferative breast disease. *J. Natl. Cancer Inst.*, 85, 1725-1732.

Moehler, T. M., Ho, A. D., Goldschmidt, H. and Barlogie, B. (2003). Angiogenesis in hematologic malignancies. *Crit Rev Oncol Hematol.*, 45, 227-244.

Mukherjee, B., Kessinger, C., Kobayashi, J., Chen, B. P., Chen, D. J., Chatterjee, A. and Burma, S. (2006). DNA-PK phosphorylates histone H2AX during apoptotic DNA fragmentation in mammalian cells. *DNA Repair (Amst).*, 5, 575-590.

Nam S, Smith DM, Dou QP. (2001). Ester bond-containing tea polyphenols potently inhibit proteasome activity in vitro and in vivo. *J Biol Chem.*, 276, 13322-13330.

Narod, S. A. (2010). Genes, the environment, and breast cancer. *Lancet.* 375, 2123-2124.

Nasulewicz. A., Mazur, A. and Opolski, A. (2004). Role of copper in tumour angiogenesis—clinical implications. *Journal of Trace Elements in Medicine and Biology*, 18, 1-8.

Naldini, A., Filippi, I., Ardinghi, C., Silini, A., Giavazzi, R. and Carraro, F. (2009). Identification of a functional role for the protease-activated receptor-1 in hypoxic breast cancer cells. *Eur J Cancer.* 45, 454-460.

Naldini, A., Filippi, I., Miglietta, D., Moschetta, M., Giavazzi, R. and Carraro, F. (2010). Interleukin-1β regulates the migratory potential of MDAMB231 breast cancer cells through the hypoxia-inducible factor-1α. *Eur J Cancer*, 46, 3400-3408.

Naujokat, C., Berges, C., Höh, A., Wieczorek, H., Fuchs, D., Ovens, J., Miltz, M., Sadeghi, M., Opelz, G. and Daniel, V. (2006) Proteasomal chymotrypsin-like peptidase activity is required for essential functions of human monocyte-derived dendritic cells. *Immunology*, 120, 120-132.

Naujokat, C., Fuchs, D. and Berges, C. (2007). Adaptive modification and flexibility of the proteasome system in response to proteasome inhibition. *Biochim Biophys Acta.*,1773, 1389-1397.

Neve, R.M., Chin, K., Fridlyand, J., Yeh, J., Baehner, F.L., Fevr, T., Clark, L., Bayani, N., Coppe, J.P., Tong, F. et al. (2006). A collection of breast cancer cell lines for the study of functionally distinct cancer subtypes, *Cancer Cell*, 10, 515-527.

Ng, C. H. *et al.* (2012). Biological and cytoselective anticancer properties of copper(II)-polypyridyl complexes modulated by auxiliary methylated glycine

ligand. (Biometals, submitted for publication). Universiti Tunku Abdul Rahman

Ng, C. H., Kong, K. C., Von, S. T., Balraj, P., Jensen, P., Thirthagiri, E., Hamada, H. and Chikira, M. (2008). Synthesis, characterization, DNA-binding study and anticancer properties of ternary metal(II) complexes of edda and an intercalating ligand. *Dalton Trans*., 4, 447-454.

Nyaga, S. G., Lohani, A., Jaruga, P., Trzeciak, A. R., Dizdaroglu, M. and Evans M. K. (2006). Reduced repair of 8-hydroxyguanine in the human breast cancer cell line, HCC1937 *BMC Cancer*, 6, 297-312.

Olivares, M. and Uauy, R. (1996). Copper as an essential nutrient. *Am. J. Clin. Nutr.*, 63, 791S-796S.

Pabla, N. and Dong, Z. (2008). Cisplatin nephrotoxicity: Mechanisms and renoprotective strategies. *Kidney Int.*, 73, 994-1007.

Paull, T. T., Rogakou, E. P., Yamazaki, V., Kirchgessner, C. U, Gellert, M. and Bonner, W. M. (2000). A critical role for histone H2AX in recruitment of repair factors to nuclear foci after DNA damage. *Curr Biol.*, 10, 886-895.

Pelicano, H., Carney, D. and Huang, P. (2004). ROS stress in cancer cells and therapeutic implications. *Drug Resist Updat.*, 7, 97-110.

Pelicano, H., Feng, L., Zhou, Y., Carew, J. S., Hileman, E. O., Plunkett, W., Keating, M. J. and Huang, P. (2003). Inhibition of mitochondrial respiration: a novel strategy to enhance drug-induced apoptosis in human leukemia cells by a reactive oxygen species-mediated mechanism. *J Biol Chem.*, 278, 37832-37839.

Podhorecka, M., Skladanowski, A. and Bozko, P. (2010). H2AX Phosphorylation: Its Role in DNA Damage Response and Cancer Therapy. *J Nucleic Acid*, 3, pii: 920161.

Popescu, A., Zuivertz, A., Olinescu, R., Tomas, S., Tomas, E. and Jucu, V. (1992). Antiviral activity of some copper complexes of symmetrical triazines. *Rev Roum Virol.*, 43, 181-184.

Portt, L., Norman, G., Clapp, C., Greenwood, M. and Greenwood, M. T. (2011). Anti-apoptosis and cell survival: a review. *Biochim Biophys Acta.*, 1813, 238-259.

Puig, S. and Thiele, D. J. (2002). Molecular mechanisms of copper uptake and distribution. *Current Opinion in Chemical Biology*, 6, 171-180.

Rajendiran, V., Karthik, R., Palandiandavar, M., Stoeckli, H., Periasamy, V. S., Akbarsha, M. A., Srinag, B. S. and Krisnamurthy, H. (2007). Mixed-ligand copper(II)-phenolate complexes: effect of coligand on enhanced DNA and protein binding, DNA cleavage, and anticancer activity. *Inorg Chem.*, 46,

8208-8221.

Rajkumar, S. V., Richardson, P. G., Hideshima, T. and Anderson, K. C. (2005). Proteasome inhibition as a novel therapeutic target in human cancer. *J Clin Oncol.*, 23, 630-639.

Raobaikady, B., Reed, M. J., Leese, M. P., Potter, B. V and Purohit, A. (2005). Inhibition of MDA-MB-231 cell cycle progression and cell proliferation by C-2-substituted oestradiol mono- and bis-3-O-sulphamates. *Int J Cancer*, 117, 150-159.

Rebbaa, A., Zheng, X., Chu, F. and Mirkin, B. L. (2006). The role of histone acetylation versus DNA damage in drug-induced senescence and apoptosis. *Cell Death Differ.*, 13,1960-1967.

Reddy, P. R., Shilpa, A., Raju, N. and Raghavaiah, P. (2011). Synthesis, structure, DNA binding and cleavage properties of ternaryamino aci d Schiff base-phen/bipy Cu(II) complexes. *J Inorg Biochem.*, 105, 1603-1612.

Reed, J. C. (2000). Mechanisms of apoptosis. *Am J Pathol.*, 157, 1415-1430.

Renschler, M. F. (2004). The emerging role of reactive oxygen species in cancer therapy. *Eur J Cancer*, 40, 1934-1940.

Ries, L., Melbert, D., Krapcho, M., Mariotto, A., Miller, B.A., Feuer, E.J., Clegg, L., Horner,M.J., Howlader, N., Eisner, M.P., Reichman, M., Edwards, B.K., (2007). SEER Cancer. Statistics Review, 1975–2004. National Cancer Institute, Bethesda.

Rogakou, E. P., Nieves-Neira, W., Boon, C., Pommier, Y. and Bonner, W. M. (2000). Initiation of DNA fragmentation during apoptosis induces phosphorylation of H2AX histone at serine 139. *J Biol Chem.*, 275, 9390-9395.

Rogakou, E. P., Pilch, D. R., Orr, A. H., Ivanova, V. S. and Bonner, W. M. (1998). DNA double-stranded breaks induce histone H2AX phosphorylation on serine 139. *J Biol Chem.*, 273, 5858-5868.

Roy, S., Saha, S., Majumdar, R., Dighe, R. R. and Chakravarty, A.R. (2010). DNA photocleavage and anticancer activity of terpyridine copper(II) complexes having phenanthroline bases. *Polyhedron*, 29, 2787-2794.

Rubino, S., Portanova, P., Girasolo, A., Calvaruso, G., Orecchio, S. and Stocco, G. C. (2009). Synthetic, structural and biochemical studies of polynuclear Platinum (II) complexes with heterocyclic ligands. *European Journal of Medicinal Chemistry*, 44, 1041-1048.

Ruiz-Ramos, R., Lopez-Carrillo, L., Rios-Perez, A. D., De Vizcaya-Ru ́z, A., Cebrian, M. E. (2009). Sodium arsenite induces ROS generation, DNA oxidative damage, HO-1 and c-Myc proteins, NF-kappaB activation and cell

proliferation in human breast cancer MCF-7 cells. *Mutat Res.*, 674, 109-115.

Saha, D. K., Sandbhor, U., Shirisha, K., Padhye, S., Deobagkar, D. and Anson, C. E. and Powell, A. K. (2004). A novel mixed-ligand antimycobacterial dimeric copper complex of ciprofloxacin and phenanthroline. *Bioorg Med Chem Lett.*, 14, 3027-3032.

Serment-Guerrero, J., Cano-Sanchez, P., Reyes-Perez, E., Velazquez-Garcia, F. and Ruiz-Azuara, L. (2011). Genotoxicity of the copper antineoplastic coordination complexes casiopeinas®. *Toxicol In Vitro.* [Epub ahead of print]

Shekhar, P. V, Chen, M. L., Werdell, J., Heppner, G. H., Miller, F. R. and Christman, J. K. (1998). Transcriptional activation of functional endogenous estrogen receptor gene expression in MCF10AT cells: A model for early breast cancer. *Int J Oncol.*, 13, 907-915.

Shibatani, T., Carlson, E. J., Larabee, F., McCormack, A. L., Früh, K. and Skach, W. R. (2006). Global organization and function of mammalian cytosolic proteasome pools: Implications for PA28 and 19S regulatory complexes. *Mol Biol Cell*, 17, 4962-4971.

Shun, M. C, Yu, W., Gapor, A., Parsons, R., Atkinson, J., Sanders, B. G. and Kline, K. (2004). Pro-apoptotic mechanisms of action of a novel vitamin E analog (alpha-TEA) and a naturally occurring form of vitamin E (delta-tocotrienol) in MDA-MB-435 human breast cancer cells. Nutr Cancer**,** 48, 95-105.

Siddik ZH. (2003). Cisplatin: mode of cytotoxic action and molecular basis of resistance. *Oncogene*, 22,7265-7279.

Silverman, B. G., Siegelmann-Danieli, N., Braunstein, R. and Kokia, E. S. (2011). Trends in breast cancer incidence associated with reductions in the use of hormone replacement therapy. *Cancer Epidemiol.*, 35, 11-16.

Simon, H. U., Haj-Yehia, A. and Levi-Schaffer, F. (2000). Role of reactive oxygen species (ROS) in apoptosis induction. *Apoptosis*, 5, 415-418.

Sluss, H. K. and Davis, R. J. (2006). H2AX is a target of the JNK signaling pathway that is required for apoptotic DNA fragmentation. *Mol Cell.* 23, 152-153.

Sparreboom, A., van Zuylen, L., Brouwer, E., Loos, W. J., de Bruijn, P., Gelderblom, H., Pillay, M., Nooter, K., Stoter, G. and Verweij, J. (1999). Cremophor EL-mediated alteration of paclitaxel distribution in human blood: clinical pharmacokinetic implications. *Cancer Res.*, 59, 1454-1457.

Srdić-Rajić, T, Zec, M, Todorović, T, Anđelković, K and Radulović, S. (2011). Non-substituted N-heteroaromatic selenosemicarbazone metal complexes induce apoptosis in cancer cells via activation of mitochondrial pathway. *Eur J Med Chem.*, [Epub ahead of print]

Srivastava, N., Gochhait, S. , de Boer, P. and Bamezai, R. N. (2009). Role of H2AX in DNA damage response and human cancers. *Mutat Res.*, 681, 180-188.

Sun, Y., Bian, J. and Wang, Y., Jacobs, C. (1997). Activation of p53 transcriptional activity by 1,10-phenanthroline, a metal chelator and redox sensitive compound. *Oncogene*, 14, 385-393.

Tanaka, T., Huang, X., Halicka, H. D., Zhao, H., Traganos, F., Albino, A. P., Dai, W. and Darzynkiewicz, Z. (2007). Cytometry of ATM activation and histone H2AX phosphorylation to estimate extent of DNA damage induced by exogenous agents. *Cytometry A.*, 71, 648-661.

Tapiero, H., Townsend, D. M. and Tew, K. D. (2003). Trace elements in human physiology and pathology. *Biomedecine & Pharmacotherapy*, 57, 386-398.

Tardito, S., Bassanetti, I., Bignardi, C., Elviri, L., Tegoni, M., Mucchino, C, Bussolati, O., Franchi-Gazzola, R. and Marchiò, L. (2011). Copper binding agents acting as copper ionophores lead to caspase inhibition and paraptotic cell death in human cancer cells. *J Am Chem Soc.*, 133, 6235-6242.

Tardito, S., Bussolati, O., Maffini, M., Tegoni, M., Giannetto, M., Dall'Asta, V. *et al*. (2007). Thioamido coordination in a thioxo-1,2,4-triazole copper(II) complex enhances nonapoptotic programmed cell death associated with copper accumulation and oxidative stress in human cancer cells. *J Med Chem.*; 50, 1916-1924.

Tardito, S. and Marchio, L. (2009). Copper compounds in anticancer strategies. Current Medicinal Chemistry. 16, 1325-1348.

Thati, B., Noble, A., Creaven, B. S., Walsh, M., McCann, M., Devereux, M., Kavanagh, K. and Egan, D. A. (2009). Role of cell cycle events and apoptosis in mediating the anti-cancer activity of a silver(I) complex of 4-hydroxy-3-nitro-coumarin-bis(phenanthroline) in human malignant cancer cells. *Eur J Pharmacol.*, 602, 203-214.

Thati, B., Noble, A., Creaven, B. S.,Walsh, M., Kavanagh, K., Egan, D. A. (2007). Apoptotic cell death: a possible key event in mediating the in vitro anti-proliferative effect of a novel copper(II) complex, [Cu(4-Mecdoa)(phen)(2)] (phen=phenanthroline, 4-Mecdoa=4-methylcoumarin-6,7-dioxactetate), in human malignant cancer cells. *Eur J Pharmacol.*, 569, 16-28.

Tisato, F., Marzano, C., Porchia, M., Pellei, M. and Santini, C. (2010). Copper in diseases and treatments, and copper-based anticancer strategies. *Med Res Rev.*,30, 708-749.

Traina, T. A, Norton, L., Drucker, K. and Singh B. (2006). Nasal septum perforation in a bevacizumab-treated patient with metastatic breast cancer. *Oncologist*., 11, 1070-1081.

Tsang, S. Y., Tam, S. C., Bremner, L. and Burkitt, M. J. (1996). Copper-1,10-phenanthrolin induces internucleosomal DNA fragmentation in HepG2 cells, resulting from direct oxidation by the hydroxyl radical, *Biochem. J.*, 317, 13-16.

Ushio-Fukai, M. and Nakamura, Y. (2008). Reactive oxygen species and angiogenesis: NADPH oxidase as target for cancer therapy. *Cancer Lett.*, 266, 37-52.

Usta, J., Kreydiyyeh, S., Knio, K., Barnabe, P., Bou-Moughlabay, Y. and Dagher, S. (2009). Linalool decreases HepG2 viability by inhibiting mitochondrial complexes I and II, increasing reactive oxygen species and decreasing ATP and GSH levels. *Chem Biol Interact.*, 180, 39-46.

Valko, M., Morris, H. and Cronin, M. T. (2005). Metals, toxicity and oxidative stress. *Curr Med Chem.*, 12, 1161-1208.

Van Cruchten, S. and Van Den Broeck, W. (2002). Morphological and biochemical aspects of apoptosis, oncosis and necrosis. *Anat Histol Embryol.*,31, 214-223.

Van Remmen, H. and Richardson, A. (2001). Oxidative damage to mitochondria and aging. *Experimental gerontology*, 36, 957-968.

Verhaegh, G. W., Richard, M. J. and Hainaut, P. (1997). Regulation of p53 by metal ions and by antioxidants: dithiocarbamate down-regulates p53 DNA-binding activity by increasing the intracellular level of copper. *Mol. Cell Biol.*, 17, 5699-5706.

Vermes, I., Haanen, C., Steffens-Nakken, H.and Reutellingspergers, C. (1995). A novel assay for apoptosis Flow cytometric detection of phosphatidylserine expression on early apoptotic cells using fluorescein labelled Annexin V. *Journal of Immunological Methods*, 184, 39-51.

Visekruna, A., Joeris, T., Seidel, D., Kroesen, A., Loddenkemper, C., Zeitz, M., Kaufmann, S. H., Schmidt-Ullrich, R. and Steinhoff, U. (2006). Proteasome-mediated degradation of IκBa and processing of p105 in Crohn disease and ulcerative colitis. *J. Clin. Invest.*, 116, 3195-3203.

Vishnu, P. and Roy, V. (2011). Safety and efficacy of nab-paclitaxel in the treatment of patients with breast cancer. *Breast Cancer (Auckl)*, 5, 53-65.

Wang, T. and Guo, Z. (2006). Copper in medicine: homeostasis, chelation therapy and antitumor drug design. *Curr Med Chem.*, 13, 525-537.

Wang. Y. and Chiu, J. F. (2008). Proteomic approaches in understanding action mechanisms of metal-based anticancer drugs. *Met Based Drugs.* 2008:716329.

Wang. Y., Zhang, X., Zhang, Q. and Yang, Z. (2010). Oxidative damage to DNA by 1,10-phenanthroline/L: -threonine copper (II) complexes with chlorogenic acid. *Biometals*, 23:265-273.

Waris, G. and Ahsan, H. (2006). Reactive oxygen species: role in the development of cancer and various chronic conditions. *J Carcinog.*, 5, 14.

Williams, S. A. and Schreier, A. M. (2004). The effect of education in managing side effects in women receiving chemotherapy for treatment of breast cancer. *Oncol Nurs Forum*, 31, E16-E23.

Xia, C., Meng, Q., Liu, L. Z, Rojanasakul, Y., Wang, X. R. and Jiang, B. H. (2007). Reactive oxygen species regulate angiogenesis and tumor growth through vascular endothelial growth factor. *Cancer Res.*, 67, 10823-10830.

Xiao, Y., Bi, C., Fan, Y., Cui, C., Zhang, X. and Dou, Q. P. (2008). L-glutamine Schiff base copper complex as a proteasome inhibitor and an apoptosis inducer in human cancer cells. *Int J Oncol.*, 33, 1073-1079.

Xing, H., Weng, D., Chen, G., Tao, W., Zhu, T., Yang X, Meng L, Wang S, Lu Y, Ma D. **(**2008). Activation of fibronectin/PI-3K/Akt2 leads to chemoresistance to docetaxel by regulating survivin protein expression in ovarian and breast cancer cells. *Cancer Lett*., 261, 108-119.

Xu, B., Guo, X., Mathew, S., Armesilla, A. L., Cassidy, J., Darling, J. L. and Wang, W. (2010). Triptolide simultaneously induces reactive oxygen species, inhibits NF-κB activity and sensitizes 5-fluorouracil in colorectal cancer cell lines. *Cancer Lett.*, 291, 200-208.

Yamamoto, N., Sawada, H., Izumi, Y., Kume, T., Katsuki, H., Shimohama, S. and Akaike, A. (2007). Proteasomeinhibition induces glutathione synthesis and protects cells from oxidative stress—relevance to Parkinson disease. *J. Biol. Chem.*, 282, 4364-4372.

Yang, H. L., Chang, W. H., Chia, Y. C., Huang, C. J., Lu, F. J., Hsu, H. K and Hseu, Y. C. (2006). Toona sinensis extracts induces apoptosis via reactive oxygen species in human premyelocytic leukemia cells. *Food Chem Toxicol.*, 44, 1978-1988.

Yde, C. W. and Issinger, O. G. (2006). Enhancing cisplatin sensitivity in MCF-7 human breast cancer cells by down-regulation of Bcl-2 and cyclin D1. *Int J Oncol.*, 29, 1397-1404.

Yde, C. W., Gyrd-Hansen, M., Lykkesfeldt, A. E., Issinger, O. G. and Stenvang, J. (2007). Breast cancer cells with acquired antiestrogen resistance are sensitized to cisplatin-induced cell death. *Mol Cancer Ther.*, 6,1869-1876.

Yip, C. H., bt Mohd Taib, N. A. and Lau, P. C. (2008). Does a positive family history influence the presentation of breast cancer? *Asian Pac J Cancer Prev.*,

9, 63-65.

Yip, C. H., Taib, N. A. and Mohamed, I. (2006). Epidemiology of breast cancer in Malaysia. *Asian Pac J Cancer Prev.*, 7, 369-374.

Zhai, S., Yang, L., Cindy Cui Q., Sun, Y., Dou, Q. P. and Yan, B. (2010). Tumor cellular proteasome inhibition and growth suppression by 8-hydroxyquinoline and clioquinol requires their capabilities to bind copper and transport copper into cells. *J Biol Inorg Chem.*, 15, 259- 269.

Zhang, C. X. and Lippard, S. J. (2003). New metal complexes as potential therapeutics. *Curr Opin Chem Biol.*, 7, 481-489.

Zhang, H., Wu, J. S. and Peng, F. (2008a). Potent anticancer activity of pyrrolidine dithiocarbamate-copper complex against cisplatin-resistant neuroblastoma cells. *Anticancer Drugs*, 19, 125-132.

Zhang, S. and Zhou, J. (2008). Ternary copper(II) complex of 1,10-phenanthroline and L-glycine: crystal structure and interaction with DNA. *Journal of Coordination Chemistry*, 61, 2488-2498.

Zhang, X., Bi, C., Fan, Y., Cui, Q., Chen, D., Xiao, Y. and Dou, Q. P. (2008b). Induction of tumor cell apoptosis by taurine Schiff base copper complex is associated with the inhibition of proteasomal activity. *Int J Mol Med.*, 22, 677-682.

Zheng, J., Lou, J. R., Zhang X. X, Benbrook, D. M., Hanigan, M. H., Lind, S. E and Ding, W. Q. (2010). N-Acetylcysteine interacts with copper to generate hydrogen peroxide and selectively induce cancer cell death. *Cancer Letters*, 298, 186-194.

Zhou, F., Mei, H., Wu, Q. and Jin, R. (2011). Expression of histone H2AX phosphorylation and its potential to modulate adriamycin resistance in K562/A02 cell line. J Huazhong Univ Sci Technolog Med Sci. 31, 154-158.

Zhou, H., Lui, Y., Zhen, C., Gong, J., Liang, Y., Wang, C. and Zou, C. (2003). Microcalorimetric studies of the synergistic effects of copper-1,10-phenanthroline combined with hyperthermia on a liver hepatoma cell line Bel-7402. *Therm. Acta.*, 397, 87-95.

Zhou, H., Zheng, C., Zoua, G., Tao, D. and Gong, J. (2002). G1-phase specific apoptosis in liver carcinoma cell line induced by copper-1,10-phenanthroline. *The International Journal of Biochemistry & Cell Biology*, 34, 678-684.

Appendix A

MTT assay

Raw data for MDA-MB-231 cells treated with [Cu(phen)(DL-ala)(H_2O)]NO_3 2½H_2O (set 1)

Dose (μM)	Optical density			Average optical density	SD	SD (%)	Cell viabilities (%)
0	0.721	0.718	0.629	0.689	0.052	7.59	100.00
1.563	0.692	0.621	0.577	0.630	0.058	8.42	91.44
3.125	0.531	0.512	0.535	0.526	0.012	1.78	76.34
6.25	0.247	0.150	0.234	0.210	0.053	7.64	30.53
12.5	0.036	0.006	0.048	0.030	0.022	3.14	4.35
25	0.025	0.001	0.011	0.012	0.012	1.75	1.79

Raw data for MDA-MB-231 cells treated with [Cu(phen)(DL-ala)(H_2O)]NO_3 2½H_2O (set 2)

Dose (μM)	Optical density			Average optical density	SD	SD (%)	Cell viabilities (%)
0	0.537	0.572	0.655	0.588	0.061	10.31	100.00
1.563	0.620	0.543	0.537	0.567	0.046	7.87	96.37
3.125	0.318	0.382	0.442	0.381	0.062	10.55	64.74
6.25	0.260	0.362	0.334	0.319	0.053	8.96	54.20
12.5	0.042	0.025	0.063	0.043	0.019	3.24	7.37
25	0.035	0.005	0.019	0.020	0.015	2.55	3.34

Raw data for MDA-MB-231 cells treated with [Cu(phen)(DL-ala)(H_2O)]NO_3 2½H_2O (set 3)

Dose (μM)	Optical density			Average optical density	SD	SD (%)	Cell viabilities (%)
0	0.531	0.657	0.583	0.590	0.063	10.73	100.00
1.563	0.477	0.434	0.564	0.492	0.066	11.23	83.33
3.125	0.421	0.586	0.367	0.458	0.114	19.34	77.63
6.25	0.227	0.176	0.176	0.193	0.029	4.99	32.71
12.5	0.049	0.026	0.046	0.040	0.013	2.12	6.84
25	0.030	0.005	0.009	0.015	0.013	2.28	2.49

Raw data for MCF10A cells treated with [Cu(phen)(DL-ala)(H_2O)]NO_3 2½H_2O (set 1)

Dose (µM)	Optical density			Average optical density	SD	SD (%)	Cell viabilities (%)
0	0.968	0.945	1.034	0.982	0.046	4.71	100.00
1.563	0.905	0.813	0.993	0.904	0.090	9.17	92.02
3.125	1.038	0.869	1.003	0.970	0.089	9.08	98.78
6.25	0.865	0.951	0.976	0.931	0.058	5.93	94.77
12.5	0.409	0.465	0.408	0.427	0.033	3.32	43.52
25	0.011	0.001	0.005	0.006	0.005	0.51	0.58

Raw data for MCF10A cells treated with [Cu(phen)(DL-ala)(H_2O)]NO_3 2½H_2O (set 2)

Dose (µM)	Optical density			Average optical density	SD	SD (%)	Cell viabilities (%)
0	0.448	0.464	0.475	0.462	0.014	2.94	100.00
1.563	0.435	0.440	0.435	0.437	0.003	0.63	94.52
3.125	0.385	0.354	0.36	0.366	0.016	3.56	79.29
6.25	0.382	0.340	0.341	0.354	0.024	5.19	76.70
12.5	0.244	0.274	0.312	0.277	0.034	7.38	59.88
25	0.121	0.100	0.018	0.080	0.054	11.78	17.24

Raw data for MCF10A cells treated with [Cu(phen)(DL-ala)(H_2O)]NO_3 2½H_2O (set 3)

Dose (µM)	Optical density			Average optical density	SD	SD (%)	Cell viabilities (%)
0	0.328	0.330	0.386	0.348	0.033	9.46	100.00
1.563	0.241	0.328	0.297	0.289	0.044	12.67	82.95
3.125	0.257	0.290	0.193	0.247	0.049	14.17	70.88
6.25	0.263	0.277	0.229	0.256	0.025	7.09	73.66
12.5	0.231	0.198	0.175	0.201	0.028	8.09	57.85
25	0.018	0.008	0.008	0.011	0.006	1.66	3.26

Raw data for MDA-MB-231 cells treated with [Cu(phen)(sar)(H_2O)]NO_3 (set 1)

Dose (µM)	Optical density			Average optical density	SD	SD (%)	Cell viabilities (%)
0	0.537	0.572	0.655	0.588	0.061	10.31	100.00
1.563	0.648	0.574	0.666	0.629	0.049	8.29	107.03
3.125	0.505	0.514	0.619	0.546	0.063	10.78	92.86
6.25	0.184	0.204	0.248	0.212	0.033	5.57	36.05
12.5	0.051	0.046	0.049	0.049	0.003	0.43	8.28
25	0.030	0.018	0.033	0.027	0.008	1.35	4.59

Raw data for MDA-MB-231 cells treated with $[Cu(phen)(sar)(H_2O)]NO_3$ (set 2)

Dose (μM)	Optical density			Average optical density	SD	SD (%)	Cell viabilities (%)
0	0.531	0.657	0.583	0.590	0.063	10.73	100.00
1.563	0.549	0.631	0.678	0.619	0.065	11.07	104.97
3.125	0.351	0.457	0.658	0.489	0.156	26.43	82.82
6.25	0.137	0.146	0.308	0.197	0.096	16.31	33.39
12.5	0.049	0.056	0.051	0.052	0.004	0.61	8.81
25	0.017	0.023	0.028	0.023	0.006	0.93	3.84

Raw data for MDA-MB-231 cells treated with $[Cu(phen)(sar)(H_2O)]NO_3$ (set 3)

Dose (μM)	Optical density			Average optical density	SD	SD (%)	Cell viabilities (%)
0	0.721	0.718	0.629	0.689	0.052	7.59	100.00
1.563	0.655	0.599	0.524	0.593	0.066	9.54	86.02
3.125	0.627	0.543	0.619	0.596	0.046	6.73	86.55
6.25	0.239	0.276	0.306	0.274	0.034	4.87	39.72
12.5	0.069	0.041	0.055	0.055	0.014	2.03	7.98
25	0.023	0.032	0.036	0.030	0.007	0.97	4.40

Raw data for MCF10A cells treated with $[Cu(phen)(sar)(H_2O)]NO_3$ (set 1)

Dose (μM)	Optical density			Average optical density	SD	SD (%)	Cell viabilities (%)
0	0.448	0.464	0.475	0.462	0.014	2.94	100.00
1.563	0.377	0.392	0.405	0.391	0.012	2.55	84.70
3.125	0.448	0.455	0.471	0.458	0.014	3.03	99.13
6.25	0.409	0.382	0.411	0.401	0.016	3.51	86.72
12.5	0.431	0.401	0.404	0.412	0.017	3.58	89.18
25	0.011	0.017	0.029	0.019	0.009	1.98	4.11

Raw data for MCF10A cells treated with $[Cu(phen)(sar)(H_2O)]NO_3$ (set 2)

Dose (μM)	Optical density			Average optical density	SD	SD (%)	Cell viabilities (%)
0	0.328	0.330	0.386	0.348	0.033	9.46	100.00
1.563	0.256	0.398	0.398	0.351	0.082	23.56	100.77
3.125	0.316	0.343	0.345	0.335	0.016	4.65	96.17
6.25	0.293	0.321	0.328	0.314	0.019	5.32	90.23
12.5	0.282	0.243	0.248	0.258	0.021	6.10	74.04
25	0.021	0.022	0.028	0.024	0.004	1.09	6.80

Raw data for MCF10A cells treated with $[Cu(phen)(sar)(H_2O)]NO_3$ (set 3)

Dose (μM)	Optical density			Average optical density	SD	SD (%)	Cell viabilities (%)
0	0.968	0.945	1.034	0.982	0.046	4.71	100.00
1.563	0.986	1.025	1.043	1.018	0.029	2.97	103.67
3.125	0.978	0.975	1.042	0.998	0.038	3.85	101.66
6.25	0.893	0.895	0.95	0.913	0.032	3.29	92.94
12.5	0.523	0.568	0.563	0.551	0.025	2.51	56.14
25	0.007	0.014	0.025	0.015	0.009	0.92	1.56

Raw data for MDA-MB-231 cells treated with $[Cu(phen)(gly)(H_2O)]NO_3 \cdot 1.5H_2O$ (set 1)

Dose (μM)	Optical density			Average optical density	SD	SD (%)	Cell viabilities (%)
0	0.531	0.657	0.583	0.590	0.063	10.73	100.00
1.563	0.626	0.599	0.629	0.618	0.017	2.80	104.75
3.125	0.621	0.475	0.540	0.545	0.073	12.40	92.43
6.25	0.435	0.484	0.497	0.472	0.033	5.54	80.00
12.5	0.227	0.162	0.120	0.170	0.054	9.14	28.76
25	0.020	0.020	0.053	0.031	0.019	3.23	5.25

Raw data for MDA-MB-231 cells treated with $[Cu(phen)(gly)(H_2O)]NO_3 \cdot 1.5H_2O$ (set 2)

Dose (μM)	Optical density			Average optical density	SD	SD (%)	Cell viabilities (%)
0	0.629	0.622	0.675	0.642	0.029	4.48	100.00
1.563	0.500	0.513	0.522	0.512	0.011	1.72	79.70
3.125	0.376	0.432	0.355	0.388	0.040	6.20	60.38
6.25	0.355	0.335	0.393	0.361	0.029	4.59	56.23
12.5	0.294	0.240	0.219	0.251	0.039	6.03	39.10
25	0.041	0.029	0.039	0.036	0.006	1.00	5.66

Raw data for MDA-MB-231 cells treated with $[Cu(phen)(gly)(H_2O)]NO_3 \cdot 1.5H_2O$ (set 3)

Dose (μM)	Optical density			Average optical density	SD	SD (%)	Cell viabilities (%)
0	0.721	0.718	0.629	0.689	0.052	7.59	100.00
1.563	0.655	0.622	0.597	0.625	0.029	4.22	90.66
3.125	0.659	0.662	0.636	0.652	0.014	2.06	94.68
6.25	0.569	0.406	0.491	0.489	0.082	11.83	70.92
12.5	0.101	0.082	0.104	0.096	0.012	1.73	13.88
25	0.015	0.002	0.020	0.012	0.009	1.35	1.79

Raw data for MCF10A cells treated with $[Cu(phen)(gly)(H_2O)]NO_3 \cdot 1.5H_2O$ (set 1)

Dose (μM)	Optical density			Average optical density	SD	SD (%)	Cell viabilities (%)
0	0.448	0.464	0.475	0.462	0.014	2.94	100.00
1.563	0.402	0.396	0.389	0.396	0.007	1.41	85.64
3.125	0.386	0.373	0.472	0.410	0.054	11.64	88.82
6.25	0.388	0.431	0.484	0.434	0.048	10.41	94.01
12.5	0.301	0.244	0.361	0.302	0.059	12.66	65.37
25	0.019	0.013	0.013	0.015	0.003	0.75	3.25

Raw data for MCF10A cells treated with $[Cu(phen)(gly)(H_2O)]NO_3 \cdot 1.5H_2O$ (set 2)

Dose (μM)	Optical density			Average optical density	SD	SD (%)	Cell viabilities (%)
0	0.371	0.320	0.326	0.339	0.028	8.22	100.00
1.563	0.281	0.359	0.304	0.315	0.040	11.82	92.82
3.125	0.299	0.344	0.289	0.311	0.029	8.64	91.64
6.25	0.222	0.346	0.317	0.295	0.065	19.13	87.02
12.5	0.261	0.273	0.227	0.254	0.024	7.04	74.83
25	0.018	0.012	0.018	0.016	0.003	1.02	4.72

Raw data for MCF10A cells treated with $[Cu(phen)(gly)(H_2O)]NO_3 \cdot 1.5H_2O$ (set 3)

Dose (μM)	Optical density			Average optical density	SD	SD (%)	Cell viabilities (%)
0	0.968	0.945	1.034	0.982	0.046	4.70	100.00
1.563	0.957	0.784	0.903	0.881	0.089	9.01	89.75
3.125	1.016	0.966	0.933	0.972	0.042	4.26	98.95
6.25	0.995	0.946	0.874	0.938	0.061	6.20	95.55
12.5	0.589	0.649	0.659	0.632	0.038	3.86	64.39
25	0.023	0.002	0.018	0.014	0.011	1.12	1.46

Raw data for MDA-MB-231 cells treated with $[Cu(phen)(C\text{-}dmg)(H_2O)]NO_3$ (set 1)

Dose (μM)	Optical density			Average optical density	SD	SD (%)	Cell viabilities (%)
0	0.537	0.572	0.655	0.588	0.061	10.31	100.00
1.563	0.696	0.633	0.658	0.662	0.032	5.40	112.64
3.125	0.533	0.461	0.320	0.438	0.108	18.43	74.49
6.25	0.356	0.381	0.347	0.361	0.018	3.00	61.45
12.5	0.023	0.027	0.031	0.027	0.004	0.68	4.59
25	0.023	0.028	0.037	0.029	0.007	1.21	4.99

Raw data for MDA-MB-231 cells treated with [Cu(phen)(C-dmg)(H_2O)]NO_3 (set 2)

Dose (μM)	Optical density			Average optical density	SD	SD (%)	Cell viabilities (%)
0	0.629	0.622	0.675	0.642	0.029	4.48	100.00
1.563	0.635	0.583	0.523	0.580	0.056	8.73	90.39
3.125	0.428	0.408	0.348	0.395	0.042	6.48	61.47
6.25	0.365	0.334	0.298	0.332	0.034	5.22	51.77
12.5	0.049	0.048	0.052	0.050	0.002	0.32	7.74
25	0.039	0.049	0.052	0.047	0.007	1.06	7.27

Raw data for MDA-MB-231 cells treated with [Cu(phen)(C-dmg)(H_2O)]NO_3 (set 3)

Dose (μM)	Optical density			Average optical density	SD	SD (%)	Cell viabilities (%)
0	0.721	0.718	0.629	0.689	0.052	7.59	100.00
1.563	0.627	0.654	0.641	0.641	0.014	1.96	92.99
3.125	0.544	0.631	0.544	0.573	0.050	7.29	83.16
6.25	0.182	0.274	0.216	0.224	0.047	6.75	32.51
12.5	0.054	0.045	0.034	0.044	0.010	1.45	6.43
25	0.012	0.086	0.031	0.043	0.038	5.58	6.24

Raw data for MCF10A cells treated with [Cu(phen)(C-dmg)(H_2O)]NO_3 (set 1)

Dose (μM)	Optical density			Average optical density	SD	SD (%)	Cell viabilities (%)
0	0.448	0.464	0.475	0.462	0.014	2.94	100.00
1.563	0.482	0.403	0.445	0.443	0.040	8.56	95.96
3.125	0.434	0.449	0.454	0.446	0.010	2.25	96.46
6.25	0.418	0.468	0.371	0.419	0.049	10.50	90.69
12.5	0.457	0.332	0.321	0.370	0.076	16.35	80.09
25	0.018	0.020	0.016	0.018	0.002	0.43	3.90

Raw data for MCF10A cells treated with [Cu(phen)(C-dmg)(H_2O)]NO_3 (set 2)

Dose (μM)	Optical density			Average optical density	SD	SD (%)	Cell viabilities (%)
0	0.328	0.330	0.386	0.348	0.033	9.46	100.00
1.563	0.391	0.309	0.357	0.352	0.041	11.84	101.25
3.125	0.406	0.326	0.290	0.341	0.059	17.06	97.89
6.25	0.354	0.325	0.256	0.312	0.050	14.47	89.56
12.5	0.230	0.183	0.211	0.208	0.024	6.79	59.77
25	0.016	0.023	0.020	0.020	0.004	1.01	5.65

Raw data for MCF10A cells treated with [Cu(phen)(C-dmg)(H_2O)]NO_3 (set 3)

Dose (μM)	Optical density			Average optical density	SD	SD (%)	Cell viabilities (%)
0	0.968	0.945	1.034	0.982	0.046	4.71	100.00
1.563	1.009	0.889	1.011	0.970	0.070	7.12	98.74
3.125	0.884	0.694	0.730	0.769	0.101	10.28	78.34
6.25	0.772	0.801	0.734	0.769	0.034	3.42	78.31
12.5	0.579	0.521	0.566	0.555	0.030	3.10	56.55
25	0.005	0.008	0.009	0.007	0.002	0.21	0.75

Raw data for MDA-MB-231 cells treated with [Cu(8OHQ)$_2$] (set 1)

Dose (μM)	Optical density			Average optical density	SD	SD (%)	Cell viabilities (%)
0	0.537	0.572	0.655	0.588	0.061	10.31	100.00
1.563	0.675	0.748	0.667	0.697	0.045	7.59	118.48
3.125	0.190	0.119	0.104	0.138	0.046	7.81	23.41
6.25	0.020	0.011	0.020	0.017	0.005	0.88	2.89
12.5	0.016	0.029	0.038	0.028	0.011	1.88	4.71
25	0.037	0.023	0.038	0.033	0.008	1.43	5.56

Raw data for MDA-MB-231 cells treated with [Cu(8OHQ)$_2$] (set 2)

Dose (μM)	Optical density			Average optical density	SD	SD (%)	Cell viabilities (%)
0	0.531	0.657	0.583	0.590	0.063	10.73	100.00
1.563	0.617	0.615	0.689	0.640	0.042	7.15	108.53
3.125	0.168	0.164	0.181	0.171	0.009	1.51	28.98
6.25	0.029	0.038	0.056	0.041	0.014	2.33	6.95
12.5	0.018	0.007	0.019	0.015	0.007	1.13	2.49
25	0.002	0.002	0.002	0.002	0.000	0.00	0.34

Raw data for MDA-MB-231 cells treated with [Cu(8OHQ)$_2$] (set 3)

Dose (μM)	Optical density			Average optical density	SD	SD (%)	Cell viabilities (%)
0	0.721	0.718	0.629	0.689	0.052	7.59	100.00
1.563	0.630	0.636	0.600	0.622	0.019	2.80	90.28
3.125	0.139	0.126	0.120	0.128	0.010	1.41	18.63
6.25	0.030	0.019	0.021	0.023	0.006	0.85	3.39
12.5	0.032	0.025	0.021	0.026	0.006	0.81	3.77
25	0.031	0.025	0.028	0.028	0.003	0.44	4.06

Raw data for MCF10A cells treated with $[Cu(8OHQ)_2]$ (set 1)

Dose (μM)	Optical density			Average optical density	SD	SD (%)	Cell viabilities (%)
0	0.448	0.464	0.475	0.462	0.014	2.94	100.00
1.563	0.226	0.267	0.266	0.253	0.023	5.06	54.76
3.125	0.031	0.017	0.023	0.024	0.007	1.52	5.12
6.25	0.015	0.010	0.019	0.015	0.005	0.98	3.17
12.5	0.019	0.032	0.019	0.023	0.008	1.62	5.05
25	0.003	0.002	0.002	0.002	0.001	0.12	0.51

Raw data for MCF10A cells treated with $[Cu(8OHQ)_2]$ (set 2)

Dose (μM)	Optical density			Average optical density	SD	SD (%)	Cell viabilities (%)
0	0.371	0.320	0.326	0.339	0.028	8.22	100.00
1.563	0.205	0.249	0.234	0.229	0.022	6.60	67.65
3.125	0.046	0.036	0.035	0.039	0.006	1.79	11.50
6.25	0.015	0.017	0.018	0.017	0.002	0.45	4.92
12.5	0.019	0.029	0.023	0.024	0.005	1.48	6.98
25	0.007	0.002	0.013	0.007	0.006	1.62	2.16

Raw data for MCF10A cells treated with $[Cu(8OHQ)_2]$ (set 3)

Dose (μM)	Optical density			Average optical density	SD	SD (%)	Cell viabilities (%)
0	0.968	0.945	1.034	0.982	0.046	4.70	100.00
1.563	0.377	0.331	0.405	0.371	0.037	3.80	37.78
3.125	0.403	0.366	0.273	0.347	0.067	6.82	35.37
6.25	0.024	0.004	0.023	0.017	0.011	1.15	1.73
12.5	0.005	0.012	0.009	0.009	0.004	0.36	0.88
25	0.012	0.009	0.017	0.013	0.004	0.41	1.29

Dose response curves of the antiproliferative activity (% cell viability) of [Cu(phen)(DL-ala)(H_2O)]NO_3 2½H_2O in MDA-MB-231 and MCF 10A cells at 24 h (Set 1).

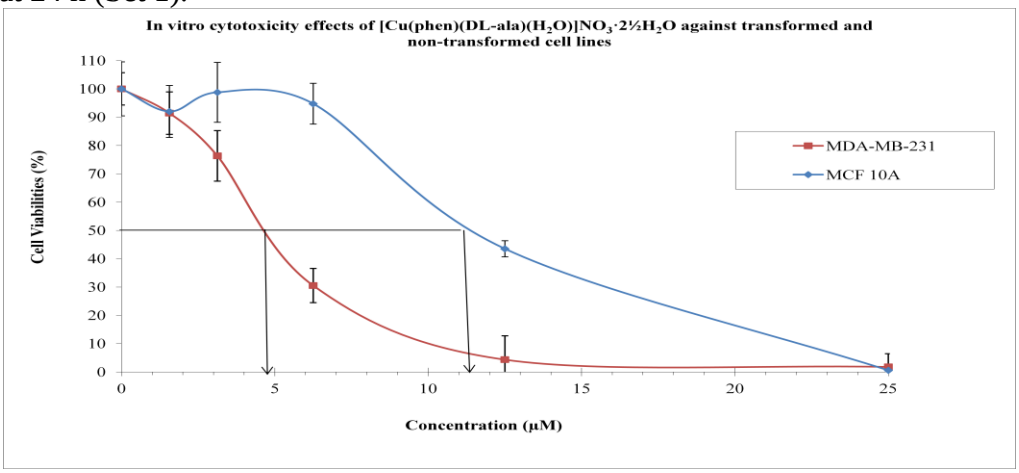

Dose response curves of the antiproliferative activity (% cell viability) of [Cu(phen)(DL-ala)(H_2O)]NO_3 2½H_2O in MDA-MB-231 and MCF 10A cells at 24 h (Set 2).

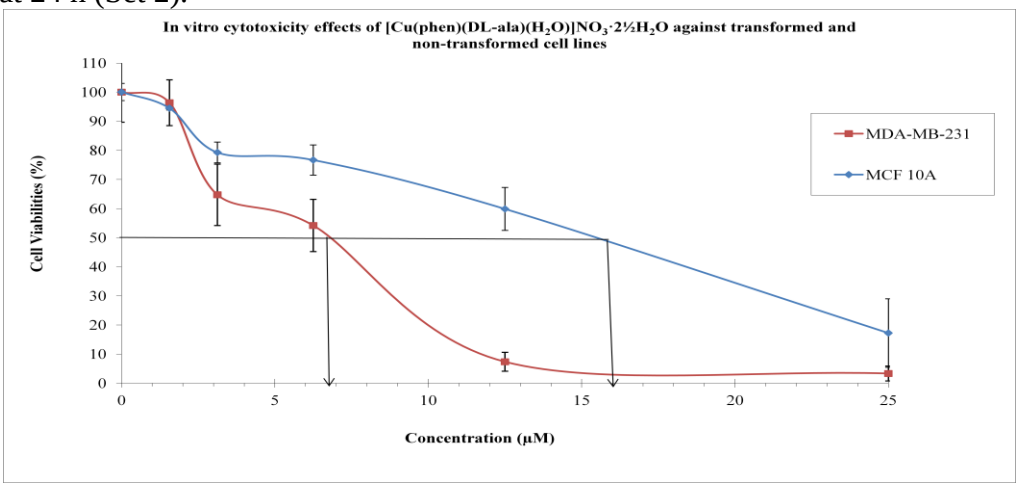

Dose response curves of the antiproliferative activity (% cell viability) of [Cu(phen)(DL-ala)(H_2O)]NO_3 2½H_2O in MDA-MB-231 and MCF 10A cells at 24 h (Set 3).

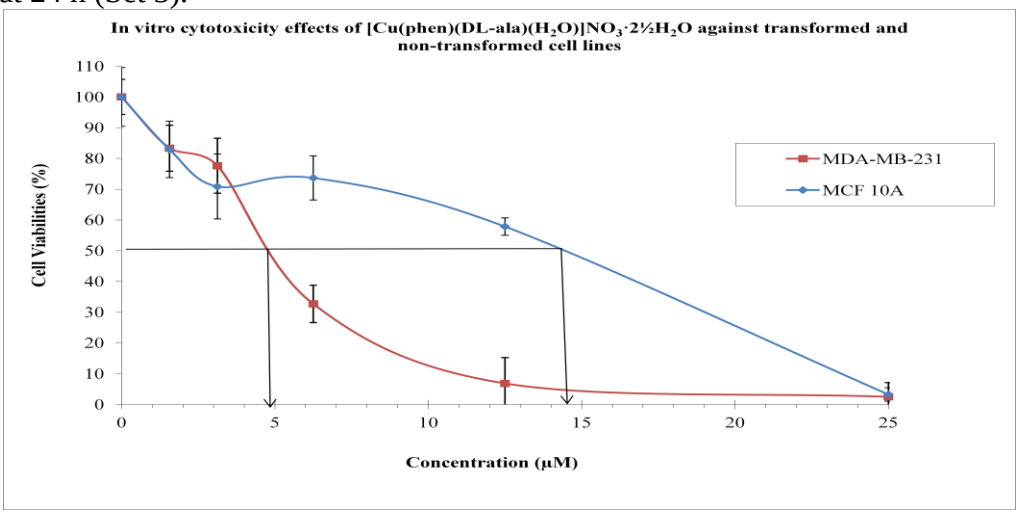

Dose response curves of the antiproliferative activity (% cell viability) of [Cu(phen)(sar)(H_2O)]NO_3 in MDA-MB-231 and MCF 10A cells at 24 h (Set 1).

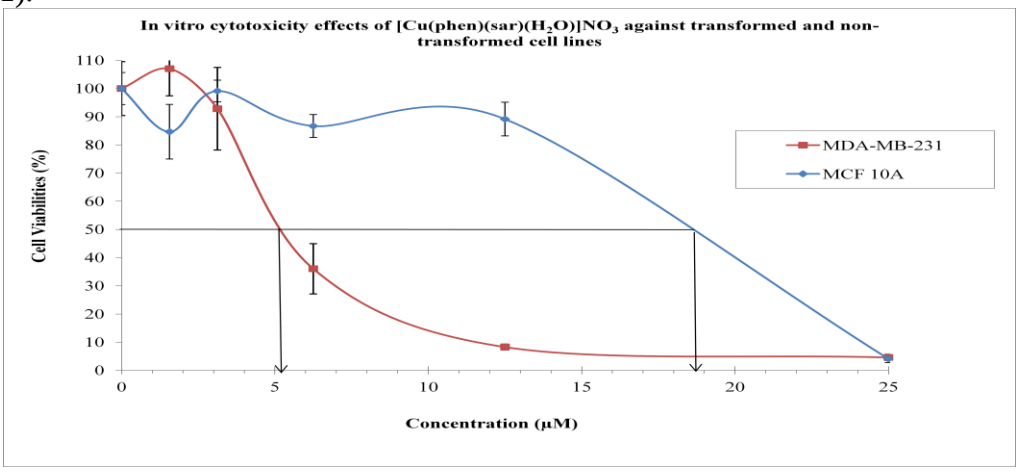

Dose response curves of the antiproliferative activity (% cell viability) of [Cu(phen)(sar)(H_2O)]NO_3 in MDA-MB-231 and MCF 10A cells at 24 h (Set 2).

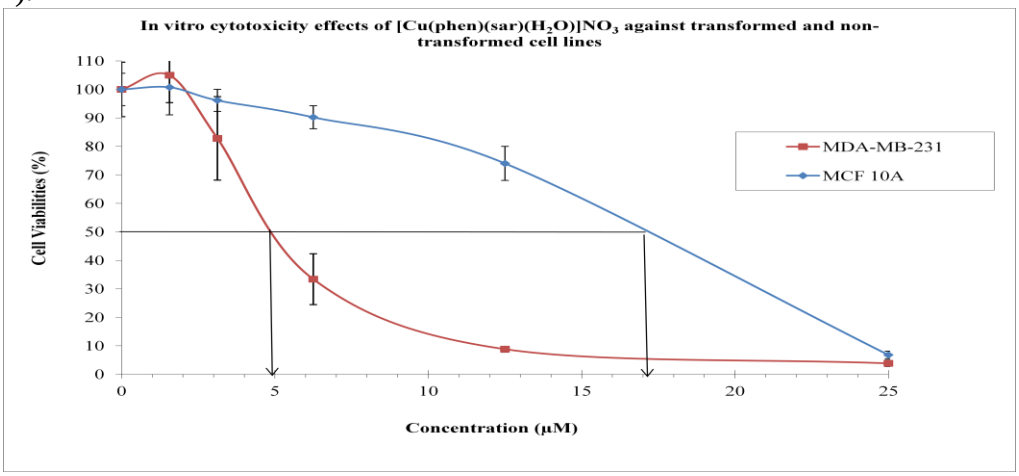

Dose response curves of the antiproliferative activity (% cell viability) of [Cu(phen)(sar)(H_2O)]NO_3 in MDA-MB-231 and MCF 10A cells at 24 h (Set 3).

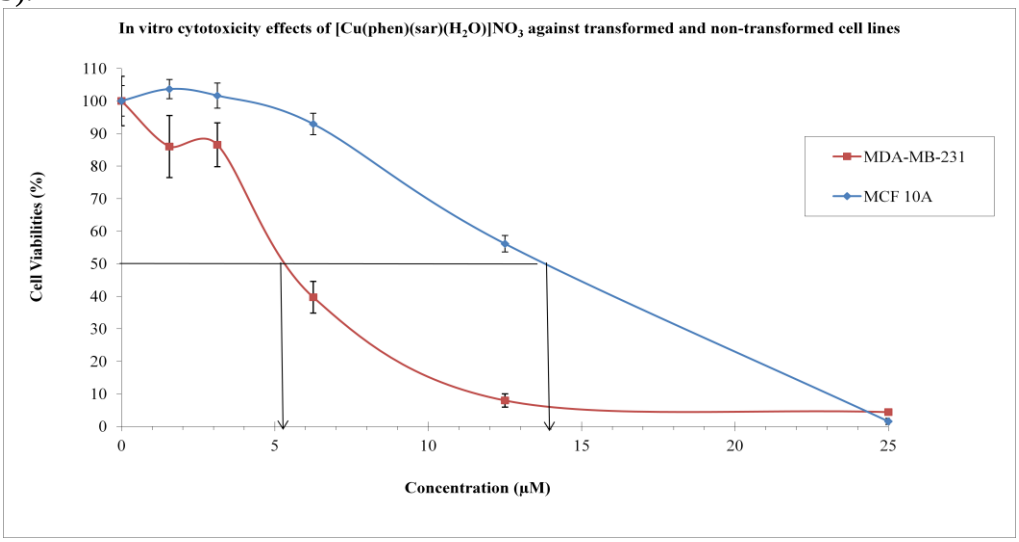

Dose response curves of the antiproliferative activity (% cell viability) of $[Cu(phen)(gly)(H_2O)]NO_3 \cdot 1.5H_2O$ in MDA-MB-231 and MCF 10A cells at 24 h (Set 1).

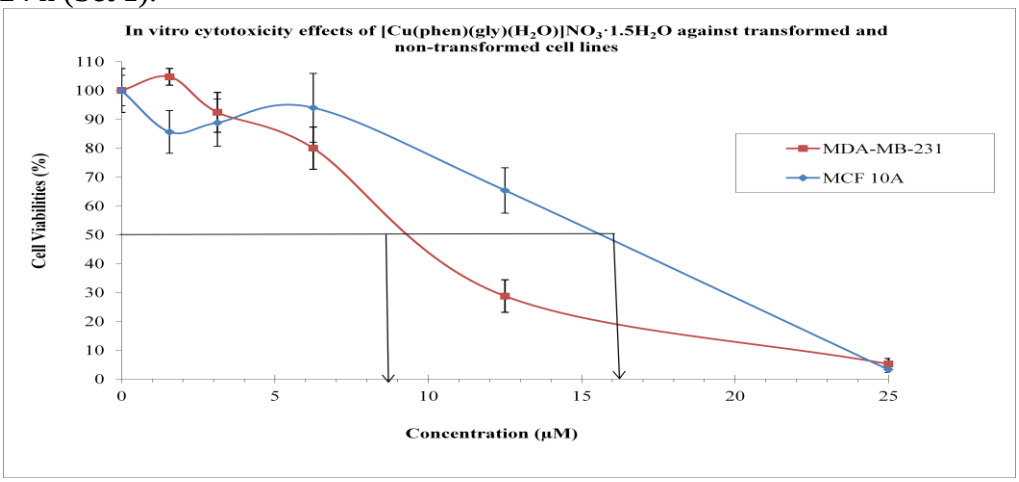

Dose response curves of the antiproliferative activity (% cell viability) of $[Cu(phen)(gly)(H_2O)]NO_3 \cdot 1.5H_2O$ in MDA-MB-231 and MCF 10A cells at 24 h (Set 2).

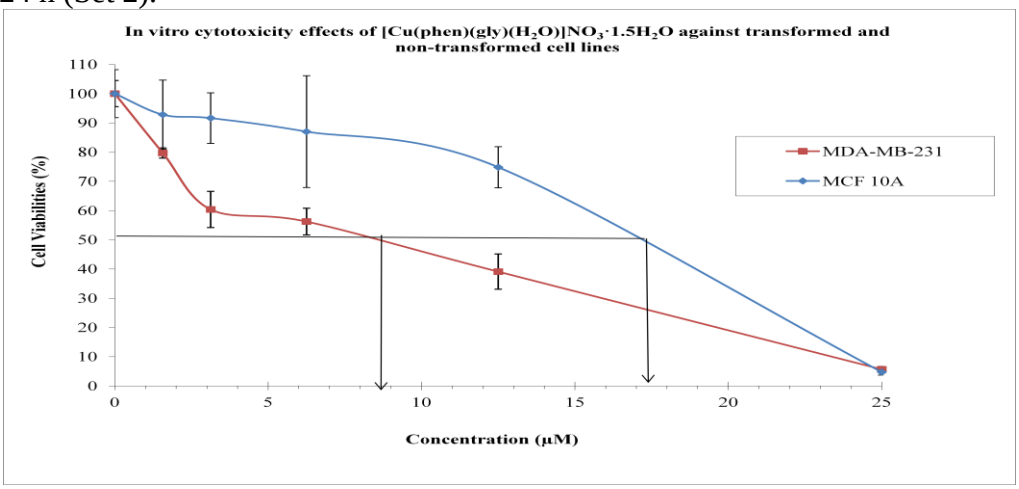

Dose response curves of the antiproliferative activity (% cell viability) of $[Cu(phen)(gly)(H_2O)]NO_3 \cdot 1.5H_2O$ in MDA-MB-231 and MCF 10A cells at 24 h (Set 3).

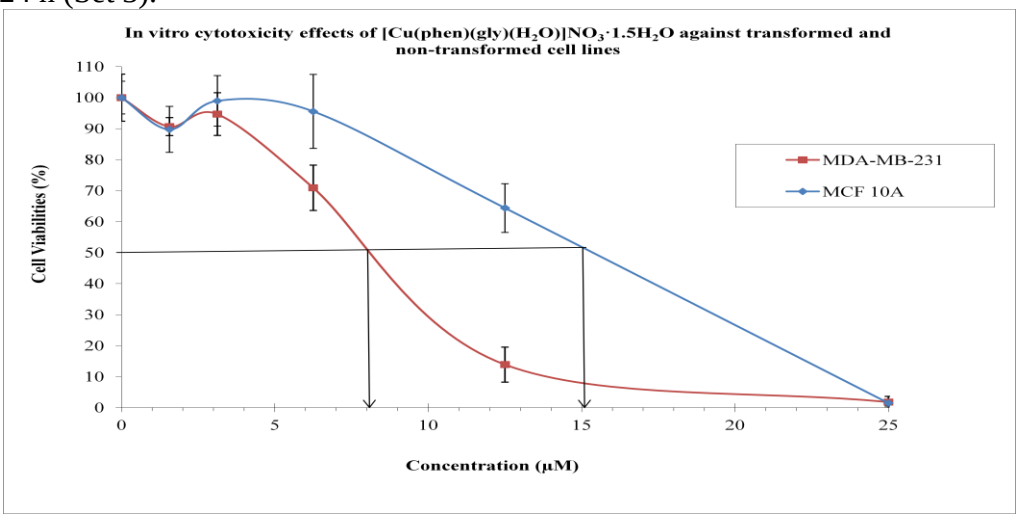

Dose response curves of the antiproliferative activity (% cell viability) of [Cu(phen)(C-dmg)(H_2O)]NO_3 in MDA-MB-231 and MCF 10A cells at 24 h (Set 1).

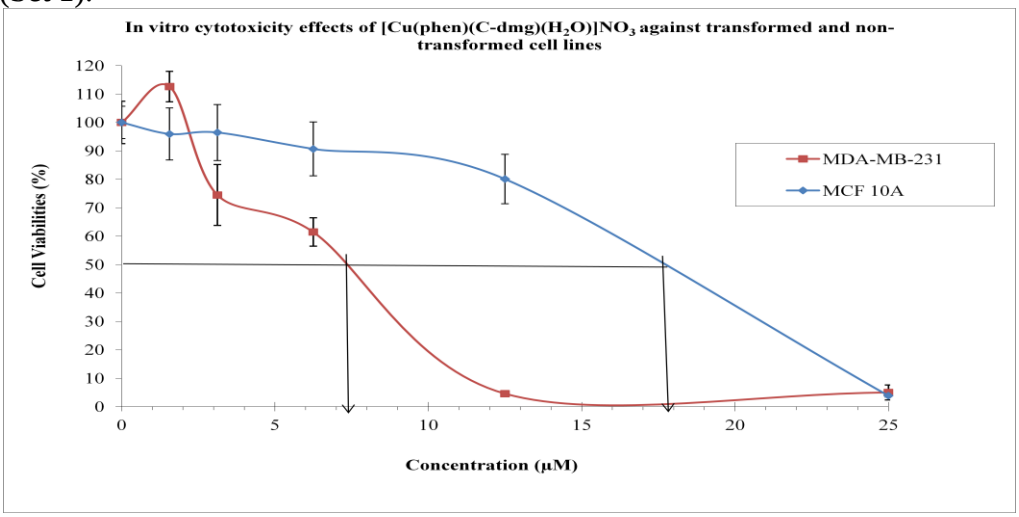

Dose response curves of the antiproliferative activity (% cell viability) of [Cu(phen)(C-dmg)(H_2O)]NO_3 in MDA-MB-231 and MCF 10A cells at 24 h (Set 2).

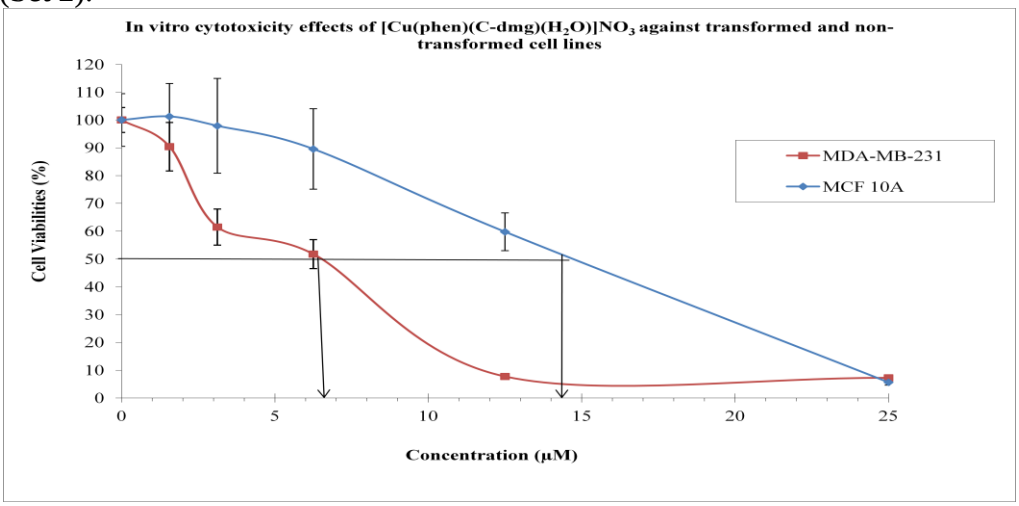

Dose response curves of the antiproliferative activity (% cell viability) of [Cu(phen)(C-dmg)(H_2O)]NO_3 in MDA-MB-231 and MCF 10A cells at 24 h (Set 3).

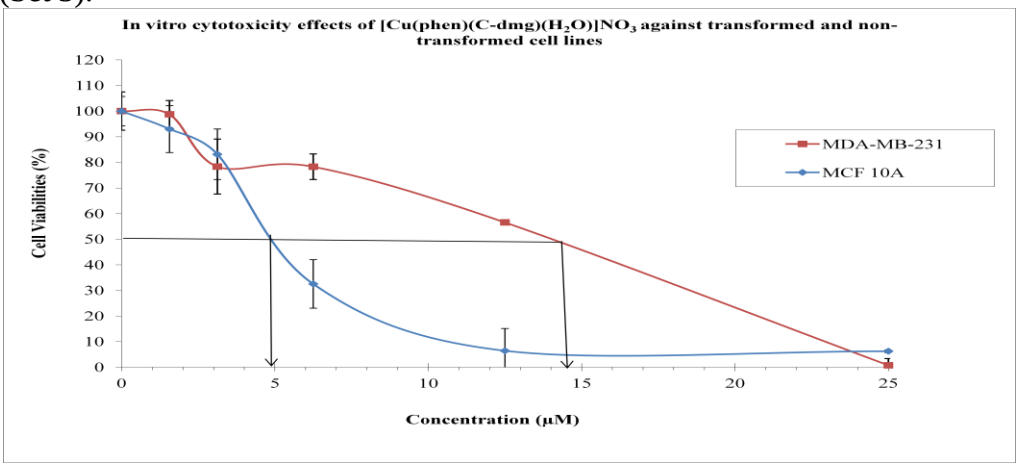

Dose response curves of the antiproliferative activity (% cell viability) of [Cu(8OHQ)$_2$] in MDA-MB-231 and MCF 10A cells at 24 h (Set 1).

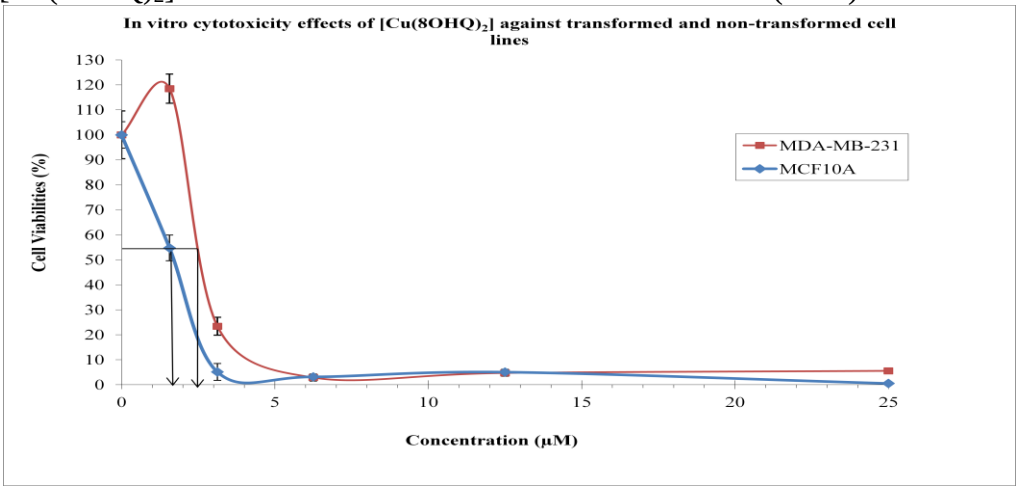

Dose response curves of the antiproliferative activity (% cell viability) of [Cu(8OHQ)$_2$] in MDA-MB-231 and MCF 10A cells at 24 h (Set 2).

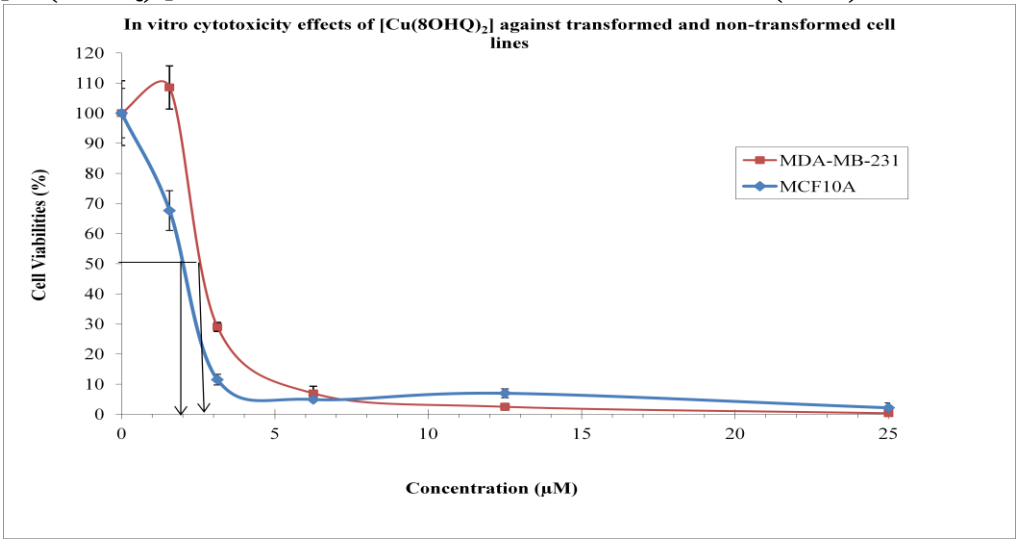

Dose response curves of the antiproliferative activity (% cell viability) of [Cu(8OHQ)$_2$] in MDA-MB-231 and MCF 10A cells at 24 h (Set 3).

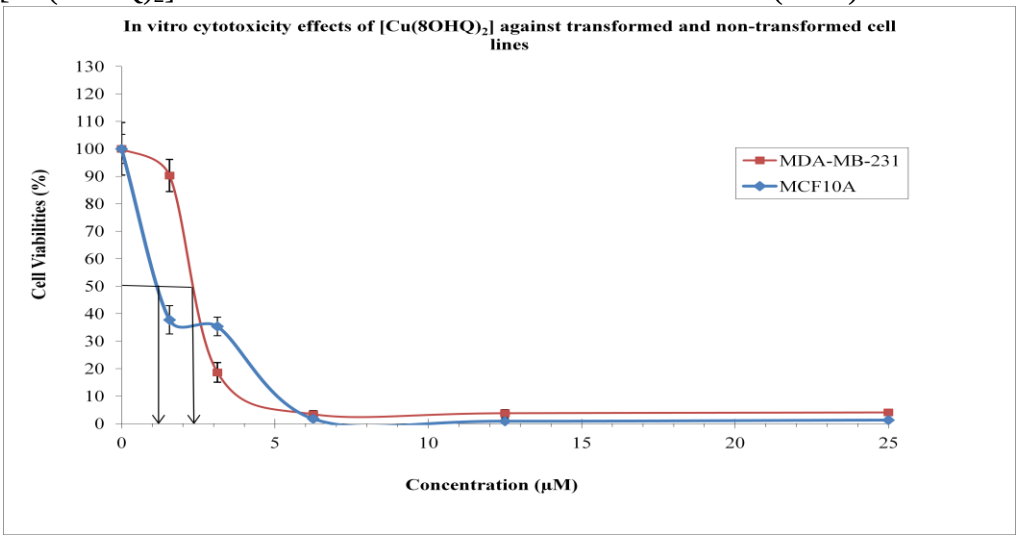

Raw data for IC_{50} values (μM) for proliferation inhibition by ternary copper(II) complexes for 24 h treatment. IC_{50} values were calculated from dose-response curves.

Compounds	IC_{50} (μM)					
	MDA-MB-231			MCF10A		
	Set 1	Set 2	Set 3	Set 1	Set 2	Set 3
$[Cu(phen)(DL\text{-}ala)(H_2O)]NO_3 \cdot 2½H_2O$	4.8	6.7	4.9	11.5	15.6	14.6
$[Cu(phen)(sar)(H_2O)]NO_3$	5.3	5.0	5.2	18.6	17.1	14.0
$[Cu(phen)(gly)(H_2O)]NO_3 \cdot 1.5H_2O$	8.8	8.5	8.2	16.2	16.1	15.2
$[Cu(phen)(C\text{-}dmg)(H_2O)]NO_3$	7.2	6.5	5.0	17	14.4	14.0
$[Cu(8OHQ)_2]$	2.5	2.7	2.8	1.7	2.0	1.3

Appendix B

Apoptosis assay

Raw data for Annexin V-FITC/PI double staining flow analysis of apoptosis assay in MDA-MB-231 cells.

Compounds	Apoptosis (%)			Average	SD
Untreated	9.62	19.85	8.75	12.74	6.17
[Cu(phen)(DL-ala)(H_2O)]NO_3 ·2½H_2O	58.75	32.77	47.47	46.33	13.03
[Cu(phen)(sar)(H_2O)]NO_3	53.49	66.75	50.29	56.84	8.73
[Cu(phen)(gly)(H_2O)]NO_3 ·1.5H_2O	42.58	46.47	34.38	41.14	6.17
[Cu(phen)(C-dmg)(H_2O)]NO_3	47.45	63.45	56.01	55.64	8.01
[Cu(8OHQ)$_2$]	92.6	79.93	87.76	86.76	6.39

Raw data for Annexin V-FITC/PI double staining flow analysis of apoptosis assay in MCF10A cells.

Compounds	Apoptosis (%)			Average	SD
Untreated	13.98	11.56	4.1	9.88	5.15
[Cu(phen)(DL-ala)(H_2O)]NO_3 ·2½H_2O	14.66	7.37	5.7	9.24	4.76
[Cu(phen)(sar)(H_2O)]NO_3	11.39	10.78	5.94	9.37	2.99
[Cu(phen)(gly)(H_2O)]NO_3 ·1.5H_2O	8.05	7.15	6.05	7.08	1.00
[Cu(phen)(C-dmg)(H_2O)]NO_3	11.53	6.8	5.04	7.79	3.36
[Cu(8OHQ)$_2$]	93.68	94.37	89.3	92.45	2.75

Appendix C

Cell cycle analysis

Raw data for cell cycle analysis assay in untreated MDA-MB-231 cells.

Cell cycle distribution	Percentage of cell			Average	Standard deviation
G0/G1	59.16	55.37	54.32	56.28	2.55
S	31.05	35.14	35.74	33.98	2.55
G2/M	9.78	9.48	9.94	9.73	0.23

Raw data for cell cycle analysis assay in MDA-MB-231 cells treated with $[Cu(phen)(DL\text{-}ala)(H_2O)]NO_3 \cdot 2½H_2O$

Cell cycle distribution	Percentage of cell			Average	Standard deviation
G0/G1	72.46	67.62	67.95	69.34	2.70
S	22.46	28.24	27.47	26.06	3.14
G2/M	5.08	4.14	4.58	4.60	0.47

Raw data for cell cycle analysis assay in MDA-MB-231 cells treated with $[Cu(phen)(sar)(H_2O)]NO_3$

Cell cycle distribution	Percentage of cell			Average	Standard deviation
G0/G1	69.02	56.19	64.86	63.36	6.55
S	24.83	38.43	30.4	31.22	6.84
G2/M	6.16	5.38	4.74	5.43	0.71

Raw data for cell cycle analysis assay in MDA-MB-231 cells treated with $[Cu(phen)(gly)(H_2O)]NO_3 \cdot 1.5H_2O$

Cell cycle distribution	Percentage of cell			Average	Standard deviation
G0/G1	71.96	57.38	60.62	63.32	7.66
S	23.81	38.37	32.63	31.60	7.33
G2/M	4.23	4.25	6.75	5.08	1.45

Raw data for cell cycle analysis assay in MDA-MB-231 cells treated with $[Cu(phen)(C\text{-}dmg)(H_2O)]NO_3$

Cell cycle distribution	Percentage of cell			Average	Standard deviation
G0/G1	68.25	58.04	66.85	64.38	5.54
S	26.53	37.87	28.68	31.03	6.02
G2/M	5.22	4.09	4.47	4.59	0.58

Raw data for cell cycle analysis assay in untreated MCF10A cells.

Cell cycle distribution	Percentage of cell			Average	Standard deviation
G0/G1	67.49	64.4	64.4	65.43	1.78
S	24.02	24.54	24.54	24.37	0.30
G2/M	8.49	11.06	11.06	10.20	1.48

Raw data for cell cycle analysis assay in MCF10A cells treated with $[Cu(phen)(DL\text{-}ala)(H_2O)]NO_3 \cdot 2½H_2O$

Cell cycle distribution	Percentage of cell			Average	Standard deviation
G0/G1	63.43	65.47	60.77	63.22	2.36
S	26.91	29.43	28.02	28.12	1.26
G2/M	9.66	5.10	11.21	8.66	3.18

Raw data for cell cycle analysis assay in MCF10A cells treated with $[Cu(phen)(sar)(H_2O)]NO_3$

Cell cycle distribution	Percentage of cell			Average	Standard deviation
G0/G1	63.11	58.4	57.47	59.66	3.02
S	27.89	32.54	29.36	29.93	2.38
G2/M	9.01	9.06	13.17	10.41	2.39

Raw data for cell cycle analysis assay in MCF10A cells treated with $[Cu(phen)(gly)(H_2O)]NO_3 \cdot 1.5H_2O$

Cell cycle distribution	Percentage of cell			Average	Standard deviation
G0/G1	65.70	63.38	63.88	64.32	1.22
S	25.50	27.04	25.30	25.95	0.95
G2/M	8.80	9.58	10.83	9.74	1.02

Raw data for cell cycle analysis assay in MCF10A cells treated with $[Cu(phen)(C\text{-}dmg)(H_2O)]NO_3$

Cell cycle distribution	Percentage of cell			Average	Standard deviation
G0/G1	61.90	62.02	62.95	62.29	0.57
S	28.05	27.97	26.74	27.59	0.73
G2/M	10.06	10.02	10.31	10.13	0.16

Appendix D

Reactive oxygen species study

The ROS production with various treatments for 6 h indicated (a) MDA-MB-231 cells and (b) MCF10A cells. Data are expressed as three independent experiments.

(a) MDA-MB-231 cells

Compounds	Mean (%)			Average	SD	SD (%)
Untreated	100	100	100	100	0	0
[Cu(phen)(DL-ala)(H_2O)]NO_3 ·2½H_2O, 5 μM	119	108	109	113	5.8	5.8
[Cu(phen)(DL-ala)(H_2O)]NO_3 ·2½H_2O, 10 μM	187	221	202	204	17.1	17.1
[Cu(phen)(sar)(H_2O)]NO_3, 5 μM	110	119	127	119	8.7	8.7
[Cu(phen)(sar)(H_2O)]NO_3, 10 μM	172	194	197	188	13.8	13.8
[Cu(phen)(gly)(H_2O)]NO_3 ·1.5H_2O, 5 μM	131	106	126	122	13.6	13.6
[Cu(phen)(gly)(H_2O)]NO_3 ·1.5H_2O, 10 μM	175	195	198	190	12.4	12.4
[Cu(phen)(C-dmg)(H_2O)]NO_3, 5 μM	139	123	133	132	8.2	8.2
[Cu(phen)(C-dmg)(H_2O)]NO_3, 10 μM	176	194	120	164	38.7	38.7

(b) MCF 10A cells

Compounds	Mean (%)			Average	SD	SD (%)
Untreated	100	100	100	100	0	0
[Cu(phen)(DL-ala)(H_2O)]NO_3·2½H_2O, 5 µM	111	122	109	114	7.3	7.3
[Cu(phen)(DL-ala)(H_2O)]NO_3·2½H_2O, 10 µM	103	113	109	109	5.0	5.0
[Cu(phen)(sar)(H_2O)]NO_3, 5 µM	113	117	109	114	3.8	3.8
[Cu(phen)(sar)(H_2O)]NO_3, 10 µM	106	116	103	109	6.6	6.6
[Cu(phen)(gly)(H_2O)]NO_3·1.5H_2O, 5 µM	116	119	109	115	5.1	5.1
[Cu(phen)(gly)(H_2O)]NO_3·1.5H_2O, 10 µM	122	111	106	114	8.0	8.0
[Cu(phen)(C-dmg)(H_2O)]NO_3, 5 µM	111	119	108	113	5.8	5.8
[Cu(phen)(C-dmg)(H_2O)]NO_3, 10 µM	135	106	106	116	16.8	16.8

Appendix E

Reactive oxygen species study

The ROS production with 5 μM treatments for 24 h indicated (a) MDA-MB-231 cells and (b) MCF10A cells. Data are expressed as three independent experiments.

(a) MDA-MB-231 cells

Compounds	Mean (%)			Average	SD	SD (%)
Untreated	100.0	100.0	100.0	100	0	0
Cu(phen)(DL-ala)NO_3	300.9	286.1	281.8	290	10	10
Cu(phen)(sar)NO_3	221.3	256.6	162.3	213	48	48
Cu(phen)(gly)NO_3	290.5	338.6	364.8	331	38	38
Cu(phen)(C-dMg)NO_3	351.2	399.6	365.4	372	25	25

(b) MCF 10A cells

Compounds	Mean (%)			Average	SD	SD (%)
Untreated	100.0	100.0	100.0	100	0	0
Cu(phen)(DL-ala)NO_3	145.3	151.7	151.9	150	4	4
Cu(phen)(sar)NO_3	124.0	104.2	134.8	121	15	15
Cu(phen)(gly)NO_3	134.3	174.5	159.8	156	20	20
Cu(phen)(C-dMg)NO_3	195.8	172.4	199.1	189	15	15

Appendix F

1. "Biological and cytoselective anticancer properties of copper(II)-polypyridyl complexes modulated by auxiliary methylated glycine ligand", *Biometals*, 2012, published online (Received: 14 January 2012 / Accepted: 10 July 2012).
2. "Copper(II)-mixed ligand complexes with anticancer propterties", UTAR REPORT FILING PI2012700421 (Patent filed with Malaysian Patent Office on 28th June 2012.
3. "Selective anticancer copper(II)-mixed ligand complexes: targeting of both ROS and proteasome", *Eur. J. Med. Chem.*, 2012, submitted for publication.